

The Pterosauria of the Early to Late Jurassic: Contributions to the understanding of the origin and global radiation of the Monofenestrata



Dissertation der Fakultät für Geowissenschaften der LudwigMaximilians-Universität München zur Erlangung des Doktorgrades in den Naturwissenschaften (Dr. rer. nat.)

Vorgelegt von
Alexandra Eugénio Fernandes
M. Sc. Vertebrate Paleontology

München, 25 July 2024

Supervisor and 1st reviewer: Prof. Dr. Oliver W. M. Rauhut

Bayerische Staatssammlung für Paläontologie und Geologie, Department of Earth and Environmental Sciences, Ludwig- Maximilians-Universität München, Richard-WagnerStr. 10, D-80333 München, Germany

2nd reviewer: Prof. Dr. Bettina Reichenbacher

Bayerische Staatssammlung für Paläontologie und Geologie, Department of Earth and Environmental Sciences, Ludwig- Maximilians-Universität München, Richard-WagnerStr. 10, D-80333 München, Germany

Date of thesis defense: 5 December 2024

CONTENTS

Statutory declaration and statement.....	IV
Abstract of the Thesis.....	IV
Kurzfassung der Dissertation.....	VI
Acknowledgements.....	IX
Chapter 1. Introduction.....	1
1.1 Introduction.....	1
1.2 Evolution of the Pterosauria.....	1
1.3 Challenges in pterosaur research.....	6
1.4 Objectives of the dissertation.....	9
1.5 Additional outputs.....	10
1.6 Overview of the studies presented in Chapters 2-6.....	11
1.7 References.....	12
Chapter 2. The oldest monofenestratan pterosaur from the Queso Rallado locality (Cañadón Asfalto Formation, Toarcian) of Chubut province, Patagonia, Argentina.....	19
2.1 Abstract.....	20
2.2 Introduction.....	21
2.3 Geographical and Paleontological Setting.....	23
2.4 Materials & Methods.....	25
2.5 Results.....	26
2.6 Discussion.....	40
2.7 Conclusion.....	46
2.8 Acknowledgements.....	47
2.9 References.....	48
Chapter 3. A new species and the earliest occurrence of the Gnathosaurinae (Pterosauria) from the Late Kimmeridgian of Brunn, Germany	56
3.1 Acknowledgements.....	57
3.2 Abstract.....	57
3.3 Introduction.....	58
3.4 Geographical and Geological Setting.....	60
3.5 Materials & Methods.....	62
3.6 Results.....	65
3.7 Discussion.....	73

3.8 Conclusion.....	83
3.9 References.....	84
Chapter 4. A new gnathosaurine (Pterosauria, Archaeoptero­dactyloidea) from the Late Jurassic of Portugal	92
4.1 Abstract.....	93
4.2 Introduction.....	93
4.2.1 History and Record of Pterosaur Discoveries in Portugal.....	94
4.3 Geographical and Geological Setting	96
4.4 Materials & Methods	97
4.5 Results	98
4.6 Discussion.....	103
4.7 Conclusion.....	109
4.8 Acknowledgments.....	109
4.9 References.....	111
Chapter 5. Pterosaur teeth from the Valmitão microfossil assemblage (upper Jurassic, Lourinhã Formation, Portugal).....	117
5.1 Abstract/Resumo.....	118
5.2 Introduction.....	118
5.3 Systematic Paleontology.....	119
5.3.1 Material Description/Remarks	119
5.5 Conclusion.....	121
5.6 References.....	121
Chapter 6. A new vertebrate assemblage from the Matute Formation of the Cameros Basin (Ágreda, Spain): implications for the diversity during the Jurassic/Cretaceous boundary.....	123
6.1 Abstract/Resumen	124
6.2 Introduction	125
6.3 Geographic and geological context	125
6.4 Materials and methods.....	127
6.5 Taphonomy	128
6.6 Vertebrate assemblage	130
6.6.1 Fishes	130
6.6.2 Crocodylomorpha.....	132
6.6.2 Testudinata.....	134

6.6.4 Pterosauria	136
6.7 Implications for the palaeobiodiversity in the Iberian ecosystems during the Jurassic/Cretaceous boundary	138
6.8 Conclusions	139
6.9 References	140
Conclusion	145
Appendix I. Chapter 2. Supplementary Information: Phylogenetic Data Matrices	148
Appendix II. Chapter 3. Supplementary Information: Phylogenetic Data Matrix	190
Appendix III. Chapter 4. Supplementary Information: Phylogenetic Data Matrix	226

Statutory declaration and statement

I hereby confirm that my thesis entitled “**The Pterosauria of the Early to Late Jurassic: Contributions to the understanding of the origin and global radiation of the Monofenestrata**”, is the result of my own original work. Furthermore, I certify that this work contains no material which has been accepted for the award of any other degree or diploma in my name, in any university and, to the best of my knowledge and belief, contains no material previously published or written by another person, except where due reference has been made in the text. In addition, I certify that no part of this work will, in the future, be used in a submission in my name, for any other degree or diploma in any university or other tertiary institution without the prior approval of the Ludwig Maximilians-University Munich.

Abstract of the thesis

Pterosaurs, the first group of tetrapods to have achieved powered flight, originated in the Triassic and survived through the Jurassic and up to the Cretaceous/Paleogene extinction. However, for all of their abundance during that prolific time span, they continue to be relatively elusive, with a remarkable amount still remaining to be understood about their paleobiology and evolution, as most of the mechanisms driving their staggering diversity and morphological disparity remain unknown. Much of this is due to their inherently thin, hollow bones, which have a very low preservational potential, except under exceptional circumstances (as seen in Konservat-Lagerstätten). However, pterosaurs, representing an early offshoot of the avian lineage of archosaur, exemplify the idea that many of their special adaptations (many of which evolved during their early evolution) evolved to maximize their flight efficiency, which, in turn, led to their subsequent radiations.

Most of the deductions that paleontologists have made thus far about the evolutionary history of pterosaurs have been based on specimens that largely originate in the northern hemisphere (which are much more abundant due to their longer and more intensive collection history). This has predetermined any inferences made, with the unintentional bias of excluding Gondwanan pterosaur taxa from the larger picture, and thus making it impossible to discern true biogeographic differences for Gondwana from the more dominant Laurasian faunas, or determine any role that Gondwanan pterosaurs might have played in Jurassic pterosaur evolution. More data collection from the southern hemisphere is therefore crucial in disentangling our biases, and for understanding the true role of this

landmass in pterosaur evolution and pterodactyloid origins.

Historically, pterosaurs were subdivided into two main groups, the “Rhamphorhynchoidea” and the Pterodactyloidea, with the pterodactyloids’ first proliferation happening during the Late Jurassic, before going on to become the most speciose group. However, recent discoveries have also shown the additional presence of several discrete lineages of closely related, non-pterodactyloid pterosaurs that were present during the Early to Middle Jurassic period, with several lines of evidence also implying a similar and concurrent origination time for the pterodactyloids, earlier than the fossil record currently marks. Part of this inference is based on the presence of an Oxfordian ctenochasmatid (a clade well nested within Pterodactyloidea), as such an earlier origin would also account for the wide diversity of pterodactyloid forms that are already known by the Late Jurassic.

The aim of the current thesis is therefore to obtain a better and more comprehensive insight into several facets of the evolution and diversification of the pterosaur lineage and its surrounding paleoenvironmental implications (namely surrounding what was happening to them during the Middle-Late Jurassic), while contributing new data from the southern hemisphere as well. With this aim in mind, a new non-pterodactyloid monofenestratan from the latest Early Jurassic of Gondwana is here introduced, representing an early step in the transition between “rhamphorhynchids” and pterodactyloids and identifying some potentially key morphological features in this transition, such as a vestigial ascending process of the maxilla.

A special focus is then put on several additional later new species of ctenochasmatids, in a worldwide context, in an attempt to unravel their role as early pterodactyloids, investigating the timeline of their potential origins, dispersion story, and what novel characteristics made them such successful paleoecological players in surviving the Jurassic-Cretaceous transition. A new gnathosaurine taxon from Brunn, Germany, marks the earliest occurrence of this subfamily of the Ctenochasmatidae and displays novel tooth characteristics, such as a veined dental enamel. Other ctenochasmatid fossils studied herein include both an extraordinarily-sized specimen, as well as microscopic fossils from Lourinhã, Portugal, and material from a new pterosaur site from Soria, Spain, whose specialized morphological features implied a flourishing diversity at a time when biodiversity was traditionally thought to have been dwindling. Altogether, the results of these academic

inquiries showcase the diversity of body sizes, rostrum shapes and dentitions shown by these filter-feeding specialists.

Pterosaurs play an important role in the evolutionary history of life on earth, having been present for all of the Mesozoic, where they reached a worldwide dispersion. Better understanding their evolutionary history and their interactions with their Mesozoic environments can thus provide important insights into the evolution of terrestrial vertebrates and their environments during that time. The new data presented in this thesis provides additional evidence for this, and for the anatomical transformations that were key to the success of the Pterosauria, with new information and inferences that contribute towards unraveling several of the open questions that still linger in respect to this topic.

Kurzfassung der Dissertation

Flugsaurier, die erste Gruppe von Tetrapoden, die einen aktiven Flug entwickelten, kamen zuerst in der Trias auf und überlebten durch den Jura bis zu ihrem Aussterben am Ende der Kreidezeit an der K/P-Grenze. Allerdings bleiben trotz dieser langen Dauer ihrer Existenz immer noch viele Fragen über ihre Evolution und Paläobiologie wenig verstanden, da die meisten Mechanismen, die ihre erstaunliche Vielfalt und morphologische Anpassungen angetrieben haben, unbekannt bleiben. Dies ist hauptsächlich auf das geringe Erhaltungspotenzial ihrer von Natur aus dünnen, hohlen Knochen zurückzuführen, die übliche taphonomische Prozesse nur unter besonderen Erhaltungsbedingungen überstehen. Dennoch demonstrieren Flugsaurier, die eine frühe Abzweigung der Archosaurier entlang der Vogellinie darstellen, dass sich viele der speziellen Merkmale dieser Knochen (die sich während ihrer frühen Evolution entwickelt haben), insbesondere im Interesse der Maximierung der Effizienz ihrer Flugfähigkeiten entwickelt haben, was wiederum ihre spätere Radiation ermöglichte.

Die meisten Schlussfolgerungen, die Paläontologen bisher über die Evolutionsgeschichte der Flugsaurier gezogen haben, basieren auf Exemplaren, die größtenteils aus der nördlichen Hemisphäre stammen (die aufgrund ihrer längeren und intensiveren Sammlungsgeschichte sehr viel besser bekannt sind). Dies hat oft unabsichtlich gondwanische Flugsaurier aus dem Gesamtbild ausgeschlossen, und es somit unmöglich gemacht, echte biogeografische Unterschiede zwischen Gondwana und den dominanteren

laurasischen Faunen zu erkennen, oder die Rolle zu erkennen, die gondwanische Flugsaurier in der Evolution der Flugsaurier im Jura gespielt haben könnten. Mehr Daten aus der südlichen Hemisphäre sind daher von entscheidender Bedeutung, um Vorstellungen zu kompletieren und die wahre Rolle dieser Landmasse bei der Entstehung und Evolution der Flugsaurier zu verstehen.

Historisch gesehen wurden Flugsaurier in zwei Hauptgruppen unterteilt, die „Rhamphorhynchoidea“ und die Pterodactyloidea, wobei die erste Verbreitung der Pterodactyloiden im späten Jura stattfand, bevor sie sich dann zur artenreichsten Gruppe entwickelten. Jüngere Untersuchungen haben jedoch auch das zusätzliche Vorhandensein mehrerer separater Linien von nahe verwandten, Nicht-Pterodactyloiden-Flugsauriern gezeigt, die während des frühen bis mittleren Jura vorhanden waren, wobei sich auch Hinweise mehren, dass die Pterodactyloiden ebenfalls bereits früher, zu einem ähnlichen Zeitpunkt entstanden sind. Ein Teil dieser Schlussfolgerung basiert auf dem Vorhandensein eines Ctenochasmatiden im Oxfordium, einer Gruppe, die tief in den Pterodactyloiden verwurzelt ist, und eine solche frühere Entstehung würde auch die große Vielfalt an Pterodactyloiden, die im späten Jura vorhanden sind.

Ziel der vorliegenden Arbeit ist es daher, einen Einblick in mehrere Facetten der Entwicklung und Diversifizierung der Flugsaurier-Linien und ihres paläoökologischen Rahmens zu erhalten, insbesondere zur Zeit des Jura. Gleichzeitig werden auch neue Daten aus der Südhalbkugel präsentiert. In Hinsicht auf den letzten Aspekt wird hier ein neues Taxon von nicht-pterodaktyloiden Monofenestratan aus dem obersten Unterjura von Gondwana vorgestellt, das einen Schritt in dem Übergang zwischen „Rhamphorhynchiden“ und Pterodaktyloiden dokumentiert und einige potenziell wichtige morphologische Merkmale dieser morphologischen Transition zeigt, wie zum Beispiel ein rudimentärer aufsteigender Fortsatz des Maxillare.

Ein besonderer Schwerpunkt wird dann auf mehrere neue Arten von Ctenochasmatiden im späteren Verlauf des Jura gelegt, um die Rolle dieser frühen Pterodactyloiden zu verstehen, ihren Ursprung, ihre Verbreitungsgeschichte und die Anpassungen, die sie paläoökologisch so erfolgreich machten, auch als Gruppe, die die Jura-Kreide-Grenze überlebt hat. Ein neues Taxon von Gnathosaurinen aus Brunn, Deutschland, stellt das früheste Vorkommen dieser Unterfamilie der Ctenochasmatidae dar und weist neuartige Zahnmerkmale auf, wie einen geäderten Zahnschmelz. Zudem wird ein

außergewöhnlich großes Exemplar und mikroskopisch kleine Fossilien von Ctenochasmatiden aus Lourinhã , Portugal, und einer neuen Flugsaurier-Fundstelle aus Soria, Spanien, beschrieben. Deren spezielle morphologische Merkmale deuteten auf eine große Vielfalt dieser Gruppe zu einer Zeit hin, als die Artenvielfalt traditionell als schwindend galt. Insgesamt unterstreichen die Ergebnisse dieser Untersuchungen die Vielfalt an Körpergröße, Kieferformen und Gebisse dieser auf eine filternde Ernährung spezialisierten Tiere.

Flugsaurier spielen eine wichtige Rolle in der Geschichte des Lebens auf der Erde, da sie im gesamten Mesozoikum präsent waren und dort eine weltweite Verbreitung erreichten. Ein besseres Verständnis ihrer Evolutionsgeschichte und ihrer Interaktionen mit ihrer Umwelt können uns daher wichtige Einsichten zur Evolution und Paläoökologie der terrestrischen Wirbeltiere zu jener Zeit geben. Die hier in dieser Arbeit präsentierten neuen Daten betonen diesen Einfluss zeigen anatomische Anpassungen, die entscheidend für ihren Erfolg waren. Die hier präsentierten Informationen und Daten helfen, die offenen Fragen zu klären, die noch immer über ihren Erfolg als Gruppe bestehen.

Acknowledgements

I would like to thank my supervisor, Prof. Dr. Oliver Rauhut, for his continued friendship and academic guidance, for entrusting me with some magnificent fossils for my studies, and for sharing some truly memorable fieldwork experiences (across 5 countries, and counting).

Innumerable thanks go to my co-authors and collaborators on these various works, and I would like to also thank all the curators and collection managers who helped in providing me access to specimens.

I would like to deeply thank the members of the Munich/Argentina fieldwork team for sharing their unlimited knowledge, experiences, laughs, and brute strength: Diego Pol, Jose Carballido, Pablo Puerta, and the entire staff of the MEF.

Sincerest gratitude is extended to the entire staff of the SNSB-BSPG, especially Elisabeth Lange and Andrea Herbert for their generosity in providing laboratory access and materials for preparation.

Thank you to Miguel Moreno-Azanza, Eduardo Puertolas-Pascual, Matyas Vremir, Mark Norell, and Roger Benson, for their professional guidance and friendship.

Heartfelt thanks are extended to Maria, Alvaro, Nicki, and Joe Fernandes, and to all of my extended family for all of their encouragements and support. Thank you to Ana Fontoura for yet again continuing to be the best personal librarian anyone could ever dream of. Thank you to Călin Şuteu, digitization wizard and life running partner. Thank you to Carl Mehling, Fiona Brady, Ana Balcarcel, Eileen Westwig, Kimberley Aparisio, Vanessa Béland, and all of my beloved family and friends.

This thesis was generously funded by the Deutsche Forschungsgemeinschaft (DFG project RA 1012/29).

Chapter 1.

1.1 Introduction

Although archosaurs are one of the most extensively studied clades in vertebrate paleontology, there remain many gaps in our understandings of their paleoecology, morphology, and evolution. Pterosaurs, the first group of tetrapods (and first archosaur subgroup) to have achieved powered flight, originated in the Triassic, and alongside the Dinosauria and Crocodylomorpha were the only clades to survive on into the Jurassic and up to the Cretaceous/Paleogene boundary (Unwin 2005; Brusatte et al., 2010; Longrich et al. 2018). And yet, for all of their abundance during that prolific time span, pterosaurs today continue to be relatively elusive since the time of their first fossil discovery in the 1700's, with a remarkable amount still remaining to be pieced together towards our understand of their paleobiology and evolution. For all of their vibrant and copious morphological disparity (reflected in their size variations, head crests, modes of flight, sexual dimorphism, etc.), most of the mechanisms driving the variations in these remarkable creatures remain unknown.

1.2 Evolution of the Pterosauria

The origin of pterosaurs is one such area in need of further elaboration, although very recently great strides have been made in this area. The oldest representatives of the Pterosauria are currently known from the Triassic of Europe (Dalla Vecchia 2013, 2019; Kellner 2015) and North America (Dalla Vecchia 2013; Britt et al. 2018), although the earlier transitional taxa are still missing from the fossil record to link them with certainty to their earlier ancestors. These earlier members of the group were likely small cursorial, non-volant dinosaur-line archosaurs, and recent findings link lagerpetids (which show a great similarity to the morphologies of Triassic pterosaurs) to bridging this morphological gap (Ezcurra et al., 2020; Müller et al., 2022). These findings also strengthen the evidence that pterosaurs belong to the avemetatarsalia (Fig. 1), the avian line of archosaurs, underpinning the idea that the specialized traits that pterosaurs evolved during their early evolution were expressly in the interest of maximizing the efficiency of their flight capabilities, which bolstered their later adaptive radiations.

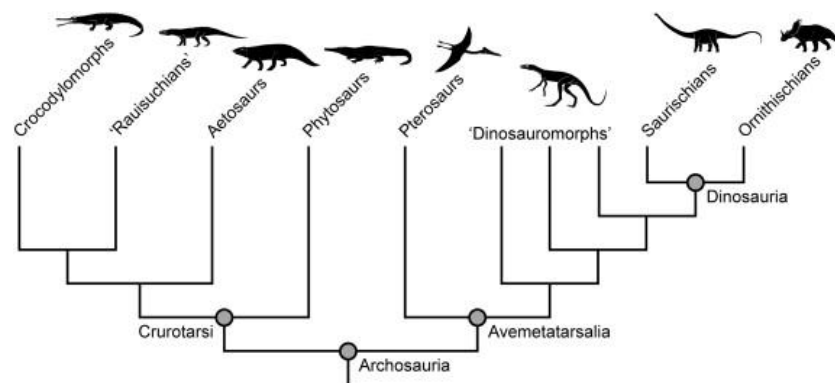


Figure 1. Cladogram of archosaur relationships (from Brusatte et al., 2010)

Historically, pterosaurs were subdivided into two main groups, the Rhamphorhynchoidea and the Pterodactyloidea. However, whereas the latter has repeatedly been demonstrated to represent a monophyletic group by modern phylogenetic systematics (Witton, 2013 and references therein), the former was basically defined as encompassing all pterosaurs that are not pterodactyloids, and is thus a paraphyletic assemblage; and as a result the name “Rhamphorhynchoidea” is no longer used in modern pterosaur systematics. There are several discrete lineages of non-pterodactyloid pterosaurs that were present during the Jurassic period, but almost all (with perhaps only the exception of the anurognathids) went on to disappear at the Jurassic-Cretaceous boundary, whereas the Pterodactyloidea (their first occurrence with *Kryptodrakon progenitor* [Andres et al., 2014]) straddled this transition and went on to become the most speciose group (Fig. 2). Their first proliferation happening during the Late Jurassic, dispersing onward to eventually achieve global representation through the end-Cretaceous extinction (Plieninger 1901; Wellnhofer 1978, 1991; Witton, 2013).

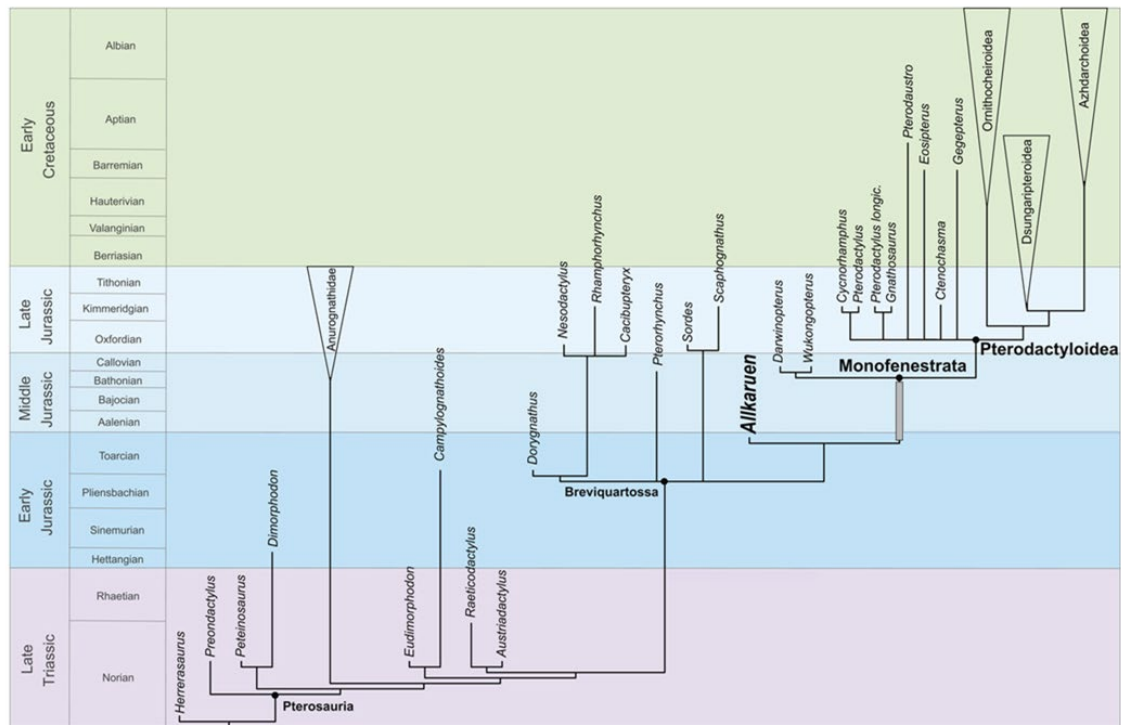


Figure 2. Simplified time-calibrated phylogeny of the Pterosauria, with the grey bar representative of the ghost lineage(s) leading to Monofenestrata (adapted from Codorniu et al., 2016)

However, several lines of evidence also imply that the origin of pterodactyloids likely happened earlier in the Middle or even in the late Early Jurassic, based on the presence of an Oxfordian ctenochasmatid (Zhou et al. 2017) (a clade well nested within pterodactyloids), as well as the wide diversity of pterodactyloid forms that came about by the Late Jurassic, (Kimmeridgian-Tithonian), including probable representatives of the derived azhdarchoids (Frey et al. 2011; Costa et al. 2015). However, exactly when and how these divisions occurred - and the evolutionary pathway between them (both temporally and morphologically) - remains obscured. What we do know is that the origin of pterodactyloids is marked by numerous anatomical novelties, most of which are apparently related with an improvement in flight capabilities (Wellnhofer 1991; Unwin 2005; Witton 2013). Some of the modifications that they underwent include the reduction of the bar separating the external nares from the antorbital fenestra, reorientation of the braincase and changes in brain flexure, elongation of the cervical vertebrae, reduction of the tail, an elongation of the wing metacarpal, and a reduction of the fifth pedal digit, among others (Fig. 3) (Wang et al. 2009, 2010, 2017; Lü et al. 2010; Rauhut 2012; Martill & Etches 2013; Tischlinger & Frey

2013; Andres et al. 2014). This evolution of the pterodactyloids seems to have led to a burst in pterosaur diversity and morphological and ecological disparity (e.g. Butler et al. 2009, 2011, 2012; Dyke et al. 2009; Prentice et al. 2011; Foth et al. 2012; Bestwick et al. 2018), and defined pterosaur success in the mid-Mesozoic and up to the Cretaceous-Paleogene boundary (Longrich et al. 2018).

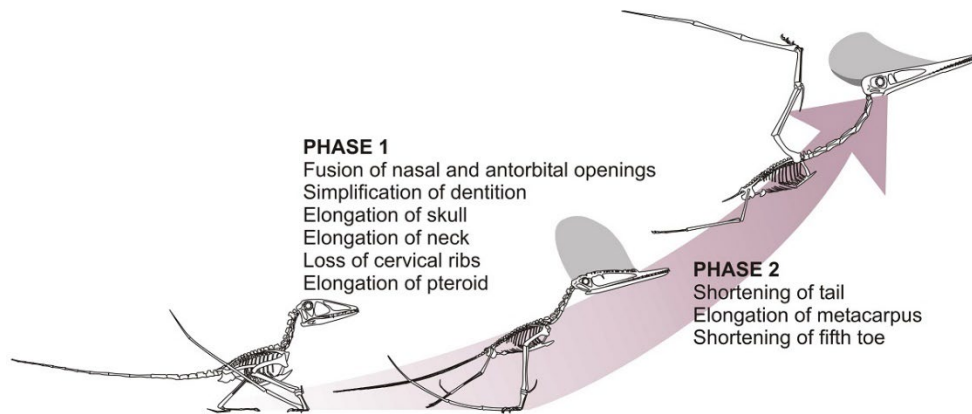


Figure 3. The phases or morphological change between “rhamphorynchoid” (left), monofenestratan (middle), and pterodactyloid(right) (Witton, 2013).

In the Middle Jurassic, at the time that these two main clades were still diverging, another less-represented group was also establishing its own foothold in the evolutionary record, despite it being shorter lived than that of the pterodactyloids. While the Pterodactyloidea were mainly bolstered by the elongation of their metacarpus (especially metacarpal IV), other recent finds of close relatives of pterodactyloids (i.e. non-pterodactyloid monofenestratans, such as the darwinopterans), have shown that this transition was more complex. They seemingly embraced modular transitions, combining traits from both more basal and derived forms to arrive at their own unique configurations that were also typified by a confluence of nares and antorbital fenestra (although the fluidity and linearity of this mechanism is challenged by some authors, e.g. Martin-Silverstone et al. 2024) (Andres et al. 2014; Wang et al. 2017).

Recent finds, especially the discovery of a pterosaur from the latest Early Jurassic of Patagonia (Cordoniú et al. 2016), have shed light on the acquisition of these transitional features and whether the process was also mosaic-like (where cranial and vertebral characteristics were seemingly changed as a unit) (Wang et al. 2009, 2010, 2017; Lü et al.,

2010; Rauhut, 2012; Martill & Etches, 2013; Tischlinger & Frey, 2013; Andres et al., 2014), or as in other finds which indicate more gradual transition, such as the braincase and endocast (Cordonú et al., 2016), or the elongation of the metacarpus (Rauhut, 2012; Tischlinger & Frey, 2013). The rarity of these taxa and their incompleteness underscores the need for more fossil material to be recovered in order to understand the exact evolution of Middle Jurassic pterosaurs and the origin of pterodactyloids.

Otherwise, middle Jurassic pterosaur remains are mainly known from Europe (Barrett et al. 2008), but they too are often isolated and fragmentary, such as the pterosaur remains known from the Great Oolite Group of England (O'Sullivan & Martill, 2018), which include several specimens that probably represent monofenestratan taxa and one poorly preserved sacrum that might indicate the oldest known pterodactyloid, further strengthening the hypothesis that the origin of pterodactyloids happened before the late Middle Jurassic. Otherwise, there are remarkably few late Early to Middle Jurassic pterosaur taxa globally (Fig. 4), which is especially true for the former Gondwanan continents in general (Barrett et al. 2008; Rauhut & López-Arbarello 2008).

Another group of importance to pterosaur evolution within the Pterodactyloidea is the Ctenochasmatidae. Ctenochasmatids were an abundant group (although one of their subfamilies, the gnathosaurines, are significantly more rare) of pterodactyloid pterosaurs that were the first subclade to appear in the fossil record, originating in the Oxfordian stage of the Jurassic (Zhou et al. 2017). They are known in the Late Jurassic already from Asia, Europe and recently also South America (Soto et al. 2021). Their presence right at the beginning of the time period of the “rhamphorhynchoid-to-pterodactyloid” transition means that they coexisted with other forms during this change (e.g. darwinopterans and anurognathids), but then also chronologically endured beyond the others, indicating that they were quite successful in filling their specific paleoenvironmental niche. As one of few groups originating in the early Late Jurassic that also crossed the J/K divide, they clearly possessed traits that were evolutionarily advantageous to their survival, representing one of the first successful major radiations of pterodactyloids. During the past few years, ctenochasmatids also have gained traction and potential for being quite informative in expressing their variety and differing levels of paleoecologic specialization that could be undergone by just one group of pterosaurs during the Jurassic.

Over the past several years, there have been many pterosaur phylogenetic analyses proposed to better understand their overall interrelationships (e.g. Kellner 2003; Unwin 2003; Wang et al. 2005, 2009, 2017; Andres & Ji 2008; Andres et al 2010, 2014, 2021; Lü et al. 2010, 2012; Vidovic & Martill 2017; Longrich et al. 2018; Pêgas et al. 2018; Martin-Silverstone et al. 2024). Although the individual results of the different analyses still differ considerably in many details, they have unanimously been in support of pterodactyloid monophyly, showing that this clade represents the major radiation of pterosaurs, accounting for almost all Cretaceous taxa known (with the exception of the Early Cretaceous anurognathid *Dendrorhynchoides curvidentatus*) (Ji & Ji 1998; Ji et al. 1999). However, more work is also needed to import data as it becomes available from the field, in order to iron out actual pterosaur interrelationships.

1.3 Challenges in pterosaur research

A significant hinderance in studying pterosaurs is their physical bone fragility, which creates a propensity for taphonomical distortion and destruction. The inherent thinness and hollow structure of their bones, under conditions of lithostatic pressure and taphonomic strain, often lose structural integrity, leading to a low preservation potential. This is also implicative that, outside of exceptional Lagerstätten environments (which tend to preserve nearly-complete, articulated specimens), any recovered fossil material is often scant, consisting of few bones, and rarely in articulation, lessening the amount of information that can be gleaned from each fossil individual and taxon. Because of this phenomenon, isolated postcranial elements are often overlooked for their difficulty in providing reliant taxonomic identification, leaving large gaps in our understanding of the mode of morphological variation over the entirety of the pterosaur post-cranial bauplan and its progression over time. This is mainly problematic when we consider that the origin of pterodactyloids was marked by numerous postcranial anatomical novelties which were related to improved flight capabilities (Wellnhofer 1991; Unwin 2005; Witton 2013; Paul 2022): the elongation of the cervical vertebrae, reduction of the tail, elongation of the wing metacarpal, reduction of the fifth pedal digit. It has also become evident by this work that in the absence of Lagerstätten environments, isolated post-cranial material (which is often overlooked or ignored by pterosaur workers for its lack of “wow-factor”) may indeed hold crucial

morphological details (such as in the case of Andres et al. (2014) describing the first known pterodactyloid based on fragmentary postcranial material), to elucidate the mode and tempo of transitional pterosaur body styles that indicate the how and why of the origin of pterodactyloids that happened during the Middle-Late Jurassic.

Another limitation in understanding pterosaurs lies in the paucity of global diversity of our data, as existing data is largely skewed in favor of select Lagerstätten preservational environments (Buffetaut, 1995). Although Dyke et al. (2009) argued that this preservational bias does not affect our general understanding of pterosaur evolution, other studies found a profound influence of the presence or absence of Lagerstätten not only on our understanding of pterosaur diversity (Butler et al. 2009, 2013), but especially on pterosaur morphological disparity (Butler et al. 2011, 2013; Prentice et al. 2011; Upchurch et al., 2015; Dean et al. 2016). Due to this bias towards exceptional Lagerstätten, our knowledge of the “rhamphorhynchoid”-to-pterodactyloid transition largely rests on material coming from the northern hemisphere (Fig. 4), from the Late Jurassic Yinliao Biota (e.g. Wang et al. 2009, 2010, 2017; Lü et al. 2010, 2011; Cheng et al. 2016, 2017) and the Solnhofen Archipelago (Rauhut, 2012; Tischlinger & Frey, 2013).

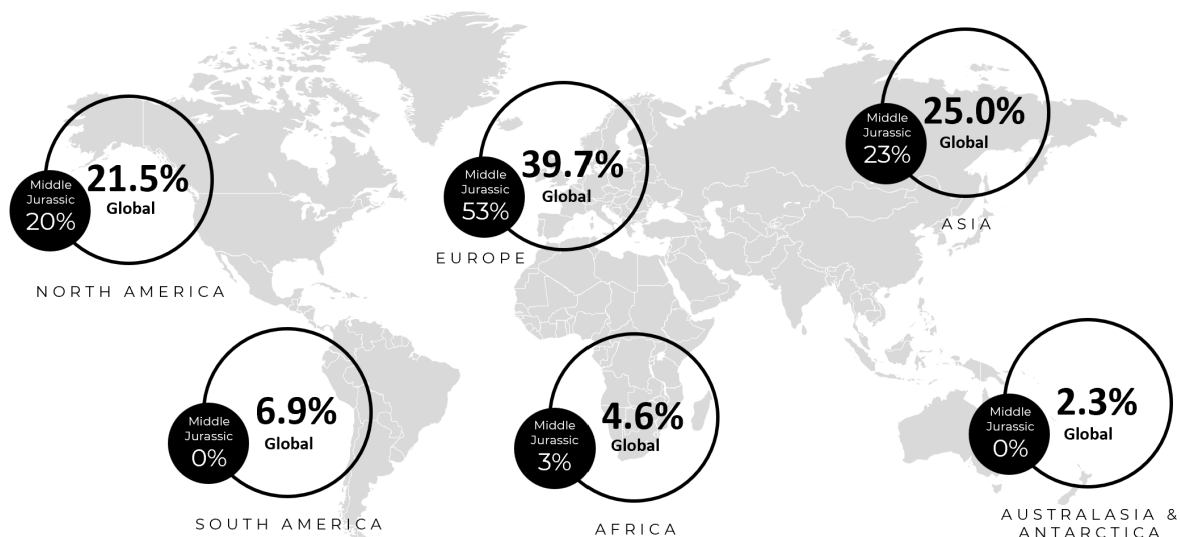


Figure 4. Distribution of pterosaur fossils worldwide (percentages calculated from Barrett et al., 2008)

Very few pterosaur remains have been described from the southern Hemisphere

(Barrett et al. 2008; Rauhut & López-Arbarello 2008). Two raeticodactylid pterosaurs, *Yelaphomte praderioi* and *Pachagnathus benitoi*, both based on skull fragments, are known from the upper Norian-Rhaetian of north-western Argentina (Martinez et al., 2022), marking the first occurrence of Triassic records for pterosaurs in the southern hemisphere, and showing that poor sampling had previously erroneously led researchers to believe that pterosaurs were absent from outside north-western Pangea during the Late Triassic. From the Early Jurassic, the only named pterosaur taxon is the rhamphorhynchid *Campylognathoides indicus* from the Kota Formation of India (Jain 1974), though its attribution has been questioned (Padian 2008), and an isolated pterosaur humerus from the Hanson Formation of Antarctica (Hammer & Hickerson, 1999). For the latest Early to early Middle Jurassic, pterosaur remains have so far only been reported from the Cañadón Asfalto Formation of Argentina (Cordoniú et al. 2016). From the Late Jurassic, Alarcón-Muñoz et al. (2020) introduced the first rhamphorhynchine pterosaur from the Oxfordian of Gondwana from Chile, based on post-cranial material, greatly extending the known range and distribution for the group outside of Laurasia, and introducing a potential dispersion scheme along the Caribbean Corridor. Otherwise, Late Jurassic pterosaurs from the southern Hemisphere have been attributed to dsungaripterids and azhdarchids, from the Tendaguru Formation of Tanzania (Reck, 1931; Unwin & Heinrich 1999; Costa & Kellner, 2009; Costa et al. 2015) and the Vaca Muerta Formation of Neuquén, Argentina, which yielded several pterodactyloids, including *Herbstosaurus pigmaeus* (Casamiquela 1975; Cordoniú & Gasparini 2007) and *Wenupteryx uzi* (Cordoniú et al., 2006; Cordoniú & Gasparini, 2013). The only other Late Jurassic pterosaur from South America is the gnathosaurine *Tacuadactylus lucaie* from the Tacuarembó Formation of Uruguay (Perea et al., 2018; Soto et al., 2021). What Gondwanan pterosaur fossils may lack in quantity, they certainly make up for in their diversity and wide distribution at that time.

Therefore, the relative absence of pterosaur representation among Gondwanan Jurassic faunas not only has previously skewed the data being analyzed by paleontologists for this time period, but biased our thinking about actual pterosaur evolution as a whole, making it impossible to discern true biogeographic differences for Gondwana from the more dominant Laurasian faunas, or the role that Gondwanan pterosaurs might have played in Jurassic pterosaur evolution. More data collection from the southern hemisphere is

therefore crucial in disentangling our biases, and for understanding the true role of this landmass in pterosaur evolution and pterodactyloid origins.

Furthermore, Lagerstätten are typically marine, but there is evidence that the origin of pterodactyloids occurred in terrestrial environments (Andres et al., 2014). Therefore, apart from the exceptional lacustrine site of the Yanliao and Jehol Biota (see also Unwin 2005; Lü et al. 2010), there is a scarcity of material from the critical exposures, especially from Gondwana, which might piece together the gaps in our knowledge simply, whether by the unavailability of natural exposures or by physical inaccessibility of sites.

1.4 Objectives of the dissertation

While it is outside the scope of this work to resolve all of the above-mentioned challenges, the aim of this thesis is indeed to make a contribution to obtaining a better and more comprehensive understanding into the mode and tempo of pterosaur (and in particular, pterodactyloid) evolution, with a focus on the Jurassic period, by providing both new discoveries and additional insights into recovered material. Therefore, the present dissertation addresses the following research questions in two stages: first by excavating, recovering, and contributing new and crucial fossil material from this critical geological time period, and then secondly by performing an analysis thereof, in order to advance our understanding of pterosaurian evolution. Therefore, two fieldwork campaigns in Portugal and two fieldwork campaigns to Argentina resulted in the recovery of numerous new specimens. Anatomical and taxonomic studies were performed on these and other specimens, including anatomical description, interpretation of CT data, and detailed comparison with other taxa (also made possible by undertaking collections visits).

By applying the above-mentioned framework, insights were gained into the main research questions: 1) What can the pterosaur fauna from the Early Jurassic terrestrial exposures of Patagonia tell us about pterosaur evolution in the Jurassic, and how do these Patagonian taxa fit into the global framework of pterosaur evolution and concurrent clades of that time period? 2) Of the new Jurassic species recovered by the various fieldwork expeditions throughout this project, what are their phylogenetic relationships to the

Pterosauria? 3) What is the significance of any new information that can be gleaned from the new specimens, regarding the morphological transition from non-monofenestratan pterosaurs to pterodactyloids, or any variations within the Pterodactyloidea themselves? As a result, the major theme of this dissertation describes how the anatomical novelties across the Early-Late Jurassic (i.e. the “prime time” for pterosaur evolution) drove such dynamic body shifts among pterosaurs, from the “rhamphorynchid” body style to pterodactyloids, and beyond.

1.5 Additional outputs (not intended for thesis publication):

One additional output of this dissertation (and also the fieldwork therein) was the collection and recognition of additional fossil material belonging to *Allkaruen koi* Cordoniu et al. 2016, which is greatly pertinent to our deeper understanding of Middle Jurassic non-pterodactyloid monofenestratans (as expounded upon in chapter 2 of this dissertation). Originating from the La Lluvia locality close to the village of Cerro C6ndor in the Chubut province of Argentina, this pterosaur had been based on a braincase, mandibles and associated cervical vertebrae, and was found to belong to the immediate outgroup of Monofenestrata. Additional new fossil material adds a second mandible, vertebrae, a significant number of new and previously-undescribed appendicular elements, thus representing at least a second individual towards our current understanding of the taxon, which could potentially change our perceptions of its biomechanics, paleoenvironment, and morphology, as well as to refine its phylogenetic standing. This additional material, analyzed by morphological comparison and detailed CT scan data, elucidated that these elements were all found in a monospecific bonebed, which also lends itself to a deeper understanding of the taphonomy and paleoecology of the region. Being of an age close to the suggested origin of monofenestratans and, probably, pterodactyloids, and representing a terrestrial setting in Gondwana, these remains have thus great potential to illuminate an important time in pterosaur evolution and, potentially, give new insights into the origin of pterodactyloids. A manuscript is already in preparation by the author, however it is pending submission for formal publication after the submission date of this dissertation, and therefore is not included here.

1.6 Overview of the studies presented in Chapters 2-6

The manuscripts in this dissertation were prepared over a period of three years, from 2021-2024, combining methodologies that were based on first-hand fieldwork experiences and laboratory preparation (both contributed by the author), and designed to then enable the formal academical inquiry into the above-mentioned themes and questions. These fieldworks and research were performed across several different countries (Argentina, Portugal, Spain, and Germany), in order to increase the global context for understanding Jurassic pterosaur evolution.

In chapter 2, the theme of anatomical transition from "rhamphorynchid"-to-pterodactyloid is further explored with the description of a new species of rare non-pterodactyloid monofenestratan (expressing a morphology between basal pterosaurs and derived pterodactyloids) from the also-rare latest Early Jurassic (Toarcian) exposure of the Queso Rallado locality with the Cañadón Asfalto Formation of Chubut province of Patagonia, Argentina. This Formation is representative of a fluviolacustrine environment of a terrestrial setting, which is much more rare in pterosaur fossil preservation (most fossils being recovered from marine environments), a rarity which is further bolstered by its Gondwanan setting. The fossil in this chapter was prepared from its encasing sediment by the author in the laboratory of the SNSB-BSPG, and was found to be a new species of non-pterodactyloid monofenestratan, preserving many significant traits. Morphological description and phylogenetic analysis was also performed to assess the evolutionary position of this new taxon within Pterosauria.

In chapter 3, the focus moves ahead in time, changing time periods and geography to the Late Kimmeridgian of Brunn, Germany, the oldest locality within the Solnhofen Archipelago, which, from younger units, has yielded the richest ctenochasmatid record from the Late Jurassic (e.g., Wellnhofer, 1970; Bennett 2007, 2021; Moser & Rauhut, 2011; Rauhut et al., 2011). In an attempt to ascertain any driving morphological features that may have affected the larger comparative evolution of pterosaurs, this article explores the Gnathosaurinae, also contributing a new species to this group of filter-feeding specialists that also crossed the Jurassic-Cretaceous boundary, marking the earliest occurrence of this subfamily of the Ctenochasmatidae. The diversity of body sizes, rostrum shapes and dentitions shown by these animals indicates a variety of dietary adaptations. Innovative

traits including a unique veined tooth texture provided insight into this taxon's potential paleoenvironmental niche, and the evolution of the pterosaurian diet. Phylogenetic analysis was also performed to assess the evolutionary position of this new taxon within Pterosauria.

In chapters 4 and 5, the focus again moves temporally forward and across borders to the Kimmeridgian/Tithonian boundary of the Lourinhã Formation, where three taxa display two extremes in size (and were collected with two extremes of practical methodologies): the former chapter sheds light on the largest Jurassic gnathosaurine known to date (excavated by rock saw and chisel by the author), which showed that larger body sizes were indeed present in the Jurassic. Phylogenetic analysis was also performed in the latter chapter, to assess the evolutionary position of this new taxon within Pterosauria, *Lusognathus almadrava*, one of the largest Jurassic gnathosaurines pterosaur specimens in general to date, which became the first pterosaur named from the Late Jurassic of Portugal. The second of these chapters scrutinizes two microvertebrate pterosaur teeth (found by microfossil picking by the author) of a rhamphorynchid and another gnathosaur, showing that both major pterosaurian morphological groups ("rhamphorynchids" and pterodactyls) were concurrently present during this time period in the Jurassic, also in the Iberian Peninsula (as their co-existence in other settings are well known for that time), shedding light on the awareness of size biases in the fossil record.

In chapter 6, the Jurassic/Cretaceous boundary is this time explored, with the introduction and preliminary report on a new fossil site in Ágreda, Spain, of the Cameros Basin, that produced an abundance of vertebrate taxa throughout its fossil assemblage. Inclusive of pterosaurs, the elements that were produced also bear the promise of being new species, whose specialized morphological features implied a flourishing diversity at a time when biodiversity was traditionally thought to have been dwindling.

1.7 References:

Alarcón-Muñoz, J., Soto-Acuña, S., Codorniú, L., Rubilar-Rogers, D., Sallaberry, M., & Suárez, M. (2020). New ctenochasmatid pterosaur record for Gondwana: discovery in the Lower Cretaceous continental deposits of the Atacama Desert, northern Chile, *Cretaceous Research*, 110, 104378.

- Andres, B. (2021). Phylogenetic systematics of *Quetzalcoatlus* Lawson 1975 (Pterodactyloidea: Azhdarchoidea). *Journal of Vertebrate Paleontology*, 41(1), 203–217.
- Andres, B., Clark, J., & Xu, X. (2010). A new rhamphorhynchid pterosaur from the Upper Jurassic of Xinjiang, China, and the phylogenetic relationships of basal pterosaurs. *J. Vertebr. Paleontol.*, 30, 163–187.
- Andres, B., Clark, J.M., & Xu, X. (2014). The earliest pterodactyloid and the origin of the group. *Current Biology* 24, 1011-1016.
- Andres, B., & Ji, Q. (2008). A new pterosaur from the Liaoning Province of China, the phylogeny of the Pterodactyloidea, and convergence in their cervical vertebrae. *Palaeontology* 51, 453–470.
- Barrett, P.M., Butler, R.J., Edwards, N.P., & Milner, A.R. (2008). Pterosaur distribution in time and space: an atlas. *Zitteliana*, 28, 61-108.
- Bennett S.C. (2007). A review of the pterosaur *Ctenochasma*: taxonomy and ontogeny. *Neues Jahrbuch für Geologie und Paläontologie—Abhandlungen*, 245(1), 23-31.
- Bennett, S.C. (2021). Complete large skull of the pterodactyloid pterosaur *Ctenochasma elegans* from the Late Jurassic Solnhofen Lithographic Limestones. *Neues Jahrbuch für Geologie und Paläontologie—Abhandlungen*, 301(3), 283–294.
<https://doi.org/10.1127/njgpa/2021/1011>
- Bestwick, J., Unwin, D.M., Butler, R.J., Henderson, D.M., & Purnell, M.A. (2018). Pterosaur dietary hypotheses: a review of ideas and approaches. *Biological Reviews*, 93, 2021-2048.
- Britt, B.B., Dalla Vecchia, F.M., Chure, D.J., Engelmann, G.F., Whiting, M.F., & Scheetz, R.D. (2018). *Caelestiventus hanseni* gen. et sp. nov. extends the desert-dwelling pterosaur record back 65 million years. *Nat Ecol Evol*, 2, 1386–1392.
<https://doi.org/10.1038/s41559-018-0627-y>
- Brusatte, S.L., Nesbitt, S.J., Irmis, R.B., Butler, R.J., Benton, M.J., & Norell, M.A. (2010). The origin and early radiation of dinosaurs. *Earth-Science Reviews*, 101(1–2), 68-100.
- Buffetaut, E. (1995). *The importance of “Lagerstätten” for our understanding of the evolutionary history of certain groups of organisms: the case of pterosaurs*. II International symposium on lithographic limestones (Lleida-Cuenca, Spain, 9–16 July 1995), Extended abstracts, pp. 49–52. Ediciones de la Universidad Autónoma de Madrid, Madrid.
- Butler, R.J., Barrett, P.M., Nowbath, S. & Upchurch, P. (2009). Estimating the effects of sampling biases on pterosaur diversity patterns: implications for hypotheses of

- bird/pterosaur competitive replacement. *Paleobiology*, 35, 432–446.
- Butler, R.J., Benson, R.B.J., Carrano, M.T., Mannion, P.D., & Upchurch, P. (2011). Sea-level, dinosaur diversity, and sampling biases: investigating the ‘common cause’ hypothesis in the terrestrial realm. *Proc. R. Soc. Lond. B*, 278, 1165–1170.
- Butler, R.J., Brusatte, S.L., Andres, B., & Benson, R.B. (2012). How do geological sampling biases affect studies of morphological evolution in deep time? A case study of pterosaur (Reptilia: Archosauria) disparity. *Evolution*, 66, 147–162.
- Butler, R.J., Benson, R.B.J., & Barrett, P.M. (2013). Pterosaur diversity: Untangling the influence of sampling biases, Lagerstätten, and genuine biodiversity signals. *Palaeogeography, Palaeoclimatology, Palaeoecology*, 372, 78–87.
- Casamiquela, R.M. (1975). *Herbstosaurus pigmaeus* (Coeluria, Compsognathidae) n. gen. n. sp. del Jurásico medio del Neuquén (Patagonia septentrional). Uno de los más pequeños dinosaurios conocidos. *Acta primero Congreso Argentino Paleontología et Bioestratigrafía*, 2, 87–102.
- Cheng, X., Jiang, S., Wang, X., & Kellner, A.W.A. (2016). New information on the Wukongopteridae (Pterosauria) revealed by a new specimen from the Jurassic of China. *PeerJ*, 4, e2177.
- Cheng, X., Jiang, S., Wang, X., & Kellner, A.W.A. (2017). New anatomical information of the wukongopterid *Kunpengopterus sinensis* Wang et al., 2010 based on a new specimen. *PeerJ*, 5, e4102.
- Codorniú, L., Carabajal, A.P., Pol, D., Unwin, D., & Rauhut, O.W.M. (2016). A Jurassic pterosaur from Patagonia and the origin of the pterodactyloid neurocranium. *PeerJ*, 4, e2311.
- Codorniú, L., & Gasparini, Z. (2007). Pterosauria. In Gasparini, Z., Salgado, L., and Coria, R.A. (Eds.). *Patagonian Mesozoic Reptiles* (pp.143–166). Bloomington, Indiana: Indiana University Press.
- Codorniú, L., & Gasparini, Z. (2013). The Late Jurassic pterosaurs from northern Patagonia, Argentina. *Earth and Environmental Science Transactions of the Royal Society of Edinburgh*, 103, 1–10.
- Costa, F.R. & Kellner, A.W.A. (2009). On two pterosaur humeri from the Tendaguru beds (upper Jurassic, Tanzania). *An. Acad. Bras. Ciências*, 81, 813–818.
- Costa, F.R., Sayão, J.M., & Kellner, A.W.A. (2015). New pterosaur material from the upper Jurassic of Tendaguru (Tanzania), Africa. *Hist. Biol.*, 27, 646–655.
- Dalla Vecchia, F.M. (2013). Triassic pterosaurs. *Geological Society, London, Special*

Publications, 379, 119–155.

- Dalla Vecchia F.M. (2019). *Seazzadactylus venieri* gen. et sp. nov., a new pterosaur (Diapsida: Pterosauria) from the Upper Triassic (Norian) of northeastern Italy. *PeerJ*, 7, e7363.
- Dean, C.D., Mannion, P.D., & Butler, R.J. (2016). Preservational bias controls the fossil record of pterosaurs. *Palaeontology*, 59, 225-247.
- Dyke, G. J., McGowan, A. J., Nudds, R. L. & Smith, D. (2009). The shape of pterosaur evolution: evidence from the fossil record. *Journal of Evolutionary Biology*, 22, 890–898.
- Ezcurra, M.D., Nesbitt, S.J., Bronzati, M., Vecchia, F.M.D., Agnolin, F.L., Benson, R.B.J., Egli, F.B., Cabreira, S.F., Evers, S.W., Gentil, A.R., Irmis, R.B., Martinelli, A.G., Novas, F.E., da Silva, L.R., Smith, N.D., Stocker, M.R., Turner, A.H., & Langer, M.C. (2020). Enigmatic dinosaur precursors bridge the gap to the origin of Pterosauria. *Nature*, 588, 445-449.
- Foth, C., Brusatte, S.L., Butler, R.J. (2012). Do different disparity proxies converge on a common signal? Insights from the cranial morphometrics and evolutionary history of Pterosauria (Diapsida: Archosauria). *Journal of Evolutionary Biology*, 25, 904-915.
- Frey, E., Meyer, C.A. & Tischlinger, H. (2011). The oldest azhdarchoid pterosaur from the Late Jurassic Solnhofen Limestone (Early Tithonian) of Southern Germany. *Swiss J. Geosci.*, 104(Suppl 1), 35–55.
- Hammer, W.R., & Hickerson, W.J. (1999). Gondwana dinosaurs from the Jurassic of Antarctica. *National Science Museum monographs*, 15, 211-217.
- Jain, S.L. (1974). Jurassic pterosaur from India. *Journal of the Geological Society of India*, 15, 330–335.
- Ji, S.A. & Ji, Q. (1998). A new pterosaur (Rhamphorhynchoidea) from Liaoning. *Jiangsu Geology*, 22, 199–206.
- Ji, S.A., Ji, Q., & Padian, K. (1999). Biostratigraphy of new pterosaurs from China. *Nature*, 398, 573–574.
- Kellner, A.W. (2003). Pterosaur phylogeny and comments on the evolutionary history of the group. In: Buffetaut E, Mazin J-M, eds. *Evolution and palaeobiology of pterosaurs*, Geological Society, London, special publications, vol. 217. London: Geological Society, 105–137.
- Kellner, A.W.A., Rodrigues, T. & Sayão, H.M. (2015). Proceedings of the Rio International Symposium on Pterosaurs. *Historical Biology*, 27.

- Longrich, N.R., Martill, D.M., & Andres, B. (2018). Late Maastrichtian pterosaurs from North Africa and mass extinction of Pterosauria at the Cretaceous-Paleogene boundary. *PLoS Biol.*, *16*, e2001663.
- Lü J., Unwin D.M., Jin X., Liu, Y., & Ji, Q. (2010). Evidence for modular evolution in a long-tailed pterosaur with a pterodactyloid skull. *Proc. R. Soc. B*, *277*, 383–389. doi:10.1098/rspb.2009.1603
- Lü, J.C., Xu, L., Chang, H., & Zhang, X. (2011). A new darwinopterid pterosaur from the Middle Jurassic of western Liaoning, northeastern China and its ecological implications. *Acta Geologica Sinica-English Edition*, *85*, 507–514.
- Lü, J.C., Ji, Q., Wei, X.F., & Liu, Y.Q. (2012). A new ctenochasmatoid pterosaur from the Early Cretaceous Yixian Formation of western Liaoning, China. *Cretaceous Research*, *34*, 26–30.
- Martill, D.M. & Etches, S. (2013). A new monofenestratan pterosaur from the Kimmeridge Clay Formation (Kimmeridgian, Upper Jurassic) of Dorset, England. *Acta Palaeontologica Polonica*, *58*, 285–294.
- Martin-Silverstone, E.M., Unwin, D.M., Cuff, A.R., Brown, E.E., Allington-Jones, L., & Barrett P.M. (2024). A new pterosaur from the Middle Jurassic of Skye, Scotland and the early diversification of flying reptiles. *Journal of Vertebrate Paleontology*, e2298741.
- Martínez, R.N., Apaldetti, C., Correa, G., Colombi, C.E., Fernández, E., Malnis, P.S., Praderio, A., Abelín, D., Benegas, L.G., Aguilar-Cameo, A., & Alcober, O.A. (2015). A New Late Triassic Vertebrate Assemblage from Northwestern Argentina. *Ameghiniana*, *52*(4), 379-390.
- Moser, M., & Rauhut, O.W.M. (2011). Der Reusengebiss-Flugsaurier Ctenochasma. *Fossilien, Sonderheft*, 47-48.
- Müller, R.T. (2022). The closest evolutionary relatives of pterosaurs: What the morphospace occupation of different skeletal regions tell us about lagerpetids. *The Anatomical Record*, *305*(12), 3456–3462.
- O’Sullivan, M., & Martill, D.M. (2015). Evidence for the presence of *Rhamphorhynchus* (Pterosauria: Rhamphorhynchinae) in the Kimmeridge Clay of the UK. *Proceedings of the Geologist’s Association*, *126*, 390–401.
- Padian K. (2008). The Early Jurassic pterosaur *Dorygnathus banthensis* (Theodori, 1830). *Special Papers in Palaeontology*, *80*, 1-107.
- Paul, G.S. (2022). *The Princeton field guide to pterosaurs*. Princeton: Princeton University Press.

- Pêgas, R.V., Costa, F.R., Kellner, & A.W.A. (2018). New information on the osteology and a taxonomic revision of the genus *Thalassodromeus* (Pterodactyloidea, Tapejaridae, Thalassodrominae). *J Vertebr Paleontol.* 38(2), e1443273.
- Perea, D., Soto, M., Toriño, P., Mesa, V., & Maisey, J.G. (2018). A Late Jurassic-?earliest Cretaceous ctenochasmatid (Pterosauria, Pterodactyloidea): The first report of pterosaurs from Uruguay. *Journal of South American Earth Sciences*, 85, 298-306.
- Plieninger, F. (1901). Beiträge zur Kenntnis der Flugsaurier. *Palaeontographica*, 48, 65-90.
- Prentice, K.C., Ruta, M., & Benton, M.J. (2011). Evolution of morphological disparity in pterosaurs. *Journal of Systematic Palaeontology*, 9(3), 337–353.
- Rauhut, O.W.M. (2012). Ein „Rhamphodactylus“ aus der Mörsheim-Formation von Mühlheim. *Freunde der Bayerischen Staatssammlung für Paläontologie und Historische Geologie e.V., Jahresbericht und Mitteilungen*, 40, 69-74.
- Rauhut, O.W.M., Heyng, A.M., & Leonhardt, U. (2011). Neue Reptilfunde aus der Mörsheim-Formation von Mühlheim. *Freunde der Bayerischen Staatssammlung für Paläontologie und Historische Geologie e.V., Jahresbericht und Mitteilungen*, 39, 61-71.
- Rauhut, O.W.M. & López-Arbarello, A. (2008). Archosaur evolution during the Jurassic: a southern perspective. *Revista de la Asociación Geológica Argentina*, 63(4), 557-585.
- Reck, H. (1931). Die deutschostafrikanischen flugsaurier. *Cent. Für Mineral. Geol. Und Paläontologie*, 7, 321–336.
- Soto, M., Montenegro, F., Toriño, P., Mesa, V. & Perea, D. (2021). A new ctenochasmatid (Pterosauria, Pterodactyloidea) from the late Jurassic of Uruguay. *Journal of South American Earth Sciences*, 11, 1-11.
- Tischlinger, H., & Frey, E. (2013). A new pterosaur with mosaic characters of basal and pterodactyloid pterosauria from the Upper Kimmeridgian of Painten (Upper Palatinate, Germany). *Archaeopteryx*, 31, 1-13.
- Unwin, D.M. (2003). On the phylogeny and evolutionary history of pterosaurs. *Geological Society, London, Special Publications*, 217(1), 139–90.
- Unwin, D.M. (2005). *The Pterosaurs from Deep Time*. Pi Press, New York.
- Unwin, D.M. & Heinrich, W.D. (1999). On a pterosaur jaw from the upper Jurassic of Tendaguru (Tanzania). *Foss. Rec.*, 2, 121–134.
- Unwin, D.M., Rauhut, O.W.M., & Haluza, A. (2004). The first “rhamphorhynchoid” from South America and the early history of pterosaurs. In: J. Reitner, M. Reich and G. Schmidt (Editors), *Geobiologie. 74. Jahrestagung der Paläontologischen Gesellschaft*,

- Göttingen, 02. bis 08. Oktober 2004. Kurzfassungen der Vorträge und Poster. Universitätsdrucke Göttingen, Göttingen, pp. 235-237.
- Upchurch, P., Andres, B., Butler, R. J., & Barrett, P. M. (2015). An analysis of pterosaurian biogeography: implications for the evolutionary history and fossil record quality of the first flying vertebrates. *Historical Biology*, 27(6), 697–717.
- Vidovic, S.U. & Martill, D.M. (2017). The taxonomy and phylogeny of *Diopecephalus kochi* (Wagner, 1837) and '*Germanodactylus rhamphastinus*' (Wagner, 1851). In: Hone, D.W.E., Witton, M.P. & Martill, D.M. (eds) *New Perspectives on Pterosaur Palaeobiology*. Geological Society, London, Special Publications, 455.
- Wang, X., Kellner, A.W.A., Zhou, Z., & Campos, D.A. (2005). Pterosaur diversity and faunal turnover in Cretaceous terrestrial ecosystems in China. *Nature*, 437, 875–879.
- Wang, X., Kellner, A.W.A., Jiang, S.X., Cheng, X., & Meng, X. (2009). An unusual long-tailed pterosaur with elongated neck from western Liaoning of China. *Anais da Academia Brasileira de Ciências* 81(4). 793–812
- Wang, X.L., Kellner, A.W.A., Jiang, S.X., Cheng, X., Meng, X., & Rodrigues, T. (2010). New longtailed pterosaurs (Wukongopteridae) from western Liaoning, China. *Anais da Academia Brasileira de Ciências*, 82, 10451062.
- Wang, X., Jiang, S., Zhang, J., Cheng, X., Yu, X., Li, Y., Wei, G., & Wang, X. (2017). New evidence from China for the nature of the pterosaur evolutionary transition. *Sci. Rep.*, 7, 42763.
- Wellnhofer, P. (1970). Die Pterodactyloidea (Pterosauria) der Oberjura-Plattenkalke Süddeutschlands. *Abhandlungen der Mathematisch-Physikalischen Klasse der Königlich Bayerischen Akademie der Wissenschaften*, 141, 1–133.
- Wellnhofer, P. (1978). Pterosauria. In: P Wellnhofer (Ed.), *Handbuch der Paläoherpetologie, Encyclopedia of Paleoherpétology*, 19 (pp. 1-82), Fischer-Verlag.
- Wellnhofer, P. (1991). *The illustrated encyclopedia of pterosaurs*. Salamander Books, London.
- Witton MP. (2013). *Pterosaurs: natural history, evolution, anatomy*. Princeton University Press.
- Zhou, C.F., Gao, K.Q., Yi, H., Xue, J., Li, Q., & Fox, R.C. (2017). Earliest filter-feeding pterosaur from the Jurassic of China and ecological evolution of Pterodactyloidea. *Royal Society Open Science*, 4, 160672.

Chapter 2. The oldest monofenestratan pterosaur from the Queso Rallado locality (Cañadón Asfalto Formation, Toarcian) of Chubut province, Patagonia, Argentina

Keywords: *Pterosauria, Monofenestrata, Jurassic, Toarcian, Patagonia, Argentina*

The chapter was submitted as: Fernandes, A.E., Pol, D. & Rauhut, O.W.M. A new monofenestratan pterosaur from the Queso Rallado locality of the Chubut province of Patagonia, Argentina. (submitted July 22, 2024 to Royal Society Open Science).

Author contributions:

- Alexandra E. Fernandes: Conceptualization, Data curation, Formal analysis, Investigation, Methodology, Software, Visualization, Writing-original draft, Writing-review & editing
- Diego Pol: Funding acquisition, Methodology, Resources, Software, Supervision, Validation
- Oliver W. M. Rauhut: Conceptualization, Formal analysis, Funding acquisition, Investigation, Methodology, Project administration, Resources, Software, Supervision, Validation, Visualization, Writing-review & editing

The oldest monofenestratan pterosaur from the Queso Rallado locality (Cañadón Asfalto Formation, Toarcian) of Chubut province, Patagonia, Argentina

Fernandes, Alexandra E. ^{1,2*}, Pol, Diego³, & Rauhut, Oliver W.M. ^{1,2,4}

¹SNSB, Bayerische Staatssammlung für Paläontologie und Geologie, Richard-Wagner-Straße 10, 80333 München, Germany

²Department of Earth and Environmental Sciences, Ludwig-Maximilians-University, Theresienstraße 41, 80333 München, Germany

³ CONICET, Museo Argentino de Ciencias Naturales "Bernardino Rivadavia", Av. Patricias Argentinas 480, C1405 Cdad. Autónoma de Buenos Aires, Argentina

⁴ GeoBioCenter, Ludwig-Maximilians Universität, Richard-Wagner-Str. 10, 80333, Munich, Germany

*Corresponding author: Alexandra E. Fernandes fernandes@snsb.de

Abstract

As the first group of tetrapods to achieve powered flight, pterosaurs first appeared in the Late Triassic. They proliferated globally, and by the Late Jurassic through the Cretaceous the majority of these taxa belonged to the clade Monofenestrata (which includes the well-known Pterodactyloidea as its major subclade), typified by their single undivided opening anterior to the orbit. Here, a new taxon *Melkamter pateko* gen. et sp. nov., represented by the specimen MPEF-PV 11530 (comprised of a partial skull and associated postcranial elements), is reported from the latest Early Jurassic (Toarcian) locality of Queso Rallado (Cañadón Asfalto Formation) and referred to the Monofenestrata, increasing our previously-known representation and temporal range for this clade. This occurrence marks the oldest record of the Monofenestrata globally and helps to shed critical light on the evolutionary processes undergone during the “rhamphorynchoid”-to-pterodactyloid transition within the Pterosauria. In addition, another single isolated tooth from the same locality shows ctenochasmatid affinities. These finds further elucidate the still-poor Gondwanan Jurassic pterosaur fossil record, underscoring that most of our current ideas about the timing and modes of pterosaur evolution during that period are largely based on (and perhaps biased by) the pterosaur fossil record of the Northern Hemisphere.

Keywords: *Pterosauria*, *Monofenestrata*, *Jurassic*, *Toarcian*, *Patagonia*, *Argentina*,

Introduction

Pterosaurs were the first clade of actively flying tetrapods, and were highly successful during the Mesozoic, achieving a global distribution from the Triassic to the Cretaceous. Over that time, the pterosaur bauplan transitioned from the basal nonmonofenestratan “rhamphorhynchoid” body style to that of the more derived pterodactyloids (Lü et al, 2009; Witton, 2013; Andres et al., 2014). This evolutionary event has become better understood in recent years, with the recognition of the Darwinoptera, which have been largely considered as “intermediate” monofenestratans that show a morphological array of attributes during this transition, combining plesiomorphic characters of “rhamphorhynchoids” with pterodactyloid features (Lü et al., 2010; Wang et al., 2017; Martin-Silverstone et al., 2024). Rather than exhibit intermediate character states, transitional pterosaurs often seemingly cherry-picked traits, exhibiting both ancestral and derived states simultaneously, which typifies mosaic evolution (Lü et al. 2010). Within Monofenestrata (the clade comprised by the Darwinoptera and the Pterodactyloidea), members of the Wukongopteridae (Darwinoptera to the exclusion of *Pterorhynchus*) exhibit characters from both basal non-pterodactyloids and derived pterodactyloids: a confluence of the nares and antorbital fenestra, a backwardly-inclined quadrate, a glenoid located on the scapula, reduced cervical ribs, and a wing metacarpal about half the length of the first wing phalanx, while still retaining an elongated tail enclosed by rod-like bony extensions made by the zygapophyses. Pterodactyloids then went on to adapt even more dramatically elongated crania and cervical vertebrae, a further reduction or loss of cervical ribs, elongation of the metacarpus, reduced tails, and a highly reduced or absent fifth toe. However, sound examples of these intermediate fossil forms are rare, particularly on the global scale, and therefore it has made challenging the process of identifying the mechanisms that underpin these transitions (Lü et al. 2010; Wang et al., 2017). Although these changes are presumed to have had their evolutionary origins during the early-middle Jurassic time period, the evolutionary pathway towards pterodactyloids is still largely unknown. Poor availability of geochronologic exposures from this time period, inadequate field sampling, and low bone preservation

rates all hinder the understanding of this critical phase in which body plans changed so drastically.

The Mesozoic pterosaur record is abundant in the Northern Hemisphere, whereas the record in the Southern Hemisphere is comparatively more scarce (Barrett et al., 2008; Codorníu & Gianechini, 2016; Pentland & Poropat, 2023). With the possible exclusion of the Argentinian *Allkaruen koi* Codorníu et al. 2016, non-pterodactyloid monofenestratan pterosaurs have thus far only been recovered from the Northern Hemisphere, namely the United Kingdom (O'Sullivan & Martill, 2018; Martin-Silverstone et al. 2024), Germany (Rauhut, 2012; Tischlinger & Frey, 2013), and China (e.g. Lü et al., 2010; Wang et al., 2017; Zhou et al., 2021), where they first appeared during the Bathonian (O'Sullivan & Martill, 2018; Martin-Silverstone et al., 2024). The apparent success of these monofenestratan forms and their pterodactyloid descendants went on to supplant the rhamphorhynchids (which disappeared in the Early Cretaceous [Unwin et al., 2000; Witton, 2013]), surviving through to the end-Cretaceous extinction. However, there is still a dearth of knowledge about non-pterodactyloid monofenestratans, specifically in terrestrial sedimentary settings (Unwin, 1996; Butler et al., 2013; Andres et al., 2014; Witton, 2015; Martin-Silverstone et al., 2024).

Pterosaur records from Gondwana are especially meager for the Jurassic (Rauhut & López-Arbarello, 2008; Pentland & Poropat, 2023), although Argentina itself contains fossil-yielding exposures from the latest Early Jurassic to the Late Cretaceous (Toarcian–Coniacian), a span of over approximately 85 ma (Codorníu & Gasparini, 2013). Specimens have been recovered from at least thirteen different fossil localities overall (Rauhut et al., 2001; Unwin et al., 2004; Codorníu & Gasparini, 2007; Rauhut & López-Arbarello, 2008; Codorníu & Gianechini, 2016), but mainly come from two geographical regions: central-western Argentina (San Juan and San Luis provinces) and Patagonia (Codorníu & Gianechini, 2016). Most of the Jurassic records come from the highest parts of the Jurassic, with the exception of the latest Early Jurassic Cañadón Asfalto Formation (Pol et al., 2020). This unit, which is exposed in the province of Chubut, comprises the bonebed containing *Allkaruen koi*, a Breviquartossan, which is based on exceptional three-dimensionally preserved cranial and postcranial material (Codorníu et al. 2010; Codorníu et al. 2016). Otherwise, only three other pterosaur taxa have been described from the Jurassic of South America thus far:

Herbstosaurus pigmaeus Casamiquela, 1975, and *Wenupteryx uzi* Codorniu and Gasparini, 2013, from the Tithonian Vaca Muerta Formation of Neuquen, Argentina, and *Tucuadactylus luciae* Soto et al., 2021, from the latest Jurassic Tacuarembó Formation of Uruguay.

Here a new pterosaur fossil species is presented, based on associated remains of preserved cranial and postcranial material from the locality of Queso Rallado, also within the Cañadón Asfalto Formation of the Chubut Province. The specimen includes a partial skull (including the premaxilla-maxilla-jugal-lacrima-postorbital-squamosal-quadratojugal-quadrato complex) and a few postcranial remains, representing a new taxon that shows clear monofenestratan affinities.

Geological and Palaeontological Setting

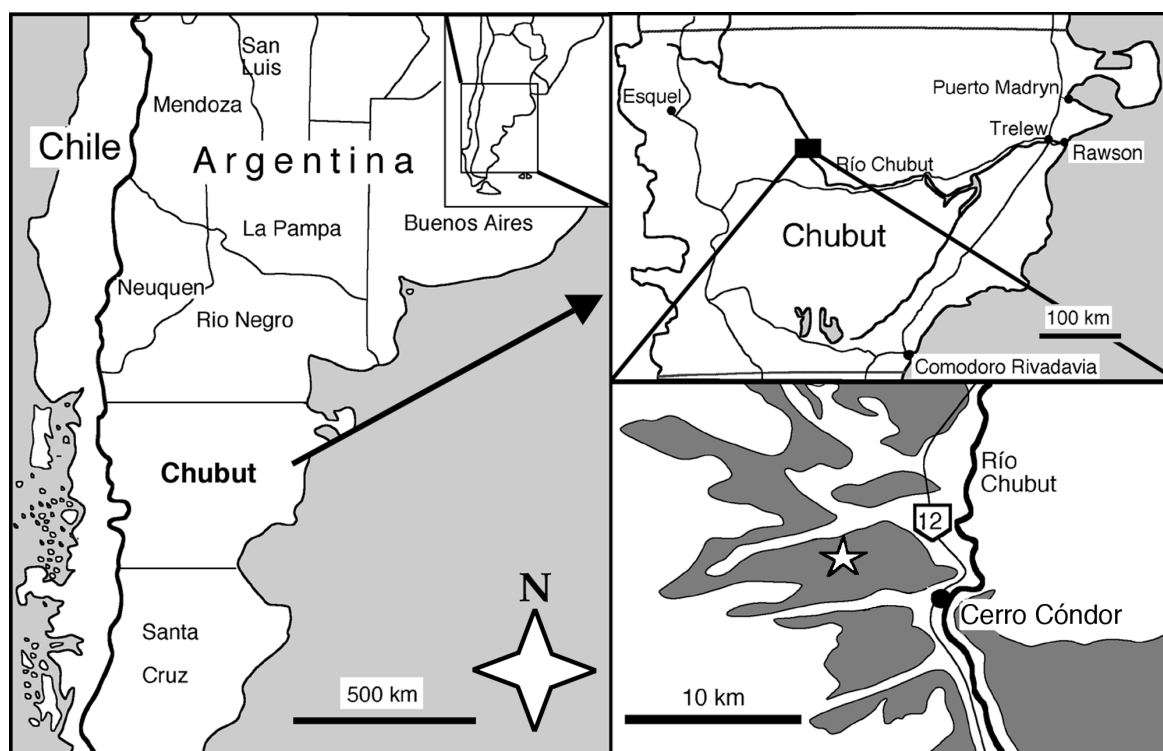


Figure 1. Map of the Queso Rallado locality (marked with a star) within the Chubut province of Argentina, with the Cañadón Asfalto Formation shaded in dark grey (modified from Rauhut, 2007).

The Cañadón Asfalto Formation crops out in the northern central part of Chubut Province, Argentina. It is part of the sedimentary infill of the Cañadón Asfalto Basin, a large semigraben structure on central Patagonia that opened with the beginning of the South

Atlantic in the Early Jurassic (Figari et al., 2015). It belongs to the megasequence 1 of this infill, which represents the synrift phase of the basin, and conformably overlies the mainly volcanic Lonco Trapial Formation. The Cañadón Asfalto Formation is mainly composed of lacustrine shales, biogenic limestones and mudstones, with intercalated basaltic flows and pyroclastic deposits in the base, and fanglomerates and conglomerates in some sections (Stipanovic et al., 1968; Figari & Courtade, 1993; Figari et al., 2015). The age of the formation has long been debated. Originally considered to be of Callovian-Oxfordian age (e.g. Bonaparte, 1978), new biostratigraphic and radiometric dates have recently indicated an uppermost Early (Toarcian) to early Middle Jurassic (Aalenian-Bajocian) age for this unit (Salani, 2008; Cúneo et al., 2013; Olivera et al., 2015). Even more recent radiometric dates, however, indicate that most (if not all) of the formation may be Toarcian in age (Pol et al., 2020; Fantasia et al., 2021).

The Queso Rallado locality is located approximately 5.5 km northwest of the village of Cerro Cóndor (Fig. 1) in the area of the mid-course of the Río Chubut. The fossiliferous level is a 0.80 m thick carbonatic and partially silicified mudstone within the lower part of the section of the Cañadón Asfalto Formation. The exact stratigraphic correlation of the outcrops at Queso Rallado awaits publication, but a Toarcian age is considered to be the age of the fossiliferous level (Cúneo et al., 2013). The fossiliferous strata at Queso Rallado have yielded a rich microvertebrate fauna of both aquatic and terrestrial animals. The fauna includes so far undescribed fishes, amphibians, crocodiles, pterosaurs, and theropod teeth, as well as the turtle *Condorchelys antiqua* Sterli, 2008, the rhynchocephalian *Sphenocondor gracilis* Apesteguía, Gómez & Rougier, 2012, the heterodontosaurid ornithischian *Manidens condorensis* Pol, Rauhut & Becerra, 2011, teeth of sauropod dinosaurs (Becerra et al., 2016; Carballido et al., 2017), and the mammaliaforms *Asfaltomylos patagonicus* Rauhut et al., 2003, *Condorodon spanios* Gaetano & Rougier, 2012, *Henosferus molus* Rougier et al., 2007, and *Argentoconodon fariarorum* Gaetano & Rougier, 2011. Other outcrops of the Cañadón Asfalto Formation have yielded the anuran *Nothobatrachus reigi* Báez & Nicoli, 2008, the sauropod dinosaurs *Volkheimeria chubutensis* Bonaparte, 1978, *Patagosaurus fariasi* Bonaparte, 1978, and *Bagualia alba* Pol et al., 2020, the theropod dinosaurs *Piatnitzkysaurus floresii* Bonaparte, 1978, *Condorraptor currumili* Rauhut, 2005,

Eoabelisaurus mefi Pol & Rauhut, 2012, and *Asfaltovenator vialidadi* Rauhut & Pol, 2019, as well as the pterosaur *Allkaruen koi* Codorniu et al., 2016.

Materials and Methods

The main specimen described herein comes from the microvertebrate locality of Queso Rallado (Rauhut et al., 2002). It was found by mechanically breaking blocks that were recovered from the fossiliferous layer, during which the partial skull was split. Subsequently, the specimen was mechanically prepared, revealing additional bones originally still covered in matrix. Although the bones were not found in articulation, they were found in close association, and consist of a partial skull, four dorsal vertebrae, one long bone, and two associated teeth. In addition, an isolated ctenochasmatid(?) tooth was recovered the same locality (but from an unknown horizon), which is also reported upon. The specimens are housed at the Museo Paleontológico “Egidio Feruglio” (MPEF) in Trelew (Province of Chubut), Argentina under the collection numbers MPEF-PV 11530 a-c and MPEF-PV 2549[2012].

CT scans were performed at the 3D Imaging Lab of the University of Tübingen, using a Nikon XT H 320 with a tungsten reflection target with maximum voltage of 225 kV. This resulted in a stack of 2714 projections (voxel size= 0.113606). The data derived from the CT-scan was segmented manually (Image Segmentation) with the software Avizo v9.2 (Thermo Fisher Scientific, MA, USA), using the brush function and interpolation, and rendered using the open-source software Blender. All CT files are available on <https://www.morphosource.org/projects/000495959>.

Phylogenetic analysis was conducted in TNT version 1.6 (Goloboff, Farris & Nixon 2008; Goloboff & Morales 2023) using two matrices: the matrix of Fernandes et al. (2023), which is in turn based on the matrix of Andres (2021), and the matrix of Martin-Silverstone et al. (2024). In both matrices, we added the new taxon, checked the codings for *Allkaruen koi* (*Dimorphodon koi* in the matrix of Andres, 2021; we changed the name back to *Allkaruen* in our matrix), based on own observations, and added an additional character, the presence or absence of an ascending process of the maxilla. Thus, the final matrix based on Fernandes et al. (2023) had 181 terminal taxa scored for 276 characters (51 continuous and 225

discrete; ordered and unordered), and the one modified from Martin-Silverstone et al. (2024) had 70 terminal taxa scored for 136 characters (ordered and unordered). The data matrices are available in the supplementary material, and also at <http://morphobank.org/permalink/?P4589>. Both matrices were analyzed under equal and implied weights (with $k=12$; Goloboff et al., 2018) using a traditional search with 2000 replicates, followed by TBR branch swapping on trees in memory. Reduced consensus methods were used to improve the resolution of the final results, using the `pcrprune` command (Pol & Escapa, 2009).

Nomenclatural Acts

The electronic edition of this article conforms to the requirements of the amended International Code of Zoological Nomenclature, and hence the new names contained herein are available under that Code from the electronic edition of this article. This published work and the nomenclatural acts it contains have been registered in ZooBank, the online registration system for the ICZN. The electronic edition of this work was published in a journal with an ISSN and has been archived and is available from the following digital repositories: PubMed Central and LOCKSS.

RESULTS

Systematic Paleontology

PTEROSAURIA Owen, 1842

MONOFENESTRATA Lü et al, 2010 sensu Andres et al. 2014

Genus ***Melkamter***, gen. nov.

Type Species ***Melkamter pateko***, sp. nov.

Etymology: Genus name "Melkamter" from the native Tehuelche word "mel" meaning (in Spanish/English) "ala/wing" and "kamter" meaning "lagarto grande/big lizard" (after the original translation of "pterosaur" as "winged lizard"); the species epithet "pateko" is derived from "pate" meaning "rallado/rasped" and "ko" meaning "conjunto de huesos/set

of bones”, an ode both to the site of Queso Rallado, and the fractured preservational state of the fossil (translations from Fernández Garay, 2004)

Holotype: MPEF-PV 11530 (Museo Paleontológico Egidio Feruglio, Trelew, Argentina), consisting of at least a partial skull (with counterslab) and two associated teeth, four dorsal vertebrae, one metacarpal (either I-III), and other bone fragments.

Type locality and Horizon: Locality Queso Rallado, close to Cerro Cóndor, northern central Chubut Province, Argentina. Lower section of the Cañadón Asfalto Formation, latest Early Jurassic, Toarcian (Cúneo et al., 2013; Pol et al., 2020).

Diagnosis: Non-pterodactyloid monofenestratan with a confluent naris and anteorbital fenestra and quadrate inclined at about 120° . Autapomorphies include: the presence of a vestigial ascending process in the maxilla that does not reach the nasal or lacrimal dorsally; a maxillary body anterior to the ascending process that is higher than posterior to it; lacrimal and posterior processes of the jugal offset at about 55° angle. The taxon can furthermore be diagnosed by a combination of characters, including the marked dorsal deflection of the dorsal margin of the skull at the beginning of the nasoantorbital fenestra, resulting in a concave rather than straight outline of the dorsal skull margin in this region in lateral view, the robust ventral process of the postorbital that reaches the mid-length of the ventral margin of the orbit, and the pointed anterior process of the quadratojugal that separates the posterior ends of the jugal and the maxilla.

Description

MPEF-PV 11530 is preserved in a block (Fig. 2A) of a very thin and fine-grained pinkish-white to gray silicified mudstone, typical for the bone-bearing layers of the Queso Rallado locality, with one small partial counterpart of the skull material (Fig. 2B). The elements that are preserved in the primary block include a partial skull with two associated teeth, four dorsal vertebrae, and a metacarpal (either I-III). There are smaller bone shards and even a long bone shaft fragment interspersed throughout the remaining surface and interior (visible with CT scans) of the block, however, they are of indeterminate morphology.

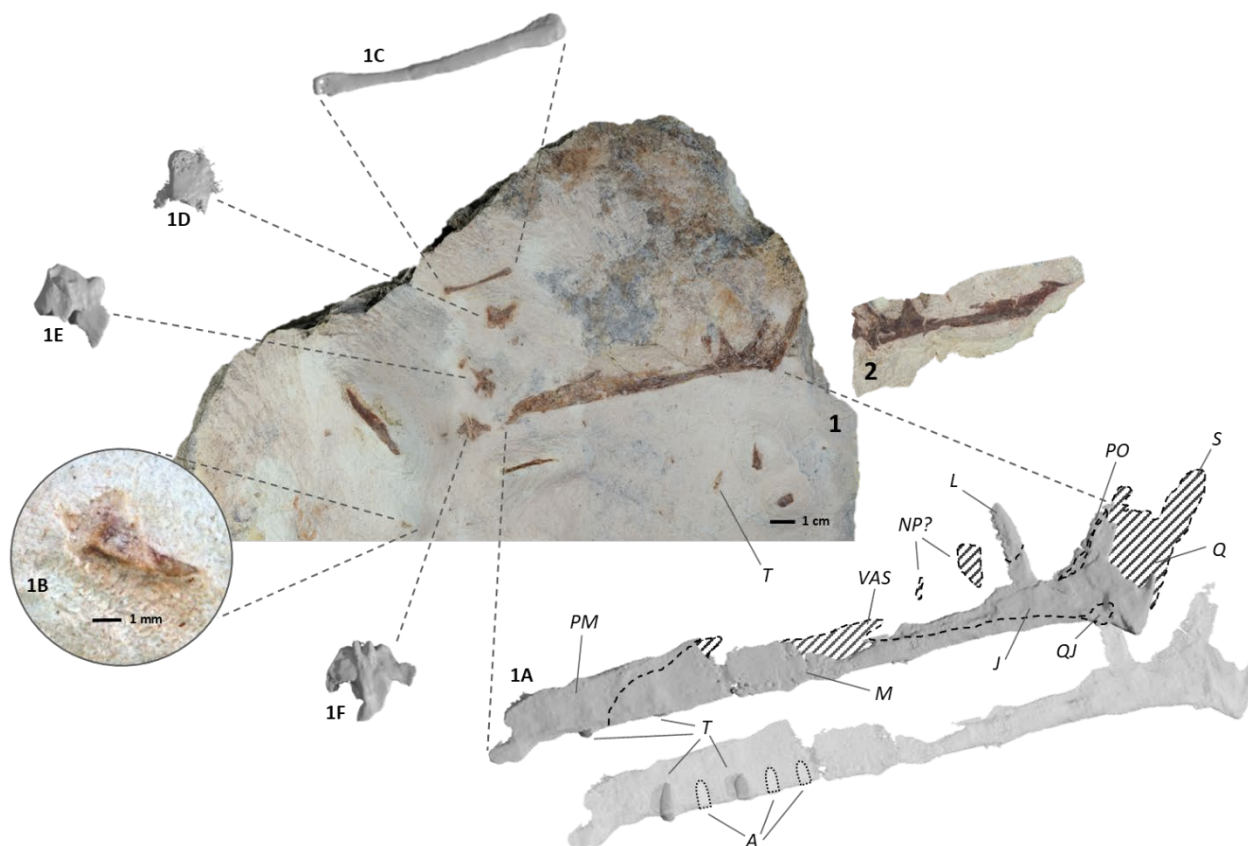


Figure 2. Photographs of MPEF-PV 115302 main block (1) with inset of tooth (1B) and counterslab (2); Rendered CT scan detail images (dashed areas represent visible bone that was too thin to be captured by the CT scan) of skull fragment (1A), manual metacarpal (1C), and dorsal vertebrae (1D-F). *Abbreviations:* A = alveoli; J = jugal; L = lacrimal; M = maxilla; NP = nasal process; P = premaxilla; PO = postorbital; Q = quadrate; QJ = quadratojugal; S = squamosal; T = tooth; VAS = vestigial ascending process.

Skull: The right side of the skull is preserved and has been split between the main slab and the counterslab during the discovery of the specimen, so that the former mainly contains the outer bone layer, with much of the bone substance preserved on the counterslab. The skull is anteroposteriorly complete, but missing the dorsal skull roof. It is laterally crushed (complicating the identification of individual elements), but appears to include the regions of the premaxilla, maxilla, jugal, ventral parts of the lacrimal and postorbital, fragments of the squamosal, partial quadratojugal, and quadrate (Fig. 2 and 3). The skull has an overall length of approx. 131.3 mm from premaxillary tip to the dorsal posterior end of the quadrate, with the rostrum anterior to the anterior margin of the orbit measuring 94.8 mm (therefore comprising about 72% of the skull, whereas the condition in derived

pterodactyls usually occupies more than 80% (Wellnhofer, 1978, 1991; Kellner, 2003; Unwin, 2003a; Andres & Ji, 2008), and a nasoantorbital fenestra (c. 51 mm) occupying about 39% of the anteroposterior skull length. The tip of the snout anterior to the nasoantorbital fenestra is approximately 39 mm long.

Of the main cranial openings, the ventral parts of the nasoantorbital fenestra, the orbit and the infratemporal fenestra are visible. The nares and anteorbital fenestra are visibly confluent to form a nasoantorbital fenestra, with a pointed anterior margin, and a ventral margin that is placed on a more dorsal level in the anterior half (probably corresponding to the original nares) than in the posterior half (probably corresponding to the original antorbital fenestra). The two portions of the ventral margin are separated by a marked step that is slightly undercut from the posterior side, and which we interpret as a vestigial ascending process of the maxilla (see below). However, above this process, the openings are confluent and there is no indication of the ascending process contacting either the nasal or the lacrimal dorsally (cortical bone striations on the process also markedly run solely in the anteroposterior plane).

A platy, triangular bone shard is dorsally placed within the posteriormost part of the nasoantorbital fenestra, with no contact made to any other bone. This might represent the free nasal process that intrudes into the nasoantorbital fenestra in many basal monofenestratans, although the bone seems to be too broad and bulky, and very posteriorly placed if compared with other taxa (e.g., Wellnhofer, 1975; Lü et al., 2010). Alternatively, a small bone shard more anteriorly within the nasoantorbital fenestra in between the triangular fragment and the end of the ascending process of the maxilla could also potentially represent this process. This fragment is thin, almost vertically and very slightly anteroventrally inclined and flexes posteriorly towards its end. In comparison with other monofenestratans, its ventral end would be relatively closer to the ventral margin of the nasoantorbital fenestra, but this might not be unexpected in a very early representative of this clade. However, as there are other bone fragments distributed all over the slab, none of these two shards can be identified as the free nasal process with any certainty.

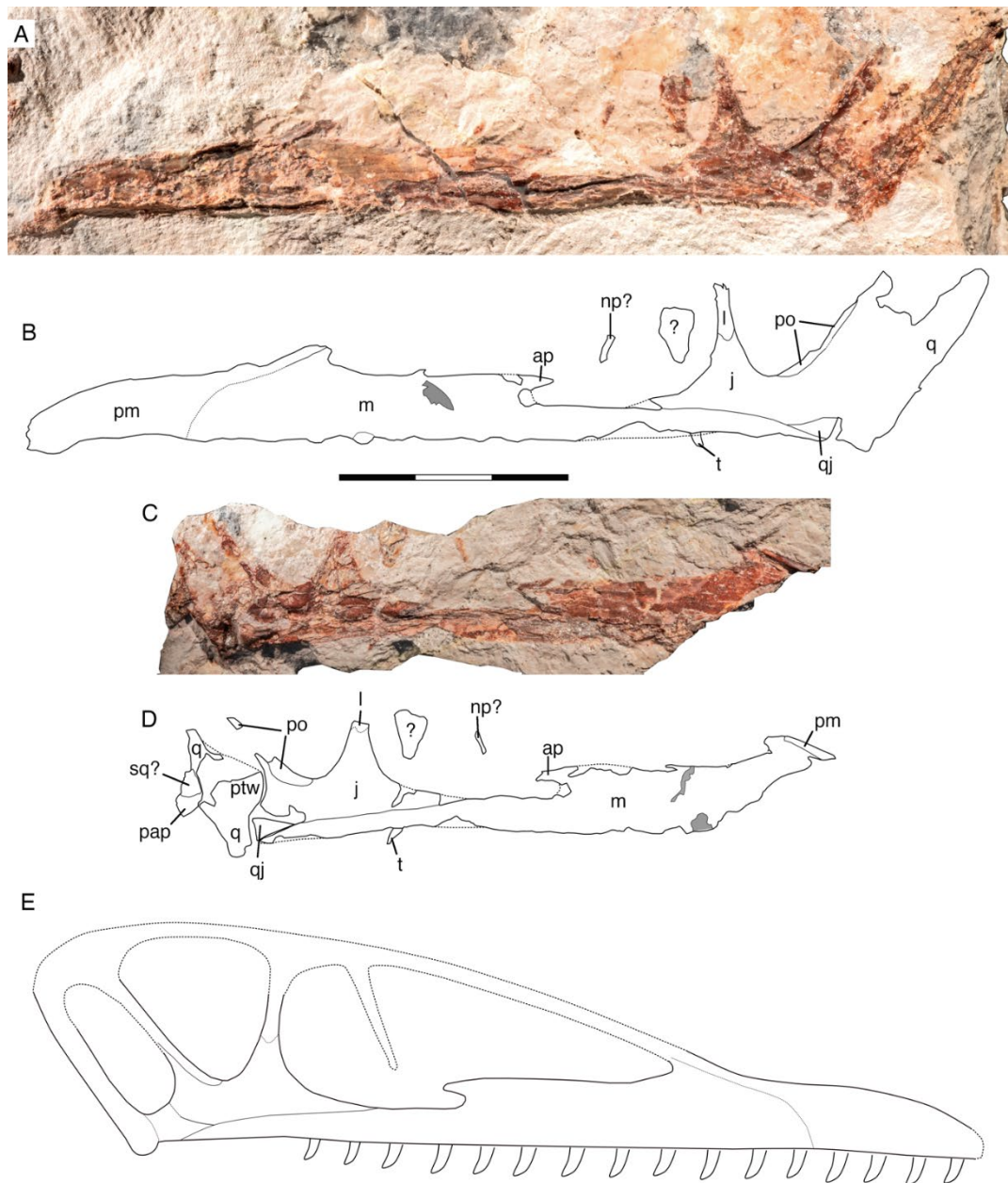


Fig. 3: Holotype skull of *Melkamter pateko* gen. et sp. nov., MPEF PV 11530. (A) photograph of the main slab; (B) interpretative camera lucida drawing of the remains on the main slab; (C) photograph of the counterslab; (D) interpretative camera lucida drawing of the remains on the counterslab; (E) reconstruction of the skull (the size, number and arrangement of the teeth is conjectural). Scale bar is 3 cm. Abbreviations: ap, ascending process of the maxilla; j, jugal; l, lacrimal; m, maxilla; np?, possible fragment of the ventral process of the nasal; pap, paroccipital process; pm, premaxilla; po, postorbital; ptw, pterygoid wing of the quadrate; q, quadrate; qj, quadratojugal; sq?, possible squamosal fragment; t, possible last tooth.

The orbit has straight anterior and posterior borders that diverge throughout the preserved height of the opening, so that its anteroposterior width increases dorsally. The entire shape of the orbit cannot be established, due to the missing dorsal region. However,

what is preserved does appear pyriform, with a rounded and approaching a v-shaped ventral margin. The orbit measures 20.3 mm at the widest preserved anteroposterior point. The jugal-lacrimal strut separating the orbit from the nasoantorbital fenestra is triangular, with a wide ventral base and its long axis almost perpendicular to the alveolar border, as in darwinopterans (e.g., Lü et al., 2010, 2011; Cheng et al., 2017) and basal pterodactyloids (e.g., Wellnhofer, 1975), but unlike the strongly anteriorly inclined strut in many non-monofenestratan pterosaurs, such as *Rhamphorhynchus* and *Scaphognathus* (Wellnhofer, 1975), *Dorygnathus* (Padian, 2008a), *Campylognathoides* (Padian, 2008b), or *Dimorphodon* (Sangster, 2021). The infratemporal fenestra was apparently high, but anteroposteriorly narrow and anteroventrally inclined, so that its ventral end was placed below the orbit, as in many pterosaurs.

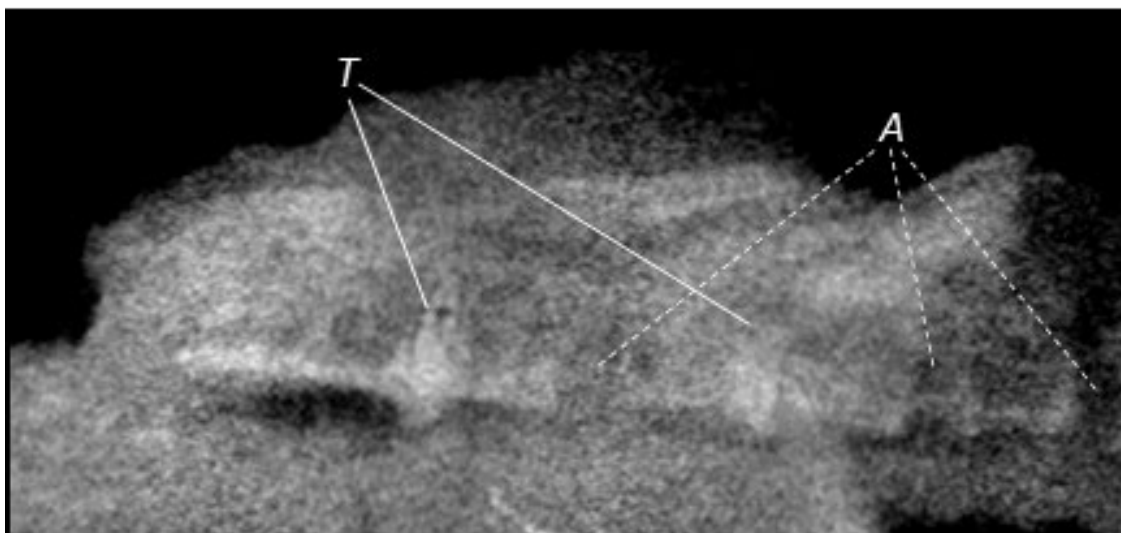


Figure 4. CT scan showing the position of two teeth (T) inside the maxilla, with three additional empty alveolar (A) sockets.

Although the crushed state of the specimen makes it difficult to discern any suturing (also further complicated by the sporadic distribution of cortical bone on either the part or counterpart of the fossil), it appears that the premaxilla is short, and is potentially fused to the maxilla where a slight dorsoventral crack occurs at about 20 mm from the anteriormost tip. A thin posterior dorsal process of the premaxilla seems to extend from here posterodorsally, flanking the dorsal margin of the maxilla and probably forming the dorsal margin of the nasoantorbital fenestra, as in other pterosaurs. There is no sign of a

premaxillary crest, although one could have been more posteriorly placed along the dorsal margin of the skull than is preserved on the specimen.

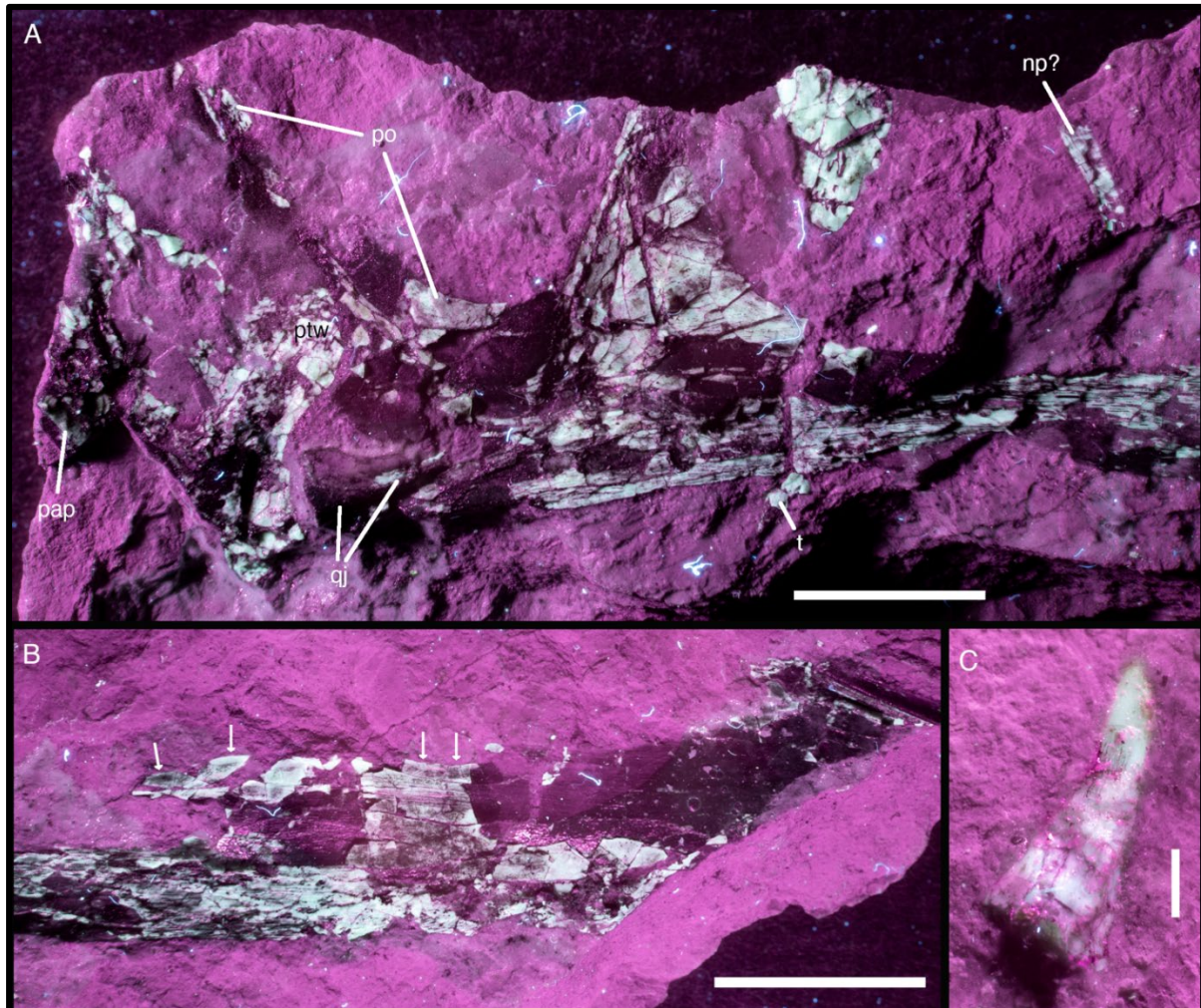


Fig. 5: Details of the holotype skull of *Melkamter pateko* gen. et sp. nov., MPEF PV 11530, under UV light. (A) posterior part of skull as preserved on the counterslab; (B) anterior part of the maxilla as preserved on the counterslab; (C) isolated tooth, preserved on the main slab. Abbreviations as in figure 3. Arrows in (B) point to preserved original margins of the base and the distal part of the ascending process of the maxilla. Scale bars are 1 cm (A, B) and 1 mm (C).

The maxilla extends posteriorly from the contact with the premaxilla, contributing to the anterior and ventral margins of the nasoantorbital fenestra, until it is overlapped dorsally by the anterior process of the jugal. The maxilla continues below the jugal to at least the mid-length of the orbit. The anterior half of the maxillary body below the nasoantorbital fenestra is approximately twice as high dorsoventrally (c. 8 mm) than the posterior half (maximally 4 mm). In between these two sections, a small incision into the

posterior end of the anterior half is present within the nasoantorbital opening. We interpret this incision as marking the posterior end of a vestigial ascending process of the maxilla, which is thus almost entirely posteriorly directed and does not contact a ventral process of the nasal or lacrimal (Fig. 3, 5B). The dorsal margin of this process is partially preserved in the counterslab, and curves downwards in its posterior part, resulting in a very slender termination of the process (Fig. 5B).

Table 1. Measurements of MPEF-PV 11530, in millimeters.

Preserved skull length (anteroposteriorly)	131.3 mm
Skull length to jaw articulation	112.1 mm
Preserved maximum skull height	24.9 mm
Rostrum to anterior nasoantorbital fenestra	40.8 mm
Skull height at anterior nasoantorbital fenestra	12.7 mm
Nasoantorbital fenestra length	51.6 mm
Preserved posterior nasoantorbital height	20.4 mm
Skull length to nasoantorbital fenestra posterior margin	93.6 mm
Mediodistal width of dental alveolus	1.7 mm
Preserved maximum orbit length	18.0 mm
Preserved maximum orbit height	15.8 mm
Infratemporal fenestra length	6.2 mm
Manual metacarpal length	29.2 mm
Manual metacarpal mid-width	1.3 mm
Dorsal vertebra centrum length	9.7 mm
Dorsal vertebra neural spine length	5.8 mm

One tooth is visibly well-preserved on the surface of the block (Fig. 2C) as well as one additional fragmentary tooth, both in close association to the skull, and although no teeth

are visibly attached to the rostrum, CT data (Fig. 4) shows that several alveoli (at least 5 per side) are indeed present and regularly spaced throughout the maxillopremaxillary region, with at least two partial teeth present within their individual alveolar sockets. Several empty sockets are also visible, but image quality precludes discerning how far anteriorly or posteriorly this toothrow extends. There is a small, posteroventrally inclined splinter in the posterior part of the maxilla that might represent a remnant of a tooth; if correctly identified, the tooth row would at least extend to the posterior margin of the nasoantorbital fenestra. Individual alveoli are widely spaced, with the distance between alveoli equaling almost two tooth widths in the anterior part of the maxilla. The completely-preserved tooth (Fig. 5C) is apicobasally short (4.3 mm), and anteroposteriorly thin (1.7 mm at the widest point of the base), with the shape of a curved cone, similar to that of basal pterodactyls. The tooth also exhibits a gradual apical taper with a gentle curvature, such that the tip is at about an 10° offset to its base.

The triradiate jugal tapers to a point anteriorly and contacts the maxilla anteriorly with a seemingly elongate process, together forming the flat ventral margin of the nasoantorbital fenestra (Fig. 3). Although the exact contact of the anteroventral jugal process with the maxilla cannot be confidently distinguished (as the anterior tip seems to be missing), it can be estimated to form approximately 13 mm of the posterior ventral margin of the nasoantorbital fenestra. The lacrimal process of the jugal rises in an almost perpendicular curve in respect to its ventral margin. Both this ascending process and the posterior postorbital ramus taper dorsally, reaching about the halfway point of the preserved orbit. The lacrimal process is considerably more massive than the postorbital process and contacts the ventral ramus of the lacrimal at about the mid-height of the orbit, or slightly lower. Although the suture is poorly preserved, the ventral end of the lacrimal seems to slot into a notch in the dorsal end of the jugal. The postorbital process is slender and reaches approximately as far dorsally as the lacrimal process (Fig. 5). Anteriorly, it is overlapped by a rather massive ventral process of the postorbital, which forms the entire posterior margin of the orbit and reaches the mid-length of this opening ventrally. The angle formed by the lacrimal and postorbital processes of the jugal is set at about 55° degrees. A short and dorsoventrally broad posterior process of the jugal is also present. Only the anterior end of the quadratojugal is preserved. It is triangular in outline, tapering anteriorly,

and inserts in between the ventral margin of the posterior end of the jugal and the dorsal margin of the posterior end of the maxilla, as in *Cycnorhamphus* (Bennett, 2012).

The quadrate appears long and broad, inclined posterodorsally backwards at about 126° from the plane of the palate. It forms the posterior boundary of the infratemporal fenestra. On its ventral-most point, there is a small, bulbous articular protuberance for articulation with the mandible. The large, anteriorly rounded pterygoid wing of the quadrate is partially preserved. It is offset from the ventral end of the quadrate and rapidly expands anteriorly in its ventral part, whereas the dorsal end grades more gradually into the quadrate shaft. On the counterslab, the end of the paroccipital process is preserved, and anterodorsal to it is a strongly eroded piece of bone that most probably represents a remnant of the squamosal.



Figure 6. Details of MPEF-PV 11530 postcranial material: (A-C) dorsal vertebrae and (D) manual metacarpal. Scale bar is 1 cm.

Four dorsal vertebrae are preserved in the block (two isolated, and two in close articulation with each other) (Fig. 6A-C). Of the two isolated vertebrae preserved, one is visible in lateral view (Fig. 6A) and one in dorsal view (Fig. 6C), with the articulated vertebrae in anterolateral view (Fig. 6B). From these perspectives, the shapes of the centra are difficult

to distinguish, but appear procoelous, and in lateral view, there is a slight dorsoventral constriction of each centrum, giving a spool-shaped profile. The transverse processes have an anteroposteriorly broad base until the capitular facet is reached, from which point they project dorsolaterally as they taper gently to a rounded tip (Fig. 5A). The location of the capitular facet (about halfway along the length of the transverse process) also contributes anteriorly to the lateral margin of the prezygapophysis, similar to darwinopterans (Martin-Silverstone et al., 2024). Due to the taphonomic state of the vertebrae, it is not possible to distinguish the presence of any foramina. The neural spines of the two articulated dorsals contact each other completely, with only a very faint line visibly demarcating them. The two articulated dorsals also potentially preserve an articulated fragmentary dorsal rib, although this is difficult to distinguish in their fractured state.

One metacarpal is completely preserved (either metacarpal I, II, or III). A shaft fragment (potentially another metacarpal I-III) and another large indeterminate bone shard are also preserved on the surface of the block, and CT scan data (Fig. X) shows an additional indeterminate long bone shaft obscured by matrix within the block. However, all are too eroded to glean any further information.

Systematic Paleontology

PTEROSAURIA Owen, 1842

PTERODACTYLOIDEA Plieninger, 1901

CTENOCHASMATIDAE(?) *indet.* Nopsca, 1928 *sensu* Unwin, 2003

In addition to the above-mentioned specimen, a separate block containing an isolated tooth was also recovered from the Queso Rallado locality of the Cañadón Asfalto Formation, which closely resembles the teeth of ctenochasmatids (Fig. 7). The sediment comprising the block is different in color and texture from the above-mentioned specimen, likely indicating that it originated from a different horizon. The tooth is in good condition overall, preserving most of the crown, and missing only the apicalmost tip (although a natural mold in the surrounding sediment retains its overall original shape). The base of the tooth appears to have been broken (likely near the crown-root boundary), perhaps during feeding, but the lack of erosion over the entire tooth surface indicates that it was not likely to be much transported after its dissociation from the rostrum. The tooth is remarkably

elongated, slightly recurved, and measuring 47 mm from base to tip, 1.5 mm wide at its base and gradually tapering to 0.5 mm wide at its apical tip. At the base it is lenticular in cross-section, but becomes more circular in cross-section as it approaches the apex, as in most ctenochasmatids. There is an ombre-like color change from base to tip, varying from gray to beige, which is also indicative of the dentine-to-enamel change, with the enamel thickening apically (the lower gray 30mm of the tooth representing exposed dentine as it is less shiny than the more apical beige enameled region). The enamel is completely smooth and lacks any ornamentation. Due to the proportion of dentine-to-enamel present, it is likely that the tooth is from the anteriormost region of a ctenochasmatid rostrum (anterior teeth are also subject to more breakage during feeding, as they more regularly contact food items and are subject to greater torsion with struggling prey [Fastnacht, 2005; Hofmann et al. 2020]).



Figure 7. Isolated ctenochasmatid(?) tooth MPEF PV 2549[2012], also from the Queso Rallado locality. Scale bar is 1 cm.

Phylogenetic Analysis

The analysis of the matrix based on Fernandes et al. (2023) under equal weights resulted in the recovery of 12 equally parsimonious trees with a score of 1388.014 (Fig. 8). The results are generally comparable to those published by Andres (2021), but show less resolution, with some polytomies being present. *Melkamter* is found in a polytomy with *Sordes* just

outside the Darwinoptera-Pterodactyloidea clade in this analysis. Interestingly, *Allkaruen* is still found in a polytomy with species of *Dimorphodon* in the Dimorphodontia, as in the original analysis of Andres (2021), despite the revised scorings for this taxon. Constraining *Allkaruen* into the clade including *Sordes* and monofenestratans (as found by Codorníu et al., 2016, and Martin-Silverstone et al., 2024) requires three additional steps (score of 1391.221) and finds this taxon within derived pterodactyloids as a member of the Istdactylinae; given that the holotype of *Allkaruen* mainly consists of a complete, three dimensionally preserved braincase (Codorníu et al., 2016), the rather limited sampling of braincase characters might account for these vastly differing results.

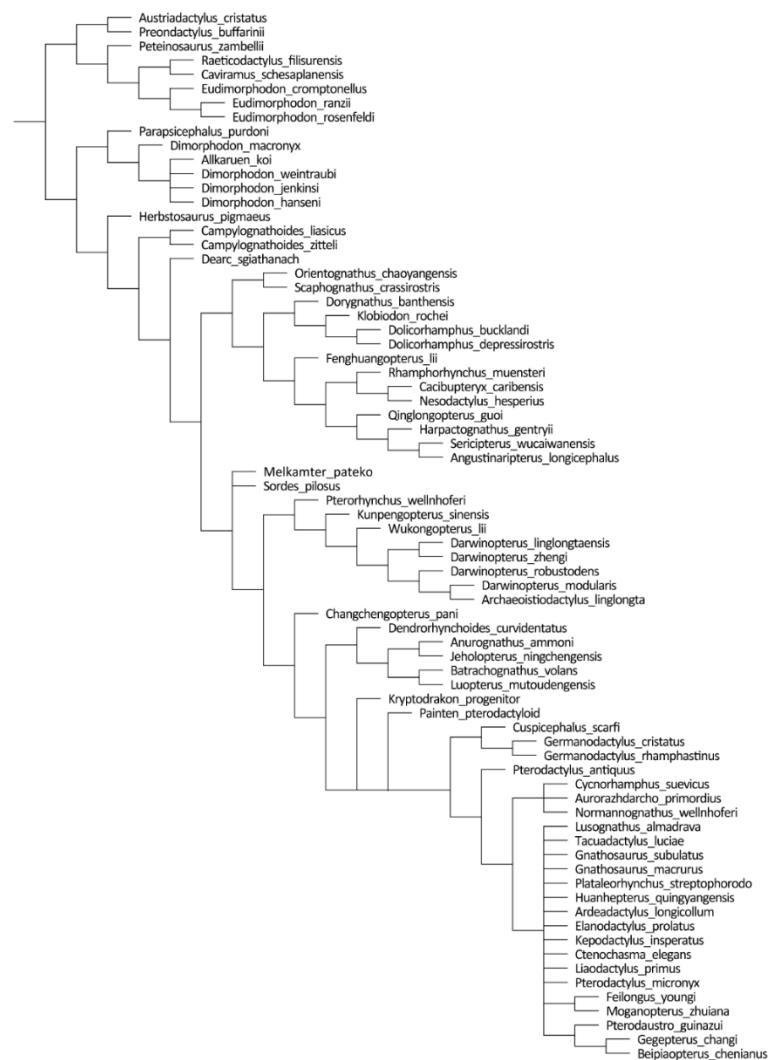


Figure 8. The relationship of *Melkamter pateko* to the Pterosauria, using the Fernandes et al. (2023) matrix (simplified in Adobe Illustrator).

The equal weights analysis using the matrix based on Martin-Silverstone et al. (2024) recovered 28560 equally parsimonious trees with a length of 556 steps (Fig. 9). The strict consensus of these trees largely confirms to the results of Martin-Silverstone et al. (2024), but shows both *Melkamter* and *Allkaruen* in a polytomy with darwinopterans at the base of Monofenestrata. Reduced consensus methods identify *Allkaruen* as a problematic taxon in this part of the tree, the *a posteriori* deletion of which results in *Melkamter* being found as the earliest branching monofenestratan, followed by a monophyletic Darwinoptera and pterodactyloids. *Allkaruen* can take multiple positions within this phylogenetic hypothesis, either below or just above *Melkamter*, as a sister taxon to the latter, as a darwinopteran, or as the earliest branching pterodactyloid. The implied weights analysis of this matrix recovered 51 trees of a score of 22.36738 and finds *Melkamter* and *Allkaruen* in a polytomy at the base of Monofenestrata.



Figure 9. The relationship of *Melkamter pateko* to the Pterosauria, using the Martin-Silverstone et al. (2024) matrix (reduced consensus; strict consensus in supplementary material).

Discussion

Phylogenetic position and evolutionary implications

The phylogenetic analyses based on both different data sets agree in placing the new taxon described here just outside the clade encompassing darwinopterans and pterodactyloids (or pterodactyliformes). In the implied weights analysis of the Fernandes et al., 2023 matrix, *Melkamter* is found above *Sordes*, as oldest and earliest branching monofenestratan, followed by the Darwinoptera and Pterodactyliformes (sensu Andres, 2021). As the Monofenestrata are an apomorphy defined clade, characterized by the presence of a confluent nasoantorbital fenestra (Andres, 2021), the presence of this trait in the material described here allows its reference to this clade. The presence of *Melkamter* in the Cañadón Asfalto Formation therefore marks the earliest occurrence (late Early Jurassic, Toarcian [Cúneo et al., 2013; Pol et al., 2020]) of a monofenestratan pterosaur worldwide, predating the currently oldest member of that clade (Martin Silverstone et al., 2024) by at least 8 and probably 10 million years. However, the clade had seemingly achieved a wider distribution by at least the Middle Jurassic (Martin-Silverstone et al., 2014), and a probably worldwide distribution by the early Late Jurassic.

Melkamter is the first and only non-pterodactyloid monofenestratan from Gondwana. However, direct comparison of *Melkamter pateko* with other non-pterodactyloid monofenestratans (outside of the darwinopterans) is complicated for lack of overlapping elements. In particular in comparison with its fellow Argentine taxon, *Allkaruen koi* from the same formation, it therefore cannot be entirely excluded that they are the same taxon as the two taxa do not have any overlapping material in common. However, in addition to the results of the phylogenetic analyses of the Fernandes et al., 2023 matrix, where these two taxa come out in widely different positions (and in which forcing together *Melkamter* and *Allkaruen* requires 5 additional steps), the only morphological evidence that is comparable, the relative size and shape of the alveoli, also contradicts this, as the alveoli of the similar-sized holotype of *Allkaruen* seem to be relatively larger and more

mediolaterally compressed than those of *Melkamter*.

Regarding comparison with darwinopterans, since the time of its initial description, *Cuspicephalus scarfi* has been further prepared from the opposite side (which is better preserved), allowing for a more direct observation of its morphology and more direct comparison with *Melkamter pateko* and other darwinopterans (Fig. 6). However, although some phylogenies do indeed regard it as a darwinopteran (i.e. Martill & Etches, 2013; Witton, O'Sullivan & Martill 2015, Martin-Silverstone et al., 2024), one phylogenetic analysis herein recovers *Cuspicephalus* as a germanodactylid (Fernandes et al., 2023), instead of its initial assignation as a non-pterodactyloid monofenestratan. Although its true phylogenetic position is outside the scope of the current work, nevertheless some of its characteristics do bear comparison. Although the skull of *Cuspicephalus* is about twice the length of that of *Melkamter*, they both exhibit broad ascending processes of their jugals, as do *Kunpengopterus sinensis* and *Darwinopterus modularis* (but unlike *Darwinopterus linglongensis*).

The overall shape of the skull in *Melkamter pateko* suggests a high skull, as in *Darwinopterus linglongtaensis* Wang et al., 2010, which is higher than both *Kunpengopterus sinensis* Wang et al., 2010 and *Darwinopterus modularis* Wang et al., 2010. *Kunpengopterus* lacks a premaxillary crest (tentatively matching the condition of *Melkamter*), making it unlike other darwinopterans. However, the quadrate of *Kunpengopterus* is inclined more dramatically than in the specimen herein (150° , as opposed to about 126° in *Melkamter*). The inclination found in *Dimorphodon* is 95° (Owen, 1859; Padian 1984), in *Parapsicephalus* it is between 115° and 130° , *Eudimorphodon* and *Scaphognathus* are at 120° (Cheng et al., 2012; Bennett, 2014), *Dorygnathus* and *Campylognathoides* are between 120° and 130° (Padian, 2008a, 2008b), *Rhamphorhynchus* is at 130° – 150° (Wellnhofer 1975, 1978; Witmer et al. 2003), and *Angustinaripterus* is at 140° (He et al., 1983). Among darwinopterans the angle varies from about 130° – 132° in *Darwinopterus linglongtaensis* to 142° in *Kunpengopterus*, and 140° in *Cuspicephalus* (Martill & Etches, 2013). Germanodactylids are further set at about 148° , with more derived pterodactyls having even larger angles of inclination. This places *Melkamter* as having a more acute angle than the darwinopterans (Fig. 10), with a value closer to those found in the more basal scaphognathines and campylognathoids than in the more derived pterodactyls.

Although potentially ontogenetically variable, the angle of the orbit (formed by the lacrimal and posterior processes of the jugal, and measured from photographs of each specimen) in *Cuspicephalus* is set at 45°, *Parapsicephalus* at 45°, *Angustinaripteus* at 46°, *Tupandactylus* at 45°, *Dimorphodon* at 47°, *Darwinopterus modularis* at 60°, *Germanodactylus cristatus* at 63°, *Pteranodon* at 65°, *Germanodactylus rhamphastinus* at 70°, *Dorygnathus* at 72°-96°, *Pterodactylus micronyx* (the neotype) at 75°, *Cycnorhamphus* at 76°, *Campylognathoides* at 77°, , *Eudimorphodon* at 80°, *Ctenochasma* at 80°-85°, *Scaphognathus* at 80°–100°, *Rhamphorhynchus* at 82°, and 90° in *Pterodactylus antiquus* (the holotype) (Wellnhofer, 1970, 1975; He et al., 1983; Bennett, 2001, 2012, 2021; Witmer et al., 2003; Padian, 2008a, 2008b; Beccari et al., 2021; O’Sullivan & Martill, 2017). *Melkamter* expresses an angle of about 55°, which places it with a value closer to those found between *Dimorphodon* and *Darwinopterus*.

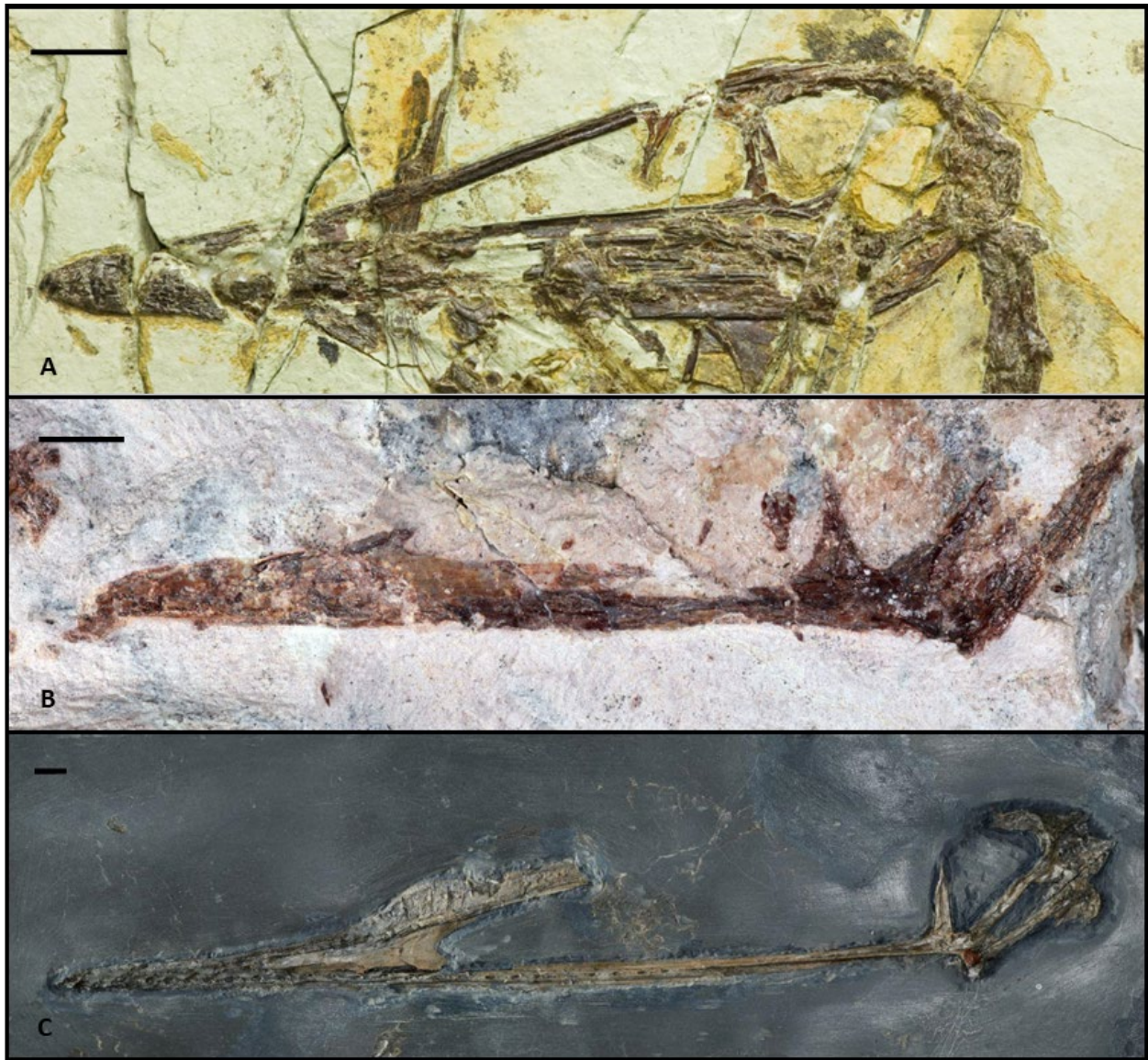


Fig 10. Comparison of (A) *Darwinopterus linglongensis* (IVPP V16049; mirror-imaged for comparison), (B) *Melkamter pateko*, and the newly-prepared left side of (C) *Cuspicephalus scarfi*. Scale bars are 1 cm.

Darwinopterans usually exhibit pterodactyloid-like elongated crania with confluent nasoantorbital fenestrae, free nasal processes, inclined quadrates, and short peg-like teeth (Lü et al., 2010; Wang et al., 2010; Witton et al., 2015; Zhou et al., 2017; Navarro et al., 2018; Bestwick, 2018), all of which are exhibited by *Melkamter*. Despite their traditionally-held modular evolution, however, it has also been recently argued that darwinopterans should no longer be considered a directly transitional group between basal “rhamphorhynchids” and the Pterodactyloidea, but rather a sister group to the

Pterodactyloidea, along with the scaphognathines and rhamphorhynchines (Martin-Silverstone et al., 2024). One significant autapomorphy seen in *Melkamter* holds merit in making this distinction: that of a vestigial ascending process of the maxilla, which is absent in all other known monofenestratans, and could potentially show the evolutionary pathway to the pterodactyloids losing this feature completely.

Concerning the tooth MPEV PV 2549, a secure identification of such an isolated element is, of course, difficult. The extreme elongation of this tooth is remarkable; such elongate teeth are unknown from any other terrestrial Mesozoic vertebrate clade, but elongate, recurved and pointed teeth are quite frequently found in pterosaurs (see Wellnhofer, 1991; Witton, 2013). A further argument for a pterosaur identification of this tooth is the unusual distribution of enamel, which is similarly found in some pterosaur clades. Inclusion of the tooth in the phylogenetic analyses above was attempted, but results were inconclusive for lack of characters. However, within pterosaurs, the tooth is most similar to the teeth of ctenochasmatids, which have strongly very elongate, slender teeth with a marked curvature in at least the mesial teeth (see e.g. Wellnhofer, 1970). If the presence of a (probably early branching) ctenochasmatid from the Cañadón Asfalto Formation can be confirmed, this would considerably extend the fossil record of pterodactyloids and place the origin of this clade firmly in the Early Jurassic. The tooth is unusually large for known ctenochasmatids, being approximately double the length of the mesial teeth of a skull of *Gnathosaurus* from the Tithonian Altmühltal Formation of Eichstätt, Germany (Wellnhofer, 1970) and even larger if compared to known large specimens of ctenochasmatids (e.g. Moser & Rauhut 2011), but the discovery of the very large jaw of *Lusognathus* demonstrates that ctenochasmatids could reach large sizes already in the Jurassic (Fernandes et al., 2023). Therefore, the tooth is here tentatively assigned to the Ctenochasmatidae, thus extending the stratigraphic range of this clade by at least 10 to 15 million years (Zhou et al., 2017). As ctenochasmatids are well nested within Pterodactyloidea, this would furthermore extend the entire clade and its early diversification into the Early Jurassic. However, as other, more basal pterosaurs also show elongate and curved teeth, including the rhamphorhynchids (e.g., Wellnhofer, 1975; Padian, 2008a, b) it cannot be excluded that this tooth represents an independent acquisition of such extremely elongate teeth, allowing for the possibility that it could belong to some

other novel taxon entirely. However that may be, the tooth certainly represents a taxon different from both *Allkaruen* and *Melkamter*, thus further increasing pterosaur diversity in the Cañadón Asfalto Formation.

Dentition and ecological implications

Great variability is shown in the basal monofenestratan dentition. The “Painten propterodactyloid” has pointed, conical long teeth with large interdental spaces and rostrally directed fangs in the rostral jaw area (Tischlinger & Frey, 2013), *Darwinopterus modularis* exhibits spike-like teeth (Lü et al. 2009), *Darwinopterus linglongtaensis* and *Kunpengopterus sinensis* have short blunted cone-shaped teeth, *Wukongopterus lii* has cone-shaped and very pointed teeth (Wang et al., 2010), and *Darwinopterus robustadens* exhibits relatively stout teeth (Lü et al., 2009; 2011b). This variation in dental morphology has been interpreted as evidence of niche partitioning (Wang et al., 2010; Lü et al., 2009, 2011b; Zhou 2021) and the feeding on different prey items, although all these taxa are overall generally regarded as being insectivorous or piscivorous (Bestwick, 2018; Zhou 2021). Based on tooth morphology alone, darwinopterans were probably insectivores (Zhou 2021), but the high tooth count of *Cuspicephalus scarfi* could also potentially indicate piscivory (Martill & Etches, 2013; Witton et al., 2015). This is all in keeping with the relative abundance of arthropods present in some concurrent deposits (e.g. Zhou, 2021), and fish in others (e.g. the Tiaojishan Formation and Daohugou beds of Wang et al., 2010b). The dental morphology and regular tooth spacing of the *Melkamter* appear to be of the insectivorous morphotype (Bestwick, 2018), warranting more similarity with wukongopterids, which also exhibit interalveolar spacing that is greater than their tooth lengths (Witton, 2015), characteristics which are shared with the specimen herein. Whereas many pterosaurs from the “classic” marine Lagerstätten show adaptations to a piscivorous diet (see Wellnhofer, 1991; Bestwick et al., 2018), this concentration of insectivorous forms in the early branching monofenestratans might support the suggestion of Andres et al. (2014) that the origin of pterodactyloids might be found in truly terrestrial rather than nearshore or insular environments. This is especially the case in the phylogenetic hypothesis based on the Andres (2021) and Fernandes et al. (2023) data sets, in which the Anurognathidae, for which there is the strongest evidence and consensus for

an insectivorous diet (Bestwick et al., 2018), represent the immediate outgroup to Pterodactyloidea. Given the otherwise expressed dietary plasticity in pterosaurs (see Bestwick et al., 2018, 2020), such a concentration on terrestrial prey in non-pterodactyloid monofenestrans might be surprising if these animals lived in nearshore environments or on islands in a lagoonal setting.

Ecological requirements (such as prey preferences) affect the dispersion of animals, even beyond their ability to fly (Upchurch et al., 2015). However, considering that the prey of insectivorous animals also fly (albeit with a likely smaller range), this could potentially indicate that insectivorous monofenestrans could have dispersed more widely (even across wider geographical barriers than those feeding solely on lacustrine fish, for example), setting different natural geospatial limits on the ecological niches that they occupied. Thus, in a still Pangean world during the Early and Middle Jurassic, a largely insectivorous diet might have represented an important adaptation to explain the success of basal monofenestrans and their descendants, the pterodactyloids.



Figure 11. Artistic reconstruction of *Melkamter pateko* by Pedro Andrade.

Conclusion

It has long been suspected that pterodactyloids were already present by the end of the Early Jurassic (Unwin, 1996; O'Sullivan & Martill, 2018), and that pterosaurs had already reached relatively high levels of taxonomic and morphological diversity by the Middle Jurassic (Martin-Silverstone et al., 2024), although the dearth of available fossil material has made these claims difficult to concretely establish. *Melkamter pateko* (Fig. 11), from the latest Early Jurassic of Chubut province, represents the so far most conclusive evidence for the presence of Monofenestrata during the late Early Jurassic, while also contributing to their morphological diversity with the novel traits expressed in this new taxon. Furthermore, if confirmed by future finds, the possible presence of a ctenochasmatid, currently indicated by a single tooth, would not only place the origin of pterodactyloids into the Early Jurassic, but even indicate that their initial diversification already happened during that time. Although the Lagerstätten of the northern hemisphere have traditionally dominated in our understanding of the diversity and dispersion of pterosaurs over time, it is clear now that Gondwana also held a high phylogenetic diversity of pterosaurs, with the Cañadón Asfalto Formation alone now exhibiting evidence for at least three distinct taxa that might all directly be relevant to the origin and early divergence of the Pterodactyloidea. This further highlights our still abysmal knowledge of Jurassic pterosaur faunas from Gondwana, and it is evident that, pending more field sampling and pterosaur fossil recovery, the inherent potential is present for the southern hemisphere to perhaps one day match the abundance of the northern hemisphere.

Acknowledgements

Thank you to Guillermo Rougier, who led the excavations in Queso Rallado. Many thanks go to José Carballido, Pablo Puerta, Ariel Aresti, Mariano Caffa, and Vanessa Béland for their invaluable research and pterosaur field assistance, and to the entire staff of the MEF. Heartfelt thanks are extended to Calin Suteu for his photographic expertise, and to Victor Beccari for his CT segmentation and UV photography assistance. Thank you to Mike Day at the NHM London and Steve Etches of the Etches Collection for granting access to specimens. Thank you to Dr. Xu Xing and Dr. Shunxing Jiang for their kindness in providing information on the Chinese taxa included in the work. We also thank Brian Andres for his critical comments on the material, and significant insights into the manuscript. We are also grateful to the reviewers for their constructive feedback, which greatly improved this work. This work was supported by the Deutsche Forschungsgemeinschaft (DFG) under project RA

1012/29. Field work was made possible by the authorities of the Secretaría de Cultura de la Provincia del Chubut, and supported by the Fundación Egidio Feruglio.

Funding

AEF is supported by funding from DFG grant number RA 1012/29.

References

- Andres, B. (2021). Phylogenetic systematics of *Quetzalcoatlus* Lawson 1975 (Pterodactyloidea: Azhdarchoidea). *Journal of Vertebrate Paleontology*, 41(1), 203–217.
- Andres, B., Clark, J., & Xu, X. (2014). The earliest pterodactyloid and the origin of the group. *Current Biology*, 24, 1011–1016.
- Andres, B., & Ji, Q. (2008). A new pterosaur from the Liaoning Province of China, the phylogeny of the Pterodactyloidea, and convergence in their cervical vertebrae. *Palaeontology* 51, 453–470.
- Apesteguía, S., Gómez, R.O., & Rougier, G.W. (2012). A basal sphenodontian (Lepidosauria) from the Jurassic of Patagonia: new insights on the phylogeny and biogeography of Gondwanan rhynchocephalians. *Zoological Journal of the Linnean Society*, 166(2), 342–360.
- Beccari, V., Pinheiro, F.L., Nunes, I., Anelli, L.E., Mateus, O., & Costa, F.R. (2021). Osteology of an exceptionally well-preserved tapejarid skeleton from Brazil: Revealing the anatomy of a curious pterodactyloid clade. *PLoS ONE*, 16(8), e0254789. <https://doi.org/10.1371/journal.pone.0254789>
- Becerra, M.G., Pol, D., Rauhut, O.W.M., & Cerda, I.A. (2016). New heterodontosaurid remains from the Cañadón Asfalto Formation: cursoriality and the functional importance of the pes in small heterodontosaurids. *Journal of Paleontology*, 90(3), 555–577. doi:10.1017/jpa.2016.24
- Bennett, S.C. (2001). The osteology and functional morphology of the Late Cretaceous pterosaur Pteranodon Part I. General description of osteology. *Palaeontographica Abteilung A*, 1–112.
- Bennett, S.C. (2012). The morphology and taxonomy of the pterosaur *Cycnorhamphus*. *Neues Jahrbuch für Geologie und Paläontologie – Abhandlungen*, 267(1), 23–41.
- Bennett, S.C. (2014). A new specimen of the pterosaur *Scaphognathus crassirostris*, with comments on constraint of cervical vertebrae number in pterosaurs. *Neues Jahrbuch*

für Geologie und Paläontologie – Abhandlungen, 271(3), 327-348.

- Bennett, S.C. (2021). Complete large skull of the pterodactyloid pterosaur *Ctenochasma elegans* from the Late Jurassic Solnhofen Lithographic Limestones. *Neues Jahrbuch für Geologie und Paläontologie, Abhandlungen*, 301(3), 283–294.
- Bestwick, J., Unwin, D.M., Butler, R.J., Henderson, D.M., & Purnell, M.A. (2018). Pterosaur dietary hypotheses: a review of ideas and approaches. *Biological Reviews*, 93, 2021-2048.
- Bestwick, J., Unwin, D.M., Butler, R.J. & Prunell, M.A. (2020). Dietary diversity and evolution of the earliest flying vertebrates revealed by dental microwear texture analysis. *Nature Communications*, 11, 5293.
- Bonaparte, J.F. (1978). *El Mesozoico de America del Sur y sus Tetrapodos*. Opera Lilloana, 26.
- Butler, R.J., Benson, R.B.J. & Barrett, P.M. (2013). Pterosaur diversity: Untangling the influence of sampling biases, Lagerstätten, and genuine biodiversity signals. *Palaeogeography, Palaeoclimatology, Palaeoecology*, 372, 78-87.
- Cabaleri, N., Volkheimer, W., Nieto, D.S., Armella, C., Cagnoni, M., Hauser, N., Matteini, M. & Pimentel, M.M. (2010). U–Pb ages in zircons from Las Chacritas and Puesto Almada members of the Jurassic Cañadón Asfalto Formation, Chubut province, Argentina. *South American Symposium Isotope Geology, Brasilia, Abstracts*, 190-193.
- Carballido, J.L, Pol, D., Otero, A., Cerda, I.A., Salgado, L., Garrido, A.C., Ramezani, J., Cúneo, N.R., & Krause, J.M. (2017). A new giant titanosaur sheds light on body mass evolution among sauropod dinosaurs. *Proc. R. Soc. B.*, 284, 20171219.
- Casamiquela, R.M. (1975). *Herbstosaurus pigmaeus* (Coeluria, Compsognathidae) n. gen. n. sp. del Jurásico medio del Neuquén (Patagonia septentrional). Uno de los más pequeños dinosaurios conocidos. *Acta primero Congreso Argentino Paleontología et Bioestratigrafía*, 2, 87-102.
- Cheng, X., Wang, X., Jiang, S., & Kellner, A.W.A. (2012). A new scaphognathid pterosaur from western Liaoning, China. *Hist. Biol.* 24, 101–111.
- Cheng, X., Jiang, S., Wang, X., & Kellner, A.W.A. (2017). New anatomical information of the wukongopterid *Kunpengopterus sinensis* Wang et al., 2010 based on a new specimen. *PeerJ*, 5,e4102.
- Codorniú, L., & Gasparini, Z. (2007). Pterosauria. In Gasparini, Z., Salgado, L., and Coria, R.A. (Eds.). *Patagonian Mesozoic Reptiles* (pp.143-166). Bloomington, Indiana: Indiana University Press.
- Cordoniú, L., Rauhut, O.W.M., & Pol, D. (2010). Osteological features of Middle Jurassic

- pterosaurs from Patagonia (Argentina). *Acta Geoscientica Sinica*, 31(suppl. 1), 12-13.
- Codorniu, L., & Gasparini, Z. (2013). The Late Jurassic pterosaurs from northern Patagonia, Argentina. *Earth and Environmental Science Transactions of the Royal Society of Edinburgh*, 103,1-10.
- Codorniu, L., & Gianchini, F.A. (2016). The flying reptiles from Argentina: An overview. *Contribuciones del MACN*, 6. In: F.L. Agnolin, G.L. Lio, F.B. Egli, N.R. Chimento, F.E. Novas (Eds.), *Historia Evolutiva y paleobiogeográfica de los vertebrados de América del Sur*.
- Codorniu, L., Carabajal, A.P., Pol, D., Unwin, D., & Rauhut, O.W.M. (2016). A Jurassic pterosaur from Patagonia and the origin of the pterodactyloid neurocranium. *PeerJ* 4:e2311.
- Cúneo, R., Ramezani, J., Scasso, R., Pol, D., Escapa, I., Zavattieri, A.M. & Bowring, S. A. 2013. High-precision U–Pb geochronology and a new chronostratigraphy for the Cañadón Asfalto Basin, Chubut, central Patagonia: Implications for terrestrial faunal and floral evolution in Jurassic. *Gondwana Research*, 24(3–4), 1267–1275.
- Fantasia, A., Föllmi, K.B., Adatte, T., Spangenberg, J.E., Schoene, B., Barker, R.T., & Scasso, R.A. (2021). Late Toarcian continental palaeoenvironmental conditions: An example from the Cañadón Asfalto Formation in southern Argentina. *Gondwana Research*, 89, 47–65. <https://doi.org/10.1016/j.gr.2020.10.001>
- Fastnacht, M. (2005). Jaw mechanics of the pterosaur skull construction and the evolution of Toothlessness. PhD thesis, Johannes Gutenberg-Universität, Mainz.
- Fernández Garay, A. (2004). *Tehuelche-Spanish dictionary, Spanish-Tehuelche index*. CNWS Research School of Asian, African and Amerindian Studies, Univ. of Leiden.
- Figari, E.G. & Courtade, S. (1993). Evolución tectosedimentaria de la cuenca de Cañadón Asfalto, Chubut, Argentina. *XII Congreso Geológico Argentino y II Congreso de Exploración de Hidrocarburos, Actas 1*, 66-77.
- Figari, E.G., Scasso, R.A., Cúneo, R.N., & Escapa, I. (2015). Estratigrafía y evolución de la Cuenca de Cañadón Asfalto, provincia del Chubut, Argentina. *Lat. Am. J. Sedimentol. Basin Anal.* 22, 135-169.
- Gaetano, L.C., & Rougier, G.W. (2011). New materials of *Argentinaconodon fariasorum* (Mammaliaformes, Ticonodontidae) from the Jurassic of Argentina and its bearing on triconodont phylogeny. *Journal of Vertebrate Paleontology*, 31(4), 829-843.
- Gaetano, L.C., & Rougier, G.W. (2012). First Amphilestid from South America: A Molariform from the Jurassic Cañadón Asfalto Formation, Patagonia, Argentina. *Journal of Mammalian Evolution*, 19, 235–248.

- Goloboff, P.A., Farris, J.S., & Nixon, K.C. (2008). TNT, a free program for phylogenetic analysis. *Cladistics*, *24*, 774–786.
- Goloboff, P.A. & Morales, M. (2023). TNT version 1.6, with a graphical interface for MacOs and Linux, including new routines in parallel. *Cladistics*, *39*(2), 144–153.
- He, X., Yan, D., & Su, C. (1983). A new pterosaur from the Middle Jurassic of Dashanpu, Zigong, Sichuan. *Journal of the Chengdu College of Geology, Suppl. 1*, 27–33.
- Hofmann, R., Besetwick, J., Berndt, G., Berndt, R., Fuchs, D. & Klug, C. (2020). Pterosaurs ate soft-bodied cephalopods (Coleoidea) *Scientific Reports* *10*, 1230. <https://doi.org/10.1038/s41598-020-57731-2>
- Kellner, A.W. (2003). Pterosaur phylogeny and comments on the evolutionary history of the group. In: Buffetaut E, Mazin J-M, eds. *Evolution and palaeobiology of pterosaurs*, Geological Society, London, special publications, vol. 217. London: Geological Society, 105–137.
- Lü, J, Unwin, D.M., Jin, X., Liu, Y., & Ji, Q. (2009). Evidence for modular evolution in a long-tailed pterosaur with a pterodactyloid skull. *Proceeding of the Royal Society B*. *277*, 383–389.
- Lü J., Unwin D.M., Jin X., Liu, Y., & Ji, Q. (2010). Evidence for modular evolution in a long-tailed pterosaur with a pterodactyloid skull. *Proc. R. Soc. B*, *277*, 383–389. doi:10.1098/rspb.2009.1603
- Lü, J.C., Xu, L., Chang, H., & Zhang, X. (2011). A new darwinopterid pterosaur from the Middle Jurassic of western Liaoning, northeastern China and its ecological implications. *Acta Geologica Sinica-English Edition*, *85*, 507–514. DOI 10.1111/j.1755-6724.2011.00444.x
- Martill, D.M. & Etches, S. (2012). A new monofenestratan pterosaur from the Kimmeridge Clay Formation (Kimmeridgian, Upper Jurassic) of Dorset, England. *Acta Palaeontologica Polonica*, *58*, 285–294.
- Martin, T., & Rauhut, O.W.M. (2005). Mandible and dentition of *Asfaltomylos patagonicus* (Australosphenida, Mammalia) and the evolution of tribosphenic teeth. *Journal of Vertebrate Paleontology*, *25*(2), 414–425.
- Martin-Silverstone EM, Unwin DM, Cuff AR, Brown EE, Allington-Jones L & Barrett PM. 2024. A new pterosaur from the Middle Jurassic of Skye, Scotland and the early diversification of flying reptiles. *Journal of Vertebrate Paleontology*, e2298741.
- Navarro C.A., Martin-Silverstone, E., & Stubbs, T.L. (2018). Morphometric assessment of pterosaur jaw disparity. *Royal Society Open Science*, *5*, 172130.
- Nopsca, F 1928, 'The genera of reptiles', *Palaeobiologica*, vol. 1, pp. 163–188.

- O'Sullivan, M., & Martill, D.M. (2015). Evidence for the presence of *Rhamphorhynchus* (Pterosauria: Rhamphorhynchinae) in the Kimmeridge Clay of the UK. *Proceedings of the Geologist's Association*, 126, 390–401.
- O'Sullivan, M., & Martill, D.M. (2017). The taxonomy and systematics of *Parapsicephalus purdoni* (Reptilia: Pterosauria) from the Lower Jurassic Whitby Mudstone Formation, Whitby, U.K. *Historical Biology*, 29, 1–10.
- O'Sullivan, M., & Martill, D.M. (2018). Pterosauria of the Great Oolite Group (Bathonian, Middle Jurassic) of Oxfordshire and Gloucestershire, England. *Acta Palaeontologica Polonica*, 63(4), 617–644.
- Owen, R. (1859). On a new genus (*Dimorphodon*) of pterodactyle, with remarks on the geological distribution of flying reptiles. *Report for the British Association for the Advancement of Science*, 28, 97–103.
- Owen, R. (1842). Report on British Fossil Reptiles, Part II. In *Proceedings of the 11th Meeting of the British Association for the Advancement of Science, Plymouth, UK, 24 July 1842*, 60–204.
- Padian, K. (1984). *Osteology and functional morphology of Dimorphodon macronyx (Buckland) (Pterosauria: Rhamphorhynchoidea) based on new material in the Yale Peabody Museum*. Peabody Museum of Natural History, New Haven.
- Padian, K. (2008a). The Early Jurassic pterosaur *Campylognathoides* Strand, 1928. *Special Papers in Palaeontology*, 80, 65–107.
- Padian, K. (2008b). The Toarcian (Early Jurassic) pterosaur *Dorygnathus* Wagner, 1860. *Palaeontology*, 80, 1–64.
- Pentland, A.H., & Poropat, S.F. (2023). A review of the Jurassic and Cretaceous Gondwanan pterosaur record, *Gondwana Research*, 119, 341–383.
- Pol, D., & Escapa, I.H. (2009). Unstable taxa in cladistic analysis: identification and the assessment of relevant characters. *Cladistics*, 25, 515–527.
- Rauhut, O.W.M. (2005). Osteology and relationships of a new theropod dinosaur from the Middle Jurassic of Patagonia. *Palaeontology* 48(1), 87–110.
- Rauhut, O.W.M. (2007). A fragmentary theropod skull from the Middle Jurassic of Patagonia. *Ameghiniana*, 44(2), 479–483.
- Rauhut, O.W.M., & López-Arbarello, A. (2008). Archosaur evolution during the Jurassic: a southern perspective. *Revista de la Asociación Geológica Argentina*, 63, 557–585.

- Rauhut, O.W.M., Martin, T., Ortiz-Jaureguizar, E., & Puerta, P. (2002). A Jurassic mammal from South America. *Nature*, *416*, 165–168.
- Rauhut, O.W.M., & Pol, D. (2019). Probable basal allosauroid from the early Middle Jurassic Cañadón Asfalto Formation of Argentina highlights phylogenetic uncertainty in tetanuran theropod dinosaurs. *Scientific Reports*, *9*, 18826. <https://doi.org/10.1038/s41598-019-53672-7>
- Rougier, G., Martinelli, A., Foraisepi, A., & Novacek, M. (2007). New Jurassic mammals from Patagonia, Argentina: a reappraisal of Australosphenidan morphology and interrelationships. *American Museum Novitates*, *54*, 1-55.
- Sangster, S. (2021). The osteology of *Dimorphodon macronyx*, a non-pterodactyloid pterosaur from the Lower Jurassic of Dorset, England, *Monographs of the Palaeontographical Society*, *175*, 1–48.
- Sterli, J. (2008). A new, nearly complete stem turtle from the Jurassic of South America with implications for turtle evolution. *Biol. Lett.* *4*, 286–289.
- Tischlinger, H., & Frey, E. (2013). A new pterosaur with mosaic characters of basal and pterodactyloid pterosauria from the Upper Kimmeridgian of Painten (Upper Palatinate, Germany). *Archaeopteryx*, *31*, 1-13.
- Unwin, D.M. (1996). The fossil record of middle Jurassic pterosaurs. In M. Morales (Ed.). *The Continental Jurassic* 291-304. *Museum of Northern Arizona Bulletin*, *60*.
- Unwin, D.M., Lü, J. & Bakhurina, N.N. (2000). On the systematic and stratigraphic significance of pterosaurs from the Lower Cretaceous Yixian Formation (Jehol Group) of Liaoning, China. *Mitteilungen aus dem Museum für Naturkunde in Berlin, Geowissenschaftliche Reihe*, *3*, 181–206.
- Unwin, D.M. (2002). On the systematic relationships of *Cearadactylus atrox*, an enigmatic Early Cretaceous pterosaur from the Santana Formation of Brazil. *Fossil Record*, *5*, 239-263.
- Unwin, D.M. (2003). On the phylogeny and evolutionary history of pterosaurs. *Geological Society, London, Special Publications*, *217*(1), 139–90.
- Unwin, D.M., Rauhut, O.W.M., & Haluza, A. (2004). The first rhamphorynchoid from south America and the early history of pterosaurs. *74th annual meeting of the Paleontologistsdhe Gesellschaft*, 235-237a.
- Unwin, D.M., Jin, X., Liu, Y., & Ji, Q. (2009). Evidence for modular evolution in a long-tailed pterosaur with a pterodactyloid skull. *Proceedings of the Royal Society, B*, *277*: 383-389.
- Unwin, D.M., & Lü, J. (2013). The basal monofenestratan *Darwinopterus* and its implication

- for the origin and basal radiation of pterodactyloid pterosaurs. *International Symposium on Pterosaurs, Rio de Janeiro; Short communications, Rio de Janeiro (Universidade Federal do Rio de Janeiro, Museu Nacional)*, 98-101.
- Upchurch, P., Andres, B., Butler, R. J., & Barrett, P. M. (2015). An analysis of pterosaurian biogeography: implications for the evolutionary history and fossil record quality of the first flying vertebrates. *Historical Biology*, 27(6), 697–717.
- Wang, X., Kellner, A.W.A., Jiang, S.X., Cheng, X., & Meng, X. (2009). An unusual long-tailed pterosaur with elongated neck from western Liaoning of China. *Anais da Academia Brasileira de Ciências* 81(4). 793–812
- Wang, X.L., Kellner, A.W.A., Jiang, S.X., Cheng, X., Meng, X., & Rodrigues, T. (2010). New longtailed pterosaurs (Wukongopteridae) from western Liaoning, China. *Anais da Academia Brasileira de Ciências*, 82, 10451062.
- Wellnhofer, P. (1970). Die Pterodactyloidea (Pterosauria) der Oberjura-Plattenkalke Süddeutschlands. *Abhandlungen der Mathematisch-Physikalischen Klasse der Königlich Bayerischen Akademie der Wissenschaften*, 141, 1–133.
- Wellnhofer, P. (1975). Die Rhamphorhynchoidea (Pterosauria) der Oberjura-Plattenkalke Süddeutschlands. *Palaeontographica*, 148,1-186; 149, 1-30.
- Wellnhofer, P. (1978). Pterosauria. In: P Wellnhofer (Ed.), *Handbuch der Paläoherpetologie, Encyclopedia of Paleoherpetology*, 19 (pp. 1-82), Fischer-Verlag.
- Wellnhofer, P. (1991). *The illustrated encyclopedia of pterosaurs*. Salamander Books, London.
- Witmer, L.M., Chatterjee, S., Franzosa, J., & Rowe, T. (2003). Neuroanatomy of flying reptiles and implications for flight, posture and behaviour. *Nature*, 425(6961), 950–953. <https://doi.org/10.1038/nature02048>
- Witton MP. (2013). *Pterosaurs: natural history, evolution, anatomy*. Princeton University Press.
- Witton, M.P. (2015). Were early pterosaurs inept terrestrial locomotors? *PeerJ* 3, e1018.
- Witton, M.P., O’Sullivan, M., & Martil, D.M. (2015). The relationships of *Cuspicephalus scarfi* Martill and Etches, 2013 and *Normannognathus wellnhoferi* Buffetaut et al. 1998 to other monofenestratan pterosaurs. *Contributions to Zoology* 84, 115–127.
- Zhou, C.F., Gao, K.Q., Yi, H., Xue, J., Li, Q., & Fox, R.C. (2017). Earliest filter-feeding pterosaur from the Jurassic of China and ecological evolution of Pterodactyloidea. *Royal Society Open Science*, 4,160672.

Zhou, X., Pêgas, R.V., Ma, W., Han, G., Jin, X., Leal, M.E.C., Bonde, N., Kobayashi, Y., Lautenschlager, S., Wei, X., Shen, C., & Ji, S. (2021). A new darwinopteran pterosaur reveals arborealism and an opposed thumb. *Current Biology*, 31, 2429–2436.

Supplementary Material:

Supplementary Material 1. Phylogenetic Data Matrix of Fernandes et al., 2023

Supplementary Material 2. Phylogenetic Data Matrix of Martin-Silverstone et al., 2024

Supplementary Material 3. The relationship of *Melkamter pateko* to the Pterosauria, using the Martin-Silverstone et al. (2024) matrix (strict consensus).

Chapter 3. A new species and the earliest occurrence of the Gnathosaurinae (Pterosauria) from the Late Kimmeridgian of Brunn, Germany

Keywords: *Pterosauria, Gnathosaurinae, Mesozoic, Jurassic, Germany, Solnhofen Archipelago*

The chapter was submitted as: Fernandes, A.E., Tischlinger, H, Rothgaenger, M., & Rauhut, O.W.M. A new species and the earliest occurrence of the Gnathosaurinae (Pterosauria) from the Late Kimmeridgian of Brunn, Germany. (submitted June 27, 2024 to PalZ)

Author contributions:

- Alexandra E. Fernandes: Conceptualization, Data curation, Formal analysis, Investigation, Methodology, Software, Visualization, Writing-original draft, Writing-review & editing
- Helmut Tischlinger: Visualization, Writing-review & editing
- Monika Rothgaenger: Resources, Writing-review & editing
- Oliver W. M. Rauhut: Conceptualization, Data curation, Formal analysis, Funding acquisition, Project administration, Software, Supervision, Validation, Writing-review & editing

A new species and the earliest occurrence of the Gnathosaurinae (Pterosauria) from the Late Kimmeridgian of Brunn, Germany

ALEXANDRA E. FERNANDES^{1,2,*}, HELMUT TISCHLINGER^{3,4}, MONIKA ROTHGAENGER⁵ and OLIVER W.M. RAUHUT^{1,2,6}

¹SNSB, Bayerische Staatssammlung für Paläontologie und Geologie, Richard-Wagner-Straße 10, 80333 München, Germany

²Department of Earth and Environmental Sciences, Ludwig-Maximilians-University, Theresienstraße 41, 80333 München, Germany

³Tannenweg 16, 85134 Stammham, Germany

⁴Jura-Museum Eichstätt, Willibaldsburg, 85072 Eichstätt

⁵Museum Solnhofen, Bahnhofstraße 8, 91807 Solnhofen, Germany

⁶GeoBioCenter, Ludwig-Maximilians-Universität, Luisenstraße 37, 80333 München, Germany

*Corresponding author: Alexandra E. Fernandes fernandes@snsb.de

Acknowledgements

We thank the excavation team at the locality of Brunn, especially the late Martin Röper, for his continued efforts in documenting the fossil assemblages from this locality. Gratitude for the support of these excavations also goes to the Bildungs- und Dokumentationszentrum Ostbayerische Erdgeschichte e.V., the Freunde der Bayerischen Staatssammlung für Paläontologie und Geologie e.V., and the Bayerische Forstverwaltung. Thank you to Alessio Ciaffi for his beautiful artwork, and to Victor Beccari for assistance in CT scan segmentation. Thank you to Dr. Xu Xing and Dr. Shunxing Jiang for their kindness in providing information on the Chinese taxa included in the work. We also thank the reviewers for their constructive feedback, which greatly improved this manuscript.

Abstract

The so-called “Solnhofen limestones” of southern Germany are widely recognized for their abundance of Late Jurassic fossil vertebrates, with pterosaurs being no exception. Within the recognized plenitude of the pterosaurs within this assemblage, although ctenochasmatid remains are relatively abundant, gnathosaurines are far more scarce, with only one known

Solnhofen representative of the group known thus far. The Late Kimmeridgian locality of Brunn (near Regensburg, Germany) represents the oldest locality of the Solnhofen complex (“Solnhofen Archipelago” in recent literature), with only one pterosaur having been described from this locality to date. Here, a second pterosaur taxon from within this locality and a new gnathosaur is introduced, *Spathagnathus roeperi* gen. et sp. nov., whose novel tooth and dental enamel features add to the known dental diversity for the group. The new taxon represents the oldest occurrence of gnathosaurines and thus contributes further to the paleoenvironmental stratigraphic range for the Gnathosaurinae within the overall fossil assemblage of the Solnhofen Archipelago. Furthermore, the new taxon adds to the known diversity of ctenochasmatids in the Late Jurassic and thus underlines the importance of this early radiation of pterodactyloid pterosaurs during this time.

Keywords: *Pterosauria*, *Gnathosaurinae*, *Mesozoic*, *Jurassic*, *Germany*, *Solnhofen Archipelago*

Introduction

The so-called “Solnhofen limestones” of southern Germany are widely recognized for being one of the most productive fossil Konservat-Lagerstätten known to date (see Arratia et al., 2015, and references therein). The localities and beds found in the area between Solnhofen and Regensburg have been continually explored for some 200+ years (throughout the present day), yielding exceptional material at a prolific rate, and thereby giving a uniquely comprehensive insight into a subtropical shallow marine paleoenvironment of the Late Jurassic. Despite this long history of research, new species are still described frequently (e.g. López-Arbarelo &

Sferco, 2011; Hone et al., 2012; Rauhut et al., 2017; Schröder, López-Arbarello & Ebert, 2012; Ebert, Lane & Kölbl-Ebert, 2016; Bever & Norell, 2017; Villa et al., 2021), highlighting the broad scope of ecological specialization and paleobiodiversity inherently held in this, or any other such exceptionally-preserved microcosm of an ancient environment.

The high paleobiodiversity of the faunal assemblage in the overarching Solnhofen region is attributed to its original depositional setting in depressions within a shallow marine reef environment at the northern shore of the Tethys Ocean (see Viohl, 2015), so that this setting has been dubbed the fossil assemblage of the Solnhofen Archipelago in the recent literature (Röper, 2005; López-Arbarello & Schröder, 2011; Rauhut et al., 2017; Villa et al., 2021). Just as modern correlate reef environments are highly productive centers of vertebrate biodiversity, so too would this paleoenvironment have been prolific, including actinopterygian, chondrichthyan and coelocanthian fishes, turtles, lepidosaurs (rhynchocephalians and squamates), crocodylomorphs, dinosaurs, and pterosaurs (Arratia et al., 2015, and references therein). Within the Solnhofen Archipelago, the locality of Brunn represents the geologically oldest fossil assemblage, and has been exploited for fossils since the early 1990's (Röper & Rothgaenger, 1995). Despite the relatively short time of exploration of this locality, it has yielded a rich flora and fauna, including numerous vertebrates (Heyng, Rothgaenger & Röper, 2015; Rauhut et al., 2017). However, only three vertebrate specimens have been described in detail and classified from Brunn thus far, the novel species of pachycormiform actinopterygian *Orthocormus roeperi* Arratia & Schultze 2013, the rhynchocephalian *Sphenofontis velserae* Villa et al., 2021, and the scaphognathine pterosaur *Bellubrunnus rothgaengeri* Hone et al., 2012. Here, we describe a fourth vertebrate specimen from Brunn, and erect a second pterosaur species, based on a

partial maxillopremaxillary fragment found in 1993. The material is housed at the Staatliche Naturwissenschaftliche Sammlungen Bayerns - Bayerische Staatssammlung für Paläontologie und Geologie, Munich, Germany under the collection number SNSB-BSPG 1993 XVIII 1006.

Institutional abbreviations. SNSB-BSPG, Staatliche Naturwissenschaftliche Sammlungen Bayerns-Bayerische Staatssammlung für Paläontologie und Geologie, München, Germany.

Geographical and Geological Setting

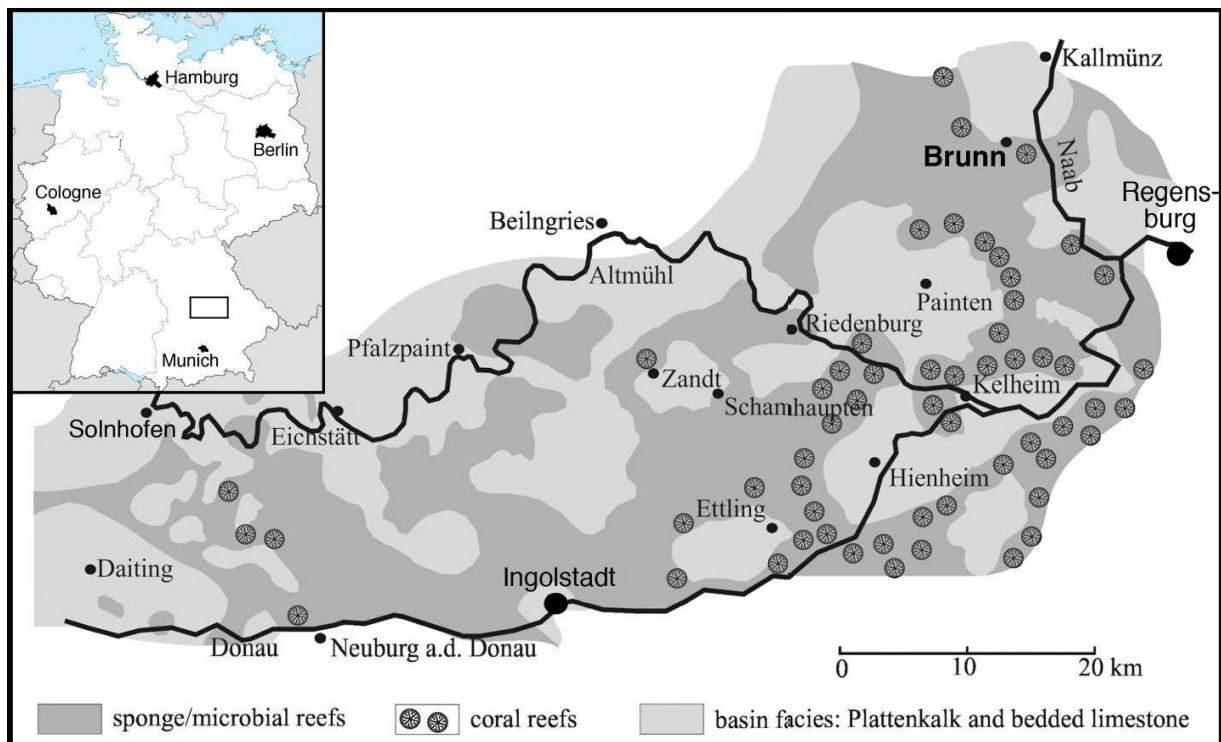


Figure 1. The locality of Brunn within the larger Solnhofen region (Rauhut et al., 2017).

In the Late Jurassic, the area that now constitutes the southern Franconian Alb in Bavaria was a lagoonal archipelago, part of a larger carbonate platform which comprised part of

a shallow epicontinental sea at the northern margin of the Tethys Ocean, bordered by the Bohemian Massif in the east and the Rhenian Massif to the north (Meyer & Schmidt-Kahler, 1990; Keupp et al., 2007; Viohl, 2015). The fossil-bearing localities of the region that are usually considered to represent the Solnhofen Archipelago (e.g. Röper, 2005; Fürsich et al., 2007; Viohl & Zapp, 2007; Ebert & Kölbl-Ebert, 2008; Heyng et al., 2011) are scattered throughout an area of some 100 km in East-West direction, from the town of Monheim to the city of Regensburg, and some 30 km in North-South extension, from the village of Kallmünz in the North to the Danube river in the south, although somewhat older but lithologically similar fossil localities are also found at Nusplingen in southern Baden-Württemberg, some 200 km to the south-west (Schweigert, 2015), and in Wattendorf, near Bamberg, some 100 km to the north (Mäuser, 2015). The sediments exposed here represent several different geological formations of the southern German Weißjura Group (Niebuhr & Pürner, 2014), which geochronologically span about 3.5 Ma from the Late Kimmeridgian to the Early Tithonian (Schweigert, 2007, 2015). The localities within the Solnhofen Archipelago are thus also stratigraphically variable, emerging from different horizons (e.g. Röper, 2005; Niebuhr & Pürner, 2014).

The locality of Brunn (Oberpfalz) is located along the northeastern border of the Solnhofen Archipelago region (Fig. 1). It is placed within the Ebenwies Member of the Torleite Formation and is the oldest locality known within the Solnhofen Archipelago *sensu stricto*, having been dated to the Subeumela Subzone of the Beckeri Ammonite Zone of the Late Kimmeridgian (Röper & Rothgaenger, 1997; Niebuhr & Pürner, 2014; Schweigert, 2007, 2015). During this time period, the region consisted of a semi-tropical shallow marine environment, housing sponge-microbial and coral reef complexes (Viohl, 2015), in between which laminated

limestones were deposited within shallow depressions. The Brunn locality sits at the southern rim of one of these depressions, at the Pfreundorf-Heitzenhofen Basin (Rauhut et al., 2017). The locality is composed of intercalated massive and finely-laminated limestones, with an approx. eight-meter section of eight different Plattenkalk layers outcropping (Heyng, Rothgaenger & Röper, 2015), yielding various fossil remains from the finely-laminated layers. Because Brunn has been recognized for its abundant plant fossils (including land plants), it is thought to have more terrestrial input than is typical of most other localities within the Solnhofen Archipelago. Vertebrate remains are relatively common in the locality of Brunn and include a diverse fauna of actinopterygian fishes, some chondrichthyans, and rare tetrapods (Rauhut et al., 2017). The latter include turtles, rhynchocephalians, crocodyliforms and pterosaurs. Regarding pterosaur material, Plattenkalk layer 1 has so far yielded an isolated pterosaur humerus (Röper, 1997; Rauhut et al., 2017) and the specimen described herein, and the pterosaur *Bellubrunnus rothgaengeri* was discovered from Plattenkalk layer 6 (Hone et al., 2012).

Materials and Methods

The specimen described here was found during systematic excavations in the Brunn quarry, led by Martin Röper and Monika Rothgaenger. It was discovered by Simone Kaulfuß, Maren Sendelbach and Andreas Heiner, then students at the school for Schule für Präparationstechnische Assistenten in Bochum, during a field trip to the locality. The specimen came from Plattenkalk layer 1, the lowest layer in the sequence, which has mainly yielded more disarticulated remains than some of the more upper layers. It was found isolated during

splitting of the layer. As it is usual in the lithographic limestones of southern Germany, the specimen has suffered moderate dorsoventral compression. It was mechanically prepared and briefly described and figured by Rauhut et al., 2017: pp.321-322, fig. 15) and is kept permanently in the collections of the Bayerische Staatssammlung für Paläontologie und Geologie in Munich under the collection number SNSB BSPG 1993 VIII 1006.

Phylogenetic analysis was conducted using TNT version 1.6 (Goloboff, Farris & Nixon, 2008; Goloboff & Morales, 2023) using the matrix of Fernandes et al. 2023 (based on the matrix of Andres, 2021), and augmented by the ctenochasmatid pterosaur *Tacuadactylus luciae* Soto et al. 2021 and the additional new taxon described herein (represented in the analysis by “Brunn”). The new character state “veined” was also added for character 174 “Dentition, texture” regarding tooth enamel. Thus, the final matrix had 181 terminal taxa scored for 275 characters (51 continuous and 260 discrete; using ordered characters as well). The data matrix is available in the supplementary material, and also at <http://morphobank.org/permalink/?P3967>. A basic traditional tree-search analysis was conducted with 2,000 random addition sequence replicates. The resulting cladogram has been simplified in the software Adobe Illustrator, the complete topology of which can also be found in the supplementary data set.

UV photography was executed by using the techniques described by Tischlinger, 2015 and Tischlinger & Arratia (2013), using a high-performance Labino UV-A lamp, Spotlight S 135, 35 watt, 365 nanometers, equipped with a custom-made midlight-reflector-inset. Photos were taken with a Lumix GX80 with a Lumix G 2,8/30 mm Macro OIS lens.

CT scans were performed in Leiria, Portugal, with a microfocus CT system GE VtomeX M 240. Scan images were segmented and assembled utilizing Avizo and Meshlab softwares (GE Sensing & Inspection Technologies GmbH., Wunstorf, Germany), and are available at MorphoSource). The segmentation of the complete specimen was done using manual selection slice-by-slice in the software Avizo v9.1 (Thermo Fisher, Waltham, MA, USA). All meshes were exported as Wavefront Files (.obj) and treated in the open-source software Blender v3.4. All meshes were smoothed for rendering using the Smooth Laplacian modifier (Lambda factor =1 and 10 repeats).

Nomenclatural Acts

The electronic edition of this article conforms to the requirements of the amended International Code of Zoological Nomenclature, and hence the new names contained herein are available under that Code from the electronic edition of this article. This published work and the nomenclatural acts it contains have been registered in ZooBank, the online registration system for the ICZN. The electronic edition of this work was published in a journal with an ISSN and has been archived and is available from the following digital repositories: PubMed Central and LOCKSS.

Data Archiving Statement

This published work and the nomenclatural acts it contains have been registered with ZooBank.

Results

Systematic Paleontology

Order **PTEROSAURIA** Owen, 1842

Suborder **PTERODACTYLOIDEA** Plieninger, 1901

Family **CTENOCHASMATIDAE** Nopsca, 1928 sensu Unwin, 2003

Subfamily **GNATHOSAURINAE** Nopsca, 1928 sensu Unwin,

2002 Genus ***Spathagnathus*** **gen. nov.**

Type species ***Spathagnathus roeperi*** **sp. nov.**

Etymology: From the Latin “spatha” for “spatula”, and “gnath” for “jaw”; “roeperi” in honor of the late Martin Röper, long term director of the Bürgermeister-Müller-Museum in Solnhofen and leader of the excavations at the locality Brunn since the early 1990’s.

Holotype: SNSB-BSPG 1993 XVIII 1006, fragment of the anterior part of a maxillopremaxillary rostrum with toothrow.

Type locality and horizon: Brunn, Germany. Southern rim of the Pfraundorf-Heitzenhofener Basin. Ebenwies Member of the Torleite Formation. *Subeumela* Subzone of the *Beckeri* ammonite Zone, Late Kimmeridgian, Upper Jurassic.

Diagnosis (autapomorphies indicated with asterisk): dorsoventrally compressed rostrum with lateral spatulate expansion on the anterior end of the premaxilla, laterally directed boomerang-shaped teeth*, tooth girth increasing from anterior to posterior end of the rostrum, dental enamel coating approximately half of tooth crowns, strongly veined enamel texture on tooth surface*, presence of carinae.

Description

The specimen SNSB-BSPG 1993 XVIII 1006 preserves the anterior-most portion of the rostrum in palatal view (Fig. 2), in a slab and counterslab (although the counterslab preserves only the very apicalmost tips of some of the teeth, embedded in sediment). The overall anteroposterior length of the preserved rostrum is 36.9 mm. The width of the posterior-most preserved end is 5.2 mm, and the widest point of the expanded proximal end is 9 mm. Despite being dorsoventrally flattened by lithostatic pressure (a typical condition for Lagerstätten specimens), the overall condition of what is preserved is relatively good as the specimen sustains only a slight overall shattered surface, with cortical bone remaining intact and in situ. Pterosaur material with a well-preserved palatal region is uncommon and there has been some recent discourse on actual palatal morphology (Ósi et al., 2010; Pinheiro & Schultz, 2012; Cheng et al., 2017; Zhou et al., 2017; Chen et al., 2024). Accordingly, it is difficult to distinguish the exact margin between the premaxilla and maxilla (as no clear suture between them is visible), so they were likely already fused, as in other pterosaurs (e.g. Howse & Milner, 1995). Although Rauhut et al., 2017 had also identified the presence of fused palatines in this specimen (following the interpretation of these bones in Howse & Milner, 1995 in *Plataleorhynchus streptophorodon*),

recent insights on the palatal morphology of pterosaurs (Ósi et al., 2010; Pinheiro & Schultz, 2012; Cheng et al., 2017, Zhou et al., 2017; Chen et al., 2024) indicate that here only the premaxilla and maxilla are actually preserved; the structure identified by Rauhut et al. more likely represents a dorsally-inset portion of the medial fused maxilla (although one cannot rule out that it could also be the vomer, such an anterior position would be unlikely for the Ctenochasmatidae), which resulted in slight grooves appearing to run between this region and the laterally-lying dentated region of the maxilla. There is a mediolateral crack visible at the portion of the rostrum where the spatula begins to expand, but this is likely taphonomic. The anterior-most spatulated portion of the premaxilla displays an antero-posterior fissure running medially (likely a taphonomic post-mortem break). There is no sign of a premaxillary crest (nor in the CT images of the dorsal side of the rostrum), although one cannot rule out the existence of one, as it may have been more posteriorly placed.



Figure 2. SNSB-BSPG 1993 XVIII 1006 *Spathagnathus roeperi* photographed under normal light (A) and UV light (B). Scale bar represents: 10 mm.

The tip of the rostrum expands laterally to form a spatulated terminal rosette (Fig 2.), the condition seen in all gnathosaurines (Wellnhofer, 1970; Howse & Milner, 1995). The expansion of the rosette begins at approximately 11.2 mm from the tip of the snout, with the

widest point of the rosette measuring 9 mm mediolaterally. Foramina are interspersed throughout the entirety of the rostrum in no discernable pattern, although they are especially concentrated throughout the spatulate region of the premaxilla. In the dentated region of the maxilla, a constant mediolateral width is maintained throughout. The alveoli face anterolaterally, and the distance between individual alveoli is consistently slightly larger than their mesiodistal length, a pattern that is preserved even as the teeth increase in girth as one moves posteriorly along the jaw. Accordingly, the size of the alveoli also increases posteriorly. The rims of each alveolus are expanded, giving the crenulated appearance typical of many gnathosaurine rostra (e.g. Wellnhofer, 1970; Howse & Milner, 1995; Soto et al., 2021).

All maxillary teeth are exposed on the sediment by their lingual side only, are in individual sockets, and all in situ. They have a distinct and unique boomerang shape, and the displacement of the tip in respect to the base (due to the tooth curvature) is more than the width of the tooth itself. Although there are no teeth on the rosette that are visible to the naked eye, the CT scan data shows roots (or potential germs) of at least four preserved teeth (Fig. 3). The right maxilla preserves six to seven tooth positions, and the left maxilla preserves seven, totaling thirteen teeth that are visibly preserved, although only two (one tooth on the right side, and one tooth on the left) remain complete from root through apex. The remainder of the teeth are broken along their crowns, with some of the apicalmost tips embedded in the sediment of the counterslab. The manner in which all of the teeth are increasingly broken along the posterior of the rostrum indicates that they were positioned more and more ventrally as one moves posteriorly in the transverse plane, a change which happens with uniformity and is therefore unlikely to be taphonomic. Otherwise, this condition could also be indicative of a

slight degree of rostral curvature, although the state of taphonomic compression makes this indiscernible.

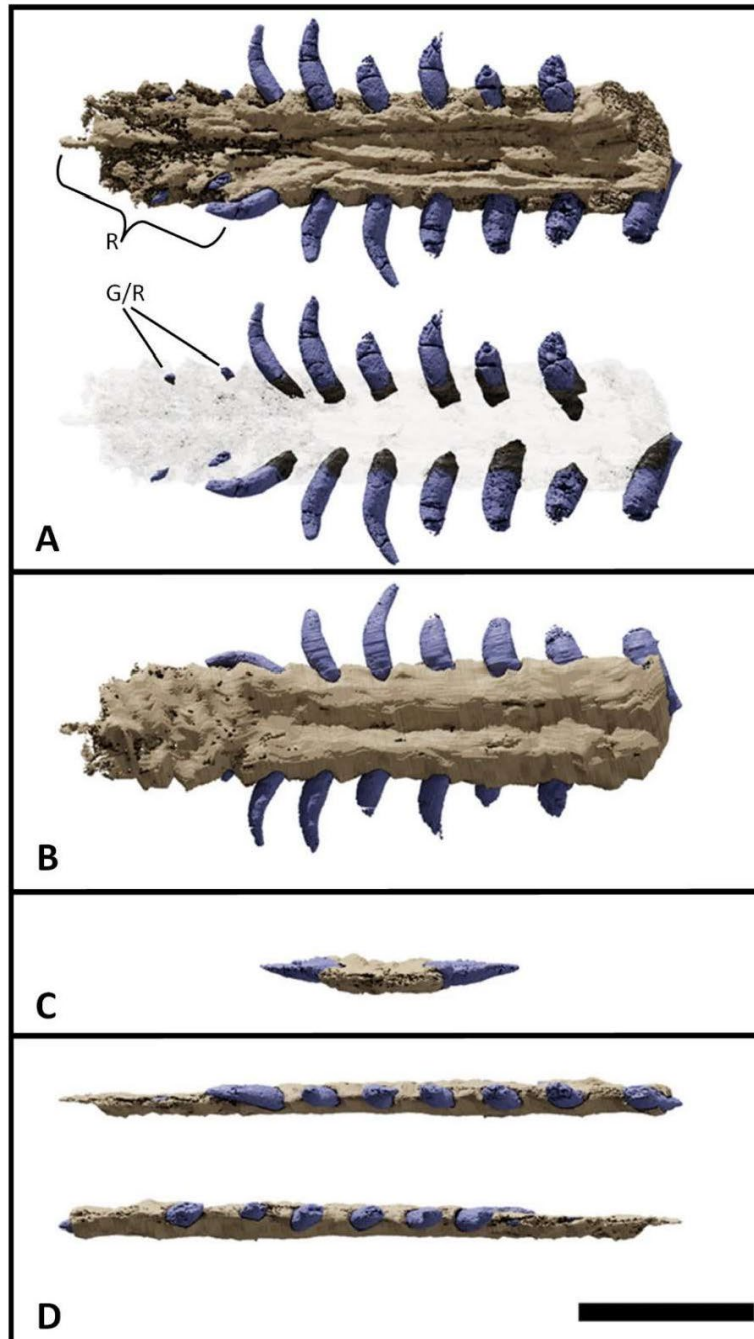


Figure 3. Rendering of CT scan data (with visible premaxillary tooth roots or germs) in palatal (A), dorsal (B), anterior (C), and lateral (D) views. R=rosette; G/R=germs/roots. Scale bar represents: 10 mm.

All teeth are conical, round to ovoid in cross-section at the root and becoming more laterally compressed apically. All teeth have a visible carina on their mesial margins, beginning at the base of the crown and running parallel to the natural curvature of each tooth through the crown apex. The carina is slightly lingually directed, resulting in a shallow longitudinal furrow adjacent to the carina on the lingual side of the crown, which is, however, restricted to its apical two thirds. The mesial teeth are slender, but the teeth seem to become more robust distally; whereas the fore-aft basal length of the third preserved tooth in the left maxilla is 1.1 mm, that of the sixth preserved tooth is 1.6 mm. All teeth are procumbent from the long axis of the jaw, and recurved mesiodistally as well as lingually (although the extent to which may be unduly exaggerated by taphonomy). In the more complete mesial teeth, the flexure seems to be concentrated in a flexure point at about half of the crown height, apical and basal to which the crown is almost straight. The teeth exhibit the typical, unique enamel extent of the Pterosauria (Wellnhofer, 1978, 1985; Fastnacht, 2005), where the tooth enamel stops at an enamel-dentine boundary (EDB), which here occurs about halfway up the crown as a slightly raised portion of the tooth, with a marked change in texture and shine (the crown base is pitted and dull, whereas the more apical enameled region of each tooth is shiny and rippled). The enamel is strongly textured overall, displaying a corrugated veined pattern of irregular longitudinal folds (Fig. 4). In cross-section, the enamel is thick (visible on the broken teeth), and the pulp cavity seems to have been rather small and restricted to the basal part of the crown. The two complete teeth have pointed tips, although their apices both show a distally-oriented wear facet (not likely to be any result of dental occlusion).



Figure 4. Detailed view of veined dental enamel patterning (A) and enamel distribution along the tooth crown (B).

Phylogenetic Analysis

Phylogenetic analysis was conducted to analyze the evolutionary relationships of the Brunn specimen within the Pterosauria. The phylogenetic analysis resulted in a single most parsimonious tree (Fig. 5) with a tree length of 1375.905 steps (consistency index [CI] = 0.287, retention index [RI] = 0.787). *Spathagnathus roeperi* was retrieved as the sister taxon of *Tacuadactylus luciae*, a relationship supported by their veined dental enamel texture (character 173). The Gnathosaurinae are phylogenetically defined as the least inclusive group including *Gnathosaurus subulatus* von Meyer, 1834 and *Huanhepterus quingyangensis* Dong, 1982 (Unwin, Lü & Bakhurina, 2000 sensu Unwin, 2002; Andres, 2021), and thus, *Spathagnathus roeperi* falls within the Gnathosaurinae, a relationship which is supported by their dorsoventrally depressed rostra, the lateral expansion at the anterior end of the rostra, and their laterally procumbent dentition.

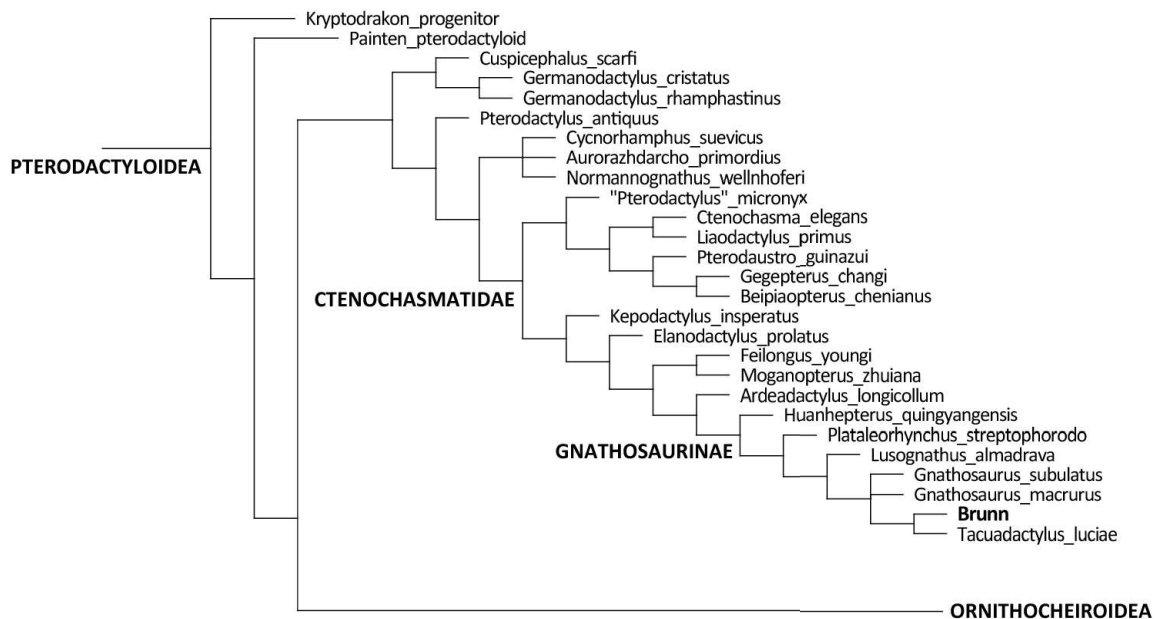


Figure 5: Phylogenetic results displayed as a simplified tree of the Pterodactyloidea, showing the relationship of *Spathagnathus roeperi* (“Brunn”) within the Gnathosaurinae, after the data matrix by Fernandes et al., 2023 (based on Andres, 2021). Non-pterodactyloid pterosaurs were removed from this figure, and the clade Ornithocheiroidea was simplified, to make the figure concise.

Discussion

Phylogenetic position of *Spathagnathus roeperi* and evolutionary implications

The recognition of SNSB-BSPG 1993 XVIII 1006 as a new taxon within the Ctenochasmatidae (and Gnathosaurinae), as originally suggested by Rauhut et al., 2017 (but not tested in a phylogenetic analysis) is here reaffirmed. This prior attribution was made based on the presence of a narrow, parallel-sided rostrum (with more laterally than ventrally pointing teeth) and the large number and shape of the elongate, slightly recurved maxillary teeth (likely involved in a style of filter feeding [i.e. Martill et al., 2022]). The gnathosaurine affinities were based on the rounded expansion of the anterior end of the rostrum, and the previous authors

also pointed out that the specimen was likely a new taxon due to the fact that it differed from other gnathosaurines in its short premaxilla (with few teeth), the change in tooth morphology in the anterior maxilla, and the “ornamented” enamel (with marked mesial carinae). Thus, *Spathagnathus roeperi* adds to the growing diversity of gnathosaurines in the Late Jurassic, most probably (depending on the exact age of *Lusognathus almadrava* Fernandes et al., 2023) representing the oldest known member of the clade (Table 1).

Table 1. A comparison of age, rostral tooth density, and size of known Gnathosaurinae species

Species	Age	Tooth Density	Wingspan	Citation
<i>Spathagnathus roeperi</i>	Kimmeridgian (~152.0 Ma)	3.27 teeth/cm	N/A	N/A
<i>Lusognathus almadrava</i>	Kimmeridgian-Tithonian (~152.0 Ma)	1.3 teeth/cm	>3.6 m	Fernandes et al. 2023
<i>Tacuadactylus luciae</i>	Late Jurassic	1.58-2 teeth/cm (according to Perea?)	N/A	Soto et. al 2021
<i>Gnathosaurus subulatus</i>	Tithonian(?)	2-3 teeth/cm	~1.7 m	Wellnhofer 1970
<i>Huanhepterus quingyangensis</i>	Late Jurassic (re-dated as Early Cretaceous)	1.6 teeth/cm	~2.5 m	Dong 1982; Howse & Milner 1995; Wang & Lü 2001
<i>Plataleorhynchus streptophorodon</i>	Tithonian/Berriasian	2-3 teeth/cm (2.9 according to Perea)	~2-2.5 m	Howse & Milner 1995
<i>Gnathosaurus macrurus</i>	Berriasian (~145-139.8 Ma)	2.0-2.5 teeth/cm	~1.8 m	Howse & Milner 1995

The immediate outgroup to gnathosaurines is represented by *Ardeadactylus longicollum* Bennett 2013, the neotype specimen of which comes from the Upper Kimmeridgian laminated limestones of Nusplingen, Baden-Württemberg (Wellnhofer, 1970; Bennet, 2013). Interestingly, the genus *Ardeadactylus* has also been identified on the basis of an isolated femur from Brunn (Rauhut et al., 2017), which also represents the oldest record of this genus. Asian representatives of gnathosaurines, or from the stem-lineage of this clade after their split from ctenochasmatines, are only known from Cretaceous deposits; whereas the oldest ctenochasmatine, *Liaodactylus primus* Zhou et al., 2017, is known from the early Late Jurassic Yanliao Biota of China (Zhou et al., 2017); this otherwise prolific pterosaur Lagerstätten has not yielded any gnathosaurine ctenochasmatids so far. The phylogenetic relationships and the distribution of gnathosaurines and their immediate outgroup in the Late Jurassic might thus indicate a European origin and early diversification of the clade, although such an interpretation should be seen with caution, given the poor fossil record of pterosaurs in the Late Jurassic outside the Solnhofen Archipelago and the Yanliao Biota in general, and in the Southern Hemisphere in particular. In this respect, the sister taxon relationship of *Spathagnathus* with the Uruguayan *Tacuadactylus luciae* is noteworthy. The occurrence of a close relative of the southern Germany taxon in South America helps to highlight our still very poor knowledge of the evolution and distribution of these early pterodactyloids. The sister group relationship between these two taxa is based in the shared characters of the presence of carinae and enamel ornamentation on the teeth, although both are much less developed in *Tacuadactylus* than in *Spathagnathus*. As such dental characters are most probably related to feeding ecology

of the animals involved (see below), more material of both taxa would be needed to rule out that these proposed synapomorphies might simply be convergence due to similar feeding ecology. The sister taxon relationship between these two taxa thus either indicates that these animals could disperse very rapidly, even over continents (which would not be impossible for flying vertebrates), or that much of their evolutionary history is still to be found, possibly in sediments of the Southern Hemisphere.

Considerations on the ontogenetic stage of *Spathagnathus roeperi*

Regarding the fused premaxillae of *Spathagnathus*, even utilizing computed tomography, the margins of the anterior rosette appear quite damaged. This is unsurprising, given that it is dorsoventrally the thinnest portion of the rostrum, and thus less taphonomically durable. However, an early ontogenetic stage could readily account for this previously-observed “short” premaxilla (Rauhut et al., 2017). In fact, changes in rostrum shape might well have occurred over the lifetime of these animals, as occurs in modern spoonbill rostra, where the bill in juveniles is more tubular and not yet spatulate, but thickens during ontogeny, becoming more bulbous with age until full bill length is reached at about 36 months of age (Hancock, Kushlan & Kahl, 1992). *Ctenochasma elegans* Wagner, 1861 was also observed to similarly have the distal end of its upper rostrum becoming more laterally expanded with age (Bennett, 2007), as was *Hamipterus tianshanensis* Wang et al., 2014, which was observed to have an ontogenetic expansion of the rostrum, becoming more progressively robust (Wang et al., 2014). In accordance with this, as pointed out by Bennett & Pankalski (2018), closely-spaced subparallel blood vessels (the presence of which can be inferred from the foramina interspersed along the

rostrum of SNSB-BSPG 1993 XVIII 1006) create the potential for increased bone deposition, which could also indicate growth over time.

There are other traits which also raise the question of the ontogenetic stage of the type specimen of *Spathagnathus roeperi*, despite most Solnhofen pterosaurs also being relatively small in size (partly because sampling favors smaller [and younger] individuals [Bennett, 1995]). In the absence of available material suitable for histological sampling or enough individuals to conduct reliable principal component analysis, identifying the ontogenetic stage of a pterosaur specimen is mainly reliant on three main factors: the degree of ossification, the fusion of skeletal elements, and the state of bone grain (Bennett, 1993). What remains of the Brunn specimen is not easy to categorize using any of three distinctions, because bone texture and suture marks may have been obscured by the taphonomic crushing that the rostrum has sustained, and although the premaxilla does preliminarily seem completely fused, there have been instances where a premaxilla can be completely fused despite ontogenetic immaturity, as pointed out in *Dorygnathus banthensis* Theodori, 1830 (Ósi et al., 2010).

Dentition and ecological implications

Morphologically, the appearance of the “needle-like” thin tooth shape and sub-circular cross-section (with slight antero-posterior compression) in *Spathagnathus* is in keeping with all ctenochasmatids (Wellnhofer, 1970; Fastnacht, 2005; Bestwick et al., 2018). However, there are also marked differences from other gnathosaurs. According to the CT scan data of the Brunn specimen (Fig. 3), all tooth roots remain firmly nested within the maxillary bone, with an additional four potentially “budding” (or simply eroded) teeth also present in the anterior-most

spatulate region of the rostrum (although it remains unclear whether these are tooth germs, or were simply full-size teeth that were eroded prior to or during deposition). The dental ontogeny of *Ctenochasma* sp. is also discussed by Bennett (2007), who found that in young individuals, the posterior teeth on the tooth row are more closely spaced than the anterior teeth (potentially reflecting rapid growth of the mandible and formation of new teeth at the posterior end of the tooth row). Although the Brunn specimen does not follow this pattern, its teeth do grow more robust from the anterior to posterior position along the toothrow, which may simply correspond to a stronger bite due to more stress during occlusion in the posterior region of the jaw, a trait which has been suggested to pertain to durophagous animals which might develop a more robust dentition in this part of the jaw (Fastnacht, 2005; Hone, Jiang & Xu, 2018). Although *Spathagnathus* was not likely to be strictly durophagous, this trait could certainly be indicative of filtering out “harder” prey items, like shellfish or other chitinous prey.

Also atypical in the teeth of the Brunn specimen is the presence of carinae. Although most pterosaurs exhibit carinae, ctenochasmatid teeth are most often devoid (Fastnacht, 2005). The distribution and phylogenetic significance of carinae in pterosaur dentition has yet to be fully explored, however, carinae make a substantial functional difference in prey acquisition, as the force needed for puncturing is much lower in a laterally compressed tooth construction with carinae than without (Fastnacht, 2005). Only one other gnathosaur is described as having carinae, *Tacuadactylus luciae* (Soto et al., 2021), although they are much more inconspicuous in that specimen. In this case, the markedly robust carinae of the Brunn specimen are unique, implying that it was more easily capable of consuming harder prey than the average ctenochasmatid.

Enamel structure and distribution are reliable metrics and stable differentiators in identifying teeth because enamel is acellular and does not have the ability to regrow (and therefore is not altered after its initial deposition). It is formed as a tooth develops (through amelogenesis), and is invariably thin in most carnivorous reptiles, both fossil and extant (Cullen et al., 2023), although *Spathagnathus* exhibits rather thick enamel compared to other pterosaurs. Enamel does not undergo any remodeling over a species' lifespan (and is unaffected by ontogenetic modifications), and so the enamel microstructure and surface morphology is fixed, and any features it contains (such as ornamentation) are formed by the enamel itself (and not reflected in the dentin below) (Sander, 1999). Enamel also bears an important functional purpose: the thickness of individual enamel layers is variable between species and/or individuals in adaptation to their different biomechanical requirements (Wilmers & Bargmann, 2020).

To date, most ctenochasmatid tooth enamel texture has been described as smooth (e.g. Knoll, 2000; Fastnacht, 2005), and among the gathosaurs, the ornamented tooth enamel of *Spathagnathus* is a feature only shared with *Tacuadactylus luciae* (along with the presence of dental carinae, although it remains ambiguous if they are mutually exclusive or not). The functional advantages of a veined enamel texture likely relate to an improved crown strength, as it has been suggested that veined enamel, although rare in small-bodied animals, may be biomechanically advantageous for more powerful occlusion, as great bite forces coupled with long teeth would require wavy enamel (with its isotropic properties of wear and abrasion resistance) (Sander, 1999). Veined enamel could even potentially be hydrodynamically advantageous for feeding in aquatic environments (Massare, 1987).

Dentin is of mesenchymal origin and continues to form after a tooth has erupted, whereas enamel originates from epithelial cells and is fully formed before the tooth erupts (Sander, 1999). The visible presence of dentine (as seen in the Brunn specimen) is common in teeth that are exposed to the environment (Cullen et al., 2023) and not shielded by extraoral tissues. Because dentine has a higher tensile strength than enamel (and is therefore much more flexible), the percentage of enamel coverage on teeth makes a big difference in tooth flexibility. Although the tooth construction of gnathosaurines and ctenochasmatids are prohibitive to having great penetrative capabilities since their thin shape makes them susceptible to failure by axial loads (Fastnacht, 2005), among these three groups gnathosaurs would have the highest resistance to high bending moments and stress, given their generously dentine-exposed tooth bases and their enamel-dentin junction being apically higher along the crown (giving increased lateral flexibility and providing a reduction of strain and stress throughout the tooth when in use). These features also provide greater elasticity than that of teeth with a complete enamel cover (Fastnacht, 2005), indicating a great resistance to breakage.

Computer modeling of pterosaur skulls show that ctenochasmatids had very low bite forces (despite fast closing jaws), which would be in accordance with feeding on small evasive prey/filter feeding (Henderson, 2018). However, gnathosaurs, with their teeth more robust and widely-spaced than other ctenochasmatids, were seemingly specialists, occupying a different ecological niche than traditional filter-feeders (whose teeth need to be closely spaced together to maximize efficacy), or at least going after larger-sized prey, seeing as how a reduction of contact between tooth and food item is required for penetrating hard food items (e.g. Evans & Sanson, 1998), potentially crustaceans or other small marine organisms. Although the more

laterally-expanded spatulas of gnathosaurines could also indicate water-feeding (with perhaps an adaptation to move larger volumes of water), the robustness of their teeth indicates greater piercing strength than in the finer-toothed ctenochasmatids, whose slighter dentition would be more appropriate for smaller sized food particles (such as plankton, i.e. Martill et al., 2022). Gnathosaur tooth spacing also implies less effective tooth–tooth occlusion (despite just one single known instance of tooth-tooth occlusion for all ctenochasmatids, in *Forfexopterus jeholensis* Jiang et al., 2016 [Zhou, Wang & Wang, 2022]). The eroded apical tips of *Spathagnathus* were therefore most likely formed by tooth–food contact during prey capture (Ósi, 2011), as the tips of the complete teeth were smoothly worn down in a fashion that is almost perpendicular to the long axis, also suggesting harder prey (i.e. Massare, 1987).

Dietary switches throughout ontogeny happen regularly in the extant animal kingdom, for example, in crocodiles, where body sizes dictate both the type and variety of foods consumed by individuals, with young animals primarily preying on insects (e.g. Coleoptera, Orthoptera and Odonata) and arachnids, and later on as they increase in age and size, intermediate size-classes feed on amphibians, small mammals, birds, reptiles, crustaceans, gastropods and arachnids in varying proportions as well as insects and fish, terminating with sub-adults and adults consuming fish and large mammals as their primary prey (Wallace, 2006). These changing appetites are a direct result of not only their changing physical size (i.e. spatial bite capacities), but also as a result of the morphological changes of their feeding apparatus throughout development (e.g. the shape-changing of rostra), especially affecting their ability to engage in disarming the various defensive mechanisms of specific prey (Wallace, 2006). In the Rhamphorhynchoidea, it has also been observed that growing teeth can produce different

patterns between juveniles, subadults, and adults: teeth start out small, but then subsequently are replaced by larger teeth at a more anterior angle as the skull grows (Bennett, 1995). These changes accommodate spatial needs, but also imply a more complex functional shift in an individual's capabilities regarding prey handling, which would lead to differences in feeding niches over the course of its lifespan (as commonly seen in reptiles, where offspring usually feed themselves [Bestwick et al., 2020]). The proportionately shorter, stouter teeth of adult individuals of the Rhamphorhynchoidea (when compared to subadults) exhibit an adaptation for feeding on larger and more powerful prey than younger individuals (Bennett, 1995). Although fish eaters generally also have a high number of slender, recurved teeth, wrinkled dental enamel is more typical of durophagous animals (Sander, 1999), and evidence from coprolites has affirmed that small foraminifera, crustaceans, worms, and various gastropods and bivalves as deliberate targets of ctenochasmatid food sources (Qvarnström et al., 2019). Therefore it is likely that gnathosaurs, with their more robust teeth, were going for the harder range of these food items. Furthermore, the higher relative abundance of foraminifera in larger coprolites also supports an ontogenetic switch to a more specialized filter feeding in adults, whereas younger individuals would have relied more on eating soft-bodied organisms from the sediments (Qvarnström et al., 2019).

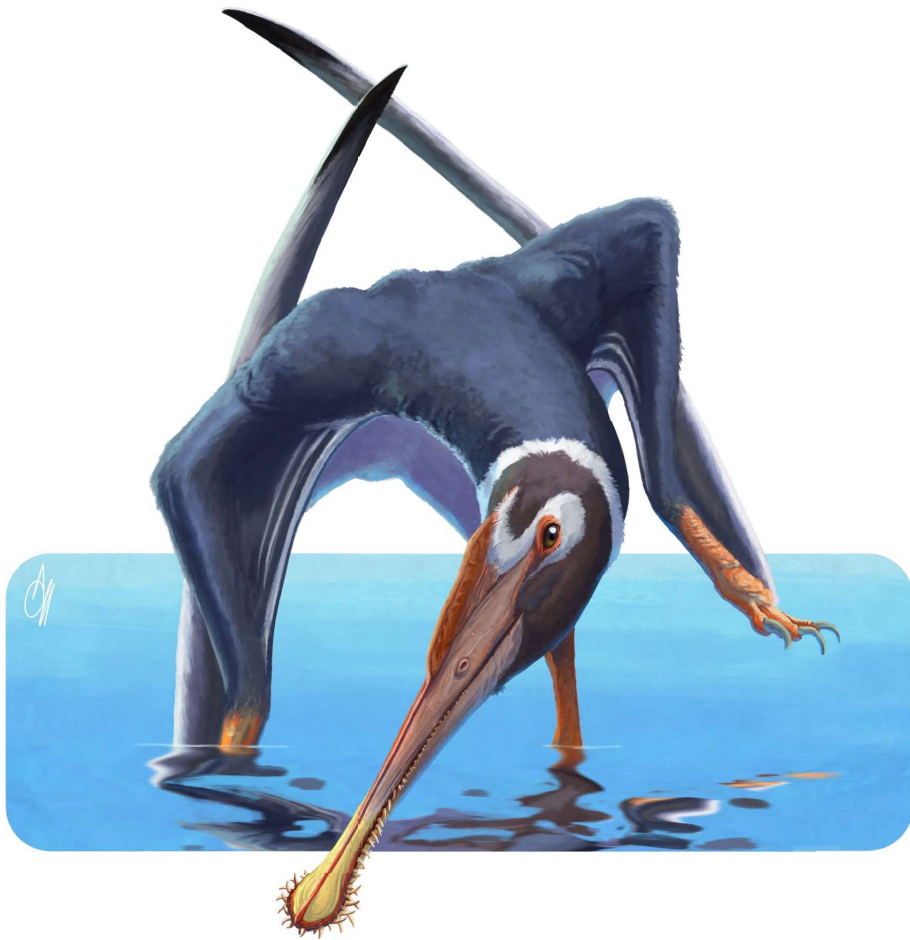


Figure 6. Artistic reconstruction of *Spathagnathus roeperi* by Alessio Ciaffi.

Conclusion

The extreme variability in the pterosaurian dental apparatus across time and space was likely an ecomorphological adaptation to their manifold inhabited environments, and reflective of their numerous different feeding strategies and diverse prey preferences throughout their evolution (Ósi, 2011). Differences in tooth morphologies and enamel patterning of globally-concurrent ctenochasmatid and gnathosaurine taxa could indicate mosaic evolution, possibly as an adaptation to their differing paleoenvironmental niches. Previous studies have already

illustrated cases of small clades comprising closely related species that are endemic to the Solnhofen Archipelago, whose evolution was driven by palaeogeographical and chronostratigraphical changes (López-Arbarello & Schröder, 2014; Konwert, 2016; Rauhut et al., 2017). The fact that the new species described herein, *Spathagnathus roeperi* (with its novel specialized tooth and dental enamel morphology suggesting hard prey preferences or even possible durophagy) (Fig. 6), was also locally-coeval with the scaphognathine *Bellubrunus rothgaengeri*, provides an even more diverse picture unfolding for the pterosaurs and general fauna of the Brunn locality, the oldest time slice of the larger Solnhofen Archipelago.

Author Contributions

Alexandra E. Fernandes contributed data curation, formal analysis, investigation, visualization, and writing-original draft. Helmut Tischlinger contributed visualizations, writing-review, and editing. Monika Rothgaenger contributed resources and writing-review. Oliver W.M. Rauhut contributed conceptualization, formal analysis, funding acquisition, project administration, supervision, and writing-review and editing.

Declarations

AEF is supported by funding from DFG grant number RA 1012/29-1.

The authors have no competing interests to declare that are relevant to the content of this article.

All authors certify that they have no affiliations with or involvement in any organization or entity with any financial interest or non-financial interest in the subject matter or materials discussed in this manuscript.

The authors have no financial or proprietary interests in any material discussed in this article.

References

- Andres, B. (2021). Phylogenetic systematics of *Quetzalcoatlus* Lawson 1975 (Pterodactyloidea: Azhdarchoidea). *Journal of Vertebrate Paleontology*, 41(1), 203–217.
- Arratia, G., Schultze, H.-P., Tischlinger, H. & Viohl, G. (2015). *Solnhofen – Ein Fenster in die Jurazeit*, Pfeil-Verlag.

- Arratia, G. & Schultze., H.-P. (2013). Outstanding features of a new Late Jurassic pachycormiform fish from the Kimmeridgian of Brunn, Germany and comments on current understanding of pachycormiforms' in G. Arratia, H.-P. Schultze, M.V.H. Wilson (Eds.), *Mesozoic Fishes 5 - Global Diversity and Evolution, Proceedings of the international meeting Saltillo 2010*, Coahuila, Mexico (pp. 87-120).
- Bennett, S.C. (1993). The ontogeny of Pteranodon and other pterosaurs. *Paleobiology*, 19, 92–106.
- Bennett, S.C. (1995). A Statistical Study of *Rhamphorhynchus* from the Solnhofen Limestone of Germany: Year-Classes of a Single Large Species. *Journal of Paleontology*, 69(3), 569–580.
- Bennett, S.C. (2007). A review of the pterosaur Ctenochasma: taxonomy and ontogeny. *Neues Jahrbuch für Geologie und Paläontologie, Abhandlungen*, 245, 23-31.
- Bennett, S.C. (2013). New information on body size and cranial display structures of *Pterodactylus antiquus*, with a revision of the genus. *Paläontologische Zeitschrift*, vol. 87, no. 2, pp. 269–289.
- Bennett, S.C. & Pankalski P. (2018). Waves of bone deposition on the rostrum of the pterosaur Pteranodon. *Geological Society, London, Special Publications*, 455, 69 – 81.
- Bestwick, J., Unwin, D.M., Butler, R.J., Henderson, D.M. & Purnell, M.A. (2018). Pterosaur dietary hypotheses: a review of ideas and approaches. *Biological Reviews*, 93, 2021-2048.
- Bestwick, J, Unwin, D.M., Butler, R.J. & Purnell, M.A. (2020). Dietary diversity and evolution of the earliest flying vertebrates revealed by dental microwear texture analysis. *Nature Communications*, 11, 1-9.
- Bever, G.S. & Norell, M.A. (2017). A new rhynchocephalian (Reptilia: Lepidosauria) from the Late Jurassic of Solnhofen (Germany) and the origin of the marine Pleurosauridae. *Royal Society Open Science*, 4, 1-16.
- Chen, H., Jiang, S., Kellner, A.W.A. & Wang, X. (2024). New insights into pterosaur cranial anatomy: X-ray imaging reveals palatal structure and evolutionary trends. *Communications Biology*, 7, 1-11.
- Cheng, X., Jiang, S., Wang, X. & Kellner, A.W.A. (2017). New anatomical information of the wukongopterid *Kunpengopterus sinensis* Wang et al., 2010 based on a new specimen. *PeerJ*, 5, 1-20.

- Cullen, T.M., Larson, D.W., Witton, M.P., Scott, D., Maho, T., Brink, K.S., Evans, D.C. & Reisz, R. (2023). Theropod dinosaur facial reconstruction and the importance of soft tissues in paleobiology. *Science*, 379, 1348-1352.
- Dong, Z.-M. (1982). On a new Pterosauria (*Huanhepterus quingyangensis* gen. et. sp. nov.) from Ordos, China. *Vertebrata Palasiatica*, 20(2), 115-121.
- Ebert, M., Lane, J.A. & Kölbl-Ebert, M. (2016). *Palaeomacrosemius thiollieri*, gen. et sp. nov., a new Macrosemiidae (Neopterygii) from the Upper Jurassic of the Solnhofen Archipelago (Germany) and Cerin (France), with a revision of the genus *Macrosemius*. *Journal of Vertebrate Paleontology*, 36(5), 1-22.
- Ebert, M. & Kölbl-Ebert, M. (2008). Predator-prey relationships in *Orthogonikleithrus hoelli* Arratia 1997. *Archaeopteryx*, 26, 11–18.
- Evans, A.R. & Sanson, G.D. (1998). The effect of tooth shape on the breakdown of insects. *Journal of Zoology*, 246, 391–400.
- Fastnacht, M. (2005). Jaw mechanics of the pterosaur skull construction and the evolution of Toothlessness. PhD thesis, Johannes Gutenberg-Universität, Mainz.
- Fastnacht, M. (2008). Tooth replacement pattern of *Coloborhynchus robustus* (pterosauria) from the Lower Cretaceous of Brazil. *Journal of Morphology*, 269, 332-348.
- Fernandes, A.E., Beccari, V., Kellner, A.W.A. & Mateus, O. (2023). A new gnathosaurine (Pterosauria, Archaeoptero-dactyloidea) from the Late Jurassic of Portugal. *PeerJ*, 11, 1-24.
- Fürsich, F.T., Mäuser, M., Schneider, S. & Werner, W. (2007). The Wattendorf Plattenkalk (Upper Kimmeridgian) – a new conservation lagerstätte from the northern Franconian Alb, southern Germany', *Neues Jahrbuch für Geologie und Paläontologie, Abhandlungen*, 245, 45–58.
- Goloboff, P.A., Farris, J.S. & Nixon, K.C. (2008). TNT, a free program for phylogenetic analysis. *Cladistics*, 24, 774–786.
- Goloboff, P.A. & Morales, M. (2023). TNT version 1.6, with a graphical interface for MacOs and Linux, including new routines in parallel. *Cladistics*, 39(2), 144–153.
- Hancock, J, Kushlan, JA & Kahl MP 1992, 'Storks, Ibises and Spoonbills of the World', Academic Press, Cambridge.

- Henderson, D.M. (2018). Using three-dimensional, digital models of pterosaur skulls for the investigation of their relative bite forces and feeding styles. *Geological Society, London, Special Publications*, 455, 25-44.
- Hone D.W.E., Tischlinger H., Frey E. & Röper M. (2012). A New Non-Pterodactyloid Pterosaur from the Late Jurassic of Southern Germany. *PLoS ONE*, 7(7), 1-18.
- Hone, D.W.E., Jiang, S. & Xu X. (2018). A taxonomic revision of *Noriopterus complicidens* and Asian members of the Dsungaripteridae. *Geological Society, London, Special Publications*, 455, 149-157.
- Howse, S.C.B. & Milner, A.R. (1995). The pterodactyloids from the Purbeck Limestone Formation of Dorset. *Bulletin of the Natural History Museum of London, Geology Series*, 51(1), 73–88.
- Heyng, A., Leonhardt, U., Krautworst, U. & Pöschl, R. (2011). Fossilien der Mörsheim-Formation am Schaudiberg. *Fossilien Sonderheft 2011*, 22–35.
- Heyng, A., Rothgaenger, M. & Röper, M. (2015). Die Grabung Brunn' in G Arratia, H-P Schultze, H. Tischlinger, G. Viohl (Eds.), *Solnhofen. Ein Fenster in die Jurazeit* (pp. 114–118). Verlag Dr. Friedrich Pfeil.
- Jiang, S., Cheng, X., Ma, Y. & Wang, X. (2016). A new archaeopteroactyloid pterosaur from the Jiufotang Formation of western Liaoning, China, with a comparison of sterna in Pterodactyloomorpha. *Journal of Vertebrate Paleontology*, 36(6), 1-12.
- Keupp, H., Koch, R., Schweigert, G. & Viohl, G. (2007). Geological history of the Southern Franconian Alb - the area of the Solnhofen Lithographic Limestone. *Neues Jahrbuch für Geologie und Paläontologie, Abhandlungen*, 245, 3–21.
- Knoll F. (2000). Pterosaurs from the Lower Cretaceous (?Berriasian) of Anoual, Morocco. *Annales de Paléontologie*, 86, 157–164.
- Konwert, M. (2016). *Orthogonikleithrus francogalliensis*, sp nov (Teleostei, Orthogonikleithridae) from the Late Jurassic plattenkalks of Cerin (France). *Journal of Vertebrate Paleontology*, 36, 1-10.
- López-Arbarello, A. & Schröder, K. (2014). The species of *Aspidorhynchus* Agassiz, 1833 (Neopterygii, Aspidorhynchiformes) from the Jurassic plattenkalks of Southern Germany. *Paläontologische Zeitschrift*, 88, 167–185.

- López-Arbarello, A. & Sferco, M.E. (2011). New semionotiform (Actinopterygii: Neopterygii) from the Late Jurassic of southern Germany. *Journal of Systematic Palaeontology*, 9, 197–215.
- Martill, D.M., Frey, E., Tischlinger, H., Mäuser, M., Rivera-Sylva, H.E. & Vidovic, S.U. (2022). A new pterodactyloid pterosaur with a unique filter-feeding apparatus from the Late Jurassic of Germany. *PalZ*, 97, 383-424.
- Massare, J.A. (1987). Tooth Morphology and Prey Preference of Mesozoic Marine Reptiles. *Journal of Vertebrate Paleontology*, 7(2), 121-137.
- Mäuser, M. (2015). Die laminierten Plattenkalke von Wattendorf in Oberfranken' in G. Arratia, H.-P. Schultze, H. Tischlinger, G. Viohl (Eds.), *Solnhofen. Ein Fenster in die Jurazeit* (pp. 515–535), Verlag Dr. Friedrich Pfeil.
- Meyer, R.K.F. & Schmidt-Kahler, H. (1990). Paläogeographie und Schwammriffentwicklung des süddeutschen Malm – ein Überblick. *Facies*, 23, 175–184.
- Ósi, A., Prondvai, E., Frey, E. & Pohl, B. (2010) New Interpretation of the Palate of Pterosaurs. *The Anatomical Record*, 293, 243-258.
- Ósi, A. (2011). Feeding-related characters in basal pterosaurs: implications for jaw mechanism, dental function and diet. *Lethaia*, 44, 136–152.
- Plieninger, F. (1901). Beiträge zur Kenntniss der Flugsaurier. *Palaeontographica*, XLVIII, 65-99.
- Niebuhr, B. & Pürner, T. (2014). Lithostratigraphie der Weißjura-Gruppe der Frankenalb (außeralpiner Oberjura) und der mittel- bis oberjurassischen Reliktorkommen zwischen Straubing und Passau (Bayern). *Schriftenreihe der Deutschen Gesellschaft für Geowissenschaften*, 83, 5–72.
- Nopsca, F. (1928). The genera of reptiles. *Palaeobiologica*, 1, 163–188.
- Owen, R. (1842). Report on British fossil reptiles, part II' in: *Proceedings of the 11th Meeting of the British Association for the Advancement of Science*, Plymouth, UK, 60–204.
- Pinheiro, F.L. & Schultz, C.L. (2012). An Unusual Pterosaur Specimen (Pterodactyloidea, ?Azhdarchoidea) from the Early Cretaceous Romualdo Formation of Brazil, and the Evolution of the Pterodactyloid Palate. *PLoS ONE*, 7(11), 1-11.
- Qvarnström, M., Elgh, E., Owocki, K., Ahlberg, P.E. & Niedźwiedzki, G. (2019). Filter feeding in

- Late Jurassic pterosaurs supported by coprolite contents. *PeerJ*, 7, 1-12.
- Rauhut, O.W.M., López-Arbarello, A., Röper, M. & Rothgaenger, M. (2017). Vertebrate fossils from the Kimmeridgian of Brunn: the oldest fauna from the Solnhofen Archipelago (Late Jurassic, Bavaria, Germany). *Zitteliana*, 89, 305-329.
- Röper M. (1997). Die Plattenkalk-Lagerstätten von Solnhofen unter besonderer Berücksichtigung der Oberkimmeridge-Vorkommen bei Brunn/Oberpfalz. *Acta Albertina Ratisbonensia*, 50, 201–216.
- Röper, M. (2005). East Bavarian Plattenkalk – Different types of Upper Kimmeridgian to Lower Tithonian Plattenkalk deposits and facies. *Zitteliana B*, 26, 57–70.
- Röper, M. & Rothgaenger, M. (1995). Eine neue Fossilagerstätte in den ostbayerischen Oberjura-Plattenkalke bei Brunn/Oberpfalz. - Erster Forschungsbericht. *Freunde der Bayerischen Staatssammlung für Paläontologie und Historische Geologie eV, Jahresbericht und Mitteilungen*, 24, 32–46.
- Röper, M. & Rothgaenger, M. (1997). Altersdatierung und Paläoökologie der Oberjura – Plattenkalke von Brunn (Oberes Kimmeridgium / Oberpfalz). *Acta Albertina Ratisbonensia*, 50, 77–122.
- Sander, P.M. (1999). The microstructure of reptilian tooth enamel: terminology, function, and Phylogeny. *Münchner Geowissenschaftliche Abhandlungen*, 38, 1-102.
- Schröder, K., López-Arbarello, A. & Ebert, M. (2012). *Macrosemimimus*, gen. nov. (Actinopterygii, Semionotiformes), from the Late Jurassic of Germany, England, and France. *Journal of Vertebrate Paleontology*, 32, 512–529.
- Schweigert, G. (2007). Ammonite biostratigraphy as a tool for dating Upper Jurassic lithographic limestones from South Germany - first results and open questions. *Neues Jahrbuch für Geologie und Paläontologie, Abhandlungen*, 245, 117–125.
- Schweigert, G. (2015). Biostratigraphie der Plattenkalke der südlichen Frankenalb' in G. Arratia, H.-P. Schultze, H. Tischlinger, G. Viohl (Eds.), *Solnhofen. Ein Fenster in die Jurazeit* (pp. 63–66), Verlag Dr. Friedrich Pfeil.
- Soto, M., Montenegro, F., Toriño, P., Mesa, V. & Perea, D. (2021). A new ctenochasmatid (Pterosauria, Pterodactyloidea) from the late Jurassic of Uruguay. *Journal of South American Earth Sciences*, 11, 1-11.
- Theodori, C. (1830). Knochen vom *Pterodactylus* aus der Liasformation von Banz', *Frorieps Notizen für Natur- und Heilkunde*, 632, 1-101.

- Tischlinger, H. (2015). Arbeiten mit ultravioletem Licht (UV)‘ in G. Arratia, H.-P. Schultze, H. Tischlinger, G. Viohl (Eds.), *Solnhofen. Ein Fenster in die Jurazeit* (pp. 109–113), Verlag Dr. Friedrich Pfeil.
- Tischlinger, H. & Arratia, G. (2013). Ultraviolet light as a tool for investigating Mesozoic fishes, with a focus on the ichthyofauna of the Solnhofen archipelago‘ in G. Arratia, H.-P. Schultze, M.V.H. Wilson (Eds.), *Mesozoic Fishes 5 - Global Diversity and Evolution, Proceedings of the international meeting Saltillo 2010, Coahuila, Mexico* (pp. 549-560).
- Unwin, D.M., Lü, J. & Bakhurina, N.N. (2000). On the systematic and stratigraphic significance of pterosaurs from the Lower Cretaceous Yixian Formation (Jehol Group) of Liaoning, China. *Mitteilungen aus dem Museum für Naturkunde in Berlin, Geowissenschaftliche Reihe*, 3, 181–206.
- Unwin, D.M. (2002). On the systematic relationships of *Cearadactylus atrox*, an enigmatic Early Cretaceous pterosaur from the Santana Formation of Brazil. *Fossil Record*, 5, 239-263.
- Unwin, D.M. (2003). On the phylogeny and evolutionary history of pterosaurs. *Geological Society, London, Special Publications*, 217(1), 139–90.
- Villa, A., Montie, R., Röper, M., Rothgaenger, M. & Rauhut, O.W.M. (2021). *Sphenofontis velserae* gen. et sp. nov., a new rhynchocephalian from the Late Jurassic of Brunn (Solnhofen Archipelago, southern Germany). *PeerJ*, 9, 1-51.
- Viohl, G. (2015). Der geologische Rahmen: die südliche Frankenalb und ihre Entwicklung‘ in G. Arratia, H.-P. Schultze, H. Tischlinger, G. Viohl (Eds.), *Solnhofen. Ein Fenster in die Jurazeit* (pp. 56–62), Verlag Dr. Friedrich Pfeil.
- Viohl, G. & Zapp, M. (2007). Schamhaupten, an outstanding Fossil-Lagerstätte in a silicified Plattenkalk around the Kimmeridgian-Tithonian boundary (Southern Franconian Alb, Bavaria). *Neues Jahrbuch für Geologie und Paläontologie, Abhandlungen*, 245, 127–142.
- von Meyer, C.E.H. (1834). *Gnathosaurus subulatus*, ein Saurus aus dem lithographischen Schiefer von Solnhofen. *Museum Senckenbergianum*, 1, 5-7.
- Wagner, A. (1861). Charakteristik einer neuen Flugeidechse, *Pterodactylus elegans*‘, *Sitzungsberichte der Bayerischen Akademie der Wissenschaften, Mathematisch-naturwissenschaftliche Abteilung*, 1, 363–365.
- Wallace, K.M. (2006). The Feeding Ecology of yearling, juvenile, and sub-adult Nile Crocodiles,

Crocodylus niloticus, in the Okavango Delta, Botswana. Master thesis, University of Stellenbosch, Stellenbosch.

- Wang, X., Kellner, A.W.A., Jiang, S., Wang, Q., Ma, Y., Paidoula, Y., Cheng, X., Rodrigues, T., Meng, X., Zhang, J., Li, N. & Zhou, Z. (2014). Sexually Dimorphic Tridimensionally Preserved Pterosaurs and Their Eggs from China. *Current Biology*, 24, 1323–1330.
- Wang, X. & Lü, J. (2001). Discovery of a pterodactylid pterosaur from the Yixian Formation of western Liaoning, China. *Chinese Science Bulletin*, 46(1), 1-6.
- Wellnhofer, P. (1970). Die Pterodactyloidea (Pterosauria) der Oberjura-Plattenkalke Süddeutschlands', *Abhandlungen der Bayerischen Akademie der Wissenschaften, Neue Folge*, 141, 1-133.
- Wellnhofer, P. (1978). Pterosauria', in: P Wellnhofer (Ed.), *Handbuch der Paläoherpetologie, Encyclopedia of Paleoherpetology*, 19 (pp. 1-82), Fischer-Verlag.
- Wellnhofer, P. (1985). Neue Pterosaurier aus der Santana-Formation (Apt) der Chapada do Araripe, Brasilien. *Palaeontographica (A)*, 187(4-6), 105-182.
- Wilmers, J. & Bargmann, S. (2020). Nature's design solutions in dental enamel: Uniting high strength and extreme damage resistance. *Acta Biomaterialia*, 107, 1-24.
- Zhou, C.-F., Gao, K.-Q., Yi, H., Xue, J., Li, Q. & Foc, R.C. (2017). Earliest filter-feeding pterosaur from the Jurassic of China and ecological evolution of Pterodactyloidea. *Royal Society Open Science*, 4(2), 1-8.
- Zhou, C.-F., Wang, X. & Wang, J. (2022). First evidence for tooth–tooth occlusion in a ctenochasmatid pterosaur from the Early Cretaceous Jehol Biota. *Geological Society, London, Special Publications*, 521, 9-17.

Supplementary Material:

Supplementary Material 1. Phylogenetic Data Matrix

Chapter 4. A new gnathosaurine (Pterosauria, Archaeopterodactyloidea) from the Late Jurassic of Portugal

Keywords: *Pterosauria, Pterodactyloidea, Gnathosaurinae, Jurassic, Portugal*

The chapter was published as: Fernandes, A.E., Beccari, V., Kellner, A.W.A. & Mateus, O. A new gnathosaurine (Pterosauria, Archaeopterodactyloidea) from the Late Jurassic of Portugal. *PeerJ* 11:e16048, 2023

Author contributions:

- Alexandra E. Fernandes: Conceptualization, Data curation, Formal analysis, Funding acquisition, Investigation, Methodology, Project administration, Resources, Software, Visualization, Writing-original draft, Writing-review & editing
- Victor Beccari: Software, Visualization, Writing-review & editing
- Alexander W. A. Kellner: Writing-review & editing
- Octavio Mateus: Supervision, Writing-review & editing

A new gnathosaurine (Pterosauria, Archaeoptero-dactyloidea) from the Late Jurassic of Portugal

Alexandra E. Fernandes^{1,2,3}, Victor Beccari^{2,3}, Alexander W. A. Kellner⁴ and Octávio Mateus^{3,5}

¹ Department of Earth and Environmental Sciences, Ludwig-Maximilians-Universität München, Munich, Bayern, Germany

² SNSB, Bayerische Staatssammlung für Paläontologie und Geologie, Munich, Germany

³ Museu da Lourinhã, Lourinhã, Portugal

⁴ Departamento de Geologia e Paleontologia, Laboratório de Sistemática e Tafonomia de Vertebrados Fósseis (LAPUG), Museu Nacional, Rio de Janeiro, Brazil

⁵ GEOBIOTEC, Department of Earth Sciences, Universidade Nova de Lisboa, Caparica, Portugal

ABSTRACT

An incomplete, yet remarkably-sized dentated rostrum and associated partial cervical vertebrae of a pterosaur (ML 2554) were recently discovered from the Late Jurassic (Late Kimmeridgian-Early Tithonian) Lourinhã Formation of Praia do Caniçal, of central west Portugal. This specimen exhibits features such as a spatulated anterior expansion of the rostrum, robust comb-like dentition, and pronounced rims of the tooth alveoli, indicating gnathosaurine affinities. Based on its further unique tooth and dentary morphology, a new genus and species, *Lusognathus almadrava* gen. et spec. nov., is proposed, making this the first named pterosaur species found within Portugal. The presence of this taxon adds yet another element to the fluvio-deltaic lagoonal environment that has been suggested as representative of the Lourinhã Formation in the Late Jurassic, further contributing to the diversity and distribution of gnathosaurines worldwide.

Subjects Evolutionary Studies, Paleontology, Taxonomy, Zoology

Keywords Pterosauria, Pterodactyloidea, Gnathosaurinae, Jurassic, Portugal

INTRODUCTION

The known global distribution and diversity of pterosaurs reinforces their success as a group, as they are found in all continents including Antarctica (*Barrett et al., 2008; Kellner et al., 2019a*), and yet their relatively sparse fossil record and often incomplete preservation (particularly when outside of Lagerstätten environments) can pose a challenge for further understanding their paleobiology, when compared with other vertebrates. Accordingly, the Jurassic of Portugal is a very productive and taxonomically diverse period concerning vertebrate fossils, especially for plesiosaurs (e.g., *Puértolas-Pascual et al., 2021*), ichthyosaurs (e.g., *Castanhinha & Mateus, 2007*), mosasaurs (e.g., *Castanhinha & Mateus, 2007*), dinosaurs (e.g., *Rauhut, 2001; Antunes & Mateus, 2003; Malafaia et al., 2010; Mocho et al., 2016; Rotatori, Moreno-Azanza & Mateus, 2020*), turtles (e.g., *Pérez-García & Ortega, 2011*), crocodylomorphs (e.g., *Guillaume et al., 2020*), and mammals (e.g., *Krebs, 1991*). However, despite this abundance, up to now, pterosaur material recovered from this

Submitted 13 June 2023
Accepted 16 August 2023
Published 18 September 2023

Corresponding author
Octávio Mateus, omateus@fct.unl.pt

Academic editor
Fabien Knoll

Additional Information and
Declarations can be found on
page 18

DOI 10.7717/peerj.16048

© Copyright
2023 Fernandes et al.

Distributed under
Creative Commons CC-BY 4.0

OPEN ACCESS

deposit has been restricted to scant and often fragmentary isolated bones and teeth, hindering any confident taxonomic assignments. This is likely due to the physical bone fragility of pterosaurs, making their remains particularly susceptible to deterrent or destructive fossilization factors such as carcass scavenging or later taphonomic duress (Dean, Mannion & Butler, 2016).

On a worldwide level, whereas ctenochasmatids occur with some regularity throughout the fossil record landscape for pterosaurs from the Late Jurassic to the Early Cretaceous, gnathosaurines are significantly more rare (Barrett et al., 2008). The currently-known gnathosaurine temporal range spans from the Late Jurassic to the Early Cretaceous, and although their distribution has so far extended throughout Europe, Asia, and South America, most of the known occurrences are attributed to isolated teeth, which have been reported from England, Portugal, Morocco, Chile, Uruguay, China, and Japan (Barrett et al., 2008; Howse & Milner, 1995; Knoll, 2000; Martill et al., 2006; Perea et al., 2018; Soto et al., 2021; Sweetman & Martill, 2010; Zhou et al., 2016; Dong, 1982; Unwin, Lü & Bakhurina, 2000).

The fossil material herein described now introduces a new taxon to the fluvio-deltaic lagoonal environment that has been suggested as representative of Lourinhã Formation in the Late Jurassic. The material is housed at the Museu da Lourinhã, in Lourinhã, Portugal, under the collection number ML 2554.

History and record of pterosaur discoveries in Portugal

The presence of pterosaurs in Portugal (Fig. 1) was first reported by Lapparent and Zbyszewski (1957: p. 58), the material consisting of four small, elongated vertebrae from the Campanian/Maastrichtian of Viso, which were initially identified as being similar to *Dimorphodon* or *Rhamphorhynchus*, and later ascribed to a maniraptoran theropod dinosaur by Galton (1994). The author also claimed in the same work that a pterodactyloid cervical vertebra from the middle portion of the neck, likely the fifth (formerly MSGP N X 213, and now belonging to the Museu Geológico (MG) in Lisbon, Portugal), discovered in the Lower Cretaceous Barremian of Serra Tiago dos Velhos was actually the first record of a pterosaur from Portugal, which he ascribed to cf. *Ornithocheirus*.

In 1968, Kühne initially attributed remains from the Kimmeridgian beds of the Guimarães mine (teeth and a terminal manual phalanx) to two different groups of pterosaurs: aff. *Rhamphorhynchus* sp. and *Pterodactylus* sp. (Kühne, 1968). Later, this material, in conjunction with other isolated fragmentary remains composed of a left scapula, wing? elements, and other appendicular elements could only be referred to the Pterodactyloidea, family *incertae sedis* (Thulborn, 1973; Wiechmann & Gloy, 2000). Guimarães has also yielded over 300 isolated pterosaur teeth, attributed to *Rhamphorhynchus* sp. and to the Pterodactyloidea (Wiechmann & Gloy, 2000). The fossils from Guimarães are also deposited in the Museu Geológico, in Lisbon, Portugal.

Other isolated teeth comprise the vast majority of pterosaur fossils from Portugal, and were recovered from the Areia do Mastro locality of the lower Barremian Papo Seco Formation of Cabo Espichel. They were assigned to the Ornithocheiridae and to the Ctenochasmatoidea (Figueiredo et al., 2020, 2022). From the Andrés fossil site of the

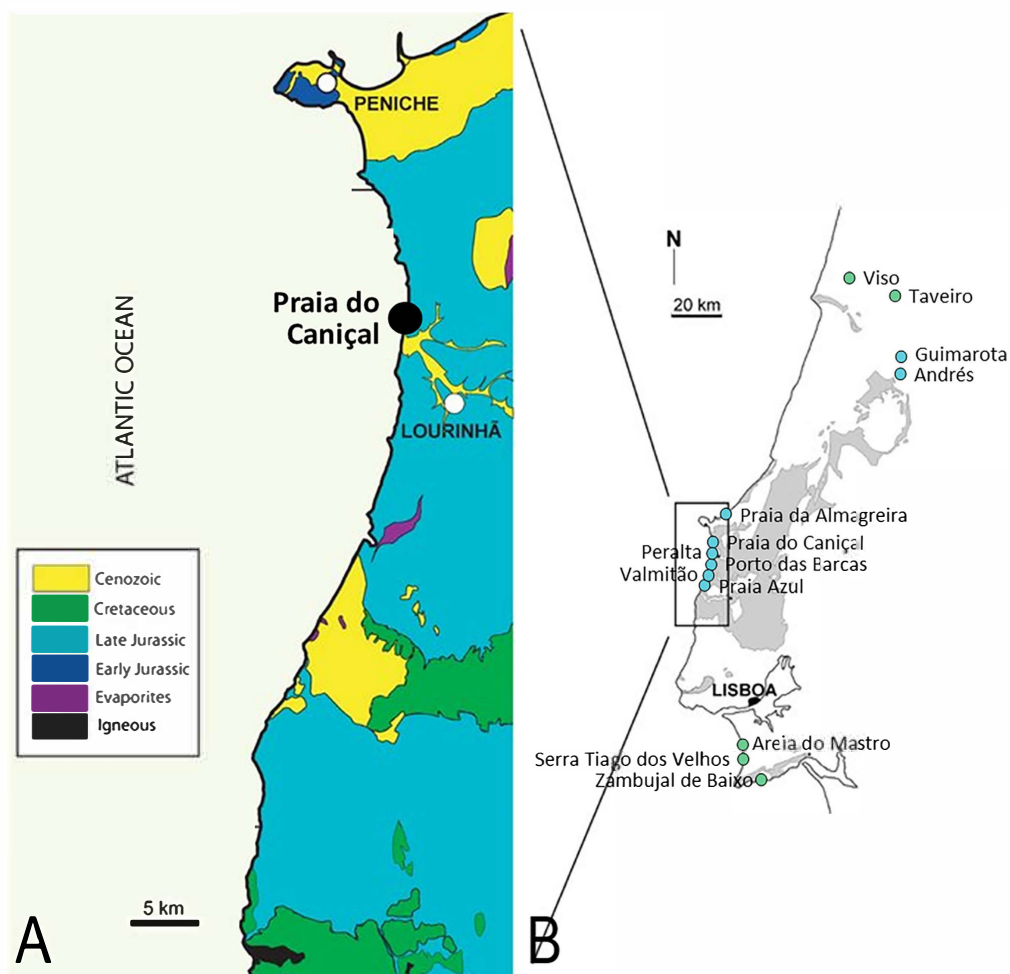


Figure 1 Pterosaur localities of Portugal. Locality of ML 2554 of Praia do Caniçal (A) and other known pterosaur localities of Portugal (B) (image modified from [Mateus, Dinis & Cunha, 2017](#))

Full-size  DOI: [10.7717/peerj.16048/fig-1](https://doi.org/10.7717/peerj.16048/fig-1)

Kimmeridgian Alcobaça Formation, isolated teeth were also attributed to Pterosauria indet. *Malafaia et al. (2010)*, based on their needle-like morphology (and similar in morphology to the *Rhamphorhynchus* sp. Guimarota teeth). Isolated teeth were also recovered in the area of Valmitão in Lourinhã ([Guillaume et al., 2020](#)), and teeth assigned to *Gnathosaurus* sp. were reported from the Sobral Formation (late Kimmeridgian-early Tithonian) locality of Praia Azul in Torres Vedras ([Bertozzo et al., 2021](#)).

Some fragmentary appendicular bones have been tentatively attributed to pterosaurs, including a large femur attributed to Dsungaripteroidea, from the locality Praia da Almagreira, Peniche ([Bertozzo et al., 2021](#)) of the upper Kimmeridgian/lower Tithonian. Some indeterminate pterosaur bone fragments were also reported from the Upper Cretaceous sediments of Taveiro, without any particular taxonomic assignment ([Antunes & Pais, 1978](#)).

About 400 *Pteraichnus* tracks have been collected from the Kimmeridgian/Tithonian Amoreira-Porto Novo Member locality of Peralta, which may correspond to the new taxon described in this work, although a more decisive attribution of these ichnofossils is beyond the scope of the current contribution. Trackways of *Pteraichnus* sp. (Mateus & Milàn, 2010) are also reported from the Upper Jurassic (Kimmeridgian) Zambujal de Baixo locality of the Azóia Formation in Sesimbra and Porto das Barcas in Lourinhã (late Kimmeridgian-early Tithonian).

Overwhelmingly, the vast majority of previous pterosaur specimens from Portugal have been assigned to *Rhamphorynchus* sp. However, this was likely a historically-generalized temporal attribution (rather than strictly based on morphology), and the known Portuguese material needs to be revised, especially considering that the range of paleobiogeographical variability has substantially grown since the time of these original attributions. In fact, no definitive non-tooth skeletal material of *Rhamphorynchus* sp. has ever even been reported in Portugal to date, which further warrants the potential for misnomers.

Here we present and describe a new specimen found by Filipe Vieira in November 2018 at Praia do Caniçal, in the municipality of Lourinhã in central west Portugal. Further excavation efforts realized in March 2019 by members of the Museu da Lourinhã collected more material from this same specimen, which is the first pterosaur taxon named from this country.

Geographical and geological setting

At Praia do Caniçal the outcropping rocks are of the Upper Jurassic of the Lourinhã Formation, namely the middle member of this unit: the Praia Azul Member. The Lourinhã Fm. displays a succession of alternated terrestrial mudstones and sandstones, some paleosol levels, and three transgressive bioclastic brackish layers. The formation is mostly continental, as evidenced by the presence of terrestrial fauna such as lissamphibians, non-aquatic mammals, and dinosaurs. The paleoclimate was arid (Myers et al., 2012) and the paleolatitude, derived from <http://paleolatitude.org> (van Hinsbergen et al., 2015), is estimated as 28°–29° North.

The Praia Azul Member is regarded to have been deposited near-shore, due to sea transgression. It is characterized by marls, mudstones, and sandstones, and is composed of three conspicuous carbonate levels (with the lower and upper levels used as the lithostratigraphic boundaries) and can be traced over distances of 20 km. The unit was mainly deposited by meandering fluvial systems flowing in a low-lying coastal plain, connected with transitional systems like deltas, sandy bay shorelines, and brackish lagoons. The brackish faunas of the shelly layers indicate short-time marine incursions (see Manuppella et al., 1999; Hill, 1989; Martinus & Gowland, 2011; Myers et al., 2012; Taylor et al., 2014; Mateus, Dinis & Cunha, 2017). So far, all studies agree to an Upper Kimmeridgian-Lower Tithonian age of those layers, which is also supported by an only non-biostratigraphic inferred date, provided by strontium isotopes by Schneider, Fürsich & Werner (2009). More precisely, the second and middle transgressive layer is at the Kimmeridgian-Tithonian boundary, which is currently at 149.2 Ma.

The Praia Azul Mb. is composed of three transgressive carbonate layers with different faunal assemblages: the lower level is categorized by *Isognomon lusitanica*, *Eomiodon securiformes*, *Arcomytilus morrisii*, dinosaur tracks, and ostreids (outcropping north of Caniçal, below the Paimogo fort) (Ribeiro et al., 2014; Mateus, Dinis & Cunha, 2017). The middle level comprises *Jurassicorbula edwarsi*, *Isognomon lusitanica*, *Nerinea*, coprolites, fish, *Eomiodon securiformes*, echinoids (outcropping at the base of Praia do Caniçal), while the upper level fauna consists of *Jurassicorbula edwarsi*, abundant ostreids, pleurosternidae turtles, and *Isognomon lusitanica* (outcropping at the top of Praia do Caniçal) (Mateus, Dinis & Cunha, 2017). The member is known to bear abundant dinosaur remains, including bones, eggs, and tracks (Ribeiro et al., 2014; Mateus et al., 2011), and also crocodylomorphs (Young et al., 2014), turtles (Pérez-García, 2015; Pérez-García & Ortega, 2022), pterosaurs (Bertoazzo et al., 2021), mammals, lissamphibians, and lepidosaurs (Mateus, Dinis & Cunha, 2017; Guillaume et al., 2023).

The specimen studied here was excavated from a stratigraphic layer at modern intertidal sea level, below the sand level of the beach itself, which is only exposed at low tide during the winter months (when sand is absent), which complicated its extraction. The fossil was preserved in a reddish micaceous fine sandstone, about 4 m above the second (and middle) transgressive layer, and below the upper transgressive layer. The age of ML 2554 is thus estimated to be about 149 Ma (Schneider, Fürsich & Werner, 2009).

MATERIALS AND METHODS

The preparation of the specimen was done mechanically, using PaleoTools Micro Jacks and a variety of manual tools, all performed at the Museu da Lourinhã in Lourinhã, Portugal. All bone surfaces were consolidated with 5% Paraloid B-72 diluted in acetone, and any breaks or deep fissures were glued and reinforced with 20% or 50% Paraloid B-72, as required.

CT scans were performed in Leiria, Portugal, with a microfocus CT system GE VtomeX M 240. Scan images were segmented and assembled utilizing Avizo and Meshlab softwares (GE Sensing & Inspection Technologies GmbH, Wunstorf, Germany). This resulted in four stacks of DICOM (.dicom) images (detailed information available at Morphobank Project 3968) (O'Leary & Kaufman, 2012). The segmentation of the complete specimen was done using manual selection slice-by-slice in the software Avizo v9.1 (Thermo Fisher, Waltham, MA, USA). All meshes were exported as Wavefrontfiles (.obj) and treated in the open-source software Blender v3.4. All meshes were smoothed for rendering using the Smooth Laplacian modifier (Lambda factor = 1 and 10 repeats). Measurements were taken both directly from the physical specimen and digitally in Blender.

Phylogenetic analysis was conducted using TNT version 1.5 (Goloboff, Farris & Nixon, 2008; Goloboff & Catalano, 2016) using the matrix by Andres (2021), augmented by the additional Portuguese specimen described here (represented in the analysis by "Lusognathus_almadrava"). A basic traditional tree-search analysis was conducted with 1,000 random addition sequence replicates. Due to the focus on the interrelationships of the new specimen and ctenochasmatids, the resulting cladogram has been simplified in the

software Adobe Illustrator. The complete topology can be found in the supplementary data set.

All specimen CT data, digital material, and phylogenetic matrix files are available at Morphobank Project 3968 ([O'Leary & Kaufman, 2012](#)).

Nomenclatural acts

The electronic edition of this article conforms to the requirements of the amended International Code of Zoological Nomenclature, and hence the new names contained herein are available under that Code from the electronic edition of this article. This published work and the nomenclatural acts it contains have been registered in ZooBank, the online registration system for the ICZN. The ZooBank LSIDs (Life Science Identifiers) can be resolved and the associated information viewed through any standard web browser by appending the LSID to the prefix "<http://zoobank.org>". The LSID for this publication is: urn:lsid:zoobank.org:pub:54B6D020-612A-4E23-ADEC-2CDE383B5C3B.

The electronic edition of this work was published in a journal with an ISSN, and has been archived and is available from the following digital repositories: PubMed Central and LOCKSS.

RESULTS

Systematic Paleontology

PTEROSAURIA [Owen, 1842](#)

PTERODACTYLOIDEA [Plieninger, 1901](#)

ARCHAEOPTERODACTYLOIDEA [Kellner, 2001](#)

CTENOCHASMATIDAE [Nopsca, 1928 sensu Unwin, 2003](#)

GNATHOSAURINAE [Nopsca, 1928 sensu Unwin, 2002](#)

Lusognathus, *gen. nov.*

L. almadrava, *sp. nov.*

Etymology: *Lusognathus* is derived from the Latin "Luso", after the prefix used for referencing things relating to Lusitania (the former name for the area of Portugal in Roman times) and "gnathus" meaning "jaw"; an "almadrava" is the name of a traditional Portuguese fishing trap for catching seafood.

Holotype: ML 2554, comprised of a fragment of the anterior part of a premaxillary rostrum, a fragment of a maxillary toothrow, two isolated fragmentary teeth, and three (or four) partial fragments of cervical vertebrae.

Locality and Horizon: Praia de Caniçal, county of Lourinhã, Portugal. Lourinhã Formation, late Kimmeridgian-early Tithonian, about 149.2 Ma ([Schneider, Fürsich & Werner, 2009](#)).

Diagnosis: A gnathosaurine pterosaur with the following combination of characters: a rounded-triangular anterior expansion of the premaxilla, constriction of the maxilla

directly posterior to the spatulate anterior expansion, robust laterally-projected teeth (spaced at 1.3 teeth per cm) with a subcircular to oval cross-section, and posterior teeth projected anterolaterally.

Specimen Description

Specimen ML 2554 is composed of a well-preserved three-dimensional maxillopremaxillary rostrum fragment with three(?) associated fragmentary mid-cervical vertebrae (two of which, although preserved in articulation, are too fragmentary to provide detailed anatomical information). The rostral fragments are divided between three blocks with only one side exposed. Two of the blocks connect and comprise the anteriormost premaxillary portion of the rostrum (Fig. 2), visible in ventral view, and the third block houses a more posterior maxillary section (of unknown exact position along the rostrum). No sutures are visible anywhere along the rostrum, although two longitudinal grooves are visible, running parallel to the toothrow (difficult to distinguish due to slight dorsoventral taphonomic compression, likely from lithostatic pressure). For precise measurements of each individual element, see Tables 1 and 2.

The anteriormost portion of the premaxilla is somewhat eroded. The increasingly anteromedial direction of the preserved roots of the anterior-most teeth indicate that the termination of the rostrum was not far beyond what is actually preserved (Figs. 2 and 3). In dorsoventral view, the rostrum begins to expand anterolaterally at approximately 28.0 mm from the anteriormost preserved edge, into a spatulate A-line or rounded-triangle shape, with the widest point terminating at the alveolar collar of the largest anterior tooth. Posterior to this point of expansion, and with no sharp demarcation (but still a distinct constriction) of the rostrum, a gradual posterolateral expansion also begins towards its posterior edge, but with a more gradual degree of increase than the anterior spatulated expansion.

The third rostrum fragment, which contains the posteriormost portion of the preserved maxilla, still preserves tooth alveoli, indicating that it was likely positioned anterior to the nasoantorbital fenestra. However, it should be noted that the actual percentage of the overall rostrum that is represented by this specimen cannot be determined.

There are twenty-nine teeth preserved in the rostrum, although in varying conditions, with one almost complete. Two additional isolated fragmentary teeth were also recovered from the surrounding sediment during preparation. Under these constraints, it is not possible to ascertain an exact overall tooth count for the taxon, although its tooth density can be calculated at approximately 1.3 teeth per cm (per side). The teeth along the premaxilla and maxilla exhibit a clear thecodont dentition, with each tooth located in a single alveolus which forms a raised collar of bone at the base of each tooth. The rostrum exhibits at least sixteen well-preserved alveoli on each side. The depressions between the alveoli gives the rostrum a crenellated appearance in dorsal and ventral views. The teeth are robust, reaching up to 5 mm in width, show a slight anterolateral tilt, and become increasingly inclined laterally and anteriorly. From the anterior to posterior end of the toothrow, the teeth also diminish in size and begin to slightly recurve posteriorly. The distance between individual teeth is greater than the tooth width, with the exception of

Table 1 Measurements of *Lusognathus almadrava* ML 2554.

Element	Left (mm)	Right (mm)
Alveoli count	11	17
Tooth 3 root length	9.1	–
Tooth 3 diameter	3.1	–
Tooth 4 length	23.5	–
Tooth 4 root length	12.1	–
Tooth 4 diameter	5.6	–
Tooth 5 length	20.4	–
Tooth 5 root length	8.1	8.3
Tooth 5 diameter	3.9	3.8
Tooth 6 root length	7.6	6.1
Tooth 6 diameter	3.7	2.7
Tooth 7 root length	4.9	3.2
Tooth 7 diameter	3.2	3.2
Tooth 8 root length	6.8	5.6
Tooth 8 diameter	3.4	2.8
Tooth 9 root length	–	4.2
Tooth 9 diameter	–	2.6
Tooth 10 root length	6.8	4.9
Tooth 10 diameter	3.5	2.9
Tooth 11 root length	–	4.5
Tooth 11 diameter	3.6	2.9
Tooth 12 root length	4.8	3*
Tooth 12 diameter	2.8	3.3
Tooth 13 root length	5	5.1
Tooth 13 diameter	1.9	2.7
Tooth 14 root length	4.8	4.9
Tooth 14 diameter	2.7	3.1
Tooth 15 root length	–	–
Tooth 15 diameter	2.1	–
Tooth 16 root length	5.1	–
Tooth 16 diameter	2.5	–
Tooth 17 root length	5.2	–
Tooth 17 diameter	1.7	–
Tooth 18 root length	5.8	–
Tooth 18 diameter	2.6	–
Average root length	6.6	
Average tooth diameter	3.5	

the largest preserved tooth at the anterior end. In the transverse view, the gradation of the tooth row is not perfectly horizontal, and shifts slightly dorsally at the posterior region.

The preserved teeth have straight crowns, tapering towards the apex. They are subcircular to oval in cross-section, with a slight compression on their anteroventral and

Table 2 Measurements of *Lusognathus almadrava* ML 2554.

Element	Left (mm)	Right (mm)
Maxilla length	127.8	
Maxilla maximum width	40.5	
Mid-maxilla width	25.5	
Maxilla height	7.5	
Mid-premaxilla width	8.9	
Distance Tooth (T) 3 to 4	–	3.5
Distance T4-5	–	3.2
Distance T5-6	–	4
Distance T6-7	3.6	3.9
Distance T7-8	5.2	4.9
Distance T8-9	4	–
Distance T9-10	5.3	–
Distance T10-11	5.8	4.7
Distance T11-12	5.4	–
Distance T12-13	6.4	6
Distance T13-14	3.9	4.9
Distance T14-15	6	6.9
Distance T15-16	7.1	6.7
Distance T16-17	–	6.9
Distance T17-18	–	5.5
Distance T18-19	–	6.3
Cervical vertebra centrum length	35.7	
Cervical vertebra preserved length	49.9	
Cervical vertebra centrum width	20.9	
Cervical vertebra neural spine height	8.9	
Cervical vertebra preserved height	29.6	

Note:

Tooth distances were measured from the distal margin of the tooth to the mesial margin of the following tooth.

posterodorsal sides, resulting in keel-like attenuations running longitudinally. The tooth enamel is completely smooth and lacks any ornamentation (Fig. 3A). Where teeth have been broken, pulp cavities are readily visible.

The best-preserved vertebral fragment consists of the incomplete anterior portion of a cervical centrum (Fig. 4), exhibiting the prezygapophyseal and cotylar region. It exhibits slight taphonomic distortion but preserves its three-dimensionality. The neural spine is low. The neural canal, flanked by two depressions on either side, is visible as a deep divot centered on the anterior end. The bifid prezygapophyses project anterolaterally, and their articular faces turn anteromedially.

There are three (possibly four) remaining vertebral fragments. One block contains one or two fragmentary vertebrae preserved in the sediment, and are potentially the posterior end of the atlas-axis complex articulated with the first cervical vertebra. Of the two other articulated fragments, one appears to be an elongated posterior part of a centrum, and the



Figure 2 The upper jaw of the holotype (ML 2554) of *Lusognathus almadrava* gen. et sp. nov. (ML 2554). (A) Photograph of both jaw fragments; (B) CT-scan reconstruction of the jaw in dorsal view, showing minimum possible preserved length, in dorsal view; (C) ventral view; (D) left lateral view; (E) right lateral view; (F) anterior view. [Full-size !\[\]\(528510d7a4b5a92b21675489a72c4b79_img.jpg\) DOI: 10.7717/peerj.16048/fig-2](https://doi.org/10.7717/peerj.16048/fig-2)

other an anterior prezygapophyseal region of another vertebra (with a pronounced neural spine). This material, however, is too damaged to provide much information. Judging by the height of the neural spine (when compared with the most complete vertebra), this spine appears slightly taller and more pronounced.

No sign of a premaxillary crest could be distinguished along the rostrum. However, since premaxillary crest in gnathosaurines usually begin to take shape in a more posterior position (e.g., *Gnathosaurus*), and the part of the rostrum preserved in *Lusognathus almadrava* is most likely well anterior to the nasoantorbital fenestra, we cannot be certain if this taxon would in fact bear one.

Phylogenetic Analysis

Phylogenetic analysis was conducted analyzing the evolutionary relationships of *Lusognathus almadrava* and other pterosaurs using the data matrix of [Andres \(2021\)](#). The analysis resulted in a single most parsimonious tree ([Fig. 5](#)). *Lusognathus almadrava*

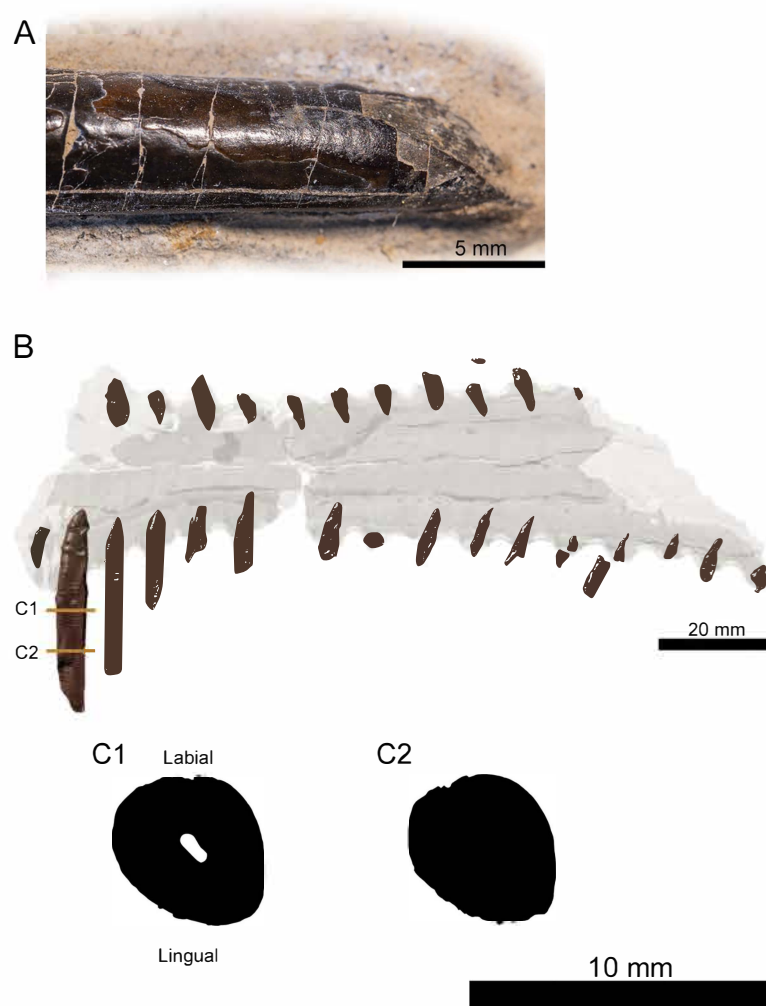


Figure 3 Tooth morphology of *Lusognathus almadrava* gen. et sp. nov. holotype (ML 2554). (A) Photography of the best-preserved tooth in labial view; (B) transparent 3D representation of the upper jaw in ventral view, showing the insertion of teeth, with cross-section cuts (C1 and C2) of the best-preserved tooth. [Full-size !\[\]\(95c552df6353b48e62ab71c0e20270ca_img.jpg\) DOI: 10.7717/peerj.16048/fig-3](https://doi.org/10.7717/peerj.16048/fig-3)

was retrieved as the sister taxon of *Gnathosaurus*, a relationship supported by a triangular lateral expansion of the anterior end of the rostrum (character 59.1). The Gnathosaurinae was phylogenetically defined as the least inclusive group including *Gnathosaurus subulatus* von Meyer, 1834 and *Huanhepterus quingyangensis* Dong, 1982 (Andres, 2021), and hence, *Lusognathus almadrava* falls within the Gnathosaurinae.

Discussion/Taxonomic Assignment

Typically, the defining feature of the Ctenochasmatidae (Nopsca, 1928) has been the tip of the rostrum being dorsoventrally depressed and rounded, whereas the designation for the gnathosaurines therein is the significant lateral expansion of the anterior end of the

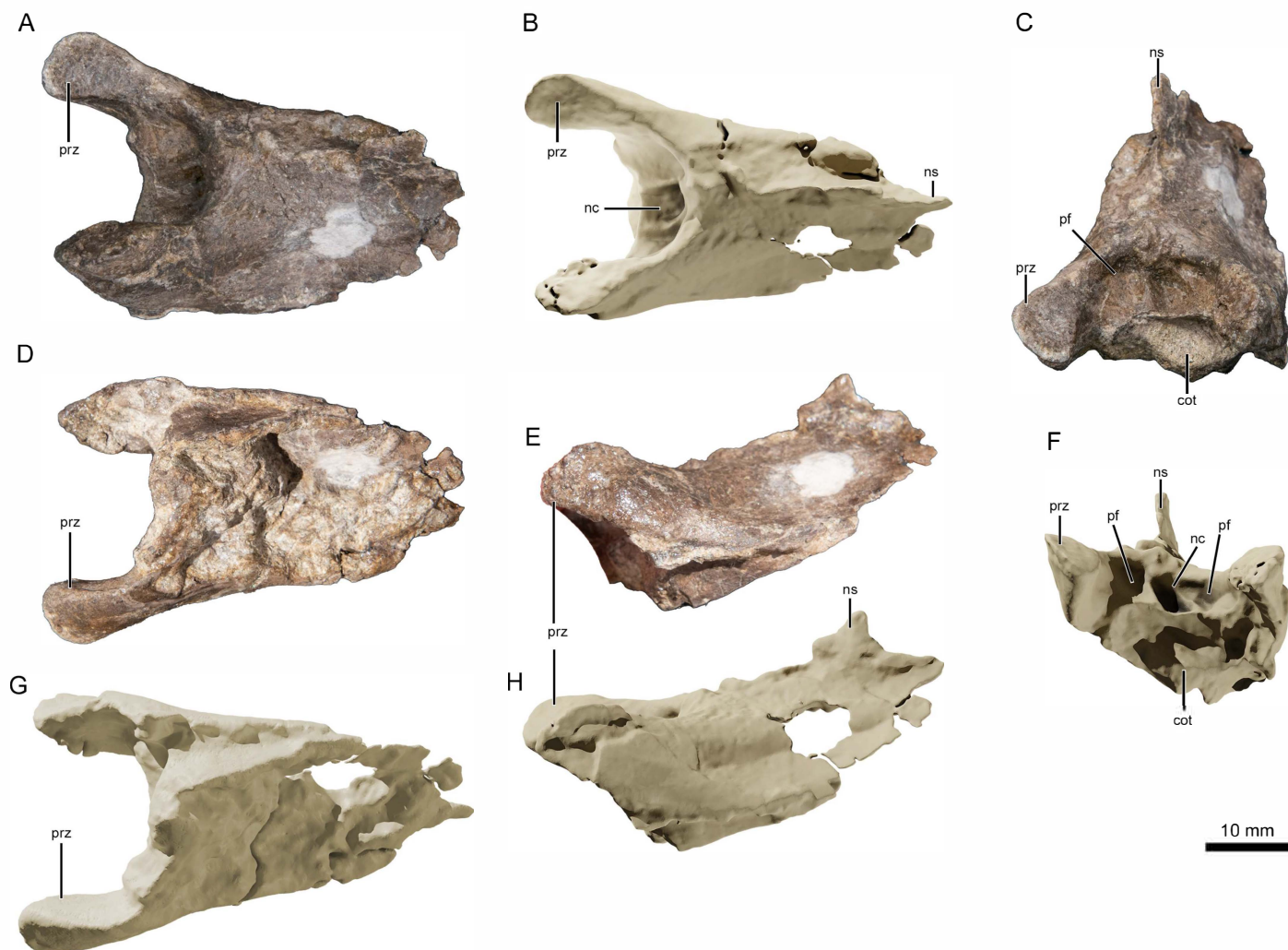


Figure 4 Photographs and virtual three-dimensional renderings of the mid-cervical vertebra of *Lusognathus almadrava* gen. et sp. nov. holotype (ML 2554). (A and B) Photograph and 3D rendering in dorsal view; (C and F) photograph and 3D rendering in anterior view; (D and G) photograph and 3D rendering in ventral view; (E and H) photograph and 3D rendering in left lateral view. Abbreviations: cot, cotyle; nc, neural canal; ns, neural spine; pf, pneumatic foramen; prz, prezygapophysis. Full-size [DOI: 10.7717/peerj.16048/fig-4](https://doi.org/10.7717/peerj.16048/fig-4)

rostra (Unwin, 2002). However, this expanded feature is not exclusive to gnathosaurines alone, as it also presents to a degree in anhanguerids (e.g., Kellner, 2003), istiodactylids (e.g., Lü, Xu & Ji, 2008), and ornithocheirids (e.g., Unwin, 2002, but see Rodrigues & Kellner, 2013 for the status of Ornithocheiridae). What does make this feature unique for gnathosaurs (beyond the aforementioned dorsoventral rostral composition of the larger Ctenochasmatidae) is the pronounced extent and variation of the spatula, e.g., the spoon-shaped spatulas of *Tucuaedactylus luciae* (Soto et al., 2021), *Gnathosaurus macrurus* (Howse & Milner, 1995), and *Gnathosaurus subulatus* (Meyer, 1833) (Fig. 6A), and the more bulbously circular end of *Plataleorhynchus streptophorodon* (Howse & Milner, 1995) (Fig. 6C). The extent of the diversity of these shapes has only been revealed as more specimens have been discovered (e.g., Soto et al., 2021). Specimen ML 2554 sustained

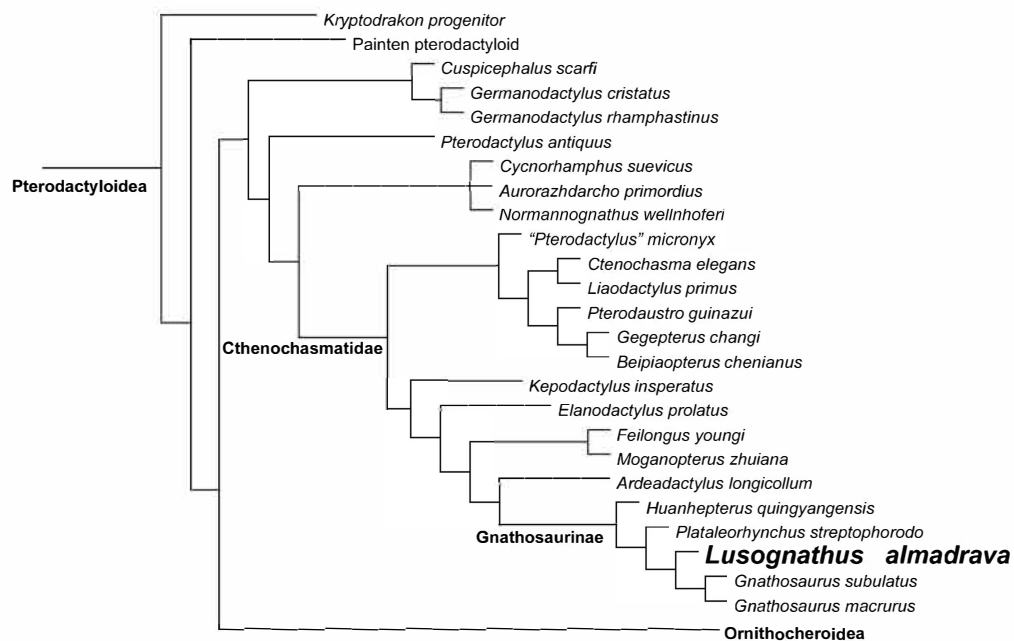


Figure 5 Phylogenetic results. Simplified tree of the Pterodactyloidea, showing the relationship of *Lusognathus almadrava* gen. et sp. nov., and gnathosaurines, after the data matrix by [Andres \(2021\)](#). Non-pterodactyloid pterosaurs were removed from this figure, and the clade Ornithocheiroidea was simplified, in order to make the figure concise. [Full-size](#) DOI: [10.7717/peerj.16048/fig-5](https://doi.org/10.7717/peerj.16048/fig-5)

damage at its anterior edge, and therefore is more difficult to precisely determine the rostrum shape, but it seems to exhibit a rounded-triangular anterior rostrum shape (Fig. 6B). ML 2554 also shares in common a constriction of the rostrum just posterior to the spatulated end with the mandible of *G. macrurus* ([Howse & Milner, 1995](#)), a demarcation of the spatula which is more pronounced than in the other afore-mentioned gnathosaurines. This overall variability in rostrum shape and dental apparatus is likely linked to contrasting functional feeding movements, and perhaps even prey differences ([Ósi, 2011](#); [Kellner et al., 2019b](#)), just as modern spoonbills today also vary in bill shape (e.g., the Yellowbilled Spoonbill *Platalea flavipes* has a longer bill and narrower spoon than the Royal Spoonbill *Platalea regia*, with both occupying the same habitat but consuming different prey ([Hancock, Kushlan & Kahl, 1992](#))).

Other defining features of the Ctenochasmatidae pertain to their dentition; namely, 25 or more teeth per side (with seven or more teeth in the premaxilla), the most rostrally-situated teeth being elongate with cylindrical crowns that project laterally from the dental border ([Unwin, 2003](#)). ML 2554 exhibits at least sixteen preserved teeth per side, with at least eight preserved in the spatula (damage impeding exact further determinations), making for an assignation therein, and making it further comparable with the tooth distribution of *G. macrurus* and *T. luciae*. Furthermore, if calculations of maximum tooth density are made based on the preserved portion, we can infer approximately 1.3 teeth per centimeter, making ML 2554 the gnathosaurine with the least dense dentition known so far. Tooth density is also informative in the Gnathosaurinae



Figure 6 Comparison of the ventral rostra of: (A) *Gnathosaurus subulatus* Meyer, 1833 (JME-SOS 4580); (B) *Lusognathus almadrava* n. gen. et sp. (ML 2554), and (C) *Plataleorhynchus streptophorodon* Howse & Milner, 1995 (BMNH R 11957). [Full-size !\[\]\(d05e99f54f2116973a3261aa569ffd8a_img.jpg\) DOI: 10.7717/peerj.16048/fig-6](https://doi.org/10.7717/peerj.16048/fig-6)

(Soto *et al.*, 2021), and even often autapomorphic within the Ctenochasmatidae, given that it can also potentially differentiate feeding specializations.

As in ctenochasmatids as a whole, gnathosaurines have conspicuous teeth set in alveoli, but gnathosaurines differ in having a raised collar of bone around their tooth bases (Perea *et al.*, 2018), which is much more pronounced than in other ctenochasmatids, a feature well exhibited by ML 2554. This feature also contributes to the appearance of an inter-dental crenulation in ML 2554, what has been previously reported in *P. streptophorodon* (Howse & Milner, 1995), *G. subulatus*, and *T. luciae* (Perea *et al.*, 2018; Soto *et al.*, 2021). This collar also differs in being much more subtle than the distinctive alveolar parapet typically used to describe lonchodectids, which exhibit a more raised margin of the alveoli, usually

elevated above the medial portion of the occlusal surface (Unwin, 2001; Averianov, 2020), and which also have vertically-inclined teeth.

Similar to all ctenochasmatids, the teeth of ML 2554 show a sub-circular to ovoid cross-section, with smooth enamel. However, one significant difference of gnathosaurines from other ctenochasmatids is in their tooth robustness. Ctenochasmatids are mostly filter-feeding, foraging in shallow waters with “needle-like” thin teeth, indicative of smaller prey items (Wang et al., 2007; Bestwick et al., 2018; Paul, 2022). The marked robustness of individual gnathosaur teeth suggests different feeding habits for their teeth being substantially larger and too widely-spaced for a true “filtration” functionality (Bestwick et al., 2018; Knoll, 2000), instead likely more associated to larger prey (e.g., piscivory). This is not dissimilar to modern gavials, whose teeth are conical and slender, with pointed apices, the shape of which is widely associated with fish-piercing, since the pointed apex would facilitate penetration of prey items, and the slenderness of the teeth would enable teeth to slide between the bones of prey, minimizing breakage (Massare, 1987). Accordingly, the finer teeth of ctenochasmatids (other than gnathosaurines) would therefore be more utile in squashing or gripping prey items rather than for directly piercing them.

Another differentiation in the dentition of the Gnathosaurinae can be made in that their teeth taper overall, from base to tip (whereas ctenochasmatid teeth are only most apically tapered) (Knoll, 2000). Additionally, tooth projection itself can also be a relevant differentiator of feeding function, as the torsional stresses applied to teeth throughout prey capture and feeding also vary, depending on the nature and agility of that prey. Whereas procumbent dentition is found in *Rhamphorhynchus* sp. and also in most ctenochasmatids (e.g., *Gegepterus changi*, *Ctenochasma elegans*, *G. subulatus*, and *T. luciae*), lateral projection is also found in certain rhamphorhynchids (e.g., *Sericipterus wucaiwanensis*) and in ctenochasmatids (*P. streptophorodon*, *Liaodactylus primus*, *C. elegans* and *T. luciae*). ML 2554 has laterally-projected teeth in the spatular region, and also anterolaterally projected teeth posterior to the spatula (a feature that is found in other taxa such as *T. luciae* and *G. macrurus*), but different from taxa with posterolateral projections as inferred in *P. streptophorodon* (Howse & Milner, 1995). The recurvature of dentition could potentially aid in maneuvering prey back towards the gullet, as in modern gavials consuming fish (Massare, 1987), and because ontogeny could also potentially change tooth orientation (Bennett, 2007), this could potentially allow for feeding niches to change somewhat over the course of an animal’s lifespan, and therefore this feature should be considered in a fluctuating capacity. Making any deductions on teeth alone should also be made prudently, since many taxonomic attributions for members of the clade are based on isolated teeth, and so may not be a wholly reliable metric.

Regarding vertebrae, the condition exhibited in one the partial vertebra of ML 2554 appears to follow the anteroposterior elongation typically found in both ctenochasmatids and azhdarchids (e.g., Howse, 1986; Martill, Sadaqah & Houry, 1998; Unwin, 2003; Andres & Ji, 2008), although its fragmentary state of preservation does not allow for any kind of insightful overall measurement. However, it is still informative in that there are no obvious



Figure 7 Reconstruction of *Lusognathus almadrava* and its paleoenvironment by © Jason Brougham.

Full-size  DOI: 10.7717/peerj.16048/fig-7

sutures between the vertebral centrum and the neural arch, suggesting that it belonged to an osteologically-mature individual (e.g., [Bennett, 1993](#)).

Portrayals of pterosaurs throughout the Triassic and Jurassic have traditionally been as relatively small animals, with wingspans constrained to around 1.6–1.8 m or less, whereas Cretaceous pterosaurs reached well above 3 m ([O’Sullivan, Martill & Grocock, 2013](#); [Jagielska et al., 2022](#)). Of late, it has been increasingly postulated that Jurassic pterosaurs have been previously underestimated for their size range (and particularly when considering the larger end of the spectrum). Some previously-known larger-sized examples include the 1.73 m minimum wingspan of *Sericipterus* ([Andres, Clark & Xing, 2010](#)), the 1.8 m wingspans of *Camplognathoides* ([Padian, 2008](#)) and *Rhamphorhynchus* ([Wellnhofer, 1975](#)), the 1.9 m wingspan of the rhamphorhynchine pterosaur from the Whitby Mudstone Formation ([O’Sullivan, Martill & Grocock, 2013](#)), and the 2.5 m wingspan of the Middle Jurassic sub-adult *Dearc sgiathanach* [Jagielska et al. \(2022\)](#). There are also the proposed (but not wholly reliable) over 2.5 m wingspans of *Harpactognathus gentryii* [Carpenter et al. \(2003\)](#) (the fossil has been removed from museum collections since its publication) and the gnathosaurine *Huanhepterus quingyangensis* [Dong \(1982\)](#) (of unreliable age), the 3.3 m wingspan of a very fragmentary potential *Rhamphorhynchus* ([Spindler & Ifrim, 2021](#)), and the 3.5–5 m wingspan of a specimen described by [Meyer & Hunt \(1999\)](#), but which may be scaled using an uncertain attribution, according to [O’Sullivan, Martill & Grocock \(2013\)](#). Pterosaurs over the 2.5 m wingspan have therefore not typically been found to be older than the Early Cretaceous ([Meyer & Hunt, 1999](#)).

Notwithstanding these larger size estimates, the pterosaurs of the Jurassic of Portugal are especially remarkable for the time period (i.e., the 4 m estimated wingspan of the fossil femur described by [Bertoazzo et al., 2021](#)), with ML 2554 being no exception in corroborating the evidence of large Jurassic pterosaurs. The minimum overall length of the

preserved rostrum of *Lusognathus almadrava* begins at 20.2 cm (when all three rostral blocks are lined up) but could potentially be even larger. This means that if we scale the specimen with the overall skull dimensions of *Gnathosaurus subulatus* (following the skull/skeleton scaling by [Carpenter et al., 2003](#)), where the calculated total minimum skull length of ML 2554 would be 60.8 cm, then *Lusognathus almadrava* would have achieved a minimum wingspan starting at 3.6 m. Additionally, the coeval pterosaur track site of Peralta, less than 10 km to the south of Praia do Caniçal, records about 400 *Pteraichnus*-like tracks of different sizes (half manus/half pes). The pes track length varies from 5.5 to 15 cm, which indicates the occurrence of very large pterosaurs, preliminarily making *Lusognathus almadrava* a likely candidate for the trackmaker. Based on ML 2554, *Lusognathus almadrava* could potentially reach these larger sizes, making it one of the largest Jurassic pterosaurs known, and the largest known Jurassic gnathosaurine, having a size matched only by some Cretaceous records of the group.

CONCLUSION

A new pterosaur taxon has been found from the Late Jurassic of Portugal, introduced here as *Lusognathus almadrava* gen et sp. nov. Several characters allow to ascribe this specimen to the Gnathosaurinae, namely its spatulate rostrum, robust comb-like dentition, and the pronounced rims of its tooth alveoli. The presence of this taxon in the fluvio-deltaic lagoonal environment that has been suggested to be representative of Lourinhã Formation in the Late Jurassic ([Fig. 7](#)) is in keeping with the modern analog of modern-day spoonbills, whose habitats generally include more shallow-water estuarine, tidal flat, coastal marshland, or even inland lake areas (areas where there are mud, clay, or fine-sand bottoms) with inflows of fresh, brackish, or salt water ([Hancock, Kushlan & Kahl, 1992](#)).

The paleobiological implications of such an exceptionally large-sized pterosaur in the Jurassic of Portugal denote and reinforce a thriving ecosystem, abundant with prey, in this case perhaps fish (as indicated by the robust teeth of ML 2554). Although it has been generally agreed upon that pterosaur body size steadily increased throughout and up to the end of the Cretaceous, ML 2554 adds more evidence for body sizes already having increased substantially by the end of the Late Jurassic (when compared with earlier forms); this growth having potentially been a response to filling a different ecological niche than their competitors, the birds ([Benson et al., 2014](#); [Tennant et al., 2017](#)). Although transitioning to this larger size may have inadvertently contributed to their downfall later on (since fewer niches are available for larger animals, making big species more likely predisposed to decline ([Cardillo et al., 2005](#))), and since larger terrestrial animals are sometimes disproportionately affected by extinctions ([Benson et al., 2014](#)), at least in the Late Jurassic paleoenvironments this extraordinary growth was potentially advantageous for their flourishing success.

ACKNOWLEDGEMENTS

Immense gratitude is extended to Filipe Viera for his invaluable scientific discovery and donation of the fossil to the Museu da Lourinhã. Thank you to the Lourinhã Paleoteam for their good-humored willingness to excavate a partially-underwater specimen (in winter,

and at a moment's notice), with a special thank you to Alexandre Audigane and Miguel Moreno-Azanza for assisting in mobilizing the excavation permits (also in winter, and at a moment's notice). Heartfelt thanks are also extended to Carla Alexandra Tomás, Micael Martinho, Laura de Jorge, and Carla Hernandez for their impeccable preparation of the specimen, and to the rest of the staff of the Museu da Lourinhã. Thank you to the DinoParque da Lourinhã and the Museu da Lourinhã, and to Bruno Pereira and Maria Rios for being coordinators of the Departamento de Investigação do GEAL. Many thanks to Bruno Camillo Silva of the Sociedade de História Natural de Torres Vedras, Pedro Aquino, Flávio Domingues, and Tiago Ferreira at Micronsense Metrologia Industrial, Lda. for their invaluable CT scan implementation. Oliver Rauhut is thanked for constructive suggestions, as are Fabian Knoll, Dave Hone, Matías Soto, and a third anonymous reviewer, whose feedback greatly improved this manuscript.

ADDITIONAL INFORMATION AND DECLARATIONS

Funding

This work was funded by the Horacio Matues (PIIHM) Grant. Alexander W. A. Kellner received funding from the Fundação Carlos Chagas Filho de Amparo à Pesquisa do Rio de Janeiro (FAPERJ #E-26/201.095/2022) and the Conselho Nacional de Desenvolvimento Científico e Tecnológico (CNPq #313461/2018-0, #406779/2021-0, #406902/2022-4). Octavio Mateus was funded by the Fundação para Ciência e a Tecnologia, I. P. with National Funds from the Ministério da Ciência, Tecnologia e Ensino Superior. (Grant Numbers: UIDB/04035/2020, GeoBioTec). The funders had no role in study design, data collection and analysis, decision to publish, or preparation of the manuscript.

Grant Disclosures

The following grant information was disclosed by the authors:

Horacio Matues (PIIHM) Grant.

Fundação Carlos Chagas Filho de Amparo à Pesquisa do Rio de Janeiro: FAPERJ #E-26/201.095/2022.

Conselho Nacional de Desenvolvimento Científico e Tecnológico: CNPq #313461/2018-0, #406779/2021-0, #406902/2022-4.

Fundação para Ciência e a Tecnologia, I. P. with National Funds from the Ministério da Ciência, Tecnologia e Ensino Superior.

GeoBioTec: UIDB/04035/2020.

Competing Interests

The authors declare that they have no competing interests.

Author Contributions

- Alexandra E. Fernandes conceived and designed the experiments, performed the experiments, prepared figures and/or tables, authored or reviewed drafts of the article, and approved the final draft.

- Victor Beccari performed the experiments, prepared figures and/or tables, authored or reviewed drafts of the article, and approved the final draft.
- Alexander W. A. Kellner analyzed the data, authored or reviewed drafts of the article, and approved the final draft.
- Octávio Mateus analyzed the data, authored or reviewed drafts of the article, and approved the final draft.

Data Availability

The following information was supplied regarding data availability:

The TNT Phylogenetic Data Matrix is available in the [Supplemental File](#).

The data is available at Morphobank: Project 3968.

https://morphobank.org/index.php/Projects/ProjectOverview/project_id/3968

The CT data is available at MorphoSource:

<https://doi.org/10.17602/M2/M530357>.

<https://doi.org/10.17602/M2/M530372>.

<https://doi.org/10.17602/M2/M530404>.

<https://doi.org/10.17602/M2/M530331>.

New Species Registration

The following information was supplied regarding the registration of a newly described species:

Publication LSID: urn:lsid:zoobank.org:pub:54B6D020-612A-4E23-ADEC-2CDE383B5C3B.

Lusognathus genus LSID: urn:lsid:zoobank.org:act:0681BFD9-A50C-4D5B-BC12-0E4EBA10E280.

Lusognathus almadrava species LSID: urn:lsid:zoobank.org:act:F36E8148-61FE-4CE8-AF4F-5F099364F817.

Supplemental Information

Supplemental information for this article can be found online at <http://dx.doi.org/10.7717/peerj.16048#supplemental-information>.

REFERENCES

- Andres B. 2021.** Phylogenetic systematics of *Quetzalcoatlus* Lawson 1975 (Pterodactyloidea: Azhdarchoidea). *Journal of Vertebrate Paleontology* **41**(1):203–217
DOI 10.1080/02724634.2020.1801703.
- Andres B, Clark JM, Xing X. 2010.** A new rhamphorhynchid pterosaur from the Upper Jurassic of Xinjiang, China, and the phylogenetic relationships of basal pterosaurs. *Journal of Vertebrate Paleontology* **30**(1):163–187 DOI 10.1080/02724630903409220.
- Andres B, Ji Q. 2008.** A new pterosaur from the Liaoning Province of China, the phylogeny of the pterodactyloidea, and convergence in their cervical vertebrae. *Palaeontology* **51**(2):453–469
DOI 10.1111/j.1475-4983.2008.00761.x.
- Antunes MT, Mateus O. 2003.** Dinosaurs of Portugal. *Comptes Rendus Palevol* **2**(1):77–95
DOI 10.1016/S1631-0683(03)00003-4.

- Antunes MT, Pais J. 1978.** Notas sobre depósitos de Taveiro: estratigrafia, paleontologia, idade, paleoecologia [Notes on the Taveiro deposits: stratigraphy, paleontology, age, paleoecology]. *Ciências da Terra* **4**:108–128.
- Averianov AO. 2020.** Taxonomy of the Lonchodectidae (Pterosauria, Pterodactyloidea). *Proceedings of the Zoological Institute RAS* **324**(1):41–55 DOI [10.31610/trudyzin/2020.324.1.41](https://doi.org/10.31610/trudyzin/2020.324.1.41).
- Barrett PM, Butler RJ, Edwards NP, Milner AR. 2008.** Pterosaur distribution in time and space: an atlas. *Zitteliana* **B**(28):61–107.
- Bennett SC. 2007.** A review of the pterosaur *Ctenochasma*: taxonomy and ontogeny. *Neues Jahrbuch für Geologie und Paläontologie—Abhandlungen* **245**(1):23–31 DOI [10.1127/0077-7749/2007/0245-0023](https://doi.org/10.1127/0077-7749/2007/0245-0023).
- Benson R, Frigot R, Goswami A, Andres B, Butler RJ. 2014.** Competition and constraint drove Cope's rule in the evolution of giant flying reptiles. *Nature Communications* **5**(1):3567 DOI [10.1038/ncomms4567](https://doi.org/10.1038/ncomms4567).
- Bennett SC. 1993.** The ontogeny of pteranodon and other pterosaurs. *Paleobiology* **19**(1):92–106.
- Bertozzo F, Camilo da Silva B, Martill D, Vorderwuelbecke EM, Aureliano T, Schouten R, Aquino P. 2021.** A large pterosaur femur from the Kimmeridgian, Upper Jurassic of Lusitanian Basin, Portugal. *Acta Palaeontologica Polonica* **66**(4):815–825 DOI [10.4202/app.00858.2020](https://doi.org/10.4202/app.00858.2020).
- Bestwick J, Unwin DM, Butler RJ, Henderson DM, Purnell MA. 2018.** Pterosaur dietary hypotheses: a review of ideas and approaches. *Biological Reviews* **93**:2021–2048 DOI [10.1111/brv.12431](https://doi.org/10.1111/brv.12431).
- Cardillo M, Mace GM, Jones KE, Bielby J, Bininda-Emonds OR, Sechrest W, Orme CD, Purvis A. 2005.** Multiple causes of high extinction risk in large mammal species. *Science* **309**(5738):1239–1241 DOI [10.1126/science.1116030](https://doi.org/10.1126/science.1116030).
- Carpenter K, Unwin D, Cloward K, Miles C, Miles C. 2003.** A new scaphognathine pterosaur from the Upper Jurassic Morrison Formation of Wyoming, USA. In: Buffetaut E, Mazin J-M, eds. *Evolution and Palaeobiology of Pterosaurs*. Vol. 217. London: Geological Society, Special Publications, 45–54.
- Castanhinha R, Mateus O. 2007.** A review on the marine reptiles of Portugal: ichthyosaurs, plesiosaurs and mosasaur [Poster presentation abstract]. *Journal of Vertebrate Paleontology* **27**(suppl. 3):57A DOI [10.1080/02724634.2007.10010458](https://doi.org/10.1080/02724634.2007.10010458).
- Dean CD, Mannion PD, Butler RJ. 2016.** Preservational bias controls the fossil record of pterosaurs. *Palaeontology* **59**:225–247 DOI [10.5061/dryad.td570](https://doi.org/10.5061/dryad.td570).
- Dong Z. 1982.** A new pterosaur (*Huanhepterus quingyangensis* gen. et sp. nov.) from Ordos, China. *Vertebrata Palasiatica* **20**(2):115–121.
- Figueiredo SD, Cunha PP, Pereda-Suberbiola X, de Carvalho CN, de Souza Carvalho I, Buffetaut E, Tong H, Sousa MF, Antunes V, Anastácio R. 2022.** The dinosaur tracksite from the lower Barremian of Areia do Mastro Formation (Cabo Espichel, Portugal): implications for dinosaur behavior. *Cretaceous Research* **137**:105219 DOI [10.1016/j.cretres.2022.105219](https://doi.org/10.1016/j.cretres.2022.105219).
- Figueiredo SD, Rosina P, Strantzali IB, Antunes V, Figueiredo S. 2020.** Paleoenvironmental approach on the Lower Cretaceous sequences of Areia do Mastro (Cabo Espichel, Southern Portugal). *Journal of Environmental Science and Engineering A* **(9)**:66–71 DOI [10.17265/2162-5298/2020.02.003](https://doi.org/10.17265/2162-5298/2020.02.003).
- Galton PM. 1994.** Notes on Dinosauria and pterodactylia from the Cretaceous of Portugal. *Neues Jahrbuch für Geologie und Paläontologie* **194**(2–3):253–267 DOI [10.1127/njgpa/194/1994/253](https://doi.org/10.1127/njgpa/194/1994/253).
- Goloboff P, Catalano S. 2016.** TNT version 1.5, with a full implementation of phylogenetic morphometrics [computer software]. *Cladistics* **32**(3):221–238 DOI [10.1111/cla.12160](https://doi.org/10.1111/cla.12160).

- Goloboff PA, Farris JS, Nixon KC. 2008.** TNT, a free program for phylogenetic analysis. *Cladistics* 24:774–786 DOI [10.1111/j.1096-0031.2008.00217.x](https://doi.org/10.1111/j.1096-0031.2008.00217.x).
- Guillaume ARD, Moreno-Azanza M, Puértolas-Pascual E, Mateus O. 2020.** Palaeobiodiversity of crocodylomorphs from the Lourinhã Formation based on the tooth record: insights into the palaeoecology of the Late Jurassic of Portugal. *Zoological Journal of the Linnean Society* 189(2):549–583 DOI [10.1093/zoolinnean/zlz112](https://doi.org/10.1093/zoolinnean/zlz112).
- Guillaume ARD, Natário C, Mateus O, Moreno-Azanza M. 2023.** Plasticity in the morphology of the fused frontals of Albanerpetontidae (Lissamphibia; Allocaudata). *Historical Biology* 35(4):537–554 DOI [10.1080/08912963.2022.2054712](https://doi.org/10.1080/08912963.2022.2054712).
- Hancock J, Kushlan JA, Kahl MP. 1992.** *Ibises and spoonbills of the world*. London: Bloomsbury Publishing Plc.
- Hill G. 1989.** The sedimentology and lithostratigraphy of the Upper Jurassic Lourinhã Formation, Lusitanian Basin, Portugal. Doctoral dissertation. The Open University. Available at <http://oro.open.ac.uk/54566/1/328171.pdf>.
- Howse SCB. 1986.** On the cervical vertebrae of the Pterodactyloidea (Reptilia: Archosauria). *Zoological Journal of the Linnean Society* 88:307–328 DOI [10.1111/j.1096-3642.1986.tb02249.x](https://doi.org/10.1111/j.1096-3642.1986.tb02249.x).
- Howse SCB, Milner AR. 1995.** The pterodactyloids from the Purbeck Limestone Formation of Dorset. *Bulletin of the Natural History Museum of London, Geology Series* 51(1):73–88.
- von Meyer H. 1834.** *Gnathosaurus subulatus*, ein Saurus aus den lithographischen Schiefer von Solnhofen. *Museum Senckenbergianum* 1:1–26.
- Jagielska N, O’Sullivan M, Funston GF, Butler IB, Challands TJ, Clark NDL, Fraser NC, Penny A, Ross DA, Wilkinson M, Brusatte SL. 2022.** A skeleton from the Middle Jurassic of Scotland illuminates an earlier origin of large pterosaurs. *Current Biology* 32:1446–1453 DOI [10.1016/j.cub.2022.01.073](https://doi.org/10.1016/j.cub.2022.01.073).
- Kellner AWA. 2001.** New hypothesis of pterosaur phylogeny. In: Barros LM, Nuvens PC, Filgueira JBM, eds. *I e II Simpósios sobre a Bacia do Araripe e bacias interiores do Nordeste, Comunicações*. Crato: Crato-CE, Colecao Chapada do Araripe, No. 1, Universidade Regional do Cariri, 249–258.
- Kellner AWA. 2003.** Pterosaur phylogeny and comments on the evolutionary history of the group. In: Buffetaut E, Mazin J-M, eds. *Evolution and Palaeobiology of Pterosaurs*. Vol. 217. London: Geological Society, Special Publications, 105–137.
- Kellner AWA, Caldwell MW, Holgado B, Dalla Vecchia FM, Nohra R, Sayão JM, Currie PJ. 2019a.** First complete pterosaur from the Afro-Arabian continent: insight into pterodactyloid diversity. *Scientific Reports* 9:17875 DOI [10.1038/s41598-019-54042-z](https://doi.org/10.1038/s41598-019-54042-z).
- Kellner AWA, Rodrigues T, Costa FR, Weinschütz LC, Figueiredo RG, Souza GAD, Brum AS, Eleutério LHS, Mueller C, Sayão JM. 2019b.** Pterodactyloid pterosaur bones from Cretaceous deposits of the Antarctic Peninsula. *Anais da Academia Brasileira de Ciências* 91(Suppl. 2):e20191300 DOI [10.1590/0001-3765201920191300](https://doi.org/10.1590/0001-3765201920191300).
- Knoll F. 2000.** Pterosaurs from the Lower Cretaceous (?Berriasian) of Anoual, Morocco. *Annales de Paléontologie* 86:157–164 DOI [10.1016/S0753-3969\(00\)80006-3](https://doi.org/10.1016/S0753-3969(00)80006-3).
- Krebs B. 1991.** Das Skelett von *Henkelotherium guimarotae* gen. et sp. nov. (Eupantotheria, Mammalia) aus dem Oberen Jura von Portugal. *Berliner geowissenschaftliche Abhandlungen/A* 133:1–110.
- Kühne WG. 1968.** History of discovery, report on the work performed, procedure, technique and generalities. In: *Contribuição para a fauna do Kimeridgiano da Mina de lignito Guimarota (Leiria, Portugal), I parte*. Vol. 14. Lisboa: Memórias dos Serviços Geológicos de Portugal, (N.S.), 7–20.

- Lü J, Xu L, Ji Q. 2008. Restudy of *Liaoxipterus* (Istiodactylidae: Pterosauria), with comments on the Chinese istiodactylid pterosaurs. *Zitteliana* **B28**:229–241.
- Malafaia E, Ortega F, Escaso F, Dantas P, Pimentel N, Gasulla JM, Ribeiro B, Barriga F, Sanz JL. 2010. Vertebrate fauna at the *Allosaurus* fossil-site of Andrés (Upper Jurassic), Pombal, Portugal. *Journal of Iberian Geology* **36**(2):193–204 DOI 10.5209/rev_JIGE.2010.v36.n2.7.
- Manuppella G, Antunes M, Pais J, Ramalho M, Rey J. 1999. Notícia explicativa da folha 30-A (Lourinhã) da Carta Geológica de Portugal. Esc. 1/50 000. Instituto Geológico e Mineiro. Available at https://geoportal.lneg.pt/pt/dados_abertos/cartografia_geologica/cgp50k/30-A.
- Martill DM, Frey E, Bell CM, Diaz GC. 2006. Ctenochasmatid pterosaurs from early Cretaceous deposits in Chile. *Cretaceous Research* **27**(5):603–610 DOI 10.1016/j.cretres.2006.03.002.
- Martill DM, Sadaqah RM, Khoury HN. 1998. Discovery of the holotype of the giant pterosaur *Titanopteryx philadelphiae* Arambourg 1959, and the status of Arambourgiania and Quetzalcoatlus. *Neues Jahrbuch für Geologie und Paläontologie* **207**(1):57–76 DOI 10.1127/njgpa/207/1998/57.
- Martinius AW, Gowland S. 2011. Tide-influenced fluvial bedforms and tidal bore deposits (late Jurassic Lourinhã Formation, Lusitanian Basin, Western Portugal). *Sedimentology* **58**(1):285–324 DOI 10.1111/j.1365-3091.2010.01185.x.
- Massare JA. 1987. Tooth morphology and prey preference of mesozoic marine reptiles. *Journal of Vertebrate Paleontology* **7**(2):121–137 DOI 10.1080/02724634.1987.10011647.
- Mateus O, Dinis J, Cunha PP. 2017. The Lourinhã Formation: the Upper Jurassic to lower most Cretaceous of the Lusitanian Basin, Portugal-landscapes where dinosaurs walked. *Ciências da Terra/Earth Sciences Journal* **19**(1):75–97 DOI 10.21695/cterra/esj.v19i1.355.
- Mateus O, Milàn J. 2010. First records of crocodile and pterosaur tracks in the Upper Jurassic of Portugal. *New Mexico Museum of Natural History and Science Bulletin* **51**:83–87.
- Mateus O, Milàn J, Romano M, Whyte MA. 2011. New finds of stegosaur tracks from the Upper Jurassic Lourinhã Formation, Portugal. *Acta Palaeontologica Polonica* **56**(3):651–658 DOI 10.4202/app.2009.0055.
- Meyer CA, Hunt AP. 1999. The first pterosaur from the Late Jurassic of Switzerland: evidence for the largest Jurassic flying animal. *Oryctos* **2**:111–116.
- Mocho P, Royo-Torres R, Malafaia E, Escaso F, Ortega F. 2016. Systematic review of late Jurassic sauropods from the Museu Geológico collections (Lisboa, Portugal). *Journal of Iberian Geology* **42**(2):227–250 DOI 10.5209/rev_JIGE.2016.v42.n2.52177.
- Myers TS, Tabor NJ, Jacobs LL, Mateus O. 2012. Estimating soil p CO₂ using paleosol carbonates: implications for the relationship between primary productivity and faunal richness in ancient terrestrial ecosystems. *Paleobiology* **38**(4):585–604 DOI 10.1666/11005.1.
- Nopsca FJ. 1928. The genera of reptiles. *Palaeobiologica* **1**:163–188.
- Ősi A. 2011. Feeding-related characters in basal pterosaurs: implications for jaw mechanism, dental function and diet. *Lethaia* **44**:136–152 DOI 10.1111/j.1502-3931.2010.00230.x.
- Owen R. 1842. Report on British fossil reptiles, part II. In: *Proceedings of the 11th Meeting of the British Association for the Advancement of Science*, Plymouth, UK60–204.
- O’Leary MA, Kaufman SG. 2012. MorphoBank 3.0: web application for morphological phylogenetics and taxonomy [computer software]. Available at <http://morphobank.org/permalink/?3968>.
- O’Sullivan M, Martill DM, Grocock D. 2013. A pterosaur humerus and scapulocoracoid from the Jurassic Whitby Mudstone Formation, and the evolution of large body size in early

- pterosaurs. *Proceedings of the Geologists' Association* **124**(6):973–981
DOI [10.1016/j.pgeola.2013.03.002](https://doi.org/10.1016/j.pgeola.2013.03.002).
- Padian K. 2008.** The early jurassic pterosaur campylognathoides strand, 1928. *Special Papers in Palaeontology* **80**:65–107.
- Paul GS. 2022.** *The Princeton field guide to pterosaurs*. Princeton: Princeton University Press.
- Perea D, Soto M, Toriño P, Mesa V, Maisey JG. 2018.** A late Jurassic-? earliest Cretaceous ctenochasmatid (Pterosauria, Pterodactyloidea): the first report of pterosaurs from Uruguay. *Journal of South American Earth Sciences* **85**:298–306 DOI [10.1016/j.jsames.2018.05.011](https://doi.org/10.1016/j.jsames.2018.05.011).
- Puértolas-Pascual E, Marx M, Mateus O, Saleiro A, Fernandes AE, Marinheiro J, Tomás C, Mateus S. 2021.** A new plesiosaur from the lower Jurassic of Portugal and the early radiation of Plesiosauroidea. *Acta Palaeontologica Polonica* **66**(2):369–388 DOI [10.4202/app.00815.2020](https://doi.org/10.4202/app.00815.2020).
- Pérez-García A. 2015.** Revision of the British record of Tropidemys (Testudines, Plesiochelyidae) and recognition of its presence in the Late Jurassic of Portugal. *Journal of Iberian Geology* **41**(1):11–20 DOI [10.5209/rev_JIGE.2015.v41.n1.48651](https://doi.org/10.5209/rev_JIGE.2015.v41.n1.48651).
- Pérez-García A, Ortega F. 2011.** *Selenemys lusitanica*, gen. et sp. nov., a new pleurosternid turtle (Testudines: Paracryptodira) from the upper Jurassic of Portugal. *Journal of Vertebrate Paleontology* **31**(1):60–69 DOI [10.1080/02724634.2011.540054](https://doi.org/10.1080/02724634.2011.540054).
- Pérez-García A, Ortega F. 2022.** New finds of the turtle Plesiochelys in the Upper Jurassic of Portugal and evaluation of its diversity in the Iberian Peninsula. *Historical Biology* **34**(1):121–129 DOI [10.1080/08912963.2021.1903000](https://doi.org/10.1080/08912963.2021.1903000).
- Rauhut OWM. 2001.** Herbivorous dinosaurs from the Late Jurassic (Kimmeridgian) of Guimarota, Portugal. *Proceedings of the Geologists' Association* **112**(3):275–283
DOI [10.1016/S0016-7878\(01\)80007-9](https://doi.org/10.1016/S0016-7878(01)80007-9).
- Ribeiro V, Mateus O, Holwerda F, Araújo R, Castanhinha R. 2014.** Two new theropod egg sites from the Late Jurassic Lourinhã Formation, Portugal. *Historical Biology* **26**(2):206–217
DOI [10.1080/08912963.2013.807254](https://doi.org/10.1080/08912963.2013.807254).
- Rodrigues T, Kellner AWA. 2013.** Taxonomic review of the Ornithocheirus complex (Pterosauria) from the Cretaceous of England. *ZooKeys (Monographs)* **308**:1–112
DOI [10.3897/zookeys.308.5559](https://doi.org/10.3897/zookeys.308.5559).
- Rotatori FM, Moreno-Azanza M, Mateus O. 2020.** New information on ornithopod dinosaurs from the Late Jurassic of Portugal. *Acta Palaeontologica Polonica* **65**(1):35–57
DOI [10.4202/app.00661.2019](https://doi.org/10.4202/app.00661.2019).
- Schneider S, Fürsich FT, Werner W. 2009.** Sr-isotope stratigraphy of the Upper Jurassic of central Portugal (Lusitanian Basin) based on oyster shells. *International Journal of Earth Sciences* **98**(8):1949–1970 DOI [10.1007/s00531-008-0359-3](https://doi.org/10.1007/s00531-008-0359-3).
- Soto M, Montenegro F, Toriño P, Mesa V, Perea D. 2021.** A new ctenochasmatid (Pterosauria, Pterodactyloidea) from the late Jurassic of Uruguay. *Journal of South American Earth Sciences* **111**(2):1–11 DOI [10.1016/j.jsames.2021.103472](https://doi.org/10.1016/j.jsames.2021.103472).
- Spindler F, Ifrim C. 2021.** Die Spur einer Spur—ein möglicher erster Flugsaurier aus Ettling. *Archaeopteryx* **37**:75–83.
- Sweetman SC, Martill DM. 2010.** Pterosaurs of the Wessex Formation (Early Cretaceous, Barremian) of the Isle of Wight, southern England: a review with new data. *Journal of Iberian Geology* **36**(2):225–242 DOI [10.5209/rev_JIGE.2010.v36.n2.9](https://doi.org/10.5209/rev_JIGE.2010.v36.n2.9).
- Taylor AM, Gowland S, Leary S, Keogh KJ, Martinius AW. 2014.** Stratigraphical correlation of the Late Jurassic Lourinhã Formation in the Consolação Sub-basin (Lusitanian Basin), Portugal. *Geological Journal* **49**(2):143–162 DOI [10.1002/gj.2505](https://doi.org/10.1002/gj.2505).

- Tennant JP, Mannion PD, Upchurch P, Sutton MD, Price GD. 2017.** Biotic and environmental dynamics through the Late Jurassic-Early Cretaceous transition: evidence for protracted faunal and ecological turnover. *Biological Reviews* **92**:776–814 DOI [10.1111/brv.12255](https://doi.org/10.1111/brv.12255).
- Thulborn RA. 1973.** Teeth of ornithischian dinosaurs from the Upper Jurassic of Portugal with description of a Hypsilophodontid (*Phylodon henkeli* gen. et sp. nov.) from the Ouimarota lignite. In: *Contribuição para o conhecimento da fauna do Kimeridgiano da mina de lignito Ouimarota (Leiria, Portugal), III parte*. Vol. 22. Lisboa: Memórias dos Serviços Geológicos de Portugal (N.S.), 89–134.
- Unwin DM. 2001.** An overview of the pterosaur assemblage from the Cambridge Greensand (Cretaceous) of Eastern England. *Fossil Record* **4**:189–221 DOI [10.5194/fr-4-189-2001](https://doi.org/10.5194/fr-4-189-2001).
- Unwin DM. 2002.** On the systematic relationships of *Cearadactylus atrox*, an enigmatic Early Cretaceous pterosaur from the Santana Formation of Brazil. *Fossil Record* **5**:239–263 DOI [10.1002/mmng.20020050114](https://doi.org/10.1002/mmng.20020050114).
- Unwin DM. 2003.** On the phylogeny and evolutionary history of pterosaurs. In: Buffetaut E, Mazin J-M, eds. *Evolution and Palaeobiology of Pterosaurs*. Vol. 217. London: Geological Society, Special Publications, 139–190.
- Unwin DM, Lü J, Bakhurina NN. 2000.** On the systematic and stratigraphic significance of pterosaurs from the Lower Cretaceous Yixian Formation (Jehol Group) of Liaoning, China. *Mitteilungen aus dem Museum für Naturkunde in Berlin, Geowissenschaftlichen Reihe* **3**:181–206 DOI [10.1002/mmng.20000030109](https://doi.org/10.1002/mmng.20000030109).
- van Hinsbergen DJJ, de Groot LV, van Schaik SJ, Spakman W, Bijl PK, Sluijs A, Langereis CG, Brinkhuis H. 2015.** A paleolatitude calculator for paleoclimate studies. *PLOS ONE* **10**(6):e0126946 DOI [10.1371/journal.pone.0126946](https://doi.org/10.1371/journal.pone.0126946).
- Wang X, Kellner AWA, Zhou Z, Campos DA. 2007.** A new pterosaur (Ctenochasmatidae, Archaeopterodactyloidea) from the Lower Cretaceous Yixian Formation of China. *Cretaceous Research* **28**:245–260 DOI [10.1016/j.cretres.2006.08.004](https://doi.org/10.1016/j.cretres.2006.08.004).
- Wellnhofer P. 1975.** Die Rhamphorhynchoidea (Pterosauria) der Oberjura-Plattenkalke Süddeutschlands. Teil II Systematische Beschreibung. *Palaeontographica A* **148**(4–6):132–186.
- Wiechmann MF, Gloy U. 2000.** Pterosaurs and Urvogels from the Guimarota mine. In: Verlag FP, ed. *Guimarota: a Jurassic Ecosystem*. München: Verlag Dr. Friedrich Pfeil, 83–86.
- Young MT, Hua S, Steel L, Foffa D, Brusatte SL, Thuring S, Mateus O, Ruiz-Omeñaca JJ, Havlik P, Lepage Y, De Andrade MB. 2014.** Revision of the Late Jurassic teleosaurid genus *Machimosaurus* (Crocodylomorpha, Thalattosuchia). *Royal Society Open Science* **1**(2):140222 DOI [10.1098/rsos.140222](https://doi.org/10.1098/rsos.140222).
- Zhou CF, Gao KQ, Yi H, Xue J, Li Q, Fox RC. 2016.** Earliest filter-feeding pterosaur from the Jurassic of China and ecological evolution of Pterodactyloidea. *Royal Society Open Science* **4**(2):160672 DOI [10.1098/rsos.160672](https://doi.org/10.1098/rsos.160672).

Chapter 5. Pterosaur teeth from the Valmitão microfossil assemblage (upper Jurassic, Lourinhã Formation, Portugal)

Keywords: *Pterosauria, Pterodactyloidea, Gnathosaurinae, Jurassic, Portugal*

The chapter was published as: Fernandes, A.E., Saleiro, A., Tomás, C., Martinho, M., Guillaume, A.R.D. (2024). Pterosaur teeth from the Valmitão microfossil assemblage (Upper Jurassic, Lourinhã Formation, Portugal). In: P. Fialho, R. da Silva, B. Camilo & H. Cândido (Eds.), *Paleolusitana: Proceedings of the Paleo Spring Meeting*, Vol. 2 (pp. 46-50).

Author contributions:

- Alexandra E. Fernandes: Conceptualization, Formal analysis, Investigation, Methodology, Writing-original draft
- André Saleiro: Resources, Validation, Writing-review & editing
- Carla Tomás: Resources, Supervision
- Micael Martinho: Resources
- Alexandre R. D. Guillaume: Conceptualization, Data curation, Methodology, Project administration, Visualization, Writing-review & editing

PTEROSAUR TEETH FROM THE VALMITÃO MICROFOSSIL ASSEMBLAGE (UPPER JURASSIC, LOURINHÃ FORMATION, PORTUGAL)

DENTES DE PTEROSSAURO DA AGLOMERAÇÃO DE MICROFÓSSEIS DE VALMITÃO (JURÁSSICO SUPERIOR, FORMAÇÃO LOURINHÃ, PORTUGAL)

Alexandra E. Fernandes ^{1,2,3*}, André Saleiro ^{3,4}, Carla Tomás ^{3,4}, Micael Martinho ³ & Alexandre R. D. Guillaume ^{3,4}

¹ SNSB - Bayerische Staatssammlung für Paläontologie und Geologie.

² Department of Earth and Environmental Sciences, Ludwig-Maximilians-Universität.

³ GEAL - Museu da Lourinhã.

⁴ GeoBioTec, FCT-NOVA.

* fernandes@snsb.de

ABSTRACT

Two pterosaur teeth recovered from the Valmitão vertebrate microfossil assemblage of the Lourinhã Formation of Portugal (Upper Jurassic) are here described and evaluated on several dental criteria, including: shape, dimension, curvature of their crowns and apices, degree of labiolingual compression, position of the enamel-dentine-boundary (EDB), enamel ornamentation, shape of the cross-sections, and size of the pulp cavity. Their morphologies and dental features reveal two distinct taxa with different ecomorphotypes, each representative of different feeding strategies, and supporting different attributions: one to Gnathosaurinae and another to Rhamphorynchinae. These attributions are congruent with previous pterosaur records from the Lourinhã Fm, and both highlight and expound upon the diversity of feeding behaviors exhibited by pterosaurs during the Late Jurassic, contributing additional crucial and diverse paleoecological niche elements towards reconstructing their paleoenvironment role that, in the likely absence of non-tooth fossil material, might otherwise have been overlooked completely.

Keywords: Pterosauria, microfossil teeth, Valmitão, Lourinhã Formation, Jurassic.

RESUMO

Dois dentes de pterossauro recuperados da aglomeração de microfósseis vertebrados de Valmitão, Formação da Lourinhã de Portugal (Jurássico Superior), são aqui descritos e avaliados sob diversos critérios dentários, incluindo: forma, dimensão, curvatura das suas coroas e ápices, grau de compressão labiolingual, posição do limite esmalte-dentina (EDB), ornamentação do esmalte, formato das secções transversais e tamanho da cavidade pulpar. As suas morfologias e características dentárias revelam dois taxa distintos com diferentes ecomorfotipos, cada um representativo de diferentes estratégias alimentares, e suportando diferentes atribuições: uma a Gnathosaurinae e outra a Rhamphorynchinae. Estas atribuições são congruentes com registos anteriores de pterossauros da Fm. da Lourinhã, onde ambas destacam e expõem a diversidade de comportamentos alimentares exibidos pelos pterossauros durante o Jurássico Superior. Estes exemplares contribuem com cruciais e diversos dados adicionais referentes a nichos paleoecológicos, permitindo a reconstrução do seu papel no paleoambiente que, na provável ausência de material fóssil não dentário, poderiam ter sido completamente ignorados.

Palavras-chave: Pterosauria, dentes microfósseis, Valmitão, Formação Lourinhã, Jurássico.

Introduction

Pterosaurs originated in the Late Triassic and later diversified into various groups, eventually reaching a worldwide distribution throughout the Jurassic and Cretaceous (Butler et al., 2012, 2013; Ezcurra et al., 2020; Foffa et al., 2022; Martill et al., 2014; Martinez et al., 2011; Müller et al., 2023). This extensive time range allowed for a plethora of morphological adaptations,

with such great variability being reflected throughout their bodies, including their dentition. Generally, basal pterosaurs exhibited more heterodont dentitions, with large numbers of conical teeth at the tips of their rostra and multicusped teeth toward the rear. By and large, this heterodonty decreased over time, even disappearing in the early pterodactyls, which diversified their dentition with more slender, elongate, and/or recurved teeth. With some exceptions, tooth

number also generally decreased over time, with the most derived pterosaurs becoming edentulous. This diverse variability in the pterosaurian dental apparatus was plausibly an adaptation to their ever-changing environments, and reflective of their numerous different feeding strategies and diverse prey preferences throughout their evolution (Ósi, 2011).

The overall preservation potential for pterosaur fossil material found outside of Lagerstätten environments is usually low, in great part due to their bone fragility, which makes them highly susceptible to taphonomic processes (Butler et al., 2013; Dean et al., 2016). Accordingly, their presence is often known only from isolated teeth, due to their in vivo tooth replacement and tendency to dislodge post-mortem (Brougham et al., 2017). Fossil teeth, in general, also preserve well and with frequency, due to their durable and highly-mineralized enamel, the hardest material in the vertebrate body (Wilmers & Bargmann, 2020). Pterosaur teeth are largely identifiable based on the characteristic enamel distribution and patterning that is restricted to pterosaurs: an apical enamel cap and dentine base to their tooth crowns, in which the dentine and enamel are well differentiated by a pronounced junction (the EDB), which slopes down at the anterior and posterior sides (or at the carinae, when present), but not to the alveolar level, leaving the lateral and medial sides mostly enamel-free (Fastnacht, 2005; Wellnhofer, 1985; Witton, 2013). Therefore, dental enamel structure, coupled with the position of the EDB along the crown, can be informative in ascertaining the functional limitations of various morphological differences, potentially eking out the dietary niches of taxa and their phylogenetic relationships (Fastnacht, 2005). However, factors such as size, overall morphology, and the thickness of enamel and dentine layers are known to vary both inter- and intra-specifically, either due to ontogeny or in adaptation to different biomechanical requirements (Fastnacht, 2005); a broad diversity which complicates the study of isolated teeth (especially considering the overall lack of specifically-indicative in situ associated diagnostic skeletal material). Despite this, certain tooth construction types generally can be recognized and identified to a lower-rank taxonomic level, such as family (Avarianov et al., 2005).

The Late Jurassic of Portugal is well representative of faunas in the J/K transition, which was a transformative and taxonomically selective time for pterosaurs (Tennant et al., 2017). Non-pterodactyloid pterosaurs (e.g. rhamphorhynchoids) were still present but already becoming extinct, while pterodactyloids (e.g. pterodactylids, ctenochasmatis, ornithocheiroids) originated and diversified during this time (Andres et al., 2014; Butler et al., 2013; Ji et al., 1999; Liu et al., 2012; Paul, 2022). However, although Portugal is quite productive for other Late Jurassic vertebrate fossils, it is no exception in its relative dearth of pterosaur fossil material (outside of isolated teeth), with only one confident tooth-bearing species described to date, the gnathosaurine *Lusognathus almadrava* Fernandes et

al., 2023, from the Kimmeridgian-Tithonian Lourinhã Formation. However, if considering teeth alone, remarkably the Guimarota beds have yielded over 300 in isolation, assigned to both *Rhamphorhynchus* sp. von Meyer, 1847, *Pterodactylus* sp. Cuvier, 1809, and to the Pterodactyloidea (Kühne, 1968; Wiechmann & Gloy 2000). More isolated teeth are also known from the Alcobaça Fm (Malafaia et al., 2010) and the Sobral Fm (Bertozzo et al., 2021), respectively referred to Pterosauria indet. and *Gnathosaurus* sp. von Meyer, 1933.

Recently, two miniscule pterosaur teeth were recovered from the Valmitão microfossil assemblage of the Lourinhã Fm (which has yielded a rich diversity in vertebrates from the Upper Jurassic of Portugal, i.e. Guillaume et al., 2023), revealing two distinct morphotypes. Here, we describe and evaluate the teeth on several dental criteria, including: shape, dimension, curvature of their crowns and apices, degree of labiolingual compression, position of the enamel-dentine-boundary (EDB), enamel ornamentation, shape of the cross-sections, and size of the pulp cavity. These identifications contribute additional crucial and diverse paleoecological niche elements towards reconstructing the role of pterosaurs in this Late Jurassic paleoenvironment that, in the likely absence of non-tooth fossil material, might otherwise have been overlooked completely.

Systematic paleontology

PTEROSAURIA Owen, 1842

PTERODACTYLOIDEA Plieninger, 1901

ARCHAEOPTERODACTYLOIDEA Kellner, 2001

CTENOCHASMATIDAE Nopsca, 1928 sensu Unwin, 2003

GNATHOSAURINAE Nopsca, 1928 sensu Unwin, 2002
Gnathosaurinae indet. (Figure 1)

Material description. Tooth ML 2846 (Figure 1) is preserved as an elongated subulate crown, with a pointed apex. It is missing the root and is slightly eroded at the apical-most tip, but is otherwise mostly complete. In lingual view, it measures 5.33mm high and 1.25mm wide at the base of the crown, making it about 4.26 times longer apicobasally tall than mesiodistally wide. The crown is moderately curved in the mesio-distal plane, and near the apex also becomes slightly lingually recurved. The overall displacement of these curvatures is less than the individual tooth width. It is rounded to ovoid in cross-section (displaying slight lateral compression). The enamel is smooth overall, lacking ornamentation, with the EDB occurring about halfway up the preserved crown. There are no visible carinae. A small pulp cavity is visible at the bottom of the crown, occupying about 25% of the cross-sectional area.

Remarks. Morphologically, tooth ML 2846's "needle-like" thin tooth shape, sub-circular cross-section (with slight antero-posterior compression), very narrow



Figure 1. ML 2846 in lingual (A), basal (B), apical (C), and posterior (D) views.

Figura 1. ML 2846 nas vistas lingual (A), basal (B), apical (C) e posterior (D).

pulp cavity, and smooth enamel is in keeping with all ctenochasmatids (Bestwick, 2018; Fastnacht, 2005; Wellnhofer, 1970). Its lack of carinae is also significant, as most pterosaurs exhibit them (with few exceptions, e.g. most ctenochasmatids and ornithocheirids), and functionally makes a difference in prey acquisition, as the force needed for puncturing is much lower in a laterally compressed tooth construction with carinae than without (Fastnacht, 2005). This is in keeping with the more passive filter-feeding styles of the ctenochasmatids (when compared to other groups like the ornithocheirids). Furthermore, while ctenochasmatid teeth are known to be only most apically tapered, gnathosaurine teeth instead taper overall from base to tip (Knoll, 2000; Wellnhofer, 1970), with gnathosaurs sustaining a proportionately more robust tooth shape (Fernandes et al., 2023) and more pronounced EDB. Cumulatively, these features, coupled with the tooth proportions of known gnathosaurines and the presence of gnathosaurs being definitively known from the Lourinhã Fm (e.g. *Lusognathus almadrava* Fernandes et al., 2023), indicate an attribution to Gnathosaurinae.

PTEROSAURIA Owen, 1842

RHAMPHORYNCHOIDEA Plieninger, 1901

RHAMPHORYNCHINAE Nopsca, 1928

Rhamphorynchinae indet. (Figure 2)

Material description. Tooth ML 2831 (Figure 2) is preserved as a mostly-complete elongate crown, missing the root. There is a distinct wear facet on the apical-most tip of the lingual side. In lingual view, it measures 10.22mm high and 1.78mm wide at the base of the crown, making it about 5.74 times longer apicobasally tall than mesiodistally wide. In the lingual view, the crown is almost straight, though curved slightly anteriorly at the apex. In lateral view, the tooth is substantially lingually recurved, with an overall displacement of more than the individual tooth width. It is lenticular in cross-section (labiolingual compressed), exhibiting two distinct carinae on the mesial and distal surfaces of the tooth. The enamel is smooth overall, with the EDB occurring in the upper third margin of the crown. A large pulp cavity is visible at the bottom of the crown, occupying about 80% of the cross-sectional area.



Figure 2. ML 2831 in lingual (A), basal (B), apical (C), and posterior (D) views.

Figura 2. ML 2831 nas vistas lingual (A), basal (B), apical (C) e posterior (D).

Remarks. Morphologically, ML 2831 differs significantly from ML 2846, particularly in being almost twice its size. Additionally, the presence of ML 2831's well-defined carinae, enamel distribution, and laterally-compressed cross-section shape (features of rhamphorynchids, i.e. Bennett, 1995; Fastnacht, 2005; Wellnhofer, 1978) indicate that less force would have been necessary for this tooth to puncture potential prey than as exhibited by the morphology of ML 2846 (i.e. Abler, 1992; Fastnacht, 2005). The more apically-placed EDB also carries great significance in function, as the distribution of more dentine along the crown overall would indicate a potential for more tooth flexure than in ML 2846, indicative of a more active feeding style. The presence of a larger pulp cavity can also be inferred to be biomechanically indicative of a tooth with more force acting upon it, because the lack of hard tooth material implies a larger surface area for the pulp to defensively function in forming reparative dentin in response to irritation (Yu & Abbott, 2007).

These features, coupled with the proportions of the tooth matching those reported for rhamphorynchids (i.e. Fastnacht, 2005), all indicate an attribution to Rhamphorynchinae.

Conclusion

Here two isolated pterosaur teeth are described from the vertebrate microsite of Valmitão, Portugal (Upper Jurassic, Lourinhã Fm). Their distinct morphologies and enamel distributions imply two different ecomorphotypes, each representative of different feeding strategies, and supporting different attributions: one to Gnathosaurinae and one to Rhamphorynchinae (assessing isolated teeth alone prevents any more specific identification). These attributions are congruent with previous pterosaur records from the Lourinhã Fm, and both highlight and expound upon the diversity of feeding behaviors exhibited by pterosaurs during the Late Jurassic.

REFERENCES

- Abler, W. L. (1992). The serrated teeth of tyrannosaurid dinosaurs, and biting structures in other animals. *Paleobiology*, 18(2), 161–183. <https://doi.org/10.1017/S0094837300013956>
- Andres, B., Clark, J., & Xu, X. (2014). The Earliest Pterodactyloid and the origin of the group. *Current Biology*, 24(9), 1011–1016. <https://doi.org/10.1016/j.cub.2014.03.030>
- Avarianov, A. O., Martin, T., & Bakirov, A. A. (2005). Pterosaur and dinosaur remains from the Middle Jurassic Balabansai Svita in the Northern Fergana Depression, Kyrgyzstan (Central Asia). *Palaeontology*, 48(1), 135–155. <https://doi.org/10.1111/j.1475-4983.2004.00437.x>
- Bennett, S. C. (1995). A Statistical Study of *Rhamphorhynchus* from the Solnhofen Limestone of Germany: Year-Classes of a Single Large Species. *Journal of Paleontology*, 69(3), 569–580. <https://doi.org/10.1017/S0022336000034946>
- Bertozzo, F., da Silva, B. C., Martill, D., Vorderwuelbecke, E. M., Aureliano, T., Schouten, R., & Aquino, P. (2021). A large pterosaur femur from the Kimmeridgian, Upper Jurassic of Lusitanian Basin, Portugal. *Acta Palaeontologica Polonica*, 66(4), 815–825. <https://doi.org/10.4202/app.00858.2020>
- Bestwick, J., Unwin, D. M., Butler, R. J., Henderson, D. M., & Purnell, M. A. (2018). Pterosaur dietary hypotheses: a review of ideas and approaches. *Biological Reviews*, 93(4), 2021–2048. <https://doi.org/10.1111/brv.12431>
- Brougham, T., Smith, E. T., & Bell, P. R. (2017). Isolated teeth of *Anhangueria* (Pterosauria: Pterodactyloidea) from the Lower Cretaceous of Lightning Ridge, New South Wales, Australia. *PeerJ*, 5, e3256. <https://doi.org/10.7717/peerj.3256>
- Butler, R. J., Benson, R. B. J., & Barrett, P. M. (2013). Pterosaur diversity: Untangling the influence of sampling biases, Lagerstätten, and genuine biodiversity signals. *Palaeogeography, Palaeoclimatology, Palaeoecology*, 372, 78–87. <https://doi.org/10.1016/j.palaeo.2012.08.012>
- Butler, R. J., Brusatte, S. L., Andres, B., & Benson, R. B. J. (2012). How do geological sampling biases affect studies of morphological evolution in deep time? A case study of pterosaur (Reptilia: Archosauria) disparity. *Evolution*, 66(1), 147–162. <https://doi.org/10.1111/j.1558-5646.2011.01415.x>
- Dean, C. D., Mannion, P. D., & Butler, R. J. (2016). Preservational bias controls the fossil record of pterosaurs. *Palaeontology*, 59(2), 225–247. <https://doi.org/10.1111/pala.12225>
- Ezcurra, M. D., Nesbitt, S. J., Bronzati, M., Vecchia, F. M. D., Agnolin, F. L., Benson, R. B. J., Egli, F. B., Cabreira, S. F., Evers, S. W., Gentil, A. R., Irmis, R. B., Martinelli, A. G., Novas, F. E., da Silva, L. R., Smith, N. D., Stocker, M. R., Turner, A. H., & Langer, M. C. (2020). Enigmatic dinosaur precursors bridge the gap to the origin of Pterosauria. *Nature*, 588, 445–449. <https://doi.org/10.1038/s41586-020-3011-4>
- Fastnacht, M. (2005). *Jaw mechanics of the pterosaur skull construction and the evolution of toothlessness* [Doctoral dissertation, Johannes Gutenberg-Universität Mainz]. Universitäts Bibliothek Mainz. <http://doi.org/10.25358/openscience-3460>
- Fernandes, A. E., Beccari, V., Kellner, A. W. A., & Mateus O. (2023). A new gnathosaurine (Pterosauria, Archaeopterygiformes) from the Late Jurassic of Portugal. *PeerJ*, 11, e16048. <https://doi.org/10.7717/peerj.16048>
- Figueiredo, S. D., Cunha, P. P., Pereda-Suberbiola, X., de Carvalho, C. N., Carvalho, I. S., Buffetaut, E., Tong, H., Sousa, M. F., Antunes, V., & Anastácio, R. (2022). The dinosaur tracksite from the lower Barremian of Areia do Mastro Formation (Cabo Espichel, Portugal): implications for dinosaur behavior. *Cretaceous Research*, 137, 105219. <https://doi.org/10.1016/j.cretres.2022.105219>

- Figueiredo, S. D., Rosina, P., Strantzali, I. B., Antunes, V., & Figueiredo, S. (2020). Paleoenvironmental approach on the Lower Cretaceous sequences of Areia do Mastro (Cabo Espichel, Southern Portugal). *Journal of Environmental Engineering and Science*, 9(2), 66–71. <http://dx.doi.org/10.17265/2162-5298/2020.02.003>
- Foffa, D., Dunne, E. M., Nesbitt, S. J., Butler, R. J., Fraser, N. C., Brusatte, S. L., Farnsworth, A., Lunt, D. J., Valdes, P. J., Walsh, S., & Barrett, P. M. (2022). *Scleromochlus* and the early evolution of Pterosauroomorpha. *Nature*, 610(7931), 313–318. <https://doi.org/10.1038/s41586-022-05284-x>
- Guillaume, A. R. D., Ezquerro, L., Moreno-Azanza, M., & Mateus O. (2023). Vertebrate microfossil assemblages from the Lourinhã Formation: a sneak peek on the paleoecology of the Late Jurassic in Portugal. *The Anatomical Record*, 306(S1), 118–121. <https://doi.org/10.1002/ar.25219>
- Ji, S. -A., Ji, Q., & Padian, K. (1999). Biostratigraphy of new pterosaurs from China. *Nature*, 398(6728), 573–573. <https://doi.org/10.1038/19221>
- Knoll, F. (2000). Pterosaurs from the Lower Cretaceous (?Berriasian) of Anoual, Morocco. *Annales de Paléontologie*, 86(3), 157–164. [https://doi.org/10.1016/S0753-3969\(00\)80006-3](https://doi.org/10.1016/S0753-3969(00)80006-3)
- Kühne, W. G. (1968). History of discovery, report on the work performed, procedure, technique and generalities. In Serviços Geológicos de Portugal (Ed.), *Contribuição para a fauna do Kimeridgiano da Mina de lignito Guimarães (Leiria, Portugal), I parte* (Vol. 14, pp. 7–20). Memórias dos Serviços Geológicos de Portugal, Nova Série. <https://docbase.ineg.pt/docs/Memorias/14.pdf>
- Liu, Y. -Q., Kuang, H. -W., Jiang, X. -J., Peng, N., Xu, H., Sun, H. -Y. (2012). Timing of the earliest known feathered dinosaurs and transitional pterosaurs older than the Jehol Biota. *Palaeogeography, Palaeoclimatology, Palaeoecology*, 323–325, 1–12. <https://doi.org/10.1016/j.palaeo.2012.01.017>
- Malafaia, E., Ortega, F., Escaso, F., Dantas, P., Pimentel, N., Gasulla, J. M., Ribeiro, B., Barriga, F., & Sanz, J. L. (2010). Vertebrate fauna at the *Allosaurus* fossil-site of Andrés (Upper Jurassic), Pombal, Portugal. *Journal of Iberian Geology*, 36(2), 193–204. <https://revistas.ucm.es/index.php/JIGE/article/view/JIGE1010220193A>
- Martill, D., Unwin, D., & Loveridge, R. (Eds.) (2014). *The Pterosauria*. Cambridge: Cambridge University Press.
- Martinez, R. N., Sereno, P. C., Alcober, O. A., Colombi, C. E., Renne, P. R., Montanez, I. P., & Currie, B. S. (2011). A basal dinosaur from the dawn of the dinosaur era in southwestern Pangaea. *Science*, 331, 206–210. <https://doi.org/10.1126/science.1198467>
- Muller, R. T., Ezcurra, M. D., Garcia, M. S., Agnolin, F. L., Stocker, M. R., Novas, F. E., Soares, M. B., Kellner, A. W. A., & Nesbitt, S. J. (2023). New reptile shows dinosaurs and pterosaurs evolved among diverse precursors. *Nature*, 620(7974), 589–594. <https://doi.org/10.1038/s41586-023-06359-z>
- Ósi, A. (2011). Feeding-related characters in basal pterosaurs: implications for jaw mechanism, dental function and diet. *Lethaia*, 44(2), 136–152. <https://doi.org/10.1111/j.1502-3931.2010.00230.x>
- Paul, G. S. (2022). *The Princeton field guide to pterosaurs*. Princeton University Press.
- Tennant, J. P., Mannion, P. D., Upchurch, P., Sutton, M. D., & Price, G. D. (2017). Biotic and environmental dynamics through the Late Jurassic–Early Cretaceous transition: evidence for protracted faunal and ecological turnover. *Biological Reviews*, 92(2), 776–814. <https://doi.org/10.1111/brv.12255>
- Wellnhofer, P. (1970). Die Pterodactyloidea (Pterosauria) der Oberjura-Plattenkalke Süddeutschlands. *Abhandlungen der Bayerischen Akademie der Wissenschaften, Neue Folge*, 141, 1–133. https://www.zobodat.at/pdf/Abhandlungen-Akademie-Bayern_NF_141_0001-0133.pdf
- Wellnhofer, P. (Ed.) (1978). *Pterosauria*. In *Handbuch der Paläoherpétologie, Encyclopedia of Paleoherpétology* (pp. 1–82). G. Fischer-Verlag.
- Wellnhofer, P. (1985). Neue Pterosaurier aus der Santana-Formation (Apt) der Chapada do Araripe, Brasilien. *Palaeontographica (A)*, 187(4–6), 105-182.
- Wiechmann, M. F., & Gloy, U. (2000). Pterosaurs and Urvogels from the Guimarota mine. In F. P. Verlag (Ed.), *Guimarota: a Jurassic Ecosystem* (pp. 83–86). Verlag Dr. Friedrich Pfeil.
- Wilmers, J., & Bargmann, S. (2020). Nature's design solutions in dental enamel: Uniting high strength and extreme damage resistance. *Acta Biomaterialia*, 107, 1–24. <https://doi.org/10.1016/j.actbio.2020.02.019>
- Witton, M. P. (Ed.) (2013). *Pterosaurs: Natural History, Evolution, Anatomy*. Princeton: Princeton University Press.
- Yu, C., & Abbott, P. V. (2007). An overview of the dental pulp: its functions and responses to injury. *Australian Dental Journal Supplement*, 52(s1), S4–S6. <https://doi.org/10.1111/j.1834-7819.2007.tb00525.x>

Chapter 6. A new vertebrate assemblage from the Matute Formation of the Cameros Basin (Ágreda, Spain): implications for the diversity during the Jurassic/Cretaceous boundary

Keywords: *Osteichthyes, Crocodylomorpha, Testudinata, Pterosauria, Tera Group, Tithonian-Barresian*

The chapter was published as: Puértolas-Pascual, E., Aurell, M., Bermúdez-Rochas, D.D., Canudo, J.I., Fernandes, A.E., Galobart, À., Moreno-Azanza, M., Pérez-García, A. & Castanera, D. (2023). A new vertebrate assemblage from the Matute Formation of the Cameros Basin (Ágreda, Spain): implications for the diversity around the Jurassic–Cretaceous boundary. *Journal of Iberian Geology*, 50, 83-103.

Author contributions:

- Alexandra E. Fernandes: Formal analysis, Investigation, Writing-original draft, Writing-review & editing



A new vertebrate assemblage from the Matute Formation of the Cameros Basin (Ágreda, Spain): implications for the diversity during the Jurassic/Cretaceous boundary

E. Puértolas-Pascual¹  · M. Aurell¹  · D. D. Bermúdez-Rochas²  · J. I. Canudo¹  · A. E. Fernandes^{3,4} · A. Galobart⁵  · M. Moreno-Azanza^{1,6}  · A. Pérez-García⁷  · D. Castanera⁸ 

Received: 15 March 2023 / Accepted: 13 September 2023 / Published online: 25 October 2023
© The Author(s) 2023

Abstract

The Ribota site (Ágreda, Soria, Spain) is a new locality in the Matute Formation (Tithonian–Berriasian) composed of several carbonate layers, outstandingly rich in macrovertebrate remains. Fossils show an unusual replacement of the original bioapatite by quartz, and are found as positive reliefs protruding from lacustrine limestone beds. This type of conservation has allowed the identification of around one hundred vertebrate bone accumulations in an outcrop of more than 10 hectares. Osteichthyans (articulated partial skeletons, cranial material, and isolated postcranial bones and scales), crocodylomorphs (disarticulated cranial material, isolated teeth, vertebrae and osteoderms), turtles (partial carapaces and plastras, but also isolated plates) and pterosaurs (cranial and appendicular elements) have been identified. Around 80 specimens have been collected and a preliminary study of part of the collection (35 specimens) has allowed the identification of at least 5 different taxa: Halecomorphi indet., Neoginglymodi indet., Goniopholididae indet., Testudinata indet., and Pterodactyloidea indet. This new site represents one of the few sites from this time interval preserved in a fully lacustrine environment, so these vertebrate assemblages are unique and composed of different animals that presumably lived around and within the lake. They are dominated by aquatic and amphibian vertebrates and was formed by attrition in this lacustrine environment, possibly far from the lake shoreline. These macrovertebrate assemblages provide new data about the diversity in the faunal ecosystems from the Jurassic/Cretaceous transition of the Iberian Basin Rift System.

Keywords Osteichthyes · Crocodylomorpha · Testudinata · Pterosauria · Tera Group · Tithonian–Berriasian

Resumen

El yacimiento de Ribota (Ágreda, Soria, España) es una nueva localidad en la Formación Matute (Titoniense-Berriasiense) compuesta por varios estratos de calizas excepcionalmente ricos en restos de macrovertebrados. Los fósiles muestran una sustitución inusual del bioapatito original por cuarzo, y se encuentran como relieves positivos sobresaliendo de la superficie de las calizas lacustres. Este tipo de conservación ha permitido la preservación e identificación de alrededor de cien acumulaciones de huesos de vertebrados en una superficie de más de 10 hectáreas. Se han identificado peces osteíctios (esqueletos parciales articulados, material craneal y escamas y huesos postcraneales aislados), cocodrilomorfos (material craneal desarticulado, dientes aislados, vértebras y osteodermos), tortugas (caparazones y plastrones parciales, pero también placas aisladas) y pterosaurios (elementos craneales y apendiculares). Se han recuperado alrededor de 80 especímenes y un estudio preliminar de parte de la colección (35 especímenes) ha permitido la identificación de al menos 5 taxones diferentes: Halecomorphi indet., Neoginglymodi indet., Goniopholididae indet., Testudinata indet. y Pterodactyloidea indet. Este nuevo yacimiento representa uno de los pocos yacimientos de este intervalo temporal conservados en un ambiente completamente lacustre, por lo que estas asociaciones de vertebrados son únicas y están compuestas por

diferentes animales que presumiblemente vivieron alrededor y dentro del lago. Están dominadas por vertebrados acuáticos y anfibios, y se formaron por atrición en este entorno lacustre, posiblemente dentro del lago y lejos de la orilla. Estas asociaciones de macrovertebrados proporcionan nuevos datos sobre la diversidad faunística en los ecosistemas presentes durante la transición Jurásico/Cretácico del Sistema de Rift de la Cuenca Ibérica.

Palabras clave Osteichthyes · Crocodylomorpha · Testudinata · Pterosauria · Grupo Tera · Titiense–Berriasiense

1 Introduction

The sedimentary successions deposited during the Jurassic/Cretaceous transition in the eastern Cameros basin (north central Spain) are well known for their large number of tracksites. The diverse ichnofauna of the Berriasian deposits (Oncala Group) of the Huérteles Formation in the North of Soria province stands out. This region has such an ichnological richness, (containing more than 7,000 vertebrate footprints produced mainly by dinosaurs, but also from pterosaurs, crocodylomorphs and turtles [e.g., Fuentes Vidarte et al., 2005; Hernández Medrano et al., 2006; Castanera et al., 2018]), that it gave rise to the creation of the touristic project “Ichnite Route of Soria” (Barco et al., 2013; Castanera et al., 2018), where a selection of dinosaur tracksites are prepared for tourist visits. This contrasts with the very scarce osteological fossil record found in the geological units that span around the Jurassic/Cretaceous (Tithonian–Berriasian) transition of the Tera Group (Agreda, Magaña and Matute Fms) in this sector of the Cameros basin.

One of the Tithonian–Berriasian geological units from the eastern Cameros basin that has yielded some fossil bones is the Matute Fm (Salomon, 1982a, b; Fernández and Meléndez, 1994). The latter authors indicate that remains of fishes and reptiles are relatively frequent in this unit, however only two notable specimens have been described in this formation. One corresponds to an articulated ginglymodian actinopterygian fish described as *Camerichthys lunae* Bermúdez-Rochas & Poyato-Ariza, 2015, from the locality of San Andrés de San Pedro (northeast of Soria province). The second is the freshwater aquatic stem turtle *Pleurosternon moncayensis* Pérez-García et al., 2022 (represented by a partial skull and several postcranial remains of a pleurosternid), recovered from the surroundings of Ágreda (east of Soria province), and only two kilometers away from the site here studied. In addition, also within the eastern Cameros basin in the town of Tera (north of Soria), some dinosaur remains of similar age from the Magaña Fm have also been reported (Canudo et al., 2010), and an articulated fish assigned to *Lepidotes* sp. has been described from the Berriasian of the Valdeprado Fm (Pascual-Arribas et al., 2007). South of Soria, in the Torrelapaja subbasin, the vertebrate fossil site of La Atalaya (Bijuesca Fm) includes large sized sauropod and crocodylomorph remains preserved in palustrine facies,

most probably formed during the Tithonian–Berriasian transition (Aurell et al., 2021). This scarce vertebrate fossil content contrasts with the relatively abundant osteological record (mostly sauropod dinosaurs) with similar age, found in the western Cameros basin (mainly in Burgos Province) (e.g., Torcida Fernández-Baldor et al., 2020), in other areas of the Iberian Range, such as the Maestrazgo and South Iberian basins (northwest of Valencia and southwest of Teruel provinces) (e.g., Ruiz-Omeñaca et al., 2004; Aurell et al., 2016; Campos-Soto et al., 2019), or in the northern Aquitaine Basin in SW France (Allain et al., 2022).

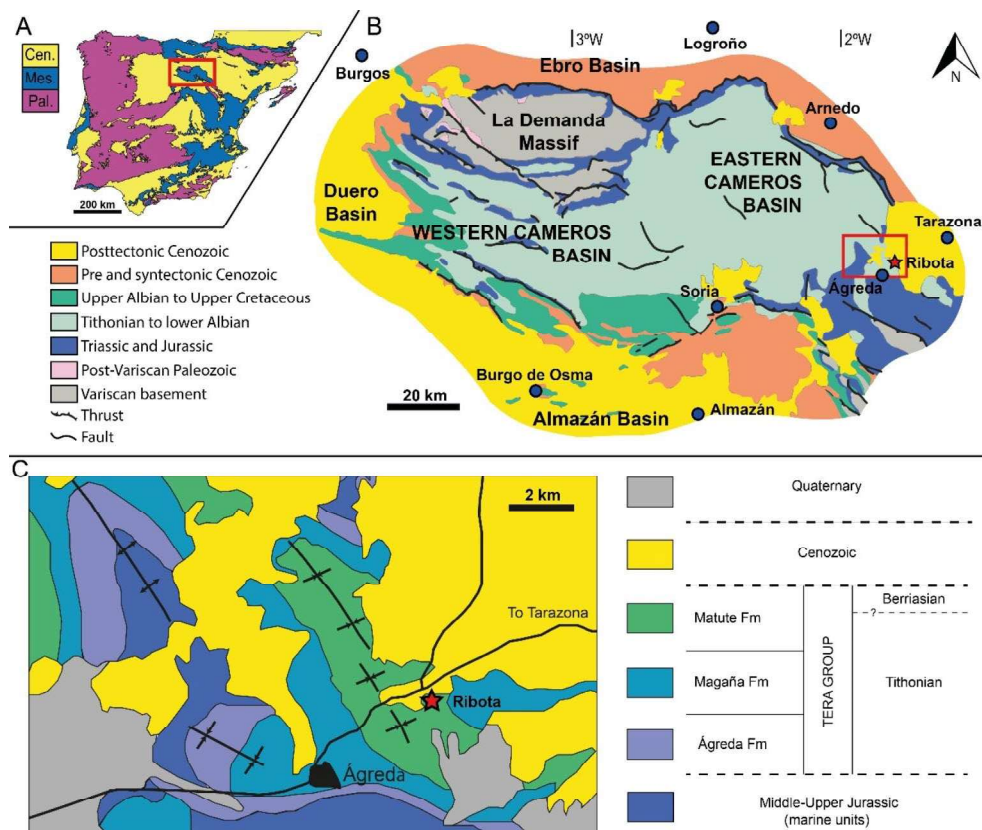
Here we present the new palaeontological site of Ribota (Ágreda, Soria province, Spain) (Fig. 1), which contains one of the most abundant vertebrate fossil assemblages of the whole Cameros basin. Until now, hundreds of bone remains (Figs. 2, 3, 4, 5, 6, 7 and 8) that correspond to osteichthyan fishes (Fig. 5), crocodylomorphs (Fig. 6), turtles (Fig. 7) and pterosaurs (Fig. 8) have been identified, and some of them, including all the remains described in this work, were recovered from the field. This paper aims to present a first approach to the genesis of this site (Figs. 3 and 4) and its palaeontological assemblage, in order to reconstruct the ecosystem of this area of the Cameros basin around the Jurassic/Cretaceous boundary.

2 Geographic and geological context

The Ribota fossil site is located 5 km northeast from the village of Ágreda (Soria Province, Castilla y León, north-central Spain), a town located about 10 km northwest of the Moncayo, the highest mountain of the Iberian Chain. The site outcrops in a sparsely vegetated area adjacent to the north of a meander of the Val River, about 300 m northwest of the “Pozo de las Truchas” waterfall.

Geologically, Ribota is located within the Cameros basin. This basin is found in the northwestern part of the Iberian Basin Rift System (Fig. 1A), which was formed due to extensional tectonics during the latest Jurassic–Early Cretaceous rifting stage. This rifting has been related to the opening of the Western Tethys Sea and the Northern Atlantic Ocean (see Salas et al., 2001; Mas et al., 2002, 2004, 2011; Aurell et al., 2019, 2021 and references therein). The Ribota site is located in the easternmost part of the eastern Cameros basin (Fig. 1B, C).

Fig. 1 **A)** Geographic and geological location of the Ribota site (Soria, Castilla y León, Spain) within the Iberian Peninsula; **B)** geological location of the site within the Cameros basin, modified from Rodríguez-Barreiro et al. (2022); **C)** detailed geological map of the area and its stratigraphic framework, modified Gómez Fernández and Meléndez (1994)

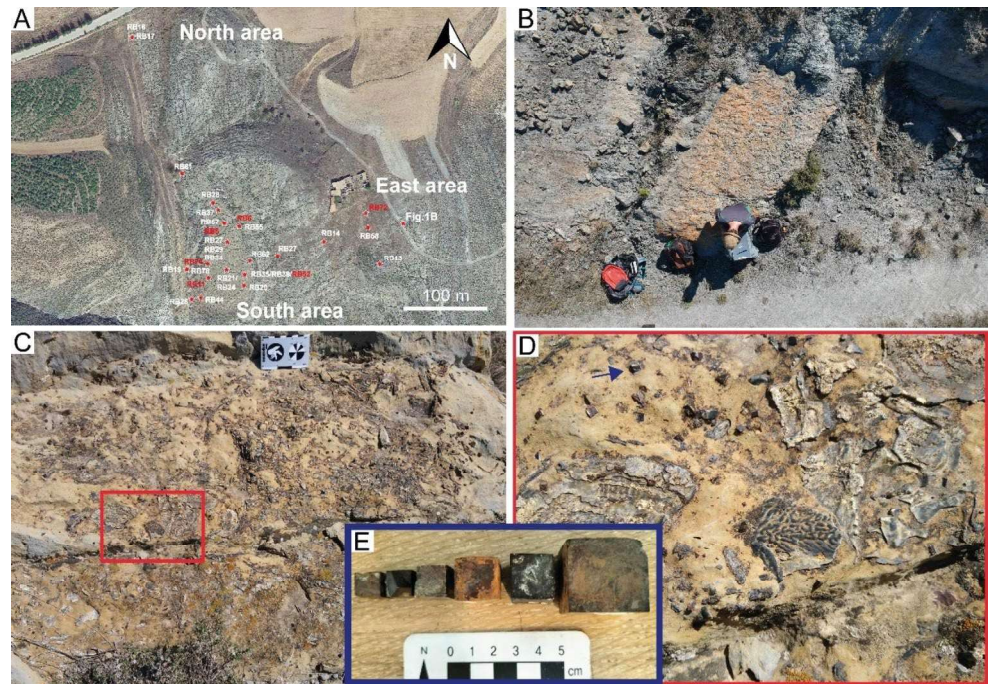


The depocenter of the Cameros basin is filled with more than 8,000 m of Upper Jurassic–Lower Cretaceous lacustrine/coastal carbonates and evaporites alternated with fluvial siliciclastic deposits (Salas et al., 2001; Mas et al., 2004). Tischer (1996) divided this succession into five groups (Tera, Oncala, Urbión, Enciso, and Oliván). Successive genetic units were recognised, and the Tera Group was divided into three alloformations (Gómez-Fernández & Meléndez, 1994), that were subsequently used as lithostratigraphic units (e.g., Mas et al., 2004; Clemente, 2010; Martín-Chivelet et al., 2019). The lower Ágreda Fm consists of shallow marine, alluvial, lacustrine to palustrine deposits; the middle Magaña Fm is characterised by fluvial facies, and the upper Matute Fm (also known as the Sierra Matute Fm) is dominated by lacustrine deposits and includes the Ribota site studied in this work (Fig. 1C). This unit was originally interpreted as early Berriasian in age (Salomon, 1982a, b). The Berriasian age assignment for this unit, based on biostratigraphy, was also supported by Martín-Closas and Alonso Millán (1998), Salas et al. (2001), Mas and Salas (2002) or Clemente (2010). However, other authors considered the Matute Fm as Tithonian in age (Mas et al., 1993; Gómez-Fernández & Meléndez, 1994), although the top of the unit could even reach the beginning of the Berriasian (Gómez-Fernández, 1992; Meléndez & Gómez-Fernández, 2000). Accordingly, the precise age of this unit remains uncertain.

The late Tithonian–earliest Berriasian age assumed here for the Matute Fm (Fig. 1C; see also Pérez-García et al., 2022) is based on the charophyte and ostracod content described in previous works (Gómez Fernández and Meléndez 1994; Tejero & Fernández-Gianotti, 2004; Schudack & Schudack, 2009).

The Ribota site is located in the lower part of the lacustrine carbonates of the Matute Fm (Fig. 1C), within a carbonate-dominated interval outcropping over a large area of about 10 hectares (Fig. 2A). Ribota is a rich locality where isolated bones are found in almost every square meter of the outcrop. Based on the closeness of several specific points with the higher bone concentrations, Ribota can be divided into three main areas (north, south, and east, Fig. 2A). The north and south areas are stratigraphically equivalent (almost the same strata), whereas the east area corresponds to slightly lower strata located about 150 m east from the other areas, but in the same formation and similar limestone facies. The division into 3 areas is provisional until a more exhaustive stratigraphic study is carried out. The most important fossiliferous accumulations are in the south area within the same stratigraphic level. Except for some articulated partial skeletons of fishes and turtles (exclusively represented by shell elements), most of the remains appear scattered and disarticulated along the different outcrops in the area.

Fig. 2 **A)** Google Earth view of the Ribota site showing the different small outcrops with vertebrate remains; **B)** photograph and general view of the first site with vertebrate remains found in the east area, point “Fig. 1B” in the satellite photo in (A); **C)** fossiliferous point with a high concentration of disarticulated fish bones and a detail zoom of these remains (**D**) and a pyrite crystal pointed by a blue arrow; **E)** some pyrite crystals found in Ribota area



The studied geological samples are very fossiliferous wackestone limestones, whereas the most common fossils are disarticulated ostracod valves, followed by vertebrate remains. All the samples were collected in the southern zone of Ribota, except for the RB72 sample that was recovered in the eastern area (Fig. 2A). All fossiliferous remains show a variable degree of recrystallization that might be related to the low-grade hydrothermal metamorphism that affected the Matute Formation (e.g., Barrenechea et al., 2001). The invertebrate remains have been completely replaced by silica (probably quartz), whereas the vertebrate remains partially retain their original apatite composition, being partially replaced by quartz and calcite. Isolated calcite and dolomite crystals can be found dispersed in a chlorite-dominated matrix, where clay mineral crystals show no preferred orientation. Secondary idiomorphic pyrite crystals of variable size, from sub-millimetric to centimetric, have grown both in the matrix and inside the bone elements. These pyrite crystals are partially oxidised, showing concentric rings of hematite and goethite, and present very small irregular inclusions of relics of apatite and calcite, incorporated into the crystal during growth.

3 Materials and methods

To date, almost 80 vertebrate fossils have been recovered in the area. The material has been collected under the permit Exp. 37/2019-SO issued by the Dirección General de Patrimonio Cultural of the Junta de Castilla y León. Here we

study only those samples that allowed a preliminary taxonomic identification (Table 1). The fossils, together with their surrounding rock matrix, were delimited in blocks cut with a radial saw and extracted with a chisel and hammer. Each collected sample has been labelled with the acronym RB (from Ribota) and the subsequent field number (RB1 to RB79), and they have been deposited (fossil numbers, n° 2023/6/RB1 to 2023/6/RB79) in the Museo Numantino, provincial de Soria (Soria, Spain). For simplicity, throughout the text, each specimen is just referred with the field number (RB1 to RB79).

Eight standard (30-micron thin) sections of selected bone specimens within limestone matrix (one Testudinata RB5; two Neoginglymodi RB11 and RB26; and four Crocodylomorpha RB6, RB52, RB72 and RB74) were prepared, in order to analyse the fossil diagenesis processes at the Ribota site. The thin sections were examined and photographed with an Olympus BX53M petrographic polarizing microscope equipped with a digital camera, housed at the IUCA Microscopy Lab at Universidad de Zaragoza. After this preliminary analysis, samples were carbon-coated and analysed in a Merlin Carl Zeiss Field Emission Scanning Electron Microscope housed at the Servicio de Apoyo a la Investigación (SAI) of the Universidad de Zaragoza. Chemical and textural information on the mineral phases, both in the fossils and in the encasing matrix, was obtained using Backscattered electron images (BSE) and Energy Dispersive X-Ray Analysis (EDS) and were acquired at 15 kV and an IProbe of 600 pA, at a working distance of 5.5 mm, using a Cobalt standard for calibration of the semiquantitative analysis.

Table 1 List of the studied material showing the identification, taxonomy and location in the outcrop

Osteichthyes			
Acronym	Material	Taxa	Area
RB 11	articulated partial skeleton	Neoginglymodi indet.	South area
RB13	dentary	Halecomorphi indet.	East area
RB14	articulated partial skeleton	Neoginglymodi indet.	East area (exsitu)
RB26	articulated partial skeleton	Neoginglymodi indet.	South area
RB27	dentary	Neoginglymodi indet.	South area
RB58	dermopalatine fragment	Neoginglymodi indet.	East area
Crocodylomorpha			
Acronym	Material	Taxa	Area
RB6	diaphysis fragment	Goniopholididae indet.	South area
RB17	disarticulated cranial remains	Goniopholididae indet.	North area
RB21	caudal vertebra	Goniopholididae indet.	South area
RB35	ventral osteoderm	Goniopholididae indet.	South area
RB39	isolated tooth	Goniopholididae indet.	South area
RB44	dorsal vertebra	Goniopholididae indet.	South area
RB52	tooth	Goniopholididae indet.	South area
RB57	cervical vertebra	Goniopholididae indet.	South area
RB61	dorsal osteoderm	Goniopholididae indet.	South area
RB62	ventral osteoderm	Goniopholididae indet.	South area
RB66	caudal vertebra	Goniopholididae indet.	South area
RB69	sacral vertebra	Goniopholididae indet.	East area
RB72	osteoderm	Goniopholididae indet.	East area
RB74-78	vertebrae	Goniopholididae indet.	South area
Testudinata			
Acronym	Material	Taxa	Area
RB5	Shell fragment	Testudinata indet.	South area
RB16	bridge peripheral	Testudinata indet.	South area
RB18	costal	Testudinata indet.	North area
RB20	hypoplastron	Testudinata indet.	South area
RB24	costal	Testudinata indet.	South area
Pterosauria			
Acronym	Material	Taxa	Area
RB19	mandibular fragment	Pterodactyloidea indet.	South area
RB28	Femur	Pterodactyloidea indet.	South area
RB29	humerus	Pterodactyloidea indet.	South area
RB34	epiphyseal fragment	Pterodactyloidea indet.	South area
RB37	Partial radius	Pterodactyloidea indet.	South area
RB55	digit IV phalanx	Pterodactyloidea indet.	South area

4 Taphonomy

No meaningful differences concerning the lithology, abundance, and diversity of fossils, or taphonomic patterns have been observed between the sampled areas. The preliminary taphonomic analysis here reported, and supported by field and thin section observations, considers the working hypothesis that all of them represent a single bonebed (north and south areas), or successive bonebeds (e.g., east area), accumulated by similar non-differentiable processes. Thus, all the specimens will be analysed as coming from a single locality.

The fossil taphonomic history of the site is unusual and interesting. In the field, the fossils outcrop as dark brown to black positive reliefs protruding from the limestone, harder

than the rock, and showing a very well-preserved external morphology. However, when broken, the bone tissue appears highly recrystallised, presenting conchoidal fractures, bright white and grey colours, and barely retaining its internal structure, making it almost indistinguishable from the encasing rock.

Bone remains appear distributed throughout the outcrop, without an appreciable distribution pattern, and no significant variation in the concentration of fossils is observed along the thickness of the studied section, within its several bone-bearing levels. Nevertheless, some areas show a relative increase in fossils elements, specifically of fossil fish bones (Fig. 2B-D) and some accumulations of crocodylomorph remains (Fig. 6F). Most fossils are bone fragments, but complete disarticulated elements are also frequent, and

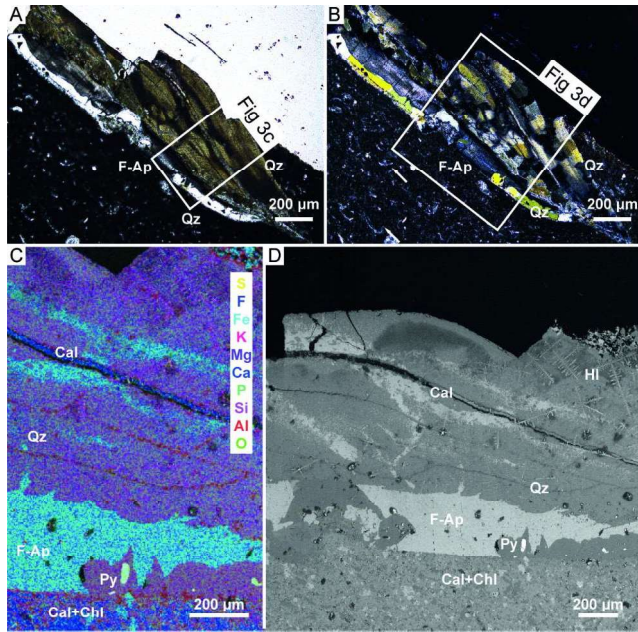


Fig. 3 Thin section of one scale of RB26 *Neoginglymodi* indet. **(A)** polarized transmitted light showing the preserved lamination of the histostructure of the scale, and diagenetic fractures infilled with quartz. **(B)** cross polarized transmitted light image of the same view as **(A)**, showing that most of the bone has been replaced by quartz (brown and yellow interference colours), whereas only a small amount of the original fluorapatite is preserved in the bottom part of the scale (denim blue interference colours). Note that two different quartz phases can be observed in **(A)** but are indistinguishable in **(B)**, one that is brown in **(A)** and another that is completely transparent suggesting the presence of an epitaxial growth of quartz after the bone replacement. White arrows point to recrystallized ostracod shells. **(C)** EDS map showing the elemental composition of the area in the white square in **(A)**. Fluorapatite in light blue whereas quartz is shown in purple. Dark blue calcite infilled cracks can be observed in the top half of the map. Note the presence of small greenish pyrite crystal in the bottom part of the image. **(D)** BSE image of the squared area in 3D. The encasing sediment is a mixture of calcitic micrite and chlorite. Anatomical abbreviations: Cal., Calcite; Chl., Chlorite; F-Ap., Fluorapatite; Hl., Halite; Py., Pyrite; Qz., Quartz

associated remains of crocodylomorphs and articulated remains of Testudinata and Osteichthyes have also been identified. No preferent orientation of long or flat bones has been observed on the field, and there is no apparent classification by size or shape of the specimens. Individual bones show various degrees of preservation, from bone splinters and fragments, to complete delicate elements such as a pterosaur limb and cranial bones. No evidence of subaerial exposure or weathering has been observed, including flaking or any presence of crusts or dissolutions. No plastic deformations have been identified in any of the specimens, and fractures caused by bone-to-bone contacts are also absent.

The fossil diagenetic history of the osteological elements analysed is of special interest, as all elements are heavily recrystallized. Concerning its geochemical composition, BSE images and EDX analyses show that the original

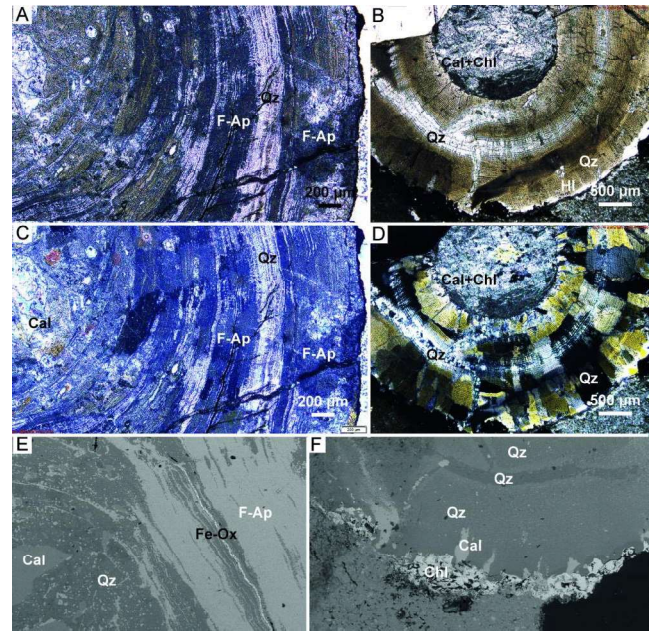


Fig. 4 **(A, C, D)** RB6 *Goniopholididae* indet. thin section of the diaphysis of an undetermined long bone. **(B, D, F)** RB52 *Goniopholididae* indet. thin section of a tooth cut at the base of the crown. **(A)** polarized transmitted light image showing the preserved lamination of the histostructure of the cortical and trabecular bone. Note both biomineralized tissues preserve the fibrous aspect of the bioapatite, and Haversian channels can be observed in the trabecular bone. **(B)** polarized transmitted light image. Dentine of the teeth still shows lamination, whereas enamel is not present. Note fractures caused by diagenetic compression. **(C)** cross polarized transmitted light image. The general denim blue interference colour of the fluorapatite suggests the original composition of the bone is preserved, except for some relatively small areas were quartz, with a white interference colour, has replaced the structure. Large calcite crystals can be observed in the medullary cavity of the bone, together with indetermined silicate minerals of bright interference colours. **(D)** cross polarized transmitted light image, showing that the bone has been completely recrystallized by medium quartz crystals of brownish-yellowish interference colour. Drusy infillings are seen filling the fractures, both radially and around the teeth. The pulp cavity is filled with a calcite and chlorite matrix, similar to the encasing sediment. **(E)** BSE image. Note the presence of large areas preserving its original fluorapatite composition, interstratified with quartz, which has started the replacing process. Some cracks are filled with Iron oxides. Large calcite crystals with relics of fluorapatite grow in the medullary cavity. **(F)** BSE image of the teeth, completely replaced by quartz. A slightly lighter phase of quartz is filling the cracks, but no significant differences in composition were detected by EDS. The surface of the teeth, where the enamel should have been, has been replaced by chlorite. Anatomical abbreviations: Cal., Calcite; Chl., Chlorite; F-Ap., Fluorapatite; Fe-Ox., Iron oxides; Hl., Halite; Py., Pyrite; Qz., Quartz

bioapatite of the bones have been partially (Fig. 3 A, C, D) or totally (Fig. 4B, D, F) replaced by silica. Petrographic thin sections confirm that the SiO₂ is actually crystalline quartz, which is characterized by white and brown interference colours and small to medium crystals with prismatic habits and blocky to undulating extinction, contrasting to the large, denim-blue fluorapatite crystals with fibrous habits.

Contrary to what it is observed in hand samples, petrographic thin sections show that the internal structure of the bone tissue is relatively well preserved, despite the extensive mineralization. Bone growth lines can be observed, although are partially distorted. Occasional calcite and pyrite crystals have partially replaced the bone tissue (Fig. 3D) and are also present in the calcite matrix. Fractures, probably caused by lithostatic compaction of the specimens, are filled with calcite, quartz (which may be enriched with clay minerals), and occasionally iron oxides (Fig. 4E). The sediment infilling the bone cavities, such as medullary cavities or vascularization in osteoderms, is mainly micrite, and has abundant neoformed calcite crystals, chlorites, other silicate minerals, and euhedral pyrites. Some bones (especially those where the replacement by quartz has been completed) may show a chlorite coating.

No significative differences in mineralogical or chemical composition have been observed between the bones attributed to different taxa, suggesting that there is no taxonomic control of the diagenetic processes.

Preliminary taphonomic analysis allows the characterization of the assemblages as time-averaged, osteichthyan dominated, multitaxic bonebeds (especially the south area). The apparent lack of evidence of transport, with no preferred orientation or sorting of elements, together with the range of degrees of articulation of the specimens suggest that the assemblage formed by attrition and accumulation of bone fragments, and disarticulated and partially articulated skeletal remains in a lacustrine environment.

Despite the relatively small sample analysed, preliminary taphonomic and palaeoecological hypothesis about the composition of the assemblage can be postulated. The assemblage is dominated by obligate aquatic taxa (osteichthyan fishes), which represent the more articulated specimens. They are followed by amphibian organisms (Crocodylomorpha and Testudinata), which show partial articulation and some degree of association, suggesting that the environment was an extensive lake with a permanent water level, and the accumulation was produced far from the coast of the lake. This is also supported by the lack of fully terrestrial animals, outside of disarticulated elements of flying pterosaurs which would have been incorporated to the assemblage after falling to their deaths inside the lake.

The low degree metamorphism present in the Matute Fm has resulted in a very particular mode of preservation of the fossil bones in the Ribota bonebeds. Opalized vertebrate bones are known in the literature (e.g., Pewklian et al., 2008), where the microstructure of the fossils is perfectly preserved at the level of the individual osteons. It seems that an analogue process may have occurred in the Ribota bonebed, which allowed the preservation of the detailed histostructure of the bone, but it was followed

by a recrystallization of the opal into quartz. This process was also sufficiently slow to allow the survival of the bone laminations during this replacement. During the peak of low-grade metamorphism in the Cameros basin, the temperatures may have reached 350–370°C and pressures of up to 1 Kbar (e.g., Casquet et al., 1992, Barrenechea et al., 2001), which probably caused this unusual preservation of the fossil bones. Further research is needed to explore the detailed mechanisms of the fossildiagenetic pathways in the context of low-grade metamorphism.

5 Vertebrate assemblage

In the outcrop, the most abundant remains correspond to isolated and disarticulated fish bones and scales (Fig. 2C, D), although some partial skeletons of indeterminate osteichthyans were also collected (Fig. 5). Other vertebrate remains include crocodylomorph isolated teeth, osteoderms, postcranial and a few cranial bones (Fig. 6); Testudinata isolated plates and partial shells (Fig. 7); and a few isolated cranial and appendicular pterosaur bones (Fig. 8). Interestingly, not a single dinosaur bone has been identified in the area so far.

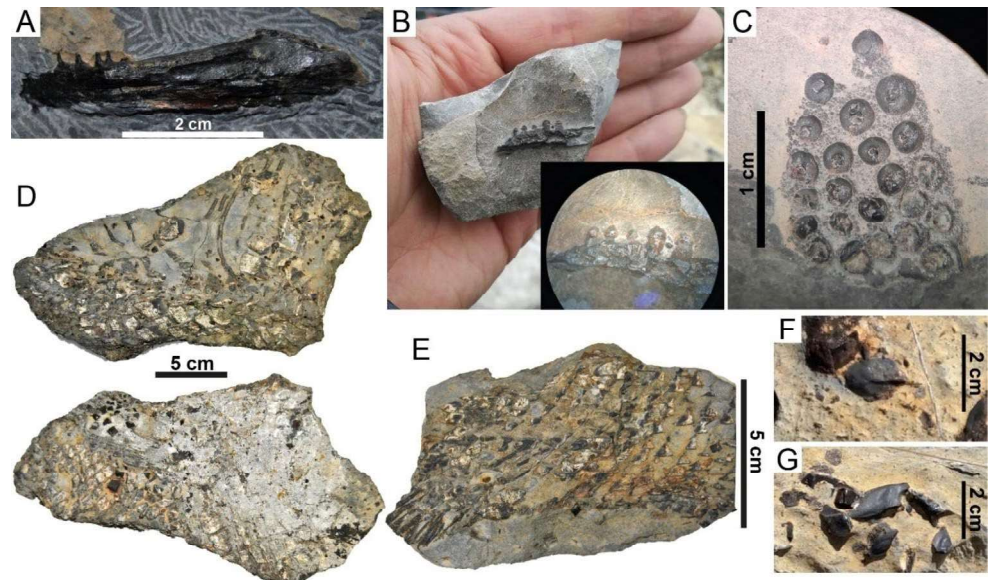
5.1 Fishes

The Late Jurassic to the Early Cretaceous actinopterygian fish faunas from continental or transitional environments of Europe are commonly characterized by the presence of remains of ginglymodians and halecomorphs, together with other groups, such as pycnodontiforms or basal teleosts (e.g. Forey & Sweetman, 2011; Pouech et al., 2015; Ruiz-Omeñaca and Bermúdez-Rochas, 2010). The Early Cretaceous of the Cameros Basin is no exception and the presence of remains of these groups of fishes have also been recorded in the Enciso Group (Bermúdez-Rochas & Poyato-Ariza, 2007), with also abundant ginglymodian remains in the Urbion Group.

Fish faunas in the Ribota site are represented by abundant osteichthyan isolated remains (teeth, ganoid scales and bone fragments), and some incomplete articulated or semi-articulated remains. A preliminary study of these remains points to a low fish faunal diversity with specimens of two major groups of actinopterygians, namely: Halecomorphi and Neoginglymodi.

The Jurassic-Cretaceous boundary osteichthyan fishes record is scarce in Spain (Poyato-Ariza et al., 1999) and the data that the Ribota site could provide is potentially interesting in order to understand the distribution and evolution of these fish faunas during the development of the Iberian Basin Rift System.

Fig. 5 Fish remains from the Ribota fossil site. **(A)** left dentary RB13 of Halecomorphi indet. in lateral view; **(B)** possible right dentary RB27 of Neoginglymodi indet. in medial view; **(C)** possible dermopalatine fragment RB58 of Neoginglymodi indet. in ventral view; **(D)** slab of an articulated partial skeleton RB14 of Neoginglymodi indet. in lateral view; **(E)** articulated partial skeleton RB26 of Neoginglymodi indet. in lateral view; **F and G)** Isolated scales in the field assigned to Neoginglymodi indet



Osteichthyes Huxley, 1880.

Actinopterygii Cope, 1887.

Neopterygii Regan, 1923.

Holostei Müller, 1844 (sensu Grande, 2010).

Halecomorphi Cope, 1872 (sensu Grande & Bemis, 1998).

Halecomorphi indet.

5.1.1 Description

Halecomorph fishes are represented by one isolated remain (RB13) corresponding to a partial left dentary with at least four incomplete teeth attached (Fig. 5A). The specimen was recovered in the east area (Fig. 2A) and partially exposed in lateral view, and as a result, the lateral surface of the dentary is quite damaged and abraded by erosion. Despite this, remains of the mandibular sensory canal can be observed. This canal traverses the bone parallel to its ventral margin, with three large pores visible, where the anterior and posterior ones are larger than the middle one. The dentary is elongated, robust and shallow, with a total length of 4.75 cm and a maximum height of approximately 1 cm at its posterior end. Teeth are only present in its anterior section. They are slightly conical and well-spaced, but poorly preserved (their tips are missing), without any presence of acrodine caps or potential carinate terminations. The two anterior teeth are slightly posteriorly curved.

Holostei Müller, 1844 (sensu Grande, 2010).

Ginglymodi Cope, 1872 (sensu Grande, 2010).

Neoginglymodi López-Arbarello & Sferco, 2018.

Neoginglymodi indet.

5.1.2 Description

Neoginglymodian fishes' remains are abundant in the Ribota Site, with the presence of scales, teeth, and bones. Most of them have been located isolated and scattered all over the site, but several articulated or semiarticulated remains have been recovered. Among them, there are some cranial and postcranial bones, at least three mandibular bones with teeth attached, and some sets of scales in connection. Most of the specimens are partially covered by limestone and their exposed surfaces are damaged by meteorization, so further preparation is required in order to study them properly.

Two specimens (RB27 and RB58) are bone fragments with several teeth in connection (Fig. 5B, C). These specimens are incomplete and still partially covered by limestone, so it is difficult to identify them. One specimen seems to correspond to a right dentary (RB27, Fig. 5B) and the other one could be a dermopalatine (RB58, Fig. 5C). Both specimens show some degree of heterodonty, as the inner teeth are more robust and bigger than the marginal ones. In the dentary the posterior teeth are about twice the size of the anterior ones. All teeth are rounded to oval in section and present a conspicuous papilla in the centre of their occlusal surface. This character is also present in the teeth of *Camericichthys lunae* (Bermúdez-Rochas & Poyato-Ariza, 2015).

The abundant scales recovered are ganoid type scales, approximately rhomboidal in shape (RB14, RB26, Fig. 5D, E, F, G). There is no evidence of surface ornamentation or serration in their posterior borders, but the ganoine surface of exposed scales is heavily worn, and most of their posterior borders are broken. Despite this, a variation in their general morphologies, that corresponds to the different body region that they occupied, can be observed. Based on this morphology, in the Ribota site there are scales corresponding to all

the regions of the body. Among the morphologies observed, at least one scale corresponds to the dorsal ridge, and seems to bear a short spine (Fig. 5F), as it occurs in the dorsal spines of *C. lunae* (Bermúdez-Rochas & Poyato-Ariza, 2015). The so-called peg-and-socket articulation (typical of ganoid scales) is not visible in the remains exposed. However, some specimens show a well-developed rostro-caudal articulation, with the corresponding two anteriorly oriented processes (Fig. 5G).

5.1.3 Remarks

Halecomorph fishes are common in the Jurassic and Cretaceous faunas of Spain (i.e., Wenz, 1995; Ruiz-Omeñaca et al., 2006; Martín-Abad & Poyato-Ariza, 2017) and, as commented above, remains of this group, assigned to Amiiformes, have been previously cited in the Early Cretaceous of the Cameros basin (Bermúdez-Rochas & Poyato-Ariza, 2007). Their finding in the Ribota site represents their first record in the Matute Formation, and their oldest record in the basin. Unfortunately, the preservation condition of the only specimen recovered does not allow a higher taxonomic precision to be achieved at this time.

The presence of isolated ganoid scales in the Matute Fm was recorded for the first time in the Virgen del Prado site (Inestrillas-Aguilar del Río Alhama, La Rioja, Spain) by Moratalla (1993), and assigned to the genus *Lepidotes* at the time. After the revised classification of the ginglymodian fishes made by López-Arbarello (2012), the assessment of these kind of isolated ganoid scales to the genus *Lepidotes* can no longer be considered valid (see Bermúdez-Rochas & Poyato-Ariza, 2015). More than twenty years later, the taxon *Camerichthys lunae* was erected in the San Andrés de San Pedro Site (Soria), based on an articulated specimen with the skull and the anterodorsal portion of the body preserved (Bermúdez-Rochas & Poyato-Ariza, 2015). The rostro-caudal articulation present in the Ribota site ganoid scales is known in several ginglymodian genera, such as *Callipurbeckia* or *Scheenstia*, belonging to the orders Semi-onotiformes and Lepisosteiformes, respectively (see López-Arbarello & Sferco, 2018). Therefore, although they present similarities with *C. lunae*, the attribution of these scales to this taxon cannot be assured, and a higher taxonomic assignment cannot be made until more complete material is recovered.

5.2 Crocodylomorpha

The crocodylomorphs of the Late Jurassic and Early Cretaceous of Europe are dominated by the Neosuchia, a clade of mesoeucrocodylian crocodyliformes, with their oldest record in the Early Jurassic (Sinemurian) of North America

(Tykoski et al., 2002). The group survived to the present with the crown group Crocodylia as the clade that includes all extant species and their closest fossil relatives. In terrestrial to transitional environments from the Middle Jurassic to the Early Cretaceous of Europe, the most typical crocodylomorph fossil assemblage is dominated by the neosuchian clades Atoposauridae, Bernissartiidae, and Goniopholididae (e.g., Brinkmann, 1989; Buscalioni et al., 2008; Schwarz-Wings et al., 2009; Gasca et al., 2012; Puértolas-Pascual et al., 2015b; Tennant et al., 2016a; Guillaume et al., 2020). However, deposits with crocodylomorphs from the Jurassic–Cretaceous transition are still scarce, giving the Ribota site greater interest. At this site, the most abundant reptiles correspond to crocodylomorphs remains (Fig. 6), which represent more than half of the collected bones.

Crocodylomorpha Hay, 1930 (sensu Walker, 1970).

Crocodyliformes Hay, 1930.

Mesoeucrocodylia Whetstone & Whybrow, 1983.

Neosuchia Gervais, 1871 (sensu Benton & Clark, 1988).

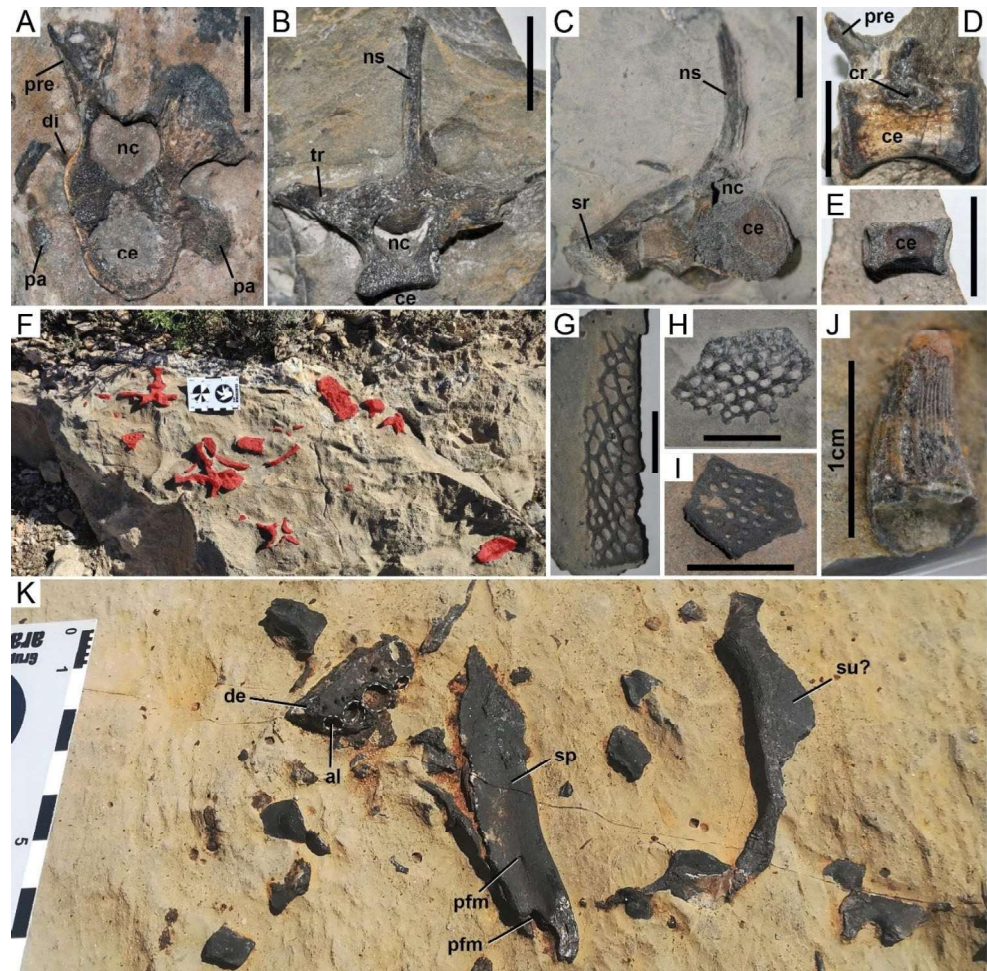
Neosuchia indet.

5.2.1 Description

Most of these crocodylomorph remains correspond to isolated vertebrae (Fig. 6A–E), however, some of them were recovered associated in an area of less than 1 m² and presenting similar sizes (Fig. 6F), so they could belong to the same individual. Since most of the vertebrae are partially eroded and/or contained within the rock matrix, some details have been hidden. However, their general morphology, shape of the vertebral centra, and the position of the ribs, diapophyses and parapophyses (when these are preserved) have allowed for assigning them to different regions of the vertebral column. Both in anterior and posterior views, the articular surfaces of the centra are sub-circular and gently concave due to the presence of a shallow central depression (amphicoelous condition), and they are almost as dorsoventrally tall as they are mediolaterally wide. The ventral and lateral surfaces of the centra are slightly concave, giving them the typical hourglass shape. At least one cervical vertebra has been recovered (RB57; Fig. 6A). This vertebra is identified by the shape and position of the diapophyses and parapophyses. The presence of parapophyses on the lateral surfaces of the centrum (but in its dorsal half), would indicate that it is one of the last posterior cervical vertebrae (e.g., Mook, 1921; Puértolas-Pascual et al., 2015a). The most abundant vertebrae correspond to the dorsal region of the trunk (RB44; Fig. 6B), and they have been identified based on the presence of long transverse processes located dorsally in the vertebral centrum and at the same height as the neural arch. A sacral vertebra has also been identified (RB69; Fig. 6C). It has

Fig. 6 Crocodylomorph remains from the Ribota fossil site.

(A) cervical vertebra RB57 in anterior view; (B) dorsal vertebra RB44 in anteroposterior view; (C) sacral vertebra RB69 in anteroposterior view; (D) caudal vertebra RB21 in lateral view; (E) caudal vertebra RB66 in lateral view; (F) disarticulated vertebrae (RB74–78) and osteoderms highlighted in red that could correspond to the same individual; (G) dorsal osteoderm RB61 in dorsal view; (H) ventral osteoderm RB62 in ventral view; (I) ventral osteoderm RB35 in ventral view; (J) isolated tooth RB39; (K) disarticulated cranial remains RB17. Anatomical abbreviations: al., alveolus; ce., centrum; cr., caudal rib; de., dentary; di., diapophysis; nc., neural canal; ns., neural spine; p.a., parapophysis; pfm., posterior foramen for the mandibular ramus of cranial nerve V; pre., prezygapophysis; tr., transversal process; sp., splenial; su., surangular. Unnumbered scale bars = 2 cm



been recognised as a sacral element due to the presence of a very stout fused rib (also referred to as the transverse process) (Gomes de Souza, 2018) attached to the lateral margin of the vertebral centrum (Mook, 1921). Whether it belongs to the first or second sacral vertebra cannot be confirmed with certainty since it is incomplete and partially covered by matrix. At least one caudal vertebra (RB21; Fig. 6D) from the anterior or middle region of the tail has been identified. Although it is not complete, this caudal vertebra is characterized by the presence of an elongated vertebral centrum with a more quadrangular articular surface, and transverse processes (= fused caudal ribs according to Gomes de Souza, 2018) arising from the dorsal region of the centrum rather than from the neural arch. In addition, the ventral region of this centrum appears to possess two articulation facets for the chevrons attached to two subtle anteroposterior parallel ridges (Mook, 1921). Interestingly, some small isolated centra (RB66; Fig. 6E), (tentatively assigned to caudal vertebrae) were found disarticulated by the opened neurocentral suture. If these vertebrae are confirmed to be caudal, they would indicate the presence of juvenile individuals in addition to adults, since

juveniles fuse their caudal vertebrae very early in ontogeny (Brochu, 1996; Ikejiri, 2012).

Neosuchia Gervais, 1871 (sensu Benton & Clark, 1988).

Goniopholididae Cope, 1875.

Goniopholididae indet.

5.2.2 Description

The second most abundant crocodylomorph elements at the site are osteoderms (Fig. 6G–I). Although most of them appear isolated and fragmented, making their identification difficult, some characteristics of the most complete ones allow to assign them anatomically and taxonomically. At least three positional types of osteoderms have been identified: dorsal, ventral, and appendicular. One of the largest and most complete osteoderms (RB61) has been interpreted as belonging to the dorsal region of the trunk. This dorsal osteoderm (Fig. 6G) is twice as wide as it is long, with a smooth non-ornamented articular facet in the anterior margin, an anterolateral peg, and the lateral margin ventrally deflected with a high angle. These osteoderms are typical of crocodylomorphs with biseriate armour (two dorsal

rows) and a closed paravertebral bracing system (Salisbury & Frey, 2001; Puértolas-Pascual et al., 2015a; Puértolas-Pascual & Mateus, 2020). At least two ventral osteoderms (RB62 and RB35) have been identified (Fig. 6H, I). They are flat, equidimensional (as wide as they are long), polygonal with pentagonal to hexagonal contours, with straight edges, and present the typical ornamentation of big circular pits evenly distributed over their ventral surface. Although they were isolated, their edges present some crenulation, indicating their sutures with adjacent osteoderms, which would form a rather rigid ventral armour (Wu et al., 1996; Salisbury & Frey, 2001). Some small, flat, elliptical to sub-circular osteoderms have been interpreted as belonging to the appendicular region. This type of osteoderm can be confused with those of the neck region, however the latter usually have a keel, at least in some goniopholidids and extant crocodylians (Wu et al., 1996).

Neosuchia Gervais, 1871 (sensu Benton & Clark, 1988).
Neosuchia indet.

5.2.3 Description

Among the cranial material recovered at the site, the most abundant elements are isolated teeth (RB39; Fig. 6J). All the teeth belong to the same generalist morphotype, consisting of conical crowns, with smooth mesial and distal carinae, and ornamentation consisting of parallel longitudinal basiapical striae. Only a group of disarticulated (but associated) cranial bones (RB17) have been recovered from the site (Fig. 6K). Although they are partially covered by rock matrix, they can be recognized as part of a mandible. A dentary fragment, probably from the symphyseal region, with five circular dental alveoli (two of them preserving tooth fragments) has been identified. In addition, these associated bones also include an indeterminate cranial element (probably a surangular fragment) and a splenial fragment in which two posterior perforations for the mandibular ramus of cranial nerve V seem to be present.

5.2.4 Remarks

Although the crocodylomorph material at the Ribota site is very fragmentary and most elements are isolated, taking it as a whole has made it possible to make a series of taxonomic inferences. Regarding the vertebrae, most of them belong to individuals of medium to large size. In addition, the presence of amphicoelous vertebral centra points to the presence of non-eusuchian taxa. Considering the known taxa in this type of palaeoenvironment, age and palaeobiogeographical region, these vertebrae most probably belong to neosuchian crocodylomorphs (e.g., Guillaume et al., 2020; Puértolas-Pascual & Mateus, 2020). The osteoderms

are more informative, since the combination of dorsal osteoderms that are twice as wide as they are long, with peg and groove articulation and a ventrally folded lateral margin, together with the presence of polygonal ventral osteoderms, points to the clade Goniopholididae (e.g., Wu et al., 1996; Salisbury & Frey, 2001; Puértolas-Pascual & Mateus, 2020). Furthermore, the presence of generalist conical teeth is also typical of this clade of neosuchian crocodylomorphs, among others (Guillaume et al., 2020). Therefore, given the palaeogeographic/chronological context, the size of the bones, the morphology of the vertebrae and teeth, and the characteristic shape of the osteoderms, most of these remains can be provisionally assigned to Goniopholididae indet.

5.3 Testudinata

The most abundant and diverse lineage of turtles in the Upper Jurassic levels of Europe is that of Thalassochelydia (Anquetin et al., 2017). Several representatives of the group of littoral thalassochelydians Plesiochelyidae have been recognized in the Iberian Peninsula, as well as the freshwater *Hylaeochelys*, the latter being the only thalassochelydian surviving after the Jurassic–Cretaceous transition (see Pérez-García, 2017; and references therein). The North American and European lineage of the paracryptodiran turtles Pleurosternidae is recognized within both the Late Jurassic and the Early Cretaceous. The Iberian record of this group of freshwater basal turtles (i.e., members of Testudinata not attributable to the crown Testudines) is currently identified as the most diverse in Europe, with several Iberian representatives having been defined from the Kimmeridgian to the Albian levels (see Pérez-García et al., 2022; and references therein). Another lineage identified in Europe from both Upper Jurassic sites (where its record is very limited) and throughout the Cretaceous is that of the terrestrial stem turtles Helochelydridae. Although the Iberian Late Jurassic record includes other lineages of turtles, the current limited availability of material does not allow us to know which lineages they belong to. However, a diverse fauna of freshwater eucryptodiran turtles is recognized in Europe, and especially in the Spanish record, after the Jurassic–Cretaceous transition, probably from the Berriasian, as a result of diachronic dispersals to this continent (see Pérez-García, 2017; and references therein).

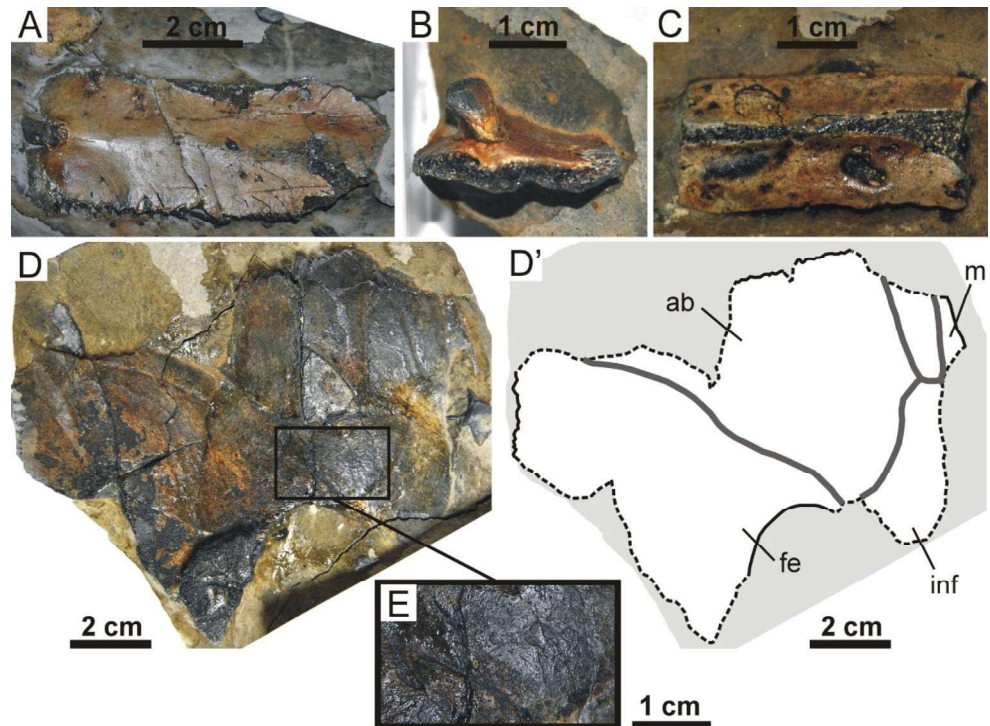
Testudinata Klein, 1760.

Testudinata indet.

5.3.1 Description

All turtle specimens so far identified in Ribota correspond to shell elements (Fig. 7). They are represented by isolated plates, both from the carapace (Fig. 7A–C) and from the

Fig. 7 Selection of turtle remains from the Ribota fossil site. **A)** visceral view of an almost complete costal RB18; **B)** anterior or posterior view of the proximal region of a costal RB24; **C)** bridge peripheral RB16, in dorsal view; **D-D')** partial left hypoplastron RB20, in ventral view. Dotted lines in D' indicate broken edges; continuous black lines correspond to the margins of the plate; and the border of the scutes are represented by thicker gray lines. Scute abbreviations: ab., abdominal; fe., femoral; inf., inframarginal; m., marginal



plastron (Fig. 7D). Although most of these remains are not complete, they generally show a well-preserved outer surface, with a rough pattern (Fig. 7E). The material currently found does not show evidence for the presence of more than one taxon in Ribota.

In visceral view, the proximal end of the dorsal ribs is well-developed (RB18 and RB24), being relatively robust (Fig. 7A, B). Both the ventro-medial margin of the bridge peripherals RB16 (Fig. 7C), and the lateral one of the only hypoplastron RB20 found (Fig. 6D), indicate that the contact between the carapace and the plastron was at least partially ligamentous. The hypoplastron corresponded to that of a taxon with inframarginals, with at least two of these scutes overlapping this plate. The anterior hypoplastral margin is not perpendicular to the axial plane (that plane being recognized by the suture of this plate with the other hypoplastron), but rather it is postero-medially directed. Thus, this taxon lacked mesoplastra between the hypoplastra and the hypoplastra. The abdominal-femoral sulcus is latero-posteriorly directed.

5.3.2 Remarks

As has been indicated in the Introduction, a turtle was described in Ágreda. It corresponded to a member of the Pleurosternidae (Paracryptodira), and was attributed to the new species *Pleurosternon moncayensis*, exclusively represented by its holotype (Pérez-García et al., 2022). That turtle was defined by both cranial and shell remains. The turtle

plates from Ribota cannot be attributed to Pleurosternidae because the taxon identified from there lacks mesoplastra, as well as an ornamental pattern composed by pits or tubercles, and by sulci on the margins of the plates (Pérez-García et al., 2022). The characters described here (i.e., absence of mesoplastra, present of inframarginal scutes), are compatible with those of the members of the lineage of Thalassochelydia, very abundant and diverse in the Late Jurassic levels of Europe, from the Oxfordian to the Tithonian (Anquetin et al., 2017; Pérez-García & Ortega, 2022). However, most of its representatives (including all members of Plesiochelyidae, a lineage exclusive to Europe and well-represented in the Iberian record) are recognized as littoral forms, which is not compatible with the sedimentary environment interpreted for the Matute Alloformation. The only freshwater member of Thalassochelydia currently known is *Hylaeochelys* which, furthermore, is the only one that survived until the Early Cretaceous (Pérez-García et al., 2023). The material analyzed here is not attributable to this genus represented in the Iberian Peninsula, considering the absence of a slightly fluted outer surface of the plates. The limited availability of characters in the turtle material found at Ribota is also compatible with that of another lineage of freshwater forms recognized in Europe: Xinjiangchelyidae. Although this group has an Asian origin, it reached Europe during the Lower Cretaceous, at the Berriasian or Valanginian. It was a diverse lineage in the European Lower Cretaceous record and especially in that of the Iberian Peninsula, where several forms have been identified (see Pérez-García,

2017; and references therein). Therefore, although the current limited information on the Ribota turtles does not allow us their precise systematic attribution, they could correspond to a single form, compatible with *Thalassochelydia* and with *Xinjiangchelyidae*. The potential future discovery of new remains in this fossil locality will be necessary to perform a more precise systematic attribution. However, the so far identified remains in Ribota are relevant since they allow the identification of two turtle lineages in Ágrede, as they are not compatible with *Paracryptodira*.

5.4 Pterosauria

The time period of the Jurassic–Cretaceous transition is a transformative time for the pterosaur faunal composition, where non-pterodactyloids were already in the process of global extinction, and the Pterodactyloidea had already begun their diversification, radiating geographically and taxonomically throughout the remainder of the Cretaceous (although the exact early evolutionary drivers behind this transition are still largely undetermined). The specific time periods of the Tithonian–Berriasian, occurring just after the peak of this marked change, were therefore still typified by residual rhamphorhynchids, but also largely occupied by anurognathids, pterodactylids and ctenochasmatis (Paul, 2022).

Today, the known Late Jurassic–Early Cretaceous pterosaur occurrences in Spain have mainly been represented by trackways (e.g., Lockley et al., 1995, 2008; Wright et al., 1998; Hernández Medrano et al., 2006; Pascual Arribas et al., 2015; Piñuela, 2015; Pascual Arribas and Hernández-Medrano, 2016), but also by disparate occurrences of

fragmentary fossil bone material (e.g. Fuentes Vidarte & Mejjide Calvo, 1996, 2010; Buffetaut, 1999; Ruiz-Omeñaca et al., 2004; Vullo et al., 2009). Most known trackway localities are found in the north and northeast of Spain, in the provinces of Asturias, La Rioja, and Soria, with some fossil bones also occurring in the latter two, and additionally in the provinces of Aragón, Valencia and Cuenca (e.g., Holgado et al., 2011). Largely these fossils consist of postcranial remains of isolated bones (mainly wing elements) and teeth, although cranial material has also been recovered, most notably in the holotype fossils of *Prejanopterus curvirostris* Fuentes Vidarte and Mejjide Calvo, 2010 (Pereda-Suberbiola et al., 2012), *Europejara olcadesorum* (Vullo et al., 2012), and *Iberodactylus andreui* (Holgado et al., 2019).

The Ribota pterosaur assemblage is thus far represented by six isolated elements: preliminary identifications designate them as a humerus (RB29, Fig. 8A), a radius fragment (RB37, Fig. 8B), a femur (RB28, Fig. 8C), a digit IV phalanx I (RB55, Fig. 8D), an epiphyseal fragment (RB34, Fig. 8E), and a mandibular fragment (RB19, Fig. 8F).

Order Pterosauria Owen, 1842 (sensu Andres & Padian, 2020a).

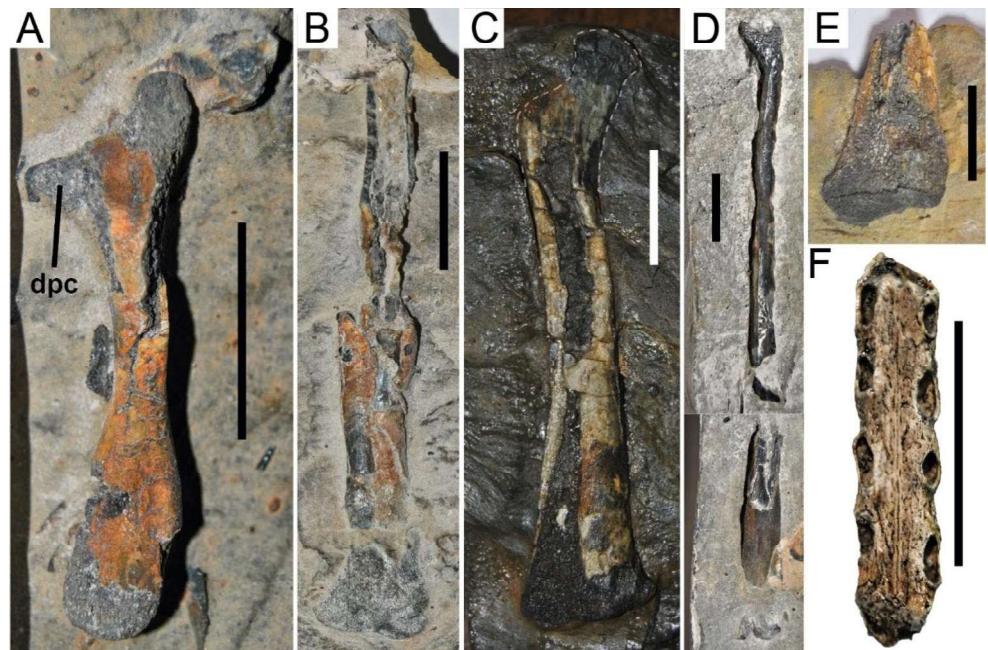
Suborder Pterodactyloidea Plieninger, 1901 (sensu Andres and Padian, 2020b).

Pterodactyloidea indet.

5.4.1 Description

RB29 is a mostly complete left humerus (Fig. 8A), visible in ventral view. Based on humerus scaling with *P. curvirostris* (the closest taxon geographically, and similar morphologically) (Pereda-Suberbiola et al., 2012), the Ribota specimen

Fig. 8 Pterosaur remains from the Ribota fossil site. (A) humerus RB29 in ventral view; (B) Partial radius RB37 in indeterminate view; (C) Femur RB28 in posterior view; (D) a digit IV phalanx RB55 in indeterminate view (note that they are two different pictures superimposed); (E) epiphyseal fragment RB34 in lateral view; (F) mandibular fragment RB19 in dorsal view. Anatomical abbreviations: dpc., deltopectoral crest. Scale bars = 2 cm



RB29 is about 30% smaller and would have achieved about one-meter wingspan. The humerus is severely eroded along both articular ends, and especially in the area of the deltopectoral crest, which is seemingly placed distal to the ulnar crest (a condition of pterodactyloids according to Unwin & Martill, 2018). At the proximal end, the ulnar crest faces anterolaterally, with a distinct concavity between it and the region of the deltopectoral crest. The humeral shaft is straight, with an ovoid cross-section at its midpoint, and moderately expanded mediolaterally towards both articular ends.

Mandibular fragment RB19 (Fig. 8F) is one of the most informative pterosaur bones in the Ribota assemblage, and is exposed dorsally and laterally, with sediment obscuring its ventral surface. The fragment is very slender, with almost parallel margins and a very thin midline rectilinear groove. The exact position of the fragment along the length of the entire mandible is indeterminate (due to being broken off both ends), but it is likely almost very near the anterior-most end of the dentary. In the mandible fragment, a total of two partial and eight complete alveoli have been preserved. Posterior to the partial alveoli (one in each side), four complete and well-developed raised alveoli are visible on each side, directed anterolaterally. The alveoli are all ovoid, elongated anteroposteriorly, although they vary in diameter, alternating between larger and smaller along the tooth row. Each pair of alveoli located laterally to each other also present asymmetry in size, with a larger alveolus in one side of the mandible and a smaller one on the opposite side. Furthermore, each alveolus is not aligned at the same anteroposterior height as its lateral counterpart, giving an extra degree of asymmetry to the dental arrangement. In transverse section, the broken ends of the symphysis show a distinctive rounded-triangle cross-section, compressed laterally, with the pointed apex facing ventrally.

Suborder Pterodactyloidea Plieninger, 1901 (sensu Andres and Padian, 2020b).

Pteranodontoidea Kellner, 2003.

Pteranodontoidea indet.

5.4.2 Description

RB28 is a left femur (Fig. 8C) only visible from its posterior face, as it is still embedded in matrix. It is highly eroded on its articular ends, and in particular in the region of the greater trochanter (which has been entirely eroded away) and in the asymmetrical distal epiphyseal region. The shaft is ovoid in cross-section, relatively straight anteroposteriorly, and slightly bowed mediolaterally, also exhibiting a slight expansion in mediolateral width to the distal end. The femoral head is strongly offset and proximally directed, capped by a mushroom-shaped constriction

of the neck, and well differentiated from the femoral shaft by an 158° angle.

5.4.3 Remarks

Although likely belonging to different individuals, since they were isolated and separated by several meters, it is not possible at the moment to determine if the pterosaur elements from Ribota belong to the same species, and since there are no overlapping elements in the assemblage, more sampling would be needed to ensure whether one or more than one species is here represented. The bones were identified as belonging to pterosaurs due to the hollowness of the bones and a cortical thinness of between 0.3 and 1.6 mm (e.g., Bennet, 2003). The preservation of these elements is excellent in terms of three-dimensionality with almost no taphonomic distortion, however significant exposure to the elements over time has led to extensive erosional damage or breakage along the bone surfaces, rendering certain features indistinguishable. Thus, some elements are not currently identifiable beyond the level of Pterosauria indet., such as a distal left radius fragment RB37 (Fig. 8B) (visible in anterior view, and missing large sections of cortical bone throughout the shaft and articular end), right digit IV phalanx I RB55 (Fig. 8D) (visible in ventral view, and although nearly complete, sustained the extensor tendon process being completely eroded away anterior to the ventral cotyle), and epiphyseal fragment RB34 (Fig. 8E) (which is too highly eroded to glean sufficient morphological information, precluding any assignment). The remaining better-preserved elements, however, are more informative.

The humeral shaft RB29 is straight (as in pterodactyloid pterosaurs), unlike the typical curved shaft of basal pterosaurs (Unwin & Martill, 2018). Humerus RB29 is therefore provisionally assigned to Pterodactyloidea indet. Regarding the femur RB28, the 158° angle of its femoral head with respect to the shaft, is consistent with the Ornithocheiridae (Unwin, 2003). Also, based on this femoral neck-shaft angle greater than 135°, it also corresponds to the Pteranodontoidea of Kellner (2003) in this analysis.

As previously stated, the cranial material is more informative. Although it is significantly smaller in size, on first glance, RB19 shows distinct morphological similarities with *Prejanopterus curvirostris*, particularly in the triangular cross-section of the symphyseal area, however the alveoli on *P. curvirostris* are organized quite differently and more symmetrical than in RB19. *P. curvirostris* was assigned to the Pterodactylidae (Pereda-Suberbiola et al., 2012), however some authors have implied that it belongs instead to the Lonchodectidae (Witton, 2003; Paul, 2022), a contentious group. However, the alveolar margins of the Ribota specimen do not appear as pronouncedly raised as

most lonchodectids (whose alveoli usually are elevated above the medial portion of the occlusal surface), nor is the midline groove as pronounced as the sulcus present in most lonchodectids (Unwin, 2001; Averianov, 2020). Mandibular fragment RB19 also shows morphological similarities with *Aetodactylus halli* Myers, 2010, which was assigned to the Ornithocheiridae (as is Ribota femur RB28), particularly in the labiolingually-compressed alveoli, but also differing in RB19's more lateral positioning of the alveoli along the symphysis (a feature more commonly associated with the Ctenochasmatidae [Unwin, 2003]). Therefore, mandibular fragment RB19 is here conservatively assigned to the Pterodactyloidea (the suborder inclusive of all the aforementioned groups), but due to the differences observed with these other taxa, could potentially be further representative of a new taxon. A more detailed study of the specimen and the possibility of more material being recovered in the future are necessary to clarify its phylogenetic position.

Although the majority of elements in this preliminary assemblage of pterosaurs have overall been informatively limited by their physical preservation, the potential of both the further preparation of these specimens, coupled with future excavation efforts will doubtlessly yield a significant and valuable picture of the pterosaur palaeodiversity of the Ribota locality, as well as the overall landscape for the Pterosauria during the transitional Tithonian–Berriasian time period worldwide.

6 Implications for the palaeobiodiversity in the Iberian ecosystems during the Jurassic/Cretaceous boundary

The Jurassic–Cretaceous transition is a significant geological period, and considerable faunal and environmental changes occurred across the Tithonian–Berriasian transition (see Tennant et al., 2016b, 2017; Allain et al., 2022). Instead of representing a significant faunal turnover between the Tithonian and the Berriasian, these faunal changes are more related with environment shifts associated to a sea level regression at the end of the Jurassic (Allain et al., 2022). Among the groups described in the present paper, Tennant et al. (2016b) indicate that marine osteichthyans and shallow marine turtles show a considerable decrease across the boundary (see also Pérez-García, 2017 and references therein) whereas freshwater and terrestrial turtles, and gonio-pholidid crocodylomorphs, seem to be unaffected. Pterodactyloids increasingly flourished right after the boundary (Butler et al., 2013; Tennant et al., 2016b). In this regard, the Iberian Peninsula has yielded many vertebrate localities from the end of the Jurassic (Kimmeridgian–Tithonian) and Jurassic–Cretaceous transition (Tithonian–Berriasian) in

different areas and is becoming a key area to understanding how those faunal changes occurred. Significant sites have been found in areas such as the Lusitanian Basin in Portugal (e.g., Martin & Krebs, 2000; Malafaia et al., 2010; Mateus et al., 2017, and references therein), the Asturian Basin (Piñuela, 2015, and references therein), and several areas of the Iberian Basin Rift System (mainly South Iberian and Maestrazgo basins) in Spain (see Aurell et al., 2016, 2019; Campos-Soto et al., 2017, 2019, and references therein). It is also worth noting that adjacent to the Iberian Peninsula, the Aquitaine Basin has also yielded rich and diverse Tithonian and Berriasian vertebrate assemblages that show strong similarities with Iberian faunas (Buffetaut et al., 1989; Mazin et al., 2008; Vullo et al., 2014; Allain et al., 2022).

Among the Lusitanian localities with abundant osteological vertebrate remains, Guimarota (Martin & Krebs, 2000) and Andrés (Malafaia et al., 2010) in Leiria (Portugal) stand out. These two localities are characterized by a highly diverse vertebrate fauna including fishes, lizards, crocodylomorphs, pterosaurs, and dinosaurs among others. There are several Spanish areas with abundant evidence of these groups of vertebrates within this time interval (Kimmeridgian–Berriasian) such as the Asturian Basin (e.g., Lockley et al., 2008; Piñuela 2015) or the Cameros basin (Hernández-Medrano et al., 2006; Castanera et al., 2018), but their records are mainly tracksites, and bone remains are comparatively scarce. In the Asturian basin, osteological remains from different groups of vertebrates have been reported and mainly represented by dinosaurs, pterosaurs, crocodylomorphs, turtles, and fishes (e.g., Ruiz-Omeñaca and Bermúdez-Rochas, 2010; Ruiz-Omeñaca et al., 2006, 2012; Rauhut et al., 2018). In the eastern Cameros basin, dinosaurs, pterosaurs, crocodylomorphs, and turtles are represented in the ichnological record (Hernández-Medrano et al., 2006; Castanera et al., 2018), and osteological fossils are also represented by isolated remains from different sites and from different vertebrate groups, such as fishes (Pascual-Arribas et al., 2007; Bermúdez-Rochas & Poyato-Ariza, 2015), turtles (Pérez-García et al., 2022), dinosaurs (Canudo et al., 2010), and pterosaurs (Fuentes Vidarte & Meijide Calvo, 1996). In the western Cameros basin and in the closely located Torrelapaja subbasin, new sites with different identified taxa (dinosaurs and crocodylomorphs) have been recently discovered, but their study is currently under way (Torcida Fernández-Baldor et al., 2020; Aurell et al., 2021).

Thus, the Ribota assemblage with a total minimum number of 5 taxa (Halecomorphi indet., Neoginglymodi indet., Goniopholididae indet., Testudinata indet. and Pterodactyloidea indet.) represents one of the highest macrovertebrate accumulations in the eastern Cameros basin, providing new data regarding vertebrate diversity in lacustrine ecosystems

during the Jurassic–Cretaceous transition of the Iberian Basin Rift System (IBRS). In this regard, the southern basins of the IBRS (Maestrazgo and South Iberian basins) have yielded many of the important vertebrate Spanish localities (with multiple sites) from the Jurassic–Cretaceous transition (e.g., Ruiz-Omeñaca et al., 2004; Royo-Torres et al., 2009; Suñer & Martín, 2009; Cobos et al., 2020), but these localities are mainly known for their dinosaur remains, whereas other groups of vertebrates are comparatively scarce or not studied in detail. It is also noteworthy that the Kimmeridgian–Berriasian deposits of the IBRS have yielded a low vertebrate diversity (see supplementary material in Aurell et al., 2016; Campos-Soto et al., 2017, 2019) when compared with other Hauterivian–Barremian localities, especially those where microvertebrate remains are abundant (Ruiz-Omeñaca et al., 2004; Canudo et al., 2010). Accordingly, the Ribota assemblage in particular, and the Matute Formation in general, open a new window towards the understanding of the vertebrate fauna during the latest Tithonian–earliest Berriasian of the Iberian Peninsula, as it shows a high concentration of macrovertebrates and a moderate number of identified taxa (6 with *Pleurosternon moncayensis*, Pérez-García et al., 2022). Although the number of taxa is not higher than other coeval sites on the IBRS, the absence of more taxa could be produced by the preliminary nature of this work, since only some of the best fossil remains recovered from the site were selected for the study. It is quite likely that additional field work, laboratory preparation, and further detailed studies of the material from Ribota site may increase the number of identified taxa. In addition, the Ribota site is a key site to providing new data about the assemblages preserved in the fully continental realm (see palaeobiogeographical reconstructions of the basin in Aurell et al., 2021) since the deposits of the Matute Formation in the area represent the deposition in a shallow carbonate lake with intense evaporation, and far from the marine influence (Gómez-Fernández and Melendez, 1994). This palaeoenvironment is compatible with the fauna identified so far, where the assemblage is dominated by obligate aquatic taxa (*Neoginglymodi* indet. and *Halecomorphi* indet.), amphibian organisms (*Testudinata* indet. and *Goniopholididae* indet.) and flying pterosaurs (*Pterodactyloidea* indet.) This palaeoenvironment is also possibly the reason why the assemblage is different to many of the mentioned sites in the IBRS that are preserved in continental to transitional units and dominated by dinosaurs.

7 Conclusions

The Ribota site represents a new locality that shows the highest bone concentration of macrovertebrate remains of the Tithonian–Berriasian sites within the eastern Cameros

Basin. The fossil diagenesis of the deposit is interesting and particular, since the bones have suffered considerable taphonomic modifications in which the original structure has been replaced by quartz. The assemblage is formed by attrition in a lacustrine environment, and dominated by fragmented bones, but with complete bones and associated and articulated specimens (mainly fishes and partial turtle shells) also present. The identified vertebrate assemblage is composed of fishes (*Halecomorphi* indet. and *Neoginglymodi* indet.), crocodylomorphs (*Goniopholididae* indet.), turtles (*Testudinata* indet.) and pterosaurs (*Pterodactyloidea* indet.). Counting with the turtle *Pleurosternon moncayensis*, described in the same formation and a few hundred meters northwest of Ribota, there is a total of 6 minimum taxa identified within the Matute Fm. The study of the vertebrate record of the Matute Fm has been neglected for years, considering the abundant vertebrate remains that have been previously mentioned (Gómez-Fernández and Melendez, 1994). Therefore, the potential of the Ribota locality in particular, and the geological unit in general (e.g., Bermudez-Rochas and Poyato-Ariza, 2014; Pérez-García et al., 2022), makes these deposits key towards the understanding of the vertebrate ecosystems in the Jurassic–Cretaceous transition of the Iberian Basin Rift System (especially because this studied assemblage is palaeoenvironmentally different from the known coeval sites described within the IBRS). Nonetheless, this is just a preliminary study and a first step towards the understanding of how the fossils have been preserved, how many bonebeds exist in the area, and how the vertebrate diversity was around the lake (for which the number of taxa will probably increase with further studies). Therefore, the preparation of the material already collected and/or new recovery may provide a considerable increase in the information about these lacustrine assemblages.

Acknowledgements E.P-P was supported by a postdoctoral contract (María Zambrano) funded by the Ministry of Universities of the Government of Spain through the Next Generation EU funds of the European Union. D.C has been supported by the Beatriu de Pinós postdoctoral programme (BP2017-00195) of the Government of Catalonia's Secretariat for Universities and Research of the Ministry of Economy and Knowledge. D.D.B-R was supported by the project PGC2018-094034-B-C21 of the Spanish Ministry of Science and Innovation. M.M-A is supported by the MCIN/AEI/<https://doi.org/10.13039/501100011033> and co-financed by the NextGeneration EU/PRTR, Ramón y Cajal contract RYC2021-034473, Fundação para a Ciência e a Tecnologia (grant number PTDC/CTA-PAL/31656/2017 and research unit UIDB/04035/2020; GeoBioTec); Fieldwork has been funded thanks to and ERG Grant of the European Association of Vertebrate Palaeontologists (EAVP). The study was subsidized in part by Project PID2021-122612OB-100 of the Spanish Ministerio de Economía y Competitividad-ERDF, as well as by the Aragón Regional Government (Grupos de referencia Aragosaur: Recursos Geológicos y Paleoambientales and E04_20R_FOCONTUR) and Unidad de Dinosaurios de Teruel financed by the Ministerio de Ciencia e Innovación (Gobierno de España). Authors would like to acknowledge the use of Servicio General de Apoyo a la Investigación-SAI, Universidad de

Zaragoza. Thanks to Marian Arlegui Sánchez, director of the Museo Numantino, provincial de Soria (Spain). Special thanks to the geologist Miguel Bartolomé for discovering us the first fossils of the Ribota site. The field assistance of the Aragosaurus members Jara Parrilla, Manuel Pérez, Eduardo Medrano, Julia Galán and Martín Linares is greatly appreciated. Thanks to the reviewers Romain Vullo and Elisabete Malafaia for their helpful comments that greatly improved the manuscript.

Funding Open Access funding provided thanks to the CRUE-CSIC agreement with Springer Nature.

Declarations

Conflict of interest On behalf of all authors, the corresponding author states that there is no conflict of interest.

Open Access This article is licensed under a Creative Commons Attribution 4.0 International License, which permits use, sharing, adaptation, distribution and reproduction in any medium or format, as long as you give appropriate credit to the original author(s) and the source, provide a link to the Creative Commons licence, and indicate if changes were made. The images or other third party material in this article are included in the article's Creative Commons licence, unless indicated otherwise in a credit line to the material. If material is not included in the article's Creative Commons licence and your intended use is not permitted by statutory regulation or exceeds the permitted use, you will need to obtain permission directly from the copyright holder. To view a copy of this licence, visit <http://creativecommons.org/licenses/by/4.0/>.

References

- Allain, R., Vullo, R., Rozada, L., Anquetin, J., Bourgeois, R., Goedert, J., Lasseron, M., Martin, J. E., Pérez-García, A., De Fabrègues, C. P., Royo-Torres, R., Augier, D., Bailly, G., Cazes, L., Despres, Y., Gailliegue, A., Gomez, B., Goussard, F., Lenglet, T., Vacant, R., Mazan, & Tournepiche, J. F. (2022). Vertebrate Paleobiodiversity of the early cretaceous (Berriasian) Angeac-Charente Lagerstätte (southwestern France): Implications for continental faunal turnover at the J/K boundary. *Geodiversitas*, 44(25), 683–752.
- Andres, B., & Padian, K. (2020a). Pterosauria, R. Owen 1842. In de K. Queiroz, P. D. Cantino, & J. A. Gauthier (Eds.), *Phylonyms* (pp. 1201–1204). CRC Press.
- Andres, B., Padian, K., Pterodactyloidea, F., & Plieninger (2020b). 1901. In K. de Queiroz, P. D. Cantino, & J. A. Gauthier (Eds.), *Phylonyms* (pp. 1205–1207). CRC Press.
- Anquetin, J., Püntener, C., & Joyce, W. G. (2017). A review of the fossil record of turtles of the clade Thalassochelydia. *Bulletin of the Peabody Museum of Natural History*, 58, 31–369.
- Aurell, M., Bádenas, B., Canudo, J. I., Castanera, D., García-Penas, A., Gasca, J. M., Martín-Closas, C., Moliner, L., Moreno-Azanza, M., Rosales, I., Santos, L., Sequero, C., & Val, J. (2019). Kimmeridgian–berriasian stratigraphy and sedimentary evolution of the central Iberian Rift System (NE Spain). *Cretaceous Research*, 103, 104153.
- Aurell, M., Bádenas, B., Castanera, D., Gasca, J. M., Canudo, J. I., Laita, E., & Liesa, C. L. (2021). Latest jurassic–early cretaceous synrift evolution of the Torrelapaja Subbasin (Camereros Basin): Implications for Northeast Iberia palaeogeography. *Cretaceous Research*, 128, 104997.
- Aurell, M., Bádenas, B., Gasca, J. M., Canudo, J. I., Liesa, C. L., Soria, A. R., Moreno-Azanza, M., & Najes, L. (2016). Stratigraphy and evolution of the Galve sub-basin (Spain) in the middle Tithonian–early Barremian: Implications for the setting and age of some dinosaur fossil sites. *Cretaceous Research*, 65, 138–162.
- Averianov, A. O. (2020). Taxonomy of the Lonchodectidae (Pterosauria, Pterodactyloidea). *Proceedings of the Zoological Institute RAS*, 324(1), 41–55.
- Barco, J. L., Castanera, D., Canudo, J. I., Pascual, C., Rubio, C. J., & Rubio, C. (2013). Aula Paleontológica y Ruta de las Icnitas de Soria: Un espacio paleontológico musealizado con fines didácticos y turísticos. *HER&MUS*, 12, 132–138.
- Barrenechea, J. F., Rodas, M., Frey, M., Alonso-Azcárate, J., & Mas, J. R. (2001). Clay diagenesis and low-grade metamorphism of Tithonian and Berriasian sediments in the Cameros Basin (Spain). *Clay Minerals*, 36(3), 325–333.
- Bennett, S. C. (2003). Morphological evolution of the pectoral girdle of pterosaurs: Myology and function. In E. Buffetaut, & J. M. Mazin (Eds.), *Evolution and paleobiology of Pterosaurs* (pp. 191–215). Geological Society.
- Benton, M. J., & Clark, J. M. (1988). Archosaur phylogeny and the relationships of the Crocodylia. *The Phylogeny and Classification of the Tetrapods*, 1, 295–338.
- Bermúdez-Rochas, D. D., & Poyato-Ariza, F. J. (2007). New fossiliferous sites with fish fauna from the basque-cantabrian and Cameros basins, early cretaceous of Spain. *Journal of Vertebrate Paleontology*, 27(supplement to Number 3), 47A–48A. 67th Annual meeting of the Society of Vertebrate Paleontology. Austin, Texas.
- Bermúdez-Rochas, D. D., & Poyato-Ariza, F. J. (2015). A new semi-notiform actinopterygian fish from the Mesozoic of Spain and its phylogenetic implications. *Journal of Systematic Palaeontology*, 13(4), 265–285.
- Brinkmann, W. (1989). Vorläufige Mitteilung über die Krokodilier-Faunen aus dem ober-jura (Kimmeridgium) der Kohlegrube Guimarota, bei Leiria (Portugal) und der Unter-Kreide (Barremium) von Uña (Provinz Cuenca, Spanien). *Documenta Naturae*, 56, 1–28.
- Brochu, C. A. (1996). Closure of neurocentral sutures during crocodylian ontogeny: Implications for maturity assessment in fossil archosaurs. *Journal of Vertebrate Paleontology*, 16(1), 49–62.
- Buffetaut, E. (1999). Pterosauria from the Upper cretaceous of Laño (Iberian Peninsula): A preliminary comparative study. *Estudios del Museo de Ciencias Naturales de Álava*, 14(Número especial 1), 289–294.
- Buffetaut, E., Pouit, D., Rigollet, L., & Archambeau, J. P. (1989). Poissons et reptiles continentaux du Purbeckien de la région de Cognac (Charente). *Bulletin de la Société géologique de France*, 5(5), 1065–1069.
- Buscalioni, A. D., Fregenal, M. A., Bravo, A., Poyato-Ariza, F. J., Sanchiz, B., Báez, A. M., Moo, C., Martín, O., Closas, C., Evans, S. E., & Marugán Lobón, J. (2008). The vertebrate assemblage of Buenache de la Sierra (Upper Barremian of Serranía de Cuenca, Spain) with insights into its taphonomy and palaeoecology. *Cretaceous Research*, 29, 687–710.
- Butler, R. J., Benson, R. B., & Barrett, P. M. (2013). Pterosaur diversity: Untangling the influence of sampling biases, Lagerstätten, and genuine biodiversity signals. *Palaeogeography Palaeoclimatology Palaeoecology*, 372, 78–87.
- Campos-Soto, S., Benito, M. I., Cobos, A., Caus, E., Quijada, I. E., Suarez-Gonzalez, P., Mas, R., Royo-Torres, R., & Alcalá, L. (2019). Revisiting the age and palaeoenvironments of the Upper jurassic–lower cretaceous? Dinosaur-bearing sedimentary record of eastern Spain: Implications for Iberian palaeogeography. *Journal of Iberian Geology*, 45(3), 471–510.
- Campos-Soto, S., Cobos, A., Caus, E., Benito, M. I., Fernández-Labrador, L., Suarez-Gonzalez, P., Van Den Berghe, Q., Mas, I. E., Royo-Torres, R., & Alcalá, L. (2017). Jurassic Coastal Park: A great diversity of palaeoenvironments for the dinosaurs of the

- Villar del Arzobispo formation (Teruel, eastern Spain). *Palaeogeography Palaeoclimatology Palaeoecology*, 485, 154–177.
- Canudo, J. I., Barco, J. L., Castanera, D., & Torcida Fernández-Baldor, F. (2010). New record of a sauropod in the jurassic–cretaceous transition of the Iberian Peninsular (Spain): Palaeobiogeographical implications. *Paläontologische Zeitschrift*, 84(3), 427–435.
- Casquet, C., Galindo, C., González-Casado, J. M., Alonso, A., Mas, R., Rodas, M., García, E., & Barrenechea, J. F. (1992). El metamorfismo en la Cuenca de Los Cameros. *Geogaceta*, 11, 22–25. Geocronología e implicaciones tectónicas.
- Castanera, D., Pascual, C., Canudo, J. I., & Barco, J. L. (2018). Bringing together research, geoconservation and reaching a broad public in the form of a geotourism project: The Ichnite Route of Soria (Spain). *Geoheritage*, 10(3), 393–403.
- Clemente, P. (2010). Review of the Upper jurassic-lower cretaceous stratigraphy in western Cameros Basin, Northern Spain. *Revista de la Sociedad Geológica de España*, 23(3–4), 101–143.
- Cobos, A., Alcalá, L., & Royo-Torres, R. (2020). The dinosaur route in El Castellar (Teruel, Spain): Palaeontology as a factor of territorial development and scientific education in a sparsely inhabited area. *Geoheritage*, 12(3), 52.
- Cope, E. D. (1872). Observations on the systematic relations of the fishes. *Proceedings of the American Association for the Advancement of Science*, 2(20), 317–343.
- Cope, E. D. (1875). Check-list of North American Batrachia and Reptilia with a systematic list of the higher groups and an essay on geographical distribution based on the specimens in the U.S. National Museum. *Bulletin of the United States National Museum*, 1, 1–104.
- Cope, E. D. (1887). Zittel's manual of Palaeontology. *American Naturalist*, 21, 1014–1019.
- de Gomes, L. (2018). Comments on the serial homology and homologues of vertebral lateral projections in Crocodylia (Eusuchia). *The Anatomical Record*, 301(7), 1203–1215.
- Forey, P., & Sweetman, S. C. (2011). 18. Bony fishes. In: English Wealden fossils (Batten, D. J. ed.). The Paleontological Association, London, 225–235.
- Fuentes Vidarte, C., & Mejjide Calvo, M. (1996). Restos de pterosaurios en el Weald de Soria (España). *Studia Geologica Salmanticensis*, 32, 15–22.
- Fuentes Vidarte, C., & Mejjide Calvo, M. (2010). Un nuevo pterosaurio (Pterodactyloidea) en el Cretácico Inferior de La Rioja (España). *Boletín Geológico y Minero*, 121(3), 311–328.
- Fuentes Vidarte, C., Mejjide Calvo, M., Mejjide Fuentes, F., & Mejjide Fuentes, M. (2005). El conjunto faunístico de la base del Cretácico Inferior de Soria (cuenca de Cameros, grupo Oncala) a través del análisis icnológico. *Celtiberia*, 99, 367–404.
- Gasca, J. M., Badiola, A., Canudo, J. I., Moreno-Azanza, M., Puértolas, E., Huerta, P., & Torcida, F. (2012). In P. Huerta, T. Fernández-Baldor, F., & J. I. Canudo (Eds.), *Zaragoza, España. Actas de las V Jornadas Internacionales sobre Paleontología de Dinosaurios y su Entorno* (pp. 159–172). Colectivo Arqueológico y Paleontológico de Salas, Salas de los Infantes. La asociación de vertebrados fósiles del yacimiento Pochancalo 1 (Valanginiense-Hauteriviense, Villanueva de Huerva).
- Gervais, P. (1871). Remarques sur les reptiles provenant des calcaires lithographiques de Cerin. *Comptes Rendus Académie Sciences Paris*, 73, 603–607.
- Gómez-Fernández, J. C. (1992). Análisis de la cuenca sedimentaria de los Cameros durante sus etapas iniciales de relleno en relación con su evolución paleogeográfica. Unpublished PhD thesis, Universidad Complutense de Madrid, 343 pp.
- Gómez-Fernández, J. C., & Meléndez, N. (1994). Estratigrafía de la Cuenca de los Cameros (Cordillera Iberica Noroccidental, N de España) durante el tránsito Jurásico-Cretácico. *Revista de la Sociedad Geológica de España*, 7, 121–139.
- Grande, L. (2010). An empirical synthetic pattern study of gars (Lepisosteiformes) and closely related species, based mostly on skeletal anatomy. The resurrection of *Holosteus*. *Copeia*, 2010(2A), iii–x1. supplement.
- Grande, L., & Bemis, W. E. (1998). A comprehensive phylogenetic study of amiid fishes (Amiidae) based on comparative skeletal anatomy. An empirical search for interconnected patterns of natural history. *Memoir of Society of Vertebrate Paleontology*, 4, 1–690.
- Guillaume, A. R., Moreno-Azanza, M., Puértolas-Pascual, E., & Mateus, O. (2020). Palaeobiodiversity of crocodylomorphs from the Lourinhã formation based on the tooth record: Insights into the palaeoecology of the late jurassic of Portugal. *Zoological Journal of the Linnean Society*, 189(2), 549–583.
- Hay, O. P. (1930). Second bibliography and catalogue of the fossil vertebrata of North America. *Carnegie Institute Wash Publications*, 390, 1–1074.
- Hernández Medrano, N., Arribas, P., Latorre, C., Macarrón, P., & Sanz Pérez, E. (2006). Contribución de los yacimientos de icnitas sorianos al registro general de Cameros. *Zubia*, 23–24, 79–120.
- Holgado, B., Martínez-Pérez, C., & Ruiz-Omeñaca, J. I. (2011). Revisión actualizada del registro fósil de pterosauria en la Península Ibérica. In A. Pérez-García, F. Gascó, J. M. Gasulla, & F. Escaso (Eds.), *Viajando a Mundos Pretéritos* (pp. 183–194). Ayuntamiento de Morella.
- Holgado, B., Pêgas, R. V., Canudo, J. I., Fortuny, J., Rodrigues, T., Company, J., & Kellner, A. W. A. (2019). On a new crested pterodactyloid from the early cretaceous of the Iberian Peninsula and the radiation of the clade Anhangueria. *Scientific Reports*, 9, 1–10.
- Huxley, T. H. (1880). On the applications of the laws of evolution to the arrangement of the Vertebrata and more particularly of the Mammalia. *Proceedings of the Zoological Society of London*, 649–662.
- Ikejiri, T. (2012). Histology-based morphology of the neurocentral synchondrosis in Alligator mississippiensis (Archosauria, Crocodylia). *The Anatomical Record: Advances in Integrative Anatomy and Evolutionary Biology*, 295(1), 18–31.
- Kellner, A. W. A. (2003). Pterosaur phylogeny and comments on the evolutionary history of the group. *Geological Society London Special Publications*, 217(1), 105–137.
- Klein, I. T. (1760). *Klassifikation und kurze Geschichte der vierfüßigen Thiere*. Jonas Schmidt.
- Lockley, M. G., Garcia-Ramos, J. C., Pinuela, L., & Avanzini, M. (2008). A review of vertebrate track assemblages from the late jurassic of Asturias, Spain with comparative notes on coeval ichnofaunas from the western USA: Implications for faunal diversity in siliciclastic facies assemblages. *Oryctos*, 8, 53–70.
- Lockley, M. G., Logue, T. J., Moratalla, J. J., Hunt, A. P., Schultz, R. J., & Robinson, J. W. (1995). The fossil trackway *Pteraichnus* is pterosaurian, not crocodilian: Implications for the global distribution of pterosaur tracks. *Ichnos*, 4(1), 7–20.
- López-Arbarello, A., & Sferco, E. (2018). Neopterygian phylogeny: The merger assay. *Royal Society Open Science*, 5(3), 172337.
- Malafaia, E., Ortega, F., Escaso, F., Dantas, P., Pimentel, N., Gasulla, J. M., Ribeiro, B., Barriga, F., & Sanz, J. L. (2010). Vertebrate fauna at the Allosaurus fossil-site of Andrés (Upper jurassic), Pombal, Portugal. *Journal of Iberian Geology*, 36(2), 193–204.
- Martin, T., & Krebs, B. (2000). *Guimarota. A jurassic ecosystem* (p. 155). Verlag Dr. Friedrich Pfeil.
- Martín-Abad, H., & Poyato-Ariza, F. J. (2017). A new genus and species for the amiiform fishes previously assigned to *Amiopsis* from the early cretaceous of Las Hoyas, Cuenca, Spain. *Zoological Journal of the Linnean Society*, 181, 604–637.
- Martín-Chivelet, J., López-Gómez, J., Aguado, R., Arias, C., Arribas, J., Arribas, M. E., Aurell, M., Bádenas, B., Benito, M. I.,

- Bover-Arnal, T., Casas-Sainz, A., Castro, J. M., Coruña, F., de Gea, G. A., Fornós, J. J., Fregenal-Martínez, M., García-Senz, J., Garóano, D., Gelabert, B., Giménez, J., González-Acebrón, J., Guimerà, J., Liesa, C. L., Mas, R., Meléndez, N., Molina, J. M., Muñoz, J. A., Navarrete, R., Nebot, M., Nieto, L. M., Omodeo-Salé, S., Pedrera, A., Peropadre, C., Quijada, I. E., Quijano, M. L., Reolid, M., Robador, A., Rodríguez-López, J. P., Rodríguez-Perea, A., Rosales, I., Ruiz-Ortiz, P. A., Sàbat, F., Salas, R., Soria, A. R., Suarez-González, P., & Vilas, L. (2019). In C. Quesada, & J. T. Oliveira (Eds.), *The late jurassic–early cretaceous rifting* (pp. 170–250). Springer. The Geology of Iberia: A Geodynamic Approach, The Alpine Cycle, Volume 3.
- Martín-Closas, C., & Alonso Millán, A. (1998). Estratigrafía y biostratigrafía (Charophyta) del Cretácico Inferior en el sector occidental de la Cuenca de los Cameros (Cordillera Ibérica). *Revista de la Sociedad Geológica de España*, *11*, 253–270.
- Mas, J. R., Alonso, A., & Guimerà, J. (1993). Evolución tectonosedimentaria de una cuenca extensional intraplaca: La cuenca finijurásica-eocretácica de Los Cameros (La Rioja-Soria). *Revista de la Sociedad Geológica de España*, *6*(3–4), 129–144.
- Mas, R., Benito, M. I., Arribas, J., Alonso, A., Arribas, M. E., Lohmann, K. C., González-Acebrón, L., Hernán, J., Quijada, E., Suárez, P., Omodeo, S. Evolution of an intra-plate rift basin: the Latest Jurassic-Early Cretaceous Cameros Basin (Northwest Iberian Ranges, North Spain). In: Post-Meeting Field trips Guidebook (Arenas, C., Pomar, L., & Colombo, F. (2011). 28th IAS Meeting, Zaragoza. Sociedad Geológica de España. Geo-Guías 8, Zaragoza, pp. 117–154.
- Mas, R., Benito, M. I., Arribas, J., Serrano, A., Guimerà, J., Alonso, A., & Alonso-Azcárate, J. (2002). La Cuenca de Cameros: Desde la extensión finijurásica-eocretácica a la inversión terciaria - implicaciones en la exploración de hidrocarburos. *Zubia*, *14*, 9–64.
- Mas, R., García, A., Salas, R., Meléndez, A., Alonso, A., Aurell, M., Bádenas, B., Benito, M. I., Carenas, B., García Hidalgo, J. F., Gil, J., & Segura, M. (2004). El Rift Mesozoico Ibérico: Segunda fase de rifting: Jurásico Superior-Cretácico Inferior. In J. A. Vera (Ed.), *Geología de España* (pp. 503–510). SGE-IGME.
- Mas, R., & Salas, R. (2002). Lower cretaceous of the Iberian Basin. In W. Gibbons, & T. Moreno (Eds.), *The geology of Spain* (pp. 284–288). Geological Society.
- Mateus, O., Dinis, J., & Cunha, P. P. (2017). The Lourinhã formation: The Upper jurassic to lower most cretaceous of the Lusitanian Basin, Portugal—landscapes where dinosaurs walked. *Ciências da Terra/Earth Sciences Journal*, *19*(1), 75–97.
- Mazin, J. M., Pouech, J., Hantzpergue, P., & Lenglet, T. (2008). The Purbeckian site of Cherves-de-Cognac (Berriasian, early cretaceous, SW France): A first synthesis. *Travaux et Documents des Laboratoires de Géologie de Lyon*, *164*(1), 68–71.
- Meléndez, N., & Gómez-Fernández, J. C. (2000). Continental deposits of the eastern Cameros Basin (northern Spain) during tithonian-berriasian time. *American Association of Petroleum Geologists Studies in Geology*, *46*, 263–278.
- Müller, J. (1844). Ueber den Bau und die Grenzen der Ganoiden und über das natürliche System der Fische. *Bericht über die zur Bekanntmachung Geeigneten Verhandlungen der Akademie der Wissenschaften Berlin*, 1846, 117–216.
- Mook, C. C. (1921). Notes on the postcranial skeleton in the Crocodilia. *Bulletin of the American Museum of Natural History*, *44*, 67–100.
- Moratalla, J. J. (1993). Restos indirectos de Dinosaurios del registro español. Paleocnología de la Cuenca de Cameros (Jurásico Superior-Cretácico Inferior) y Paleocnología del Cretácico Superior, Vol. 1. Tesis doctoral inédita. Universidad Autónoma de Madrid, 421 pp.
- Myers, T. S. (2010). A new ornithocheirid pterosaur from the Upper cretaceous (Cenomanian–Turonian) Eagle Ford Group of Texas. *Journal of Vertebrate Paleontology*, *30*(1), 280–287.
- Owen, R. (1842). Report on British Fossil Reptiles, Part II. Proceedings of the 11th Meeting of the British Association for the Advancement of Science, Plymouth, UK, 24 July 1842 (pp. 60–204).
- Pascual-Arribas, C., Canudo, J. I., Perez, S., Hernández-Medrano, E., Castanera, N., D., & Barco, J. L. (2015). On the validity of *Pteraichnus palacieisaenzi*, Pascual Arribas and Sanz Pérez 2000: New data from the Huérteles formation. *Paläontologische Zeitschrift*, *89*, 459–483.
- Pascual-Arribas, C., & Hernández-Medrano, N. (2016). Huellas de *Pteraichnus* en la Muela (Soria, España): Consideraciones sobre el icnogénero y sobre la diversidad de huellas de pterosaurios en la Cuenca de Cameros. *Revista de la Sociedad Geológica de España*, *29*(2), 89–105.
- Pascual-Arribas, C., Sanz Pérez, E., Hernández Medrano, N., & Macarón, L., P (2007). *Lepidotes* sp. en la Aloformación Valdeprado del Cretácico Inferior (Berriasiense) de la cuenca de cameros (Cordillera Ibérica, Soria, España). *Studia Geologica Salmanticensis*, *43*(2), 193–206.
- Paul, G. S. (2022). *The Princeton Field Guide to Pterosaurs* (p. 184). Princeton University Press.
- Pereda-Suberbiola, X., Knoll, F., Ruiz-Omenaca, J. I., Company, J., & Fernandez-Baldor, T., F (2012). Reassessment of *Prejanopteris curvirostris*, a basal pterodactylid pterosaur from the early cretaceous of Spain. *Acta Geologica Sinica*, *86*(6), 1389–1401.
- Pewklian, B., Pring, A., & Brugger, J. (2008). The formation of precious opal: Clues from the opalization of bone. *The Canadian Mineralogist*, *46*(1), 139–149.
- Piñuela Suárez, L. (2015). Huellas de dinosaurios y otros reptiles del Jurásico Superior de Asturias. PhD Thesis, Universidad de Oviedo, 326 pp.
- Plieninger, F. (1901). *Beiträge Zur Kenntnis der Flugsaurier Paläontographica*, *48*, 65–90.
- Pouech, J., Mazin, J. M., Cavin, L., & Poyato-Ariza, F. J. (2015). A berriasian actinopterygian fauna from Cherves-de-Cognac, France: Biodiversity and palaeoenvironmental implications. *Cretaceous Research*, *55*, 32–43.
- Poyato-Ariza, F. J., Buscalioni, A. D., & Cartanyá, J. (1999). *The Mesozoic record of osteichthyan fishes from Spain* In: Mesozoic Fishes 2. Systematics and Fossil Record. Proceedings of the international meeting (Buckow, 1997) (Arratia, G., Schultze, H.-P. (eds.). Verlag Dr. Friedrich Pfeil, München, Germany, 505–533.
- Pérez-García, A. (2017). The Iberian fossil record of turtles: An update. *Journal of Iberian Geology*, *43*, 155–191.
- Pérez-García, A., Camilo, B., & Ortega, F. (2023). New data on the poorly known jurassic record of the turtle *Hylaeochelys* (Thalassochelydia), based on new finds from Portugal. *Diversity*, *15*, 167.
- Pérez-García, A., Martín-Jiménez, M., Aurell, M., Canudo, J. I., & Castanera, D. (2022). A new Iberian pleurosternid (jurassic-Cretaceous transition, Spain) and first neuroanatomical study of this clade of stem turtles. *Historical Biology*, *34*(2), 298–311.
- Pérez-García, A., & Ortega, F. (2022). New finds of the turtle *Plesiochelys* in the Upper jurassic of Portugal and evaluation of its diversity in the Iberian Peninsula. *Historical Biology*, *34*, 121–129.
- Puértolas-Pascual, E., Canudo, J. I., & Sender, L. M. (2015a). New material from a huge specimen of *Anteophthalmosuchus* cf. *escucha* (Goniopholididae) from the Albian of Andorra (Teruel, Spain): Phylogenetic implications. *Journal of Iberian Geology*, *41*(1), 41–56.
- Puértolas-Pascual, E., & Mateus, O. (2020). A three-dimensional skeleton of Goniopholididae from the late jurassic of Portugal: Implications for the Crocodylomorpha bracing system. *Zoological Journal of the Linnean Society*, *189*(2), 521–548.
- Puértolas-Pascual, E., Rabal-Garcés, R., & Canudo, J. I. (2015b). Exceptional crocodylomorph biodiversity of ‘La Cantalera’ site

- (lower barremian; lower cretaceous) in Teruel, Spain. *Palaeontology Electronica*, 18, 1–16.
- Rauhut, O. W., Pinuela, L., Castanera, D., García-Ramos, J. C., & Cela, I. S. (2018). The largest european theropod dinosaurs: Remains of a gigantic megalosaurid and giant theropod tracks from the Kimmeridgian of Asturias. *Spain PeerJ*, 6, e4963.
- Regan, C. T. (1923). The skeleton of *Lepidosteus*, with remarks on the origin and evolution of the lower neopterygian fishes. *Proceedings of the Zoological Society of London*, 93, 445–461.
- Rodríguez-Barreiro, I., Santos, A. A., Arribas, M. E., Mas, R., Arribas, J., Villanueva-Amadoz, U., Fernández-Baldor, T., F., & Díez, J. B. (2022). The Jurassic–Cretaceous transition in the West Cameros Basin (Tera Group, Burgos, Spain): Sedimentological and palynostratigraphical insights. *Cretaceous Research*, 139, 105300.
- Royo-Torres, R., Cobos, A., Luque, L., Aberasturi, A., Espílez, E., Fierro, I., González, A., Mampel, L., & Alcalá, L. (2009). High european sauropod dinosaur diversity during jurassic–cretaceous transition in Riodeva (Teruel, Spain). *Palaeontology*, 52, 1009–1027.
- Ruiz-Omeñaca, J. I., Bermúdez-Rochas, D. D. Vertebrados fósiles (restos directos). In: V Congreso de Jurásico de España. Guía de campo (excursión B). Las sucesiones litorales y marinas restringidas del Jurásico Superior. Acantilados de Tereñes (Ribadesella) y de la playa de La Griega (Colunga) (García-Ramos, J. C., & Aramburu, C. (2010). (coords.), Servitec, Oviedo: 47–50.
- Ruiz-Omeñaca, J. I., Canudo, J. I., Aurell, M., Bádenas, B., Barco, J. L., Cuenca-Bescós, G., & Ipas, J. (2004). Estado de las investigaciones sobre los vertebrados del Jurásico Superior y Cretácico Inferior de Galve (Teruel). *Estudios Geológicos*, 60, 179–202.
- Ruiz-Omeñaca, J. I., García-Ramos, J. C., Piñuela, L., Bardet, N., Bermúdez-Rochas, D. D., Canudo, J. I., & Pereda-Suberbiola, X. (2006). Restos directos de vertebrados del Jurásico de Asturias. En: Fernández-Martínez, E. (ed.), XXII Jornadas de la Sociedad Española de Paleontología y simposios de los proyectos PICG 493, 503, 499 y 467. *Libro de resúmenes. Universidad de León, León*, 171–173.
- Ruiz-Omeñaca, J. I., Piñuela, L., & García-Ramos, J. C. (2012). New ornithopod remains from the Upper jurassic of Asturias (North Spain). *Fundamental*, 20, 219–222.
- Salas, R., Guimerà, J., Mas, R., Martín-Closas, C., Meléndez, A., & Alonso, A. (2001). Evolution of the mesozoic central Iberian Rift System and its cainozoic inversion (Iberian chain). *Peri-Tethys Memoir*, 6, 145–185.
- Salisbury, S. W., & Frey, E. (2001). A biomechanical transformation model for the evolution of semi-spheroidal articulations between adjoining vertebral bodies in crocodylians. In G. C. Grigg, F. Seebacher, & C. E. Franklin (Eds.), *Crocodylian biology and evolution* (pp. 85–134). Surrey Beatty & Sons.
- Salomon, J. (1982a). El Cretácico Inferior. In A. García (Ed.), *El Cretácico de España* (pp. 345–387). Universidad Complutense de Madrid.
- Salomon, J. (1982b). Les formations continentales du Jurassique Supérieur - Crétacé Inferieur (Espagne du Nord – Chaînes Cantabriques et NW Ibérique). *Mémoires Géologiques de l'Université de Dijon*, 6, 1–227.
- Schudack, U., & Schudack, M. (2009). Ostracod biostratigraphy in the lower cretaceous of the Iberian chain (eastern Spain)/Bioestratigrafía de ostracodos en el Cretacico Inferior de la Cordillera Iberica (este de Espana). *Journal of Iberian Geology*, 35(2), 141–168.
- Schwarz-Wings, D., Rees, J., & Lindgren, J. (2009). Lower cretaceous mesocrocodylians from Scandinavia (Denmark and Sweden). *Cretaceous Research*, 30(5), 1345–1355.
- Suñer, M., & Martín, M. (2009). Un nuevo yacimiento del tránsito Jurásico–Cretácico de Alpuente (Los Serranos, Valencia, España): Resultados preliminares. *Paleolusitana*, 1, 441–447.
- Tejero, R., & Fernández-Gianotti, J. (2004). CD-Rom appendix. In J. A. Vera (Ed.), *Geología de España*. SGE-IGME.
- Tennant, J. P., Mannion, P. D., & Upchurch, P. (2016a). Environmental drivers of crocodyliform extinction across the Jurassic/Cretaceous transition. *Proceedings of the Royal Society B: Biological Sciences*, 283(1826), 20152840.
- Tennant, J. P., Mannion, P. D., & Upchurch, P. (2016b). Sea level regulated tetrapod diversity dynamics through the Jurassic/Cretaceous interval. *Nature Communications*, 7(1), 12737.
- Tennant, J. P., Mannion, P. D., Upchurch, P., Sutton, M. D., & Price, G. D. (2017). Biotic and environmental dynamics through the late jurassic–early cretaceous transition: Evidence for protracted faunal and ecological turnover. *Biological Reviews*, 92(2), 776–814.
- Tischer, G. (1966). Über die Wealden Ablagerung und die Tektonik der östlichen Sierra de los Cameros in der nordwestlichen Iberischen Ketten (Spanien). *Beihefte zum Geologischen Jahrbuch*, 44, 123–164.
- Torcida Fernández-Baldor, F., Canudo, J. I., & Huerta, P. (2020). New data on sauropod palaeobiodiversity at the jurassic–cretaceous transition of Spain (Burgos). *Journal of Iberian Geology*, 46(4), 351–362.
- Tykoski, R. S., Rowe, T. B., Ketcham, R. A., & Colbert, M. W. (2002). *Calsoyasuchus valliceptus*, a new crocodyliform from the early jurassic Kayenta formation of Arizona. *Journal of Vertebrate Paleontology*, 22(3), 593–611.
- Unwin, D. M. (2001). An overview of the pterosaur assemblage from the Cambridge Greensand (cretaceous) of Eastern England. *Fossil Record*, 4, 189–221.
- Unwin, D. M. (2003). On the phylogeny and evolutionary history of Pterosaurs. In E. Buffetaut, & J. M. Mazin (Eds.), *Evolution and paleobiology of Pterosaurs* (pp. 139–190). Geological Society.
- Unwin, D. M., & Martill, D. M. (2018). Systematic reassessment of the first Jurassic pterosaur from Thailand. Geological Society, London, Special Publications, 455(1), 181–186.
- Vullo, R., Abit, D., Ballèvre, M., Billon-Bruyat, J. P., Bourgeois, R., Buffetaut, É., Daviero-Gomez, V., Garcia, G., Gomez, B., Mazin, J. M., Morel, S., Néraudeau, D., Pouech, J., Rage, J. C., Schnyder, J., & Tong, H. (2014). Palaeontology of the Purbeck-type (Tithonian, late jurassic) bonebeds of Chassiron (Oléron Island, western France). *Comptes Rendus Palevol*, 13(5), 421–441.
- Vullo, R., Buscalioni, A. D., Marugán-Lobón, J., & Moratalla, J. J. (2009). First pterosaur remains from the Early Cretaceous Lagerstätte of Las Hoyas, Spain: palaeoecological significance. *Geological Magazine*, 146(6), 931–936.
- Vullo, R., Marugán-Lobón, J., Kellner, A. W. A., Buscalioni, A. D., Gomez, B., de la Fuente, M., & Moratalla, J. J. (2012). A New Crested Pterosaur from the Early Cretaceous of Spain: The First European Tapejarid (Pterodactyloidea: Azhdarchoidea). *PLOS ONE*, 7(7), e38900.
- Walker, A. D. (1970). A revision of the jurassic reptile *Hallopus victor* (Marsh), with remarks on the classification of crocodiles. *Philosophical Transactions of the Royal Society of London B Biological Sciences*, 257, 323–372.
- Wenz, S. (1995). Les Amiïdés du Crétacé inferieur du Montsec (Province de Lleida, Espagne): *Urocles sauvagei* (Vidal, 1915) synonyme de *vidalamia catalunica* (Sauvage, 1903). *Treballs del Museu de Geologia de Barcelona*, 4, 5–13.
- Whetstone, K. N., & Whybrow, P. J. (1983). A cursorial crocodylian from the Triassic of Lesotho (Basutoland), Southern Africa.

- Occasional Papers of the Museum of Natural History The University of Kansas*, 106, 1–37.
- Witton, M. P. (2003). *Pterosaurs: Natural history, evolution, anatomy*. Princeton University Press.
- Wright, J. L., Barret, P. M., Lockley, M. G., & Cook, E. (1998). A review of the early cretaceous terrestrial vertebrate track – bearing strata of England and Spain. *New Mexico Museum of Natural History and Science Bulletin*, 14, 143–153.
- Wu, X. C., Brinkman, D. B., & Russell, A. P. (1996). *Sunosuchus jingarensis* sp. nov. (Archosauria: Crocodyliformes) from the Upper jurassic of Xinjiang, people’s Republic of China. *Canadian Journal of Earth Sciences*, 33(4), 606–630.

Authors and Affiliations

E. Puértolas-Pascual¹ · M. Aurell¹ · D. D. Bermúdez-Rochas² · J. I. Canudo¹ · A. E. Fernandes^{3,4} · A. Galobart⁵ · M. Moreno-Azanza^{1,6} · A. Pérez-García⁷ · D. Castanera⁸

✉ E. Puértolas-Pascual
puertolas@unizar.es

M. Aurell
maurell@unizar.es

D. D. Bermúdez-Rochas
david.bermudez@uam.es

J. I. Canudo
jicanudo@unizar.es

A. E. Fernandes
fernandes@snsb.de

A. Galobart
angel.galobart@icp.cat

M. Moreno-Azanza
mmazanza@unizar.es

A. Pérez-García
a.perez.garcia@ccia.uned.es

D. Castanera
castanera@fundaciondinopolis.org

¹ Departamento de Ciencias de la Tierra, Facultad de Ciencias, Aragosaurus-IUCA Reconstrucciones Paleoambientales, Universidad de Zaragoza, Calle Pedro Cerbuna 12, 50009 Zaragoza, Spain

² Área de Didáctica de las Ciencias Experimentales, Departamento de Didácticas Específicas, Facultad de Formación de Profesorado y Educación, Universidad Autónoma de Madrid, c/ Francisco Tomás y Valiente 3, 28049 Cantoblanco, Madrid, Spain

³ Bayerische Staatssammlung für Paläontologie und Geologie, SNSB, Richard-Wagner-Str. 10, 80333 Munich, Germany

⁴ Department of Earth and Environmental Sciences, Ludwig-Maximilians-Universität, Richard-Wagner-Str. 10, 80333 Munich, Germany

⁵ Institut Català de Paleontologia Miquel Crusafont, Universitat Autònoma de Barcelona, c/ Escola Industrial 23, 08201 Sabadell, Barcelona, Spain

⁶ Department of Earth Sciences, GEOBIOTEC, NOVA School of Science and Technology, Campus de Caparica, P- 2829 516 Caparica, Portugal

⁷ Grupo de Biología Evolutiva, Facultad de Ciencias, UNED, Avda. Esparta s/n, 28232 Las Rozas, Madrid, Spain

⁸ Fundación Conjunto Paleontológico de Teruel-Dinópolis/ Museo Aragonés de Paleontología, Avenida de Sagunto s/n, 44002 Teruel, Spain

Conclusion

Pterosaurs, in their evolutionary position along the avian line of archosaurs, were the first to underpin the idea that the specialized traits expressed in their bones (and that developed during their early evolution) could evolve particularly in the interest of maximizing the efficiency of their flight capabilities, which would then go on to bolster their later adaptive radiations. Although a remarkable amount still remains to be understood about the complete spectrum of their paleobiology and evolution (including many of the mechanisms driving their staggering array of variations), by way of this dissertation, several insights were indeed gained into the pterosaur lineage, and the surrounding paleoenvironmental implications of this variation.

The morphological evidence that we previously had from the pterosaur fossil record indicated that first proliferation of the pterodactyloids happened during the Late Jurassic (the data largely based on specimens that originated in the more readily fossil-abundant northern hemisphere), although it was suspected that pterodactyloids were also present during the Early to Middle Jurassic, along with several discrete lineages of non-pterodactyloid pterosaurs. By way of the field sampling and research undertaken in this dissertation, a new non-pterodactyloid monofenestratan from the southern hemisphere was discovered and described, setting the stage for the anatomical transitions that occurred in the period ushering out the “rhamphorynchids” and ushering in the pterodactyloids, and identifying some potentially key morphological features in the mosaic evolution that may have enabled this shift, shedding light on the role of Gondwana as a key player in originating this first radiation.

This, and the several other new species presented herein add substantially to the known morphological paleobiodiversity of the pterosaur fossil record. *Melkamter pateko* from Argentina (especially pertinent for contributing its crucial data from the underrepresented southern hemisphere) displays the earliest-known confluent naris and antorbital fenestra for a pterosaur, while also retaining a previously-unknown vestigial relic of an ascending process in the maxilla. *Spathagnathus roeperi* from Germany exhibits a novel veined tooth enamel texture, a variation in the pterosaur dental apparatus that was likely acquired for feeding specialization within its particular paleoenvironmental niche. *Lusognathus almadrava* from Portugal represents the largest gnathosaurine known, adding

more evidence for pterosaurs flourishing during the Late Jurassic, with their substantially-increasing body sizes. The specialized morphological features of a suspected new ctenochasmatid (and other postcranial elements) from the Jurassic/Cretaceous boundary of Spain also imply a flourishing diversity at a time when biodiversity was traditionally thought to have been dwindling. The presence of these taxa during the transitions from the Middle-Late Jurassic-Cretaceous boundaries were here explored in the worldwide context, helping to elucidate the myriad of new traits that are representative of the plasticity and variability inherent in pterosaur adaptation. By their addition into the fossil record, new light is shed on the anatomical array of specializations that were beneficial throughout these various Jurassic paleoenvironments.

Even just within just one lineage (as seen throughout this thesis with the ctenochasmatids, for example), the wide diversity of pterodactyloid forms that came about by the Late Jurassic becomes evident, both biologically and geospatially. One such biological variability, in this case the pterosaurian dental apparatus (likely an ecomorphological adaptation to their manifold inhabited environments) is just one example of their numerous different feeding strategies and diverse prey preferences acquired throughout their evolution. Just by the two new gnathosaurines (and a potential two more ctenochasmatid relatives) presented in this dissertation alone, the marked differences in their tooth morphologies and enamel patterning could also indicate mosaic evolution, possibly as an adaptation to their differing paleoenvironmental niches.

Geospatially, *Spathagnathus roeperi* was locally-coeval with the scaphognathine *Bellubrunus rothgaengeri*. *Melkamter pateko* was locally-coeval with the Breviquartossan *Allkaruen koi*. The microvertebrate teeth, one belonging to the Gnathosaurinae and one to Rhamphorynchinae, that were recovered from the same vertebrate microsite of Valmitão, Portugal also show evidence of two different paleoecological niches being occupied simultaneously. All of these distinct morphologies of the taxa expounded upon in this dissertation imply different – but concurrently present – ecomorphotypes, each representative of different survival strategies, and each providing an even more diverse picture unfolding for the pterosaurs throughout the Jurassic.

Pterosaurs play a crucial role in the earth's evolutionary history, having been present for all of the Mesozoic, and having reached a worldwide dispersion before their

subsequent extinction. The impact that they would have had on their surrounding paleoenvironments is undeniable, and had we more fossil evidence to track and trace these dynamics, it could reinforce or even potentially reformat our perceived understandings of this early world, and lead us to a more accurate understanding of these uniquely volant creatures. The new data presented here in this dissertation emphasizes this influence, and contributes towards unraveling the anatomical transformations that were so key to their success with new information and inferences towards unraveling the open questions that still linger.

Therefore, the future directions that this research has framed have naturally unfolded as this dissertation progressed. The first immediate additional output would be to expound on the additional fossil material that was already recovered by this project, belonging to *Allkaruen koi*, given that *Allkaruen* was found to be the immediate outgroup to *Monfenestrata*. It is also very probable that the material from the Cañadón Asfalto Formation and its equivalents will provide new information on the stem lineage of pterodactyloids and the morphological transitions leading to the origin of the clade. Additional new fossils from other localities would also, of course, continue to bring great importance to these themes (particularly those originating from the depauperate Middle Jurassic, and more fossils from the southern hemisphere), but it will also be crucial to revisit extant phylogenetic matrices to revise and reinterpret the characters judged to be of importance in disentangling the pterosaur evolutionary record. We will therefore also evaluate the presence of modular evolution in the transition from non-monofenestratan to pterodactyloid pterosaurs within a phylogenetic context, through the development of statistical tests of character change.

The incompleteness of the fossil record continues to challenge paleontologists, and the customarily-fragmented pterosaurs recovered therein are certainly no exception to these trials. Therefore, to understand the full spectrum of pterosaur evolution we must continue dig deeper, analyze more critically, and continue to revisit our past assumptions in order to fully appreciate these remarkable creatures for the myriad innovative ways in which they influenced our earth's past, and helped to shape the future that we know and appreciate today.

Dimorphodon_macronyx 3.56 21.57 0.895 0.1965 0.3906 1.938 0.2117 1.024 ? ? 0.716 ? ? ?
0.6049 0.124 0.1255 11.87 3.97 0.0858 0.6596 1.279 2.58 1.889 4.0 2.029 8.0 1.387 ? 9.29 ? 1.291 0.696 0.18
0.44 0.5985 2.555 1.135 1.088 1.248 1.0 1.671 1.969 0.95 0.943 1.449 0.521 0.2902 3.934 0.3631 0.6658 0.526

Dimorphodon_hanseni ? ? ? ? ? ? ? ? ? ? ? ? ? ? ? 0.16 0.2561 14.83 2.48 0.1653 0.7363 ? ? ? ? ?
? ?

Dimorphodon_jenkinsi ?
? ?

Dimorphodon_weintraubi ? ? ? ? ? ? ? ? ? ? ? ? ? ? ? 0.1861 ? ? ? ? ? ? ? 1.779 ? ? ? ? ? 1.034 ? ? ?
1.203 0.87 0.2393 0.51 0.4657 2.171 1.212 0.938 0.938 0.778 ? ? ? ? ? ? ? ? ? ? 3.0 0.2586 0.5667 0.4

Herbstosaurus_pigmaeus ?
1.428 ?

Campylognathoides_zitteli 2.63 6.35 0.937 0.3134 0.212 4.087 0.145 1.745 ? ? 1.343 ? ? ? 0.599
0.066 0.164 8.38 2.44 ? 0.6424 1.5 1.09 1.923 5.0 1.92 9.932 1.595 ? 6.09 ? 1.06 0.766 0.2427 0.418 0.4412
2.215 2.925 1.046 0.818 0.606 ? 1.592 2.439 ? 1.314 0.955 0.4179 2.966 0.232 0.6033 0.622

Campylognathoides_liasicus 3.31 12.56 0.846 0.2336 0.2731 2.863 0.1259 1.685 ? ? 1.443 0.1137
1.144 0.5895 0.6156 0.056 0.1202 12.37 2.16 ? 0.6794 1.578 2.14 2.333 5.0 2.612 5.75 1.203 ? 7.61 ? 1.241
0.669 0.2943 0.461 0.6849 2.063 1.839 1.068 0.94 0.742 0.775 1.586 2.319 0.763 1.239 0.632 0.4267 3.594
0.264 0.6222 0.605

Scaphognathus_crassirostris 2.78 18.73 0.783 0.2649 0.1713 2.152 0.1765 1.416 ? ? 1.103 0.1381 ?
0.3554 0.5469 0.024 0.2029 9.07 2.5 ? 0.5444 1.208 2.69 2.296 4.0 1.324 5.0 1.275 ? 8.86 ? 1.7 0.843 0.1685
0.499 0.6059 2.355 1.2 1.089 1.05 0.98 1.52 1.696 2.27 0.952 1.148 0.364 0.3402 1.925 0.2429 0.4521 0.24

Orientognathus_chaoyangensis 2.14 ? ? ? ? ? ? ? ? ? ? ? ? ? ? ? 0.028 0.2671 11.73 3.51 ? 0.4432 1.342
2.79 2.0 4.0 1.657 4.221 1.101 ? 11.09 ? 0.843 0.618 0.2442 0.38 0.5556 ? 1.11 1.38 ? ? ? 3.453 1.976 0.885
1.012 0.57 0.5065 2.213 0.2224 0.4513 0.453

Dorygnathus_banthenis 3.59 15.73 0.906 0.3733 0.2783 5.358 0.1895 1.428 ? ? 1.055 0.0857
2.482 0.503 0.6338 0.04 0.3144 12.0 3.32 ? 0.6066 1.515 2.7 2.11 4.0 2.167 6.572 1.333 ? 8.43 ? 1.62 0.876
0.1721 0.506 0.618 2.068 1.231 1.205 1.204 0.992 1.41 2.161 2.039 0.837 1.359 0.581 0.3767 2.475 0.4096
0.3956 0.286

Klobiodon_rochei ? ? ? ? ? ? ? ? ? ? ? ? ? ? ? 0.028 0.244 11.62 2.11 0.1906 0.7155 ? ? ? ? ? ? ? ?
? ?

Dolicorhamphus_depressirostris ? ? ? ? ? ? ? ? ? ? ? ? ? ? ? 0.02 ? ? 2.37 ? ? ? ? ? ? ? ? ? ? ? ? ? ? ? ? ?
? ?

Dolicorhamphus_bucklandi ? ? ? ? ? ? ? ? ? ? ? ? ? ? ? 0.028 0.3333 14.29 3.33 0.3302 0.5867 ? ? ?
? ?

Fenghuangopterus_lui 2.57 14.53 0.996 ? ? ? 0.1612 ? ? ? ? ? 3.962 ? 0.7214 0.044 0.1334 12.87
2.5 ? ? 1.375 2.09 1.951 3.0 2.669 2.339 0.8 ? 12.0 ? 1.349 1.0 0.1968 0.556 0.4877 2.027 1.984 0.6 0.446 0.396
1.51 2.61 ? 0.905 1.754 0.435 0.2991 ? ? ? ? ?

Rhamphorhynchus_muensteri 3.64 17.37 0.763 0.3463 0.1375 4.276 0.0933 2.099 ? ? 1.311 0.0935
1.31 0.2298 0.579 0.036 0.4102 13.91 4.78 ? 0.6816 1.498 2.0 1.987 4.0 2.144 7.179 1.139 ? 7.28 0.753 1.633
0.762 0.2033 0.56 0.6818 2.198 2.531 0.942 0.857 0.867 1.323 2.365 2.193 0.859 1.451 0.501 0.4781 4.73
0.1875 0.5448 0.085

<i>Nesodactylus_hesperius</i>	????????????????????1.287 2.19 2.143 4.0 1.123 6.544 0.941 ? 7.75 0.717 1.72 0.653 ? 0.574 0.5247 2.604 2.946 ? ? ? 1.379 ? ? ? ? ? ? ? ? ?
<i>Cacibupteryx_caribensis</i>	3.15 ? ? ? ? 2.833 ? 2.167 ? ? 0.867 ? 1.624 0.7241 ? 0.04 ?
<i>Qinglongopterus_guoi</i>	? 9.96 1.002 0.3333 0.2376 ? 0.2376 ? ? ? ? ? 0.6455 0.64 0.028 0.3807 11.29 2.66 ? 0.6387 1.215 1.94 1.685 4.0 2.454 3.624 0.936 ? 7.09 ? 1.59 0.941 0.1413 0.511 0.4152 2.328 1.781 1.009 0.937 0.584 1.798 ? ? 0.685 1.254 0.654 0.4641 4.57 0.3521 0.4 0.24
<i>Harpactognathus_gentryii</i>	3.67 ? ? ? ? ? ? ? ? ? ? ? ? ? ? 0.028 ?
<i>Angustinaripterus_longicephalus</i>	4.02 ? 0.871 0.3114 0.2114 9.444 0.3159 2.646 ? ? 1.143 ? ? ? 0.5174 0.036 0.1425 15.78 1.92 ?
<i>Sericipterus_wucaiwansensis</i>	4.08 14.27 ? 0.301 ? ? ? ? ? ? ? 0.1279 ? ? ? 0.028 ? ? ? ? ? 1.866 2.37 2.019 ? ? ? 1.013 ? 6.81 ? ? 0.94 ? ? ? ? 1.271 0.922 ? 0.924 ? ? ? ? ? ? ? ? ? ? ? ? ?
<i>Sordes_pilosus</i>	3.51 19.2 0.736 0.2 0.1931 2.753 0.215 1.712 ? ? 1.176 0.1601 1.36 0.6188 0.5034 0.026 0.2935 15.62 5.64 ? 0.4726 1.011 2.39 2.2 5.0 1.933 4.395 1.109 ? 11.66 ? 1.639 0.867 0.1855 0.403 0.6333 2.338 1.068 1.081 1.038 0.755 3.32 1.559 2.589 0.79 1.411 0.39 0.3293 1.574 0.255 0.3269 0.359
<i>Pterorhynchus_wellnhoferi</i>	2.95 38.06 0.922 0.3215 ? ? ? ? 0.5318 5.471 1.204 ? ? 0.3315 0.5125 0.038 0.1834 14.2 2.33 ? 0.4878 1.544 4.69 1.505 5.0 2.893 7.685 ? ? 16.77 ? 1.75 0.722 0.2453 0.548 0.5507 ? 1.106 1.252 1.148 0.8 ? 2.206 2.384 0.808 1.167 0.347 ? ? ? ? ?
<i>Kunpengopterus_sinensis</i>	2.93 17.74 0.842 0.3789 ? ? ? ? 0.6632 4.025 1.1 ? ? ? ? ? 0.2444 11.69 3.79 ? ? 2.598 3.8 1.236 ? 1.792 4.502 1.21 ? 6.01 ? 1.635 0.823 0.4358 0.635 0.4463 2.416 1.128 1.07 1.092 0.9 ? ? ? 1.11 1.356 0.355 0.382 1.035 0.2718 0.2393 0.22
<i>Wukongopterus_lii</i>	4.15 ? 0.86 0.2722 ? ? ? ? 0.5072 ? ? ? ? ? 0.4952 0.056 0.1938 13.02 3.28 ? ? 2.039 ? ? 5.0 ? 5.975 1.324 ? ? ? 1.602 ? 0.1176 0.591 ? 2.342 1.179 1.243 1.287 1.127 ? ? 2.655 0.889 1.533 0.356 0.3367 1.79 0.4357 0.2307 0.199
<i>Darwinopterus_zhengi</i>	? ? ? ? ? ? ? ? ? ? ? ? ? ? ? ? ? ? ? 3.55 2.48 2.467 6.0 1.495 6.467 1.439 ? 9.34 ? 1.227 0.83 0.5161 0.656 ? ? 1.098 1.054 0.999 0.848 ? ? 3.236 0.83 1.744 0.448 0.3185 1.905 ? ? ?
<i>Darwinopterus_linglongtaensis</i>	3.78 22.88 0.842 0.413 ? ? ? ? 0.3275 2.927 0.976 ? ? ? 0.4833 ? 0.2197 20.72 3.18 ? ? 1.61 3.82 1.81 5.0 1.921 4.224 1.215 ? 7.71 ? 1.484 0.834 0.4849 0.574 0.5771 2.027 1.497 1.135 1.18 1.184 0.769 2.963 2.846 0.99 1.25 0.46 0.322 1.345 0.3493 0.2304 0.368
<i>Darwinopterus_robustodens</i>	5.0 31.38 0.863 0.3486 ? ? ? ? 0.4343 3.8 0.841 0.0662 ? ? 0.3441 0.04 0.2661 23.18 4.0 ? 0.396 2.839 2.87 1.546 ? 2.514 3.732 1.129 ? 8.97 ? 1.6 0.571 0.4375 0.6 0.3571 2.167 1.3 1.154 1.154 1.031 1.07 0.947 2.873 0.86 1.395 ? 0.35 1.0 0.3333 0.1429 0.143
<i>Archaeoistiodactylus_linglongtaensis</i>	4.2 ? ? ? ? ? ? ? ? 3.577 ? ? ? ? ? ? ? ? ? 2.493 ? ? ? ? ? ? ? ? 1.489 1.0 0.51 0.596 0.5 ? ? ? ? ? 2.597 2.636 0.936 1.409 0.251 0.3335 ? ? ? ?
<i>Darwinopterus_modularis</i>	4.65 29.58 0.834 0.3455 ? ? ? ? 0.4432 4.284 1.169 0.0852 ? ? 0.4846 0.054 0.2167 24.88 5.59 ? 0.5475 2.02 2.49 1.639 5.0 3.747 7.527 1.038 ? 9.84 ? 1.465 0.918 0.4063 0.601 0.594 2.627 1.181 1.146 1.229 1.104 1.118 2.364 2.462 0.909 1.35 ? 0.352 1.841 0.336 0.2808 1.217
<i>Changchengopterus_pani</i>	? ? ? ? ? ? ? ? ? ? ? ? ? ? ? ? ? ? ? 1.167 1.17 1.333 3.0 1.133 3.007 1.222 ? 6.48 ? 1.421 1.0 0.462 0.602 0.3509 ? 1.158 1.067 1.0 ? ? ? ? 0.811 1.19 0.471 0.4091 ? ? ? ?

Dendrorhynchoides_curvidentatus ? 10.21 1.083 0.1068 ? ? ? ? ? ? ? ? ? ? ? ? ? ? 2.466 ? ? ? ? 0.0517 18.21 1.02 ?
? ? ? 1.516 ? 0.935 0.852 1.182 ? 14.76 ? 1.298 0.908 0.1114 0.308 0.4349 2.614 1.623 0.822 0.628 ? ? ? ?
0.723 1.344 0.518 0.4523 1.211 0.2417 0.4524 0.3

Luopterus_mutoudengensis ? ? 0.801 0.1272 ? ? ? ? ? 0.1917 1.46 2.136 0.1127 3.218 ? ? ? 0.0989
12.87 ? ? ? 1.181 ? ? 5.0 ? 2.0 1.889 ? ? ? 1.556 1.0 0.1215 0.323 0.4695 2.404 1.852 0.82 0.5 0.1 ? 1.871 2.528
0.778 1.286 0.556 0.4444 1.506 0.1667 0.75 0.5

Batrachognathus_volans ? 12.29 0.977 0.0208 ? ? ? ? 0.1816 0.859 1.398 0.1406 2.923 ? 0.6351
0.048 0.0644 11.53 1.11 ? ? 1.17 1.76 1.737 ? ? ? 1.033 ? 13.13 ? 1.609 0.823 ? 0.326 ? 2.594 ? ? ? ? ? ? 0.628
1.616 0.292 0.3833 1.545 0.1477 0.5742 0.62

Jeholopterus_ningchengensis 2.76 7.52 1.065 0.0877 ? ? ? ? 0.2596 0.92 1.095 ? 2.399 ? 0.6883
0.028 0.0926 13.01 1.23 ? 0.6377 1.126 1.75 1.507 5.0 0.403 0.868 1.532 ? 13.13 ? 1.275 0.819 0.1529 0.326
0.3821 2.562 1.48 0.891 0.633 0.178 1.416 ? 3.055 0.702 1.149 0.457 0.4517 1.494 0.159 0.6528 0.494

Anurognathus_ammoni 1.66 14.15 0.891 0.0419 ? ? ? ? 0.183 1.175 1.211 0.1655 2.546 ?
0.4894 0.03 0.1651 12.88 1.33 ? 0.3678 1.384 3.12 1.321 5.0 0.556 0.894 1.22 ? 13.85 ? 1.433 0.839 0.1389
0.285 0.554 2.279 1.686 0.798 0.462 ? ? 1.622 3.139 0.796 1.463 0.475 0.4649 2.469 0.1857 0.524 0.487

Kryptodrakon_progenitor ? 1.027 ? 2.547
? ? ? ? ? ? ? ? ? ? ? ? ? ?

Painten_pterodactyloid 3.83 25.87 0.797 0.4424 ? ? ? ? 0.3042 2.241 1.065 0.0767 ? ? 0.5215
0.042 0.4741 19.96 9.52 ? 0.5753 1.375 3.05 1.275 5.0 0.579 2.229 1.515 ? 9.5 ? 1.359 0.638 0.3412 0.63
0.4827 ? 1.14 1.095 1.107 0.864 1.54 2.825 2.408 0.953 1.174 0.483 0.319 0.698 0.3412 0.2057 0.173

Cuspicephalus_scarfi 5.93 ? ? 0.3659 ? ? ? ? 0.4755 5.167 0.906 0.045 ? ? 0.6204 0.116 ? ? ? ? ? ? ?
? ?

Germanodactylus_rhamphastinus 4.54 34.81 0.862 0.3118 ? ? ? ? 0.4105 3.043 1.065 0.0446 ? ?
0.5242 0.058 0.4718 17.43 10.5 ? 0.5016 2.693 5.01 1.074 5.0 ? ? 1.253 ? 11.64 ? 1.448 0.875 ? 1.068 0.7015
1.317 1.427 0.824 0.772 0.705 1.169 2.064 3.64 1.032 1.471 0.469 0.3179 ? ? ? ?

Germanodactylus_cristatus 4.33 26.29 0.752 0.3921 ? ? ? ? 0.3552 2.404 1.149 0.068 ? ? 0.5213
0.052 0.4112 16.9 6.63 ? 0.626 3.312 3.43 1.194 5.0 0.499 1.424 1.266 ? 13.4 ? 1.274 0.812 0.5467 1.093
0.7204 1.783 1.381 0.943 0.825 0.718 1.528 1.966 3.408 0.958 1.434 0.383 0.334 1.091 0.3395 0.1957 0.092

Pterodactylus_antiquus 6.16 27.95 0.802 0.456 ? ? ? ? 0.2467 3.194 1.474 0.0766 ? ? 0.4625
0.079 0.3878 23.05 9.75 ? 0.5105 5.09 6.79 1.313 5.0 0.489 1.168 1.359 ? 10.53 ? 1.339 0.855 0.5036 0.991
0.7031 1.556 1.306 0.945 0.84 0.641 1.154 2.127 3.154 0.994 1.388 0.373 0.3668 0.969 0.3336 0.1637 0.177

Normannognathus_wellnhoferi 4.9 ?
? ? ? ? ? ? ? ? ? ? ? ? ? ?

Aurorazhdarcho_primordius ? 1.165 ? 0.48 1.333 1.25 ? 10.89
? 1.329 0.933 0.6538 1.511 ? ? 1.915 0.592 0.423 0.422 1.094 3.235 ? 1.226 1.51 0.346 0.1823 0.963 0.3278
0.1555 0.161

Cycnorhamphus_suevicus 4.42 20.62 0.827 0.4032 ? ? ? ? 0.3364 3.569 1.427 0.1623 6.016 ?
0.0514 0.012 0.3065 15.23 3.99 ? 0.0928 2.224 3.84 1.286 5.0 0.432 1.535 1.057 ? 9.3 ? 1.305 0.81 0.7317 1.63
0.616 1.788 2.123 0.818 0.595 0.499 1.19 1.666 2.645 1.152 1.482 0.339 0.228 ? ? ? ?

Pterodactylus_micronyx 5.32 30.83 0.777 0.5025 ? ? ? ? 0.1885 3.262 2.138 0.062 3.253 0.6449
0.2631 0.072 0.3878 25.0 8.72 ? 0.3248 3.038 5.44 1.192 5.0 0.624 1.587 1.099 ? 13.12 ? 1.102 0.764 0.5169
1.328 0.5138 1.874 1.646 0.778 0.594 0.518 1.303 2.443 2.731 1.039 1.379 0.301 0.2585 0.997 0.341 0.1976

0.213

Liaodactylus_primus 6.69 ? 0.88 0.5 ? ? ? ? 0.3113 3.322 1.087 0.0685 2.327 0.3762 0.5515
0.152 0.305 33.94 10.23 ? 0.5888 ?

Ctenochasma_elegans 8.11 28.39 0.806 0.6119 ? ? ? ? 0.1265 3.214 1.719 0.0878 3.561 0.1758
0.6095 0.406 0.5873 24.33 22.42 ? 0.7242 4.21 4.66 ? 5.0 0.479 1.11 1.236 ? 11.96 ? 1.235 0.765 0.5138 1.047
0.9256 1.366 1.4 0.919 0.718 0.667 1.255 2.452 3.389 0.857 1.442 0.327 0.373 1.054 0.3146 0.2332 0.152

Pterodaustro_guinazui 10.77 38.38 0.961 0.6873 ? ? ? ? 0.1419 3.79 1.262 0.0377 ? ? 0.7238 1.0
0.5955 26.11 15.67 ? 0.8843 4.294 5.21 1.228 7.0 0.822 2.854 1.039 ? 11.61 ? 1.435 0.757 ? 1.052 ? 1.865
1.604 0.975 0.753 0.602 1.273 2.94 ? 0.855 1.556 0.53 0.5125 1.69 0.3537 0.2212 0.168

Beipiaopterus_chenianus ? 3.984 8.81 0.966 5.0 0.404 1.066
1.123 0.4221 18.43 ? 1.349 0.819 0.2735 1.035 0.6092 1.687 0.927 1.575 1.317 1.102 ? ? ? 0.706 1.993 0.38
0.3428 0.927 0.3146 0.1107 0.119

Gegepterus_changi 9.94 39.19 0.861 0.67 ? ? ? ? 0.1879 4.429 1.212 0.0667 ? ? 0.4224 0.151 ?
30.98 19.08 ? 0.4718 3.672 5.06 0.987 ? ? ? ? 0.3852 ? ? ? ? ? ? ? ? ? ? 1.015 ? ? ? 2.171 ? ? ? ? ? ? ? ? ?

Kepodactylus_inspersatus ? 2.712 ? ? ? ? ? ? ? ? ? ? ? ? 1.25 ?
? ? ? ? ? ? 0.858 ? ? ? ? ? ? ? ?

Elanodactylus_prolatus ? 3.638 6.39 1.37 ? ? ? 1.321 ? 12.31 ?
1.107 0.816 ? 0.848 0.5086 1.59 1.4 1.142 1.049 0.701 1.029 2.13 2.13 ? ? ? ? 1.132 0.2248 0.2058 ?

Moganopterus_zhuiana 11.54 ? 0.913 0.888 ? ? ? ? 0.22 9.706 1.0 ? ? 0.0899 0.3067 0.064
0.3109 34.25 14.35 ? 0.3796 7.25 ?

Feilongus_youngi 10.38 ? 0.893 0.5946 ? ? ? ? 0.2261 6.332 ? 0.0414 ? 0.0788 0.3009 0.076
0.4476 29.14 15.31 ? 0.3536 6.364 ?

Ardeadactylus_longicollum 5.7 28.07 0.837 0.4952 ? ? ? ? 0.3096 3.404 1.318 0.0891 6.789 ?
0.4803 0.058 0.4087 24.73 ? ? 0.4823 5.335 7.02 1.301 5.0 0.432 1.216 1.157 ? 11.5 ? 1.29 0.754 0.6005 1.661
0.6815 1.5 2.055 0.776 0.466 0.393 1.198 2.117 2.307 1.143 1.505 0.226 0.2013 ? ? ? ?

Huanhepterus_quingyangensis 9.55 ? ? ? ? ? ? ? ? ? ? ? ? ? ? ? ? 0.1 ? ? 14.06 ? ? 8.258 8.65 0.758 5.0 ? ?
? ? 7.54 ? 1.648 0.861 ? 0.875 0.5644 1.578 1.479 0.883 0.704 0.634 0.821 ? ? 0.931 2.04 ? 0.2523 ? 0.2073 ? ?

Plataleorhynchus_streptophorodon ? ? ? ? ? ? ? ? ? ? ? ? ? ? ? ? 0.124 ? ? ? ? ? ? ? ? ? ? ? ? ? ? ? ? ? ?
? ?

Gnathosaurus_macrurus ? ? ? ? ? ? ? ? ? ? ? ? ? ? ? ? 0.12 0.3961 43.47 14.05 ? 0.5584 8.216 ? ? ? ?
? ?

Gnathosaurus_subulatus 12.44 ? ? 0.5019 ? ? ? ? 0.2927 5.179 1.461 0.0504 3.233 0.2884 0.5704
0.14 ? ? 14.51 ?

Haopterus_gracilis 3.82 26.07 0.82 0.424 ? ? ? ? 0.3555 7.616 ? ? ? ? 0.5405 0.052 0.4719 13.09
7.96 ? 0.6728 1.395 3.0 1.017 ? ? ? 0.786 ? 11.78 ? 1.438 0.888 0.3736 1.18 ? ? 2.095 0.799 0.649 0.331 ? ? ? ?
? ? ? ? 0.316 0.1111 0.169

Ornithostoma_sedgwicki 5.43 ?
? ?

Volgadraco_bogolubovi ? 7.12 ? ? 2.4 4.76 0.801 ? ? ? ? ? ? ? ? ? ? ? ?

????????????????

Tethyraco_regalis ??1.041????????????
????????????

Pteranodon_sternbergi 6.14 43.18 0.914 0.7135 ? ? ? ? 0.1789 1.986 0.716 0.0325 ? 0.0402 ? ?
0.6883 16.42 6.49 ? ? 2.15 4.09 0.937 ? 0.832 0.829 0.914 ? 13.55 ? 1.446 0.741 0.3726 2.367 0.5438 1.542
2.684 0.798 0.582 0.324 1.283 2.075 2.169 1.003 1.397 0.315 0.2479 ? ? ? ?

Pteranodon_longiceps 4.78 ? 0.87 0.6939 ? ? ? ? 0.2257 2.086 0.761 0.0497 3.475 0.0336 ? ?
0.6367 16.02 5.56 ? ? 2.07 ? ? 10.0 ? ? 0.903 ? ? ? 1.369 0.678 0.3003 2.154 0.4501 1.704 2.428 0.814 0.593
0.297 1.132 2.423 2.04 0.982 1.408 0.316 0.3196 1.074 0.413 0.0939 0.108

Alamodactylus_byrdi ??0.975????????????
????????????

Cretornis_hlavaci ??
??????????

Simurghia_robusta ??0.671????????????
????????????

Alcione_elainus ??0.999 ? ? 0.695 1.274 0.715 ?
1.504 0.5248 ? ? ? ? ? ? 1.003 ? ? ? ? ? ?

Muzquizopteryx_coahuilensis 4.08 ? ? ? ? ? ? ? 2.688 1.714 ? ? ? ? ? ? ? ? ? ? 8.0 ? ? ? ?
0.702 1.391 0.773 0.6011 ? ? ? ? ? ? 0.957 2.425 ? 0.969 1.397 ? 0.2018 ? ? ? ?

Nyctosaurus_grandis ????????????????????????????????2.345 ? ? ? ? ? ? ? 0.716 1.3 0.678 ?
0.91 0.8025 1.898 ? ? ? ? ? ? 0.878 ? ? ? ? ? ?

Nyctosaurus_lamegoi ????????????????????????????????0.74 ? ? ? ? ? ? ? ? ? ?
????????????

Nyctosaurus_nanus ????????????????????????????????0.995 ? ? ? ? ? 6.75 0.596 ? ? ? ? ?
????????????

Nyctosaurus_gracilis 5.83 31.98 0.885 0.6637 ? ? ? ? 0.269 2.759 1.109 0.0788 1.935 0.5217 ? ?
0.5612 21.58 12.11 ? ? 2.173 3.6 1.088 9.0 0.462 0.828 0.898 ? 8.88 0.626 1.837 0.697 0.7837 2.996 0.5522
1.576 3.523 0.796 0.453 0.377 0.902 3.719 2.138 0.913 1.352 0.292 0.2755 ? ? ? ?

Serradraco_sagittirostris ??
??????????

Aussiedraco_molnari ????????????????????????????4.88 ? ? ? ? ? ? ? ? ? ? ? ? ? ? ? ?
????????????

Hongshanopterus_lacustris ? ? ? 0.4895 ? ? ? ? 0.2795 ? ? 0.077 2.996 0.4516 0.5 0.072 ? ? ? ? ?
1.325 ?

Targaryendraco_wiedenrothi ????????????????????????3.38 ? ? ? ? ? ? ? ? ? ? 0.672 ? ? ? ?
????????????

Lonchodectes_compressirostris 6.9 ? ? ? ? ? ? ? ? ? ? ? ? 3.29 ? ? ? ? ? ? ? ? ? ? ? ? ? ? ? ?
????????????

<i>Ikandraco_avatar</i>	7.07 ? 0.907 0.5002 ? ? ? ? 0.3366 3.782 1.5 0.0579 4.07 0.1988 0.6059 0.08 0.5136 20.24 9.38 0.4588 0.5815 2.648 ? ? ? ? ? ? ? ? 1.644 0.524 0.7117 1.264 0.8331 1.46 2.06 0.954 ? ? ? ? ? ? ? ? ? ? ? ?
<i>Ikandraco_machaerorhynchus</i>	? ?
<i>Lonchodraco_giganteus</i>	3.26 ?
<i>Lonchodraco_microdon</i>	9.46 ?
<i>Lonchodraco_denticulatus</i>	1.66 ?
<i>Nurhachius_ignaciobrito</i>	5.16 27.86 0.881 0.3779 ? ? ? ? 0.5968 6.399 1.402 0.0648 5.966 ? 0.3506 0.047 0.3207 21.68 7.04 ? 0.375 2.311 3.25 1.407 ? ? ? 0.81 ? 10.15 ? 1.709 0.454 0.3798 1.124 0.5261 1.619 2.021 0.82 0.638 ? ? 1.889 ? 1.104 1.257 ? 0.1349 1.136 0.443 ? ?
<i>Liaopterus_brachyognathus</i>	? ? ? ? ? ? ? ? ? ? ? ? ? ? ? ? 0.044 0.2863 22.39 5.34 ? 0.3418 ?
<i>Istiodactylus_sinensis</i>	5.21 38.25 0.902 0.2097 ? ? ? ? 0.6409 4.61 1.265 0.0576 ? ? 0.2331 0.06 0.1196 17.07 2.83 ? 0.2314 2.073 3.18 1.212 ? ? ? 0.896 ? 14.4 ? 1.751 0.483 ? 1.249 0.5819 1.716 2.046 0.892 0.715 ? ? ? ? 1.206 1.134 ? ? ? ? ? ?
<i>Istiodactylus_latidens</i>	6.29 38.02 0.755 0.1748 ? ? ? ? 0.4304 3.707 1.134 0.0509 3.833 ? 0.1539 0.052 0.1655 18.42 3.09 ? 0.2279 ? 3.6 1.105 ? ? ? 0.796 ? 10.75 ? 1.732 0.442 0.252 ? 0.4913 ? ? ? ? ? ? ? ? 0.909 ? ? ? ? ? ? ? ?
<i>Pterodactylus_polyodon</i>	7.74 ?
<i>Zhenyuanopterus_longirostris</i>	8.17 32.3 0.908 0.5505 ? ? ? ? 0.2752 3.998 1.268 0.0397 ? ? 0.8073 0.172 0.5616 21.16 9.38 ? 0.8671 2.664 4.74 ? 6.0 0.593 1.012 1.333 ? 12.44 ? 1.248 0.526 0.4389 1.095 0.7071 1.317 1.714 0.764 0.583 0.528 ? ? ? 1.0 0.952 0.468 0.11 ? ? ? ?
<i>Boreopterus_giganticus</i>	6.38 ? 0.876 0.586 ? ? ? ? 0.2161 2.767 0.935 ? ? ? 0.6872 0.114 0.6353 15.09 13.21 ? 0.7897 ?
<i>Boreopterus_cuiaie</i>	5.88 ? 0.851 0.5534 ? ? ? ? 0.2261 3.96 1.094 ? ? ? 0.6628 0.112 0.65 20.13 11.91 ? 0.7771 2.198 ? ? ? ? 2.029 ? ? ? ? 1.392 ? 0.4091 1.19 ? 1.758 1.734 0.894 0.715 0.635 ? ? ? 1.038 1.0 ? 0.1585 ? ? ? ?
<i>Hamipterus_tianshanensis</i>	4.85 24.06 ? 0.5684 ? ? ? ? 0.2948 2.522 0.806 0.0695 1.431 0.1966 0.6652 0.068 0.4453 15.91 8.33 ? 0.5725 2.731 2.71 1.312 6.0 ? ? 0.905 ? 12.48 ? ? 0.5 0.4882 ? ? 1.834 1.836 0.758 ? 0.219 ? 2.629 1.622 1.133 ? ? ? ? ? ? ? ?
<i>Brasileodactylus_araripensis</i>	? 5.54 ?
<i>Barbosania_gracilirostris</i>	3.25 29.25 0.844 0.5349 ? ? ? ? 0.2455 4.545 0.851 0.0598 ? ? 0.6733 0.044 0.5128 17.6 7.88 ? 0.7098 ? ? 0.927 ? 0.619 1.467 ? ? 11.86 ? 1.407 0.528 0.5785 0.981 0.8043 ? ? ? ? ? ? ? ? 0.801 ? ? ? ? ? ? ? ?

??????????

Coloborhynchus_clavirostris ???
??????????????

Eopteranodon_lii 4.03 24.34 0.949 0.3015 ? ? ? ? 0.4478 2.14 ? ? ? ? ? 0.6131 ? ? ? ? 2.555
5.08 1.259 ? ? ? ? ? 11.56 ? 1.495 0.898 0.5443 1.539 0.6076 1.692 2.025 0.773 0.522 0.347 ? 3.146 2.543
1.182 ? ? ? ? ? ? ? ?

Huaxiapterus_jii 3.83 20.83 0.909 0.1096 ? ? ? ? 0.5257 2.201 ? ? ? ? ? 0.4752 14.72 3.32
0.6576 ? 3.399 4.43 1.171 ? ? ? ? 0.4123 10.6 ? 1.481 0.844 0.5128 1.671 0.6716 1.727 2.044 0.786 0.567 0.279
0.845 ? ? 1.266 1.41 0.355 0.2411 ? ? ? ?

Sinopterus_dongi 3.45 30.94 0.721 0.1576 ? ? ? ? 0.6829 2.983 0.867 ? ? ? ? ? 0.5184 13.13
5.4 0.5005 ? 2.448 4.0 1.14 5.0 ? ? 1.069 0.5071 11.11 ? 1.454 0.821 0.4896 1.577 0.7751 1.409 1.988 0.762
0.525 0.239 1.366 ? 2.535 1.226 1.415 0.208 0.2081 0.927 0.2607 0.2571 0.285

Sinopterus_benxiensis 3.36 ? 0.779 0.3346 ? ? ? ? 0.4705 3.003 ? 0.1009 ? ? ? ? 0.5369 15.83
7.91 0.5468 ? 2.889 ? ? ? ? ? ? ? ? 1.919 0.857 0.5042 2.145 0.7692 1.267 2.839 0.739 0.557 ? ? ? ? 1.806
1.375 ? 0.2273 ? ? ? ?

Sinopterus_corollatus 3.66 19.66 0.854 0.3073 ? ? ? ? 0.4417 2.321 ? ? ? ? ? 0.5515 13.91 5.76
0.6613 ? 1.637 2.49 ? ? ? ? 1.175 0.5086 10.08 ? 1.479 0.806 0.5408 1.941 0.5944 1.655 2.185 0.64 0.417 0.196
0.999 ? ? 1.319 1.513 0.285 0.1996 0.912 0.4092 0.1338 0.116

Bakonydraco_galaczi 5.68 ? ? ? ? ? ? ? ? ? ? ? ? ? ? 0.5 20.17 12.63 0.4822 ? ? ? ? ? ? ? ? ? ?
? ? ? ? ? ? ? ? ? ? ? ? ? ? ? ? ? ?

Keresdrakon_vilsoni 4.12 ? ? ? ? ? ? ? ? 1.482 ? ? ? ? ? ? ? ? 10.31 ? ? 2.519 1.8 ? ? ? ? ? ? 5.79 ?
1.32 0.637 ? ? ? ? 2.156 ? ? ? ? 1.526 ? ? ? ? ? ? ? ? ? ?

Caiuajara_dobruskii ? ? ? ? ? ? ? ? ? 1.542 0.807 ? ? 0.0338 ? ? 0.3677 9.78 2.23 0.3116 ? 1.712 ?
1.053 6.0 0.497 0.776 ? 0.4396 12.19 ? 1.33 0.574 ? 1.673 ? 2.027 1.932 0.907 0.955 0.291 1.489 ? ? 1.009
1.225 ? ? ? ? ? ?

Tupandactylus_navigans 3.04 ? ? 0.2531 ? ? ? ? 0.4747 2.071 0.766 0.102 1.75 0.1104 ? ? ? ? ? ? ? ?
? ?

Tupandactylus_imperator 3.52 ? ? 0.1838 ? ? ? ? 0.6803 2.68 0.772 0.0257 ? ? ? ? ? 0.51 12.86 2.92
0.51 ?

Vectidraco_daisymorrisae ? 1.75 5.0 ? ? ? ? ? ? ? ? ? ? ? ? ? ?
? ? ? 2.073 ? ? ? ? ? ? ? ? ? ?

Europejara_olcadesorum ? ? ? ? ? ? ? ? ? ? ? ? ? ? ? 0.2505 11.59 1.96 0.277 ? ? ? ? ? ? ? ? ? ? ? ?
? ? ? ? ? ? ? ? ? ? ? ? ? ? ? ? ? ? ? ?

Tapejara_wellnhoferi 2.46 14.96 0.77 0.224 ? ? ? ? 0.477 1.913 0.894 0.13 1.12 0.0415 ? ?
0.4387 7.04 1.18 0.3967 ? 2.722 2.48 0.928 ? 0.57 1.204 1.226 0.47 5.93 ? 1.406 0.79 0.4906 1.316 0.8068
1.365 1.966 0.835 0.646 0.435 ? 2.13 2.495 1.154 1.26 0.486 0.2908 ? ? ? ?

Microtuban_altivolans ? 1.282 0.3672 6.75 ? 1.363
0.7 ? 1.807 0.8272 1.409 2.0 0.848 0.47 0.026 ? ? ? ? ? ? ? ? ? ? ? ?

Noriopteris_complicidens ? ? ? ? ? ? ? ? ? ? ? ? ? ? ? 0.028 ? ? ? ? ? 3.185 3.66 1.887 7.0 0.607
2.571 ? ? 9.59 ? 1.368 0.902 ? 1.868 0.4174 1.771 2.289 0.713 ? ? 1.567 2.425 1.097 1.145 1.839 0.22 0.2 0.75

????????????010?200?00?????0?0??0-??0??0????????????????010000??000?00?????????0--
?00101000?01100[01]1042?10?????0?????0?????00?00?0101?0001?0?11?001010?????0?????1?010?0??
?????????100000?200

Eudimorphodon_rosenfeldi 10-1?0-00001??10101000-001110200-----01003000000--1?00-00210-
100000?00000100??????0010000100?000001?????00110--
0001010002011001104211010?0100000000?0??0000?00010101001??01100?101000000?00010010000000
??00?00?01??0?020?

Eudimorphodon_ranzii 10-100-000010?10101000-001110200-----01003000000--1000-00210-
1000000000??0?00--01??002000010000000010000-00110--
0001011002011001104211010?010??0000?00?1??0?00002010110100011000101000??0??1010010?????
00??000?01?0?00??0

Parapsicephalus_purdoni 10-100-?01010000111000-203000210-----01112000000--100??00100-
1001000000001??00--
01000????????????????????????????????0?????0?1????[01]1??????0????????????????????????????
??

Dimorphodon_macronyx 10-1?0-00101??00111000-203000210-----01111001000--110??00100-
100100000??10?????01??0120000-0?0000000000-2013200100124100211000011--
110000?011??0000??0010020?00012??00?00011100102000??00020100100001001320000101000000200

Dimorphodon_hanseni ???????01??????01000-
?1????21??????0111100000102??10?????-10?10?00?????0?????????0??0010000101010000-
20242001001?4300201000011--
?10?0??

Dimorphodon_jenkinsi
????????1??????1??0??[02]????????????????0????????????????0????100?10010????0010????????????
????????????????????????0??2?100????0001??
??

Dimorphodon_weintraubi
????????????????????????[01]?????1????????????????????????????????100?1????????????001000????????
??00011100000?????????00?12????00?00?10?0102000
?00??2010010000?????????????????020?

Herbstosaurus_pigmaeus
??
??
?????????????130000??101100????

Campylognathoides_zitteli 10-1?0-000010?10111000-00??0210-----02102000000--1000-00?00-
0000100?????0?0??????01220000-0000001-000??10130--100100000211100011--
10010??0?000000?0000020?00002?110001?01111??1010?001??2010010?011011310100101011?10210

Campylognathoides_liasicus 10-100-000010010111000-002110210-----02102000000--1000-00200-
00001000000010000--01??01220000-0000001-0000-10130--100100000211100011--
100100?0100000000000000200000021110001001111??10100001?020100100011011310?00?01011010210

Scaphognathus_crassirostris 10-1?0-000010210111100-002110210-----01102000000--1000-00200-
1100000000??10?????01?001120000-1000001-?????00131--102012010220100011--
10000000?00000000001002000000211??002000110??1030000100020110101002?11101[01]000010110112
20

Sericipterus_wucaiwanensis 1111?1010101011111101-?????0?11001?001011?20000?0--??0-
0?200-11?00?01?0?00?0--??11?????1001001-0000-00?31?-102025211220111121--
00?0?001000000??0?0??00?02?????000111?010300100?????????02201???????????????

Sordes_pilosus 10-100-000010110111000-002110210-----01102001000--1000-00210-
11000101-00010000--01?001100000-1000001-0001010130--102033000220100011--
100000?01100000000010020000002?110004001111??100000000?[45]01101010020111011000010110112
20

Pterorhynchus_wellnhoferi 10-100-00001011-11--100004110-?110110000----001000--??00-
0022001100010?00010?????????1100000-1000001-?????10100--102033000220101011--
100001?0?0?000??0100200?0?????????????110??100000?????0011010??0201?01000101??0??2?1

Kunpengopterus_sinensis 10-1?0-000010?1-11--100004110-11101200?0----001000--1000-
012100110001???1??0?????????01100000-1?00001-?????10100--102033000220101031--
200001???01001001000?020?00?02?110002?0??10??102000?????401?0?0?0?????????????1?11?11211

Wukongopterus_lii 10-1?0-00001011-1?--1?0?????0-?????????0----
??????????????2?01?????????????????01???1100000-1000001-?????10100--102033000220101031--
20000?0?0100?00100010020000002????002?0110??109?????0?4?110100?????????01?00001?11?1122?

Darwinopterus_zhengi
??
??
401101?0?????31?100001?11?2121?

Darwinopterus_linglongtaensis 10-1?0-00001?1-11--100004110-1111220000----001000--1000-
002100110011???10?0?0?????????01100000-1?00001-?????10100--102033000220101031--
20000?01?100100?0011020?00?021110002?01111??109?000????40110100??20113?1000?01?11021221

Darwinopterus_robustodens 10-1?0-00001?1-11--100004110-1111220000----0010?0--1000-
00210011001101-1??0?0?????????01100000-1?00001-?????10100--102033000220101031--
200001?010100?001?001?020000002?11000200011??119000?1??4011010100201131?000001?11021221

Archaeoistiodactylus_linglongtaensis ???????00010?1-??--1?0?0?1?0-?????????0-?--
?????????????????0?????????????????????0?0?110?0??10?00??1?00-?????????02033000?20101031--
??0??0?01?010?????????????????????0?1?0??11??119000????04?11??????201??11000101?11?2?22?

Darwinopterus_modularis 10-100-00001011-11--100004110-1111220000----001000--1000-
00210011001101-1??10?010001???110000-1000001-?????10100--102033000220101031--
200001?0?0?100100?00?1?020000002?1?00200?110??19000????04?110?0?02011311000?01?11021221

Changchengopterus_pani
??
??01000001?0??010?00?02????00?00?111??00000????
?401101??00201?01?0??1?11?2121?

Dendrorhynchoides_curvidentatus 10-1-0-0001?020-0?????0?????1??0-----
0?????????????????01?????????001?----10?10?100100-002000?0?00-1??0--?0103300022?100011--
??00?????100??1?0???100000002????004?001110?100000?0?0?501101?1?01????00?00?1??0?021?

Luopterus_mutoudengensis 10-?0-0001?02?-0--10000??1?????????0-?--
?????????1??????0????00?????01?----1?1?11?100-?02000?????????????????03300??20?00[01]11--
?00??0?0??0001?????1?100000?02?????????0??11?100000000?05?1101?1?3201?00100001?1?01020?

Batrachognathus_volans 10-1-0-0001?020-0?--100000111-10-----0----0---?0--1?00-
 000010?00110?????0?----10?10110010?-0020001-0000-1?220--101033000220100011--
 10000?????0001?00?????000020100004000110??100000??????110101?????1?0100?01?1??10??1

Jeholopterus_ningchengensis 10-1-0-0001?020-0?--100000111-10-----0----0---?0--1000-
 000010?001?0?????0?----10?1?1100100-?02000???00-1?22????01033000220100011--
 10000?????100??1100??0100000002????00?001110?1040000??5011010100??11100100?01?11?10201

Anurognathus_ammoni 10?1-0-00011020-0?--1000001?1-10-----0----0---00--1000-
 000010?00110?????00----10?101100100-0020001-0000-1?220--101033000220100011--
 100001?????0?1?00010100000002????????00111??104000?0??50110101??101??00100?01011010201

Kryptodrakon_progenitor
 ???
 ???
 11?000?00????????????????????????????????

Painten_pterodactyloid 10-100-000010?1-01--100004110-10-----0----001000--1100-
 00310011000001-1??0?0?????0?1100000-1000001-000?00100--102033000220100211--
 100000?000100001100010110000102????00?00111??10500000?0401110?0?03?1131101101011011201

Cuspicephalus_scarfi 20-100-00001011-11--100004110-1110320000----0?11?0--??0-
 20320011000101-11??0010--
 0?0?01????????????????????????????????020????0120??01??100?0????????????????????????????
 ???1

Germanodactylus_rhamphastinus 20-100-00001011-11--100004110-1110320000----001100--1100-
 20320011000101-1??0?1????????1110000-?000001-0?0?-10130--102033000120100011--
 110000?0?100001?0?10??0000?20?00002?0?11?1??1??0?00?4??1?0010?301130?000?01011011??1

Germanodactylus_cristatus 20-100-00001011-11--100004110-1110320000----001100--1100-
 20320011000101-1??0?1????????1110000-1000001-0?0??10130--102033000120100011--
 010100?0??0001100010??0000002????0020001110?1050?000?4??110010?3011301000101011011331

Pterodactylus_antiquus 10-100-00001011-11--100004110-10-----0----001100--1100-
 11320011000101-2??0?0?10--0????1100000-1000001-0?00-00130--102033000120100011--
 100000?0001000011000101000000020101004000111001050000000040111001003011301001101011011331

Normannognathus_wellnhoferi 10-000-000?10?2?1????????????????1122?000?-
 ???10--?????1?00200-100000??100?????????02012010110100?11--
 11000??

Aurorazhdarcho_primordius
 ???
 ???
 ?201110?000?0113??????1?10?1331

Cycnorhamphus_suevicus 10-000-00021012-11--100002110-1[01]12220000----001100--
 1101111320011000101-211?0?10--010101000200-1001001-??0-01111--10-012010110100011--
 1?0000000000001?0?1?00000?02?110002000111??108000000?4?111000003011301000101011011331

Pterodactylus_micronyx 10-100-00000112-11--100004110-10-----0----001200--1100-
 11320011000101-21100?10--010001100000-1100001-0000-00020--102012000120101111--
 100000?00110010110001010000000211??002000111??105000000?40111000002011301101101011011331

Liaodactylus_primus 10-1?0-00000112-11--110004110-?1103?0000----????0--1?0-

10000????????????????????1????2????????0???1??2071??

Lonchodraco_microdon ??-?0??10?011?1?????????????????0-----
??101?????1????????????????????????????????02?????0?20??03??
????0??

Lonchodraco_denticulatus 100100-
1??011??101?????1????????????????
????????????????02?????0110??13??1?0??
????????????????????????????

Nurhachius_ignaciobrito 10-1?0-00101011-10--10010?110-10-----0----010100--1110-
00330?11001101-1??0?10--0?0?01101000-1000001-1000-101[02]0--102044000110101031--
100011?001010101??1??????11?021?1010200?0010?0?0711010?1?4?2?10011?3?????001101?1?02?4-1

Liaoxipterus_brachyognathus ??????-
?????1??200-11??0?1-
??0?1012?????02044000000?01011--
?00??

Istiodactylus_sinensis 10-1?0-001211?1-10--100012110-10-----0----1----0--1?10-
00340011001211-1??0?11--0?0?01101?00-1100001-?????10120--102044300000101011--
100011?0?010?01??1??????1?02?????0?00001??071??00??02?00??0311?????????1?1?0????1

Istiodactylus_latidens 10-1?0-00121111-10--100012110-?0-----0----1----0--
1110?00340?11001211-1??0?1??0?0?01101200-1100001-??0-10120--102044300000101011--
10001??0?0?010??111?????111102101010?00?00101207110100114??100?1?311?????????111102??1

Pterodactylus_polyodon 10-100-0??010?1?????????????????0-----
??100?????1?????????0????????????????????02?????0110??13??
1?0?0??

Zhenyuanopterus_longirostris 10-1?0-00101??1-10--110104110-1112310??0---0110?0--
1111000220011000101-1??0??????0??11?000-1?00011-?????10100--100114?10220111231--
10001??0?1010101?111?10?111102??????2?0?001??207110?????4??110?1??????0??????1?11?214-1

Boreopterus_giganticus 10-1?0-10101??1-10--110102110-10-----0----1----0--1110-
00220011000101-11??0??????0?11101000-1?01011-?????10120--?00114110220111211--
100011??

Boreopterus_cuiaie 10-1?0-10101??1-10--110102110-10-----0----1----0--1110-
002[12]0?11000101-1????????????????1101000-1?01011-?????10120--100114?10220111211--
10001??0?010101?????10????0?????????10?????????????????21??1?0?????????????1?11?214-1

Hamipterus_tianshanensis 10-101000101002-10--100102110-1112330000----1----0--
1110000220011001001-1110010100010011101010-1000001-1011000100--102124110120101131--
100011?001010101?1??11??11110211?0??210100??207110?10?1402?100??101??11101101?1102??1

Brasileodactylus_aripensis ?????0?????0??1000010-
1000001?101?????1--?02124??0121?01131--
?001??

Barbosania_gracilirostris 10-101000101001-1?--1?0?0?110-10-----0----0?11?0--1?10-
0023?0?0?01??0?001010?0????1000010-1?00001-1?1?00101--?02124110121101131--
10001?????????????1?1?10?1??02????10?0?00??207110????402?101?0211?0?0?????1?1102??1

Cearadactylus_atrox 10-101000101001-10--11010?110-?0-----0---
01100?????????02300110101?1-?????0100011111000010-1000001-1010-00101--102124?10121101131--
10001??1

Guidraco_venator 10-1?1000101??1-10--110102110-10-----0---
?????121111200230111010001-1??0?????0?0?110??010-1?00001-?????10100--102124110121101131--
10001??001??0101??1

Ludodactylus_colorhinus 10-
11100??01??100?????1?????????0?
?????????????????02?????00?1??13??1?0??
????????????????????????????????????1

Ludodactylus_sibbicki 10-101000101??1-10--110102110-10-----0---
01101111111200230111010001-11100?0100010?11000010-1?00001-100??10100--102124110021101131--
10001??1

Aetodactylus_halli ??-??000?2??0?????????????????????0-----
??100?????11000210-1120001-1000-1?100--10112?1?0120101131-
-?001??

Camposipterus_nasutus 10-101000?211?2?????????????????????0-----
??100?????1?????????0?????????????????????02?????01?0??13???
100?1??

Cimoliopterus_dunni 10-
101000?011?2?????????????????????1104?011??100?????1??????????
?????????????????????0212??0120?01131--
120?1??

Cimoliopterus_cuvieri 10-
101000?011?2?????????????????????1104?011??100?????1??????????
?????????????????????02?2?1101?0?01131--
120?1??

Aerodraco_sedgwickii 10-
101200?01??1??100?????1?????????0?
?????????????????02?2??01?1??131--
1?0?1??

Liaoningopterus_gui 10-1010001010??-10--1101[02]2110-?110400110---
??????????1?00230?11010101-??????100?????110000?0-??0?001-?????001020??02124110121101131--
10101??001??0101??1

Anhanguera_robustus ???0?????????????--
1??10211?????????????????????????????????02?0????10?????????0??0??11000010-1000001-1000-
0010211102124100121?01131--
??101?000101010101110?0111110200111?00100001207110000114021101?1020113?110110101102????

Anhanguera_piscator 10-1?1000101001-10--110102110-1110400110---
011011021111000230111010101-1110010?????1?11000010-1000001-??0-0010201102124110121111131--
1010111001010101010010101?111020010112001001012071100?0114?2?101110211??110110101102?4-1

Anhanguera_blittersdorffi 10-101000101001-10--110102110-1110400110---1---
1021111000230111010101-1110010100011111000010-100?0?1-10????01?201?0212411012111131--

Bakonydraco_galaczi 20-200-
1?0310????????????????11010011????????????????????????????????????0--
????1121000111001111-01210001020111-----??--
0??

Keresdrakon_wilsoni 20-200-1?0310?0--?--1?0?????0-?110100110----
?????????????????0?????????????????00--?????121030[01]-100?01?002??10??201?1-----
0?100100010?????????00?121111001100011??108111?11?????????1?001??0111001111?1??1

Caiujara_dobruskii 20-210-11001000--?--100124110-?111011110----
?????112??13?0?[34]001?001101-1?101?00--0??0122000111001011-010??001021001-----
0?10?100010??0?1?100100122?1?00?21?101??108011??1004??100?102??12??111?111111??1

Tupandactylus_navigans 20-210-110010?0--1--100124110-1111011100----
00110??010?000230011001101-1??0?0?????1????????????????????????????????1-----
0??

Tupandactylus_imperator 20-2?0-1?0010?0--?--1?0123110-1111011100----1----
1120?01300230011001101-1??1?0?????????1220001010?????1-010??001?210?1-----
0??

Vectidraco_daisymorrisae
??
??
??
?????????3?1??011111???????????

Europejara_olcadesorum ??????-??0?????????--1????411?-?????????0----
?????????1??002?001?0?????????????1??010?01210001110?1111-01??010210?1-----
0??

Tapejara_wellnhoferi 20-210-11001000--1--100124110-1111010110----
001101120101300230011001101-11101110--01010121000111001111-01010001021001-----
0?10010001010100??01001221110001101011001080111110040??100010301??00111?111111114-1

Microtuban_altivolans
??
??
4?3110??0?????????????112?1????

Noripterus_complicidens ??????-
?????0??1??000-
100?00??100110??1--?020510?0220??1?31--
????0?1101000101??1?11100??12??00?0010111010801111100??11100?0210113?11111001211?4-1

Noripterus_parvus 210100-10001001-11--100012010-1111330101----1----
1120001220220?11101101-11101?0100010?11110000-1001001-1001100101--102051000220101031--
01010110010001010111????00?12??00?000011001080111110041?1100?02??1????????001211????

Domeykodactylus_ceciliae
????????????????????????0??1?2??10??11?0??1
0??001-??10?0??1?-
?02051??0220??04????010??
???????????????

Dsungaripterus_weii 210000-10001001-11--100012110-1112330101----1----
1120001220220011101101-1110110100010111010000-1001001-1001000101--102051000220101041--

02010110010001010111111001001121110001??0?0??108011111?0?11?1001123?1????1111?001211???1

Tupuxuara_leonardii 20-100-10001001--1--100124110-1100530120----1---
1100001220230011001101-111011111011111110000-1001011-1001000101--11-----
011001000101??11?????001121?10001100??11?108011111004???100110????????????1112111??1

Tupuxuara_longicristatus ???00-100010??-?-100?????0-11005?012?----
?????????????????0??0??1-?????11110????????????????????????????????1-----
0?????????0?????????????????????0?????????????????????31?0??1?????????????????????1

Thalassodromeus_sethi 20-100-10101001--1--100124110-1100530120----
010001100001220230011001101-1?1?110111011?111??000-100?011-1211000101--11-----
0??1

Lacusovagus_magnificens 20-2?0-1100100?--?-1???????-?110100?10----
?????????????????1?????????????00--0????????????????????????????????1-----
?0??1

Xericeps_curvirostris
??10??300-
110101??1011?????0--?1-----?--
0??

Alaqa_saharica 20-100-
10?011?1??111?????1??????10?01??
1?1?????????1-----?--
?0??

Argentinadraco_barrealensis
?????????????0??11??300-
11?101??101100??200?1-----?--
0??

Aerotitan_sudamericanus 20-100-
10?311?2???0--
?????0?????????????????????????????????????1-----?--
?1??

Eoazhdarcho_liaoxiensis ??????-
?????0???0?????????????????????--?????110000-10?1001-
00010??10?-?11-----
???000130?11?00?????000?22?????00?0?01?0?080??111?4?3110??10?????????????1??1?????

Shenzhoupterus_chaoyangensis 20-1?0-??010?2--1--10012?111-10-----0---1---
1101?01301230?1100020?1??1?????????1110000-1?0??1-?????00121--?1-----
0???0130?11?10?????00?22?????????01??1080?????0?31?0?1?0?????????????1?1??114-1

Jidapterus_edentus 20-100-10001002--1--100?????1-?0-----0----
?????????????????0011?001?1-?1?????00--01??11110000-1001001-?????00121--11-----
00?00013011101001000000?22111000100001????080?1?11004021100110301?????1111111211133?

Chaoyangopterus_zhangii 20-100-100010?2--?-1?0?????1-?0-----0----
?????????????????????????????????????00--?????1110000-100100?????????121--?1-----
0?000130111?00?????000?221110002?0?011??10?????1?1?40211001?02011301111?11?1211133?

Radiodactylus_langstoni

????????????????011????????????1??01??1110000-100100??????00??1--?1-----
0??200230111??1

Hatzegopteryx_thambema

????????0??0?11?????1-
11??0?????0?1?11??2???11?001??0?2?????1??-
??1100230?11????????????22????????001?????18011????????????????????????????????1

Arambourgiana_philadelphiae

??
??
????????1????????????????????????????

Quetzalcoatlus_lawsoni

??-100-10001000--1--11012?110-111[01][46]10010----1----

000000????330011010101-??0??10--011111??200-1000011-0001001101--11-----
0111002311110111?????10012211100011100000111801111100403?1000132011321111101121114-1

Quetzalcoatlus_northropi

??
??
????100?3?????????????011211????1

Dearc_sgiathanach

????0????????????????0??0??????0-----

??
?1?????????0??0??0????????????????0?0????????????????????1??1????????????????0

Tacuadactylus_luciae

??1?1????2??
????????????????????01??4?111????2??
????????????????????????????????

Lusognathus_almadrava

??1?11??2??
????????????????????02012011121?02131--
10????????23??1??

Melkamter_pateko

2??1?0-10001???

10?11??20?11????????????0????????????????0????2100100001000????????????????????
?????0?3300022??0?011--
????0????????????????0??0

Allkaruen_koi

????????????????????????[01]?????1????????????????????0--

??10????????????????101101?????????11?00??000001-
????20?????00????010????00????00??101113000????????????????????????????????
????????????????????????????

;

cnames

- { 0 Skull_aspect_ratio_length_to_maximum_height_preserved_exclusive_of_crests continuous;
- { 1 Skull_length_to_squamosal_relative_to_dorsal_vertebra_length continuous;
- { 2 Mandible_length_relative_to_skull_length_to_squamosal continuous;
- { 3 Rostrum_length_to_narial/nasoantorbital_fenestra_relative_to_skull_length_to_squamosal continuous;
- { 4 External_naris_length_relative_to_skull_length_to_squamosal continuous;
- { 5 External_naris_length_relative_to_maximum_height_in_naris continuous;
- { 6 Antorbital_fenestra_length_relative_to_skull_length_to_squamosal continuous;
- { 7 Antorbital_fenestra_length_relative_to_maximum_height_in_fenestra continuous;

{ 8 Nasoantorbital_fenestra_length_relative_to_skull_length_to_squamosal continuous;
 { 9 Nasoantorbital_fenestra_aspect_ratio_length_to_maximum_height_in_fenestra_preserved continuous;
 { 10 Orbit_length_relative_to_height continuous;
 { 11 Supratemporal_fenestra_length_relative_to_skull_length_to_squamosal continuous;
 { 12 Subtemporal_fenestra_length_relative_to_width continuous;
 { 13 Basipterygoid_processes_angle_divided_by_100 continuous;
 { 14 Rostrum_tooth_row_length_to_posterior_margin_relative_to_skull_length_to_squamosal continuous;
 { 15 Teeth_maximum_number_divided_by_1000 continuous;
 { 16 Mandible_symphysis_length_relative_to_mandible_length continuous;
 { 17 Mandible_length_relative_to_ramus_mid-depth continuous;
 { 18 Mandible_symphysis_aspect_ratio_length_to_maximum_depth_preserved_exclusive_of_crests continuous;
 { 19 Mandible_crest_length_relative_to_mandible_length continuous;
 { 20 Mandible_tooth_row_length_relative_mandible_length continuous;
 { 21 Mid-cervical_vertebra_maximum_length_relative_to_mid-width continuous;
 { 22 Mid-cervical_vertebra_maximum_length_relative_to_dorsal_vertebra_length continuous;
 { 23 Dorsal_vertebra_length_relative_to_maximum_diameter continuous;
 { 24 Synsacrum_vertebra_number continuous;
 { 25 Caudal_vertebra_length_relative_to_dorsal_vertebra_length continuous;
 { 26 Caudal_vertebra_length_relative_to_diameter continuous;
 { 27 Scapula_length_relative_to_coracoid_length continuous;
 { 28 Coracoid_deep_flange_length_relative_to_coracoid_length continuous;
 { 29 Humerus_length_relative_to_dorsal_vertebra_length continuous;
 { 30
 Humerus_deltpectoral_crest_proximodistal_constriction_width_relative_to_anterior_terminus_proximodistal_width continuous;
 { 31 Ulna_or_radius_length_relative_to_humerus_length continuous;
 { 32 Radius_mid-width_relative_to_ulna_mid-width continuous;
 { 33 Pteroid_length_relative_to_ulna_or_radius_length continuous;
 { 34 Metacarpal_IV_length_relative_to_humerus_length continuous;
 { 35 Metacarpal_IV_midpoint_dorsoventral_width_relative_to_combined_ulna_and_radius_mid-width continuous;
 { 36 Metacarpal_IV_proximal_end_dorsoventral_width_relative_to_midpoint_dorsoventral_width continuous;
 { 37 Manus_digit_IV_first_phalanx_length_relative_to_humerus_length continuous;
 { 38 Manus_digit_IV_second_phalanx_length_relative_to_first_phalanx_length continuous;
 { 39 Manus_digit_IV_third_wing_phalanx_length_relative_to_first_phalanx_length continuous;
 { 40 Manus_digit_IV_fourth_wing_phalanx_length_relative_to_first_phalanx_length continuous;
 { 41 Prepubis_length_relative_to_maximum_width continuous;
 { 42 Pubis_depth_relative_to_acetabulum_anteroposterior_length continuous;
 { 43 Ilium_preacetabular_process_length_relative_to_postacetabular_process_length continuous;
 { 44 Femur_length_relative_to_humerus_length continuous;
 { 45 Tibiotarsus_length_relative_to_femur_length continuous;
 { 46 Fibula_free_length_relative_to_tibiotarsus_length continuous;
 { 47 Metatarsal_III_length_relative_to_tibiotarsus_length continuous;
 { 48 Pes_digit_III_second_phalanx_length_relative_to_mid-width continuous;
 { 49 Pes_digit_IV_first_phalanx_length_relative_to_metatarsal_III_length continuous;
 { 50 Pes_digit_IV_second_phalanx_length_relative_to_pedal_digit_IV_first_phalanx_length continuous;
 { 51 Pes_digit_IV_third_phalanx_length_relative_to_pedal_digit_IV_first_phalanx_length continuous;
 { 52 Rostrum_anterior_tip_shape_(ordered) flat rounded pointed;
 { 53 Rostrum_rostral_process absent present;
 { 54 Rostrum_rostral_process_cross-section triangular elliptical;
 { 55 Rostrum_anterior_end_orientation_(ordered) upturned straight downturned;
 { 56 Palate_anterior_end_fossa absent present;
 { 57 Rostrum_anterior_end_lateral_expansion absent present;
 { 58 Jaws_anterior_end_lateral_expansion_horizontal_outline elliptical triangular quadrangular;

{ 59 Rostrum,_anterior_portion,_occlusal_margins,_shape rounded ridged;
 { 60 Rostrum,_middle_portion,_expansion absent present;
 { 61 Rostrum,_posterior_portion,_occlusal_margins,_shape rounded ridged;
 { 62 Rostrum,_shape laterally_compressed anteroposteriorly_truncated dorsoventrally_depressed laterally_flattened;
 { 63 Rostrum,_taper_in_sagittal_plane subparallel attenuated;
 { 64 Rostrum,_taper_in_horizontal_plane attenuated subparallel;
 { 65 Skull,_lateral_margins,_curvature_in_horizontal_plane_(ordered) concave straight convex;
 { 66 Skull,_dorsal_margin,_curvature_in_sagittal_plane_exclusive_of_cranial_crests_(ordered) convex straight concave;
 { 67 External_naris,_dorsal_and_ventral_edges,_orientation acute_angle subparallel;
 { 68 Narial/nasoantorbital_fenestra,_anterior_end,_position_relative_to_premaxillary_tooththrow dorsal posterior;
 { 69 Jugal,_lateral_surface,_antorbital/nasoantorbital_fossa present absent;
 { 70 Antorbital_fenestra,_dorsal_and_ventral_edges,_orientation subparallel angle;
 { 71 Antorbital_fenestra,_ventral_edge,_position_relative_to_external_naris_ventral_edge level ventral;
 { 72 External_naris_and_antorbital_fenestra,_configuration separate confluent_(nasoantorbital_fenestra);
 { 73 Antorbital/nasoantorbital_fenestra,_posterior_edge,_shape subangular beveled;
 { 74 Nasoantorbital_fenestra,_dorsal_and_ventral_edges,_orientation acute_angle subparallel;
 { 75 Orbit_outline subcircular inverted_piriform_to_ovate inverted_triangle;
 { 76 Orbit,_dorsal_position_in_skull
 middle_of_the_skull_with_the_ventral_margin_of_the_orbit_below_the_middle_of_the_antorbital_(or_nasoantorbital)_fenestra_and_the_dorsal_margin_of_the_orbit_above_the_dorsal_margin_of_the_antorbital_(or_nasoantorbital)_fenestra
 high_in_the_skull_with_the_ventral_margin_of_the_orbit_the_same_level_or_above_the_middle_of_the_antorbital_(or_nasoantorbital)_fenestra
 low_in_the_skull_with_the_entire_orbit_lower_than_the_dorsal_margin_of_the_antorbital_(or_nasoantorbital)_fenestra;
 { 77 Infratemporal_fenestra,_outline trapezoidal inverted_triangle upright_triangle oval elliptical;
 { 78 Infratemporal_fenestra,_position_relative_to_orbit posterior_to_orbit reaches_under_orbit;
 { 79 Infratemporal_fenestra,_orientation subvertical inclined;
 { 80 Premaxilla,_premaxillary_bar,_width wide narrow;
 { 81 Premaxilla,_maxillary_process,_posterior_end,_position_(ordered) contacts_nasal posterior_half_of_external_naris anterior_half_of_external_naris;
 { 82 Premaxilla,_premaxillary_bar,_posterior_end,_position between_nasals between_frontals;
 { 83 Premaxilla,_crest absent present;
 { 84 Premaxilla,_crest,_anterior_end,_position_relative_to_skull_anterior_end level posterior;
 { 85 Premaxilla,_crest,_anterior_margin,_orientation_(ordered) inclined_posteriorly subvertical curving_anterodorsally;
 { 86 Premaxilla,_crest,_shape tall_triangle_decreasing_in_height_posteriorly low_blade low_with_anterior_hump comb-like_with_straight_dorsal_margin semicircular tall_triangle_increasing_in_height_posteriorly rectangular;
 { 87 Premaxilla,_crest,_posterior_end,_position_(ordered) anterior_to_naris/nasoantorbital_fenestra_anterior_end between_naris/nasoantorbital_fenestra_anterior_end_and_orbit above_orbit above_occiput;
 { 88 Premaxilla,_crest,_dorsal_spine absent present;
 { 89 Premaxilla,_crest,_thickness thin,_single_plate thick,_two_plates_separated_by_trabeculae;
 { 90 Premaxilla,_crest,_texture striated smooth branching_grooves;
 { 91 Maxilla,_posterior_end,_shape narrow ventral_expansion;
 { 92 Maxilla,_nasal_process,_shape broad_tapered parallel_sided;
 { 93 Maxilla,_lateral_surface,_antorbital_fossa present absent;
 { 94 Maxilla,_nasal_contact,_position main_body_of_nasal descending_process_of_nasal;
 { 95 Maxilla,_premaxillary_process_and_posterior_ramus,_configuration posterior_ramus_wider both_narrow premaxillary_process_wider both_wide;
 { 96 Nasal,_descending_process present absent;
 { 97 Nasal,_descending_process,_position lateral medial;

{ 98 Nasal,_descending_process,_length short elongate;
 { 99 Nasal,_descending_process,_orientation_(ordered) inclined_anteriorly ventral inclined_posteriorly;
 { 100 Nasal,_descending_process,_lateral_pneumatic_foramen absent present;
 { 101 Frontal,_crest absent present;
 { 102 Frontal,_crest,_shape blunt elongate expanded;
 { 103 Frontal,_crest,_anterior_end,_position_(ordered) anterior_to_orbit above_orbit posterior_to_orbit;
 { 104 Frontal,_anterior_end,_position_relative_to_preorbital_bar_anterior_margin anterior posterior;
 { 105 Lacrimal,_foramen absent present;
 { 106 Lacrimal,_posterior_margin,_orbital_process absent present;
 { 107 Parietal,_crest absent present;
 { 108 Parietal,_crest,_shape low expanded_into_rounded_margin tapered_into_triangular_process
 elongate_process;
 { 109 Squamosal,_shape unexpanded rounded expanded;
 { 110 Squamosal,_position_relative_to_base_of_lacrimal_process_of_jugal above below;
 { 111 Quadrate,_inclination_relative_to_ventral_margin_of_skull_(ordered) acute perpendicular ~120? ~150?;
 { 112 Quadrate,_mandible_articulation,_position_relative_to_orbit_(ordered) posterior_to_orbit
 posterior_to_center_below_orbit below_orbit_center anterior_to_center_below_orbit anterior_to_orbit;
 { 113 Quadrate,_ascending_process,_shape wide thin;
 { 114 Jugal,_anterior_end,_position_relative_to_nasoantorbital_fenestra_anterior_end posterior level;
 { 115 Jugal,_maxillary_ramus absent present;
 { 116 Jugal,_ventral_margin,_curvature_in_parasagittal_plane straight concave;
 { 117 Jugal,_postorbital_process_and_lacrimal,_configuration do_not_contact
 contact_to_form_lower_orbital_bar;
 { 118 Jugal,_ascending_and_postorbital_processes,_configuration separated_by_distinct_angle
 infilled_by_concave_flange;
 { 119 Jugal,_ascending_process,_base,_width broad narrow;
 { 120 Jugal,_ascending_process,_inclination_(ordered) anterodorsal subvertical posterodorsal;
 { 121 Jugal,_postorbital_process,_anterior_margin,_orbital_process absent present;
 { 122 Jugal,_posterior_process present absent;
 { 123 Jugal,_posterior_process,_orientation posterior ventral;
 { 124 Occiput,_orientation_(ordered) posterior posteroventral ventral;
 { 125 Basioccipital,_length_relative_to_width shorter_than_wide longer_than_wide;
 { 126 Basisphenoid,_main_body,_length shorter_than_wide longer_than_wide;
 { 127 Basisphenoid,_elongate_basipterygoid_processes absent present;
 { 128 Supraoccipital,_crest absent present;
 { 129 Supraoccipital,_pneumatic_foramina absent present;
 { 130 Palate,_posterior_end,_shape concave convex;
 { 131 Palate,_median_ridge absent present;
 { 132 Palate,_median_ridge,_position tapering_anteriorly confined_posteriorly;
 { 133 Palate,_median_ridge,_shape narrow_strip wide_keel;
 { 134 Palatine,_shape broad_plate thin_bars;
 { 135 Choanae_and_maxilla,_configuration contact do_not_contact;
 { 136 Pterygoid,_ventral_margin,_position_relative_to_jaw_occlusal_margin dorsal ventral;
 { 137 Interpterygoid_vacuity,_length_relative_to_subtemporal_fenestra_length
 longer_than_subtemporal_fenestra shorter_than_subtemporal_fenestra;
 { 138 Mandible,_articulation,_helical_shape absent present;
 { 139 Jaws,_lateral_surface,_row_of_foramina_parallel_to_occlusal_margin present absent;
 { 140 Mandible,_anterior_end,_orientation_(ordered) upturned straight downturned;
 { 141 Mandible,_anterior_tip,_shape_(ordered) blunt pointed prow;
 { 142 Mandible,_odontoid_process absent present;
 { 143 Mandible,_symphysis,_shape laterally_compressed anteroposteriorly_shortened
 dorsoventrally_depressed laterally_flattened;
 { 144 Mandible,_anterior_end,_lateral_expansion absent present;
 { 145 Mandible,_symphysis,_dorsal_eminence absent present;
 { 146 Mandible,_symphysis,_dorsal_eminence,_height low high;
 { 147 Mandible,_symphysis,_fusion absent present;

{ 148 Mandible,_symphysis,_taper_in_horizontal_plane attenuated subparallel;
 { 149 Mandible,_anterior_end,_lateral_surfaces,_texture flat cup-shaped_structures pitted;
 { 150 Mandible,_anterior_portion,_occlusal_margins,_shape rounded ridged;
 { 151 Mandible,_middle_portion,_expansion absent present;
 { 152 Mandible,_posterior_portion,_occlusal_margins,_shape rounded ridged;
 { 153 Mandible,_ramus,_dorsal_eminence present absent;
 { 154 Mandible,_ramus,_dorsal_eminence,_shape rounded pointed;
 { 155 Mandible,_symphysis,_occlusal_surface,_median_sulcus absent present;
 { 156 Mandible,_symphysis,_occlusal_surface,_anterior_end,_shape flat fossa keel;
 { 157 Mandible,_symphysis,_occlusal_surface,_shape flat parasagittal_ridges median_ridge;
 { 158 Mandible,_symphyseal_cavity absent present;
 { 159
 Mandible,_symphyseal_cavity,_dorsal_shelf,_posterior_end,_position_relative_to_ventral_symphysis_posteri
 or_end dorsal_shelf_extends_posterior_to_ventral_symphysis
 ventral_symphysis_extends_posterior_to_dorsal_shelf;
 { 160 Mandible,_ramus,_dorsal_margin,_curvature_along_length_(ordered) convex straight concave;
 { 161 Mandible,_ramus,_orientation straight_to_upturned downcurved;
 { 162 Mandible,_retroarticular_process,_orientation_relative_to_ramus_(ordered) posteroventral subparallel
 posterodorsal;
 { 163 Mandible,_retroarticular_process,_outline_in_parasagittal_plane triangular subcircular elongate blunt
 rectangular;
 { 164 Mandible,_symphysis,_ventral_margin,_shape flat keel crest;
 { 165 Mandible,_crest,_shape blade-like_and_low massive_and_deep;
 { 166 Mandible,_crest,_anterior_end,_position_relative_to_mandible_anterior_end posterior level;
 { 167 Dentary,_position_relative_to_angular_and_surangular does_not_separate separates;
 { 168 Dentition present absent;
 { 169 Dentition,_spacing_along_jaws_(ordered) mesial_teeth_spaced_wider_apart even_along_the_jaws
 distal_teeth_spaced_wider_apart;
 { 170 Dentition,_tooth_shape,_variation isodont heterodont;
 { 171 Dentition,_mesial_teeth,_shape recurved_triangle slender_needle recurved_spike curved_cone
 labiolingually_compressed_triangle bulbous_triangle;
 { 172 Dentition,_cheek_teeth,_shape recurved_triangle bulbous_triangle slender_needle curved_cone
 labiolingually_compressed_triangle recurved_spike;
 { 173 Dentition,_texture smooth striated mesial_and_distal_keels median_carina veined;
 { 174 Dentition,_maximum_crown_height_relative_to_mesiodistal_base_width less_than_four_times_width
 more_than_four_times_width;
 { 175 Dentition,_lateral_orientation vertical lateral;
 { 176 Dentition,_mesial_teeth,_spacing_between_successive_teeth_(ordered) nearly_touching
 at_most_diameter_of_teeth more_than_diameter_of_teeth;
 { 177 Dentition,_cheek_teeth,_spacing_between_successive_teeth_(ordered) nearly_touching
 at_most_diameter_of_teeth more_than_diameter_of_teeth;
 { 178 Dentition,_size_variation even_transition_along_tooth_row
 distinct_disparity_in_size_between_mesial_and_distal_teeth;
 { 179 Dentition,_upper_teeth,_size_relative_to_lower_teeth_(ordered) upper_teeth_significantly_larger
 subequal lower_teeth_significantly_larger;
 { 180 Dentition,_maximum_curvature_relative_to_mesiodistal_base_width
 displacement_of_curvature_less_than_width displacement_of_curvature_more_than_width;
 { 181 Dentition,_curvature_orientation posterior lingual anterior;
 { 182 Dentition,_inclination_(ordered) upright mesial_teeth_procumbent procumbent;
 { 183 Dentition,_cheek_alveoli,_shape set_in_grooves low undulating_occlusal_margins raised_rims pedestals;
 { 184 Dentition,_cheek_teeth,_denticles present absent;
 { 185 Dentition,_cheek_teeth,_largest_denticles,_shape_(ordered) serrations cuspules crenulations low_cusps
 tall_cusps;
 { 186 Dentition,_cheek_teeth,_maximum_denticle_number_(ordered) more_than_50 between_six_and_49
 five;
 { 187 Dentition,_upper_tooth_row,_anterior_end,_position_(ordered) posterior_to_rostrum_tip rostrum_tip

rostrum_anterior_surface;
 { 188 Dentition,_maxillary_teeth,_position_of_largest_teeth mesial middle distal;
 { 189 Dentition,_fifth_and_sixth_teeth,_subequal_in_size_and_distinctly_smaller_than_fourth_and_seventh
 absent present;
 { 190 Dentition,_lower_tooth_row,_anterior_end,_position mandible_tip posterior_to_mandible_tip;
 { 191 Jaws,_occlusal_margin,_curvature_in_sagittal_plane straight dorsally_reflected;
 { 192 Cervical_vertebrae,_atlantoaxis,_fusion unfused fused;
 { 193 Cervical_vertebrae,_lateral_to_neural_canal,_pneumatic_foramina absent present;
 { 194 Cervical_vertebrae,_middle-series,_midsection,_cross-section pentagonal dorsoventrally_depressed
 wide_suboval laterally_compressed;
 { 195 Cervical_vertebrae,_middle-series,_neural_arch,_lateral_surface,_pneumatic_foramen absent present;
 { 196 Cervical_vertebrae,_middle-series,_centrum,_lateral_surface,_pneumatic_foramen absent present;
 { 197 Cervical_vertebrae,_IV?VI,_neural_spines,_height_(ordered) tall low extremely_reduced;
 { 198 Cervical_vertebrae,_IV?VI,_neural_spine,_shape rectangular subtriangular fan ridge;
 { 199 Cervical_vertebrae,_middle-series,_transverse_crest_or_ridge,_dorsal_reflection absent present;
 { 200 Cervical_vertebrae,_middle-series,_postexapophyses absent present;
 { 201 Cervical_vertebrae,_middle-series,_neural_arch_and_centrum,_configuration distinct confluent;
 { 202 Cervical_vertebrae,_middle-series,_ribs,_shape elongate reduced;
 { 203 Cervical_vertebrae,_VIII,_neural_spine,_height tall low;
 { 204 Cervical_vertebrae,_IX,_shape_similar_to_dorsal_vertebrae similar_to_cervicals;
 { 205 Dorsal_vertebrae,_notarium absent present;
 { 206 Dorsal_vertebrae,_anterior_series,_supraneural_plate absent present;
 { 207 Synsacrum,_sacral_ribs,_configuration contact_at_iliac_contact_medial_to_iliac;
 { 208 Synsacrum,_supraneural_plate absent present;
 { 209 Caudal_vertebrae,_number more_than_15 at_most_15;
 { 210 Caudal_vertebrae,_zygapophyses,_length_(ordered) short elongate extremely_elongate;
 { 211 Caudal_vertebrae,_centrum,_shape single duplex;
 { 212 Scapulocoracoid,_orientation_relative_to_vertebral_column subparallel rotated_laterally;
 { 213 Scapula_proximal_end,_shape elongate_and_compressed suboval_and_expanded;
 { 214 Scapula,_shape elongate_process stout_with_constricted_shaft;
 { 215 Scapula,_articulation_with_vertebral_column absent present;
 { 216 Coracoid,_ventral_margin,_shape flat broad_tubercle crest;
 { 217 Coracoid,_shape_(ordered) semicircular broad_shaft narrow_shaft;
 { 218 Sternum,_sternocoracoid_articulations,_configuration lateral_to_one_another
 anterior_and_posterior_to_one_another;
 { 219 Sternum,_posterior_to_sternocoracoid_articulations,_constriction present absent;
 { 220 Sternum,_cristospine,_shape shallow deep;
 { 221 Sternum,_cristospine,_length stout elongate;
 { 222 Sternocoracoid_articulations,_shape flattened oval;
 { 223 Sternocoracoid_articulations,_posterior_expansion absent present;
 { 224 Sternum,_plate,_shape narrow quadrangular semicircular triangular laterally_expanded;
 { 225 Humerus,_proximal_end,_ventral_surface,_pneumatic_foramen absent present;
 { 226 Humerus,_proximal_end,_articulation_surface,_outline crescent horseshoe;
 { 227 Humerus,_proximal_end,_dorsal_surface,_pneumatic_foramen absent present;
 { 228 Humerus,_shaft,_curvature straight bowed;
 { 229 Humerus,_mid-shaft,_shape constricted subcylindrical;
 { 230 Humerus,_entepicondyle,_dorsoventral_width_relative_to_ectepicondyle_dorsoventral_width
 entepicondyle_wider_than_ectepicondyle ectepicondyle_wider_than_entepicondyle;
 { 231 Humerus,_distal_end,_anterior_surface,_between_distal_condyles,_pneumatic_foramen absent
 present;
 { 232 Humerus,_distal_aspect,_pneumatic_foramen absent present;
 { 233 Humerus,_distal_aspect,_outline hourglass crescentic_or_D-shape triangular trapezoidal;
 { 234 Humerus,_deltopectoral_crest,_position proximal more_distal_on_shaft;
 { 235 Humerus,_deltopectoral_crest,_shape subtriangular_with_proximal_apex
 proximodistally_long_and_proximally_leaning_trapezoid proximally_curving_hook
 oblong_process_with_constricted_neck anteroposteriorly_short_and_rectangular

proximodistally_long_and_proximally_expanded hatchet-shape distally_leaning_trapezoid
 anteroposteriorly_tall_and_rectangular_process anteroposteriorly_tall_and_proximally_leaning_trapezoid;
 { 236 Humerus,_deltopectoral_crest,_curvature perpendicular_to_shaft warped_distally ERROR;
 { 237 Humerus,_ulnar_crest,_size reduced developed;
 { 238 Humerus,_ulnar_crest,_orientation posterior ventral;
 { 239 Ulna,_shaft,_proximal_end,_anterior_surface,_longitudinal_ridge absent present;
 { 240 Ulna,_distal_tuberculum,_position middle_of_the_distal_end ventral_part_of_the_distal_end;
 { 241 Radius,_distal_end,_cross-section suboval subtriangular_with_large_anterior_process;
 { 242 Distal_syncarpal_ventral_articular_facet_for_wing_metacarpal,_size_relative_to_dorsal_facet
 ventral_facet_larger subequal_in_size;
 { 243 Distal_syncarpal,_cross-section rectangular triangular;
 { 244 Pteroid,_shape angled_at_midsection stout_hook straight_and_tapered_with_expanded_proximal_end
 straight_with_expanded_ends proximally_curved_slender_rod curved_and_subparallel_sided;
 { 245 Medial_carpal,_shape longer_than_wide wider_than_long;
 { 246 Metacarpals,_number_articulating_with_carpus_(ordered) five four two one;
 { 247 Metacarpals_I?III,_distal_ends,_relative_positions disparate approximate;
 { 248 Metacarpal_IV,_proximal_end,_cross-section anteroposteriorly_compressed broad;
 { 249 Metacarpal_IV,_shaft,_cross-section cylindrical anteroposteriorly_compressed_oval;
 { 250 Metacarpal_IV,_distal_end,_intercondylar_sulcus,_median_ridge absent present;
 { 251 Manus,_unguals,_size_relative_to_pedal_unguals less_than_twice_size_of_pedal_unguals
 more_than_twice_size_of_pedal_unguals;
 { 252 Manus,_digit_IV,_first_phalanx,_proximal_end,_ventral_surface,_pneumatic_foramen absent present;
 { 253 Manus,_digit_IV,_second_or_third_phalanges,_shaft,_cross-section subtriangular concave_posteriorly
 oval ventral_keel;
 { 254 Pubis,_anterior_margin,_curvature_in_sagittal_plane_(ordered) convex straight slightly_concave
 deeply_concave;
 { 255 Pubis_and_ischium,_ventral_contact,_configuration confluent oval_opening;
 { 256 Ischium,_ventral_margin,_curvature_in_parasagittal_plane straight convex;
 { 257 Prepubis,_shaft,_constriction absent present;
 { 258 Prepubis,_shape elongate_paddle medially_curved_with_short_lateral_process triradiate expanded_fan;
 { 259 Ilium,_preacetabular_process,_anterior_margin,_shape rounded triangular sharp_rod;
 { 260 Ilium,_preacetabular_process,_orientation straight dorsiflected;
 { 261 Ilium,_postacetabular_process,_orientation subhorizontal posterodorsal;
 { 262 Ilium,_postacetabular_process,_shaft,_constriction absent present;
 { 263 Ilium,_postacetabular_process,_terminus,_expansion absent present;
 { 264 Acetabulum,_outline oval subcircular;
 { 265 Ilium,_postacetabular_process,_dorsal_margin,_shape flat convex;
 { 266 Femur,_curvature strongly_bowed straight_to_slightly_curved;
 { 267 Femur,_proximal_end,_pneumatic_foramen absent present;
 { 268 Femur,_neck,_shape indistinct constricted;
 { 269 Femur,_greater_trochanter,_shape_(ordered) reduced distinct_process hooked_process;
 { 270 Femur,_distal_end,_epicondyles,_size reduced_and_confluent_with_distal_condyles
 expanded_into_distinct_distal_flanges;
 { 271 Femur,_neck,_angle_relative_to_shaft_(ordered) perpendicular less_than_145° more_than_145°;
 { 272 Metatarsal_IV,_length_relative_to_metatarsals_I?III subequal significantly_shorter;
 { 273 Pes,_digit_V,_number_of_phalanges_(ordered) four three two one zero;
 { 274 Pedal_digit_V_ultimate_phalanx,_shape_(ordered) straight curved bent_at_midsection nubbin;
 { 275 Maxilla,_ascending_process present absent;
 ;

nstates stand;

ccode - 0.51 53.54 56.64 67.80 82.84 86 88.98 100.102 104.110 113.119 121.123 125.139 142.159 161
 163.168 170.175 178 180.181 183.184 188.196 198.209 211.216 218.245 247.253 255.268 270 272 275 + 52
 55 65.66 81 85 87 99 103 111.112 120 124 140.141 160 162 169 176.177 179 182 185.187 197 210 217 246
 254 269 271 273.274;

0???1?01??0??0??0001?????2???????????????????

Darwinopterus

00011220201122?1100111111000001110101011100010000001000000111000000011101200013
?0?112002001[1 2]00600?0[1 2][0 1 2]0[1 2]00??101010[0 1]00111310100001011011

Wukongopterus

000112??0?????11????????????????????????????10001?0000010000001??0?000000?010120001?0?0
111?0200?2?0??0?0200?0???010100?011??0?000010?101?

Kunpengopterus

00011220001122?110011111010000??110??101?1000100000010000001110000000010101200013
1??11200200110060000[1 2]001000010101002011131?100001011011

Changchengopterus

??001200002??112
002001?00600001201000?010?01201112?010000101101?

Douzhanopterus

??1??00001??102
?0200?2?1?0?003?21??2010100?01??101100?100110?

Rhamphodactylus

00011210001122?11000100100100110?210??201?100011000001000100111000000000111200103
?0010200000120051000[0 1]1?1100020111010011121010000101101

Liaodactylus

00111210001?22?11??10010?1?0100?21011201010011100000100000011100000100?????????????
??1

Pterodactylus

00011210001122?1100100100100110?2?0?02010100011000001000000111000000000111201102
00010200000120050000[0 1]0021100202110[0 1]0[0 1]0112101000010012?1

Cycnorhamphus

00111210001122?1??0?100100000110?2?0??2?20100111000001000110111000000000010001103
?011120000?120050000130211002030101010112101000?11?1??1

Eosipterus

??11120110????11?
000??1100500?00001110??0201010001??01000010012??

Aurorazhdarcho

01112220001122?1?00?100100100100?210??20101011110000010000001110000010010111201103
?00112000001000500000302110021[2 3]0001?10112111000?11012??

Gnathosaurus

01112210201122?11?00100100100110121011201010111100000100000011100000100?????????????
??0??1

Gegepterus

00113220001122?11000100100000110?2?0??201?10?11?0?00010000001?100000110111120?????
?0?120??01?????????0????02???012?01????0?0??10????1

Gladocephaloideus

00113220001122?11000101100000110?210??202?100111000001000000111000001001?11120????

??1?2000011?05?00?10010?002120101200?????10?0010012?1

Ctenochasma 00113220[0
2]01122?1?000100100000110?2?0??201?10011100000100000011100000110??11120110??0?1?20000011?0
50000[0 1]0?111002020101?101?2101000010012?1

Pterodaustro
00113220001122?111001001001001100210??201?10011100010100000011000000110111112?0103
10111200000100050000000211002120101010112101000010012?1

Istiodactylus 00110110001122?11?0011021?[0
1]00000??0??102010011000000100000010?000000011101011????1012020111113017111?211?0100213?1
02?10?????110002?????1

Nurhachius
00110220001122?1110011021010000001????102010011100000100000011100000001?101011????
1??20201??1?0?7?11?2??110021??102?201????100?21?1??1

Haopterus
001101?000??22?1??010?????0?????????10??10011100000100000011100100001??010?0???300
1202?10101??7?11??1?110?00203110?010?????????????12??

Ornithocheirus
01011220101122?1??0?10111?001000?1?0?1102110101100001100000011100100000?????????????
??

Anhanguera 01011220101122?1110010111000000011101110211010110000[0
1]10000001110010000011010111103?1?2021110130171100[1 2]11211??2121102010105?11100021????1

Coloborhynchus
01011220101122?1??0?10111?000000?1101110211010110000110000001110010000011010111103
1102011110130171110111?1??02121102010101?01100021?12?1

Ludodactylus
01011220001122?111001011?0001000??0??102?10?01100000100000011100100000?????????????
???1

Boreopterus 00012220[0
1]01122?1?0010111??00000??0??102?100011000001000000111001000001?0101?110??????2??11111???
?1?111?1110?2121102?10????01100?21?12?1

Nyctosaurus
00013220001122?1??0?10110?00200001?0111020100011001001??111??1??????100101111010
002120111012108?1012212?100224?[0 1]03020112201100020?12?1

Muzquizopteryx
??0??0001122?1??0?1?110??02000??0??1?2?1??????1?01??111??1????????010?11101010
?1??11101??08?1?01??2?100?23??????1??20110002??2?1

Pteranodon
00013220001122?1??0?10111?00200011?0111020100011001101??111??1??????110101111010
11202011111107110?101111002241103010103201100011012?1

Germanodactylus crist
00011210200122?11100100100100000?1?1??1?1?1000110000010000001101011000?101000?10?
??1?20000001?050001130?1100202010[0 1]?10??2?11011010012?1

Germanodactylusrhamp

00011210200122?1100110100100000?1?1?101?10001100000100000001101010000?101000110?
0??1020000011?050001200??002020000?10122111011?11012?1

Dsungaripterus

00011210200122?1??0?10010?00300011?11110101000110001000000000?00101100011011011101
101112000110?005001??0??100??0?0?2??124?1101101?????1

Tatalpterosaur

00011210200122?1??0?10011?103000??1??101?10001?000?000000000?010110001101100?????
??112?00??02005001?130?11002130?012?0????11011011?????

Noripterus

????????0????????????????????????????????1?001?000?0?000?00?101?1?000?0112?????????
21??0?0?0?5001??0??00??????2??104??100101?0??1

Lonchodectes

000????[0 1]0?????1????????????????????????110011?000?[0
1]100000001100000000101112????????1?????0?1050????????????????????0011???????

Tapejara

10020110401122?1??0?11011?2130001110??1020100011000211???111???1??????1011120???11
01112000111?005001?1?0??1002130?1?0?0102??1000011??2?1

Tupandactylus

10020210401122?1??0?11011?214000?11011102?100011000?11???111???1??????10111211101?
01112000?11110500?01302??002230011?20112?11001111012?1

Sinopterus

1002021000?122?1??0?11011?213000??0??101?100011000[0
2]11???111???1??????1?111201101?01112?0?1?11??5?010130211002?3001102010211?001?11012?1

Huaxiapterus

1002021040?122?1??0?11010?214000??0??1010100011000211???111???1????????1112?110???
?1120?0??11105001?1302110?21300110[1 2]0????11?001?11????1

Shenzhoupterus

00021211001122?1??0?11021?215000??0??1?2?10001?001?01???111???1????????11120?10???
?112?00??11??500?1230?1?0?2240011020????1100??1?2?1

Chaoyangopterus

0002?2?100??22?1??0?1?????2????????????1???100011001?0????111???1????????1112??1??1?11
?2??0??11?????1013?21100223?010020????1100??11??2??

Tupuxuara

00020220301122?1??0?11021?215000??0111021100011000?01???111???1??????110110111011
01112000?1111050010030211002230011020102?11001111012?1

Thalassodromeus

00020?20301122?1??0?11021?215000??0?11021100011000?01???111???1????????????????????
??1

Quetzalcoatlus

00021220501?22?1??0?10021?21?????????1020100011001001???111???1??????1021121????10
1112000111105001?1302?1002240011320?????1001121??2?1

Zhejiangopterus

00020220001122?1??0?11020?210000??0??1?2?100011001001???111??1?????????21121110??0
1112?00??11?05?01023?2110?2?400113?0102011001?21012?1

Azhdarcho

000?????0?????1????????????????????????????????0001?00???????111??1???????1021121?????1?1??
2??0111?1050?1??0??00?????3???????10011???????

;

cnames

{0 Tip_of_rostrum_downturned absent present;
 {1 Tip_of_rostrum_laterally_expanded absent present;
 {2 Tip_of_rostrum laterally_compressed dorsoventrally_compressed;
 {3 Rostrum_high_with_convex_outline_low_with_straight_or_concave_dorsal_outline
 anterior_region_of_rostrum_low_but_antorbital_region_expanded_dorsally;
 {4 Rostrum_length_anterior_to_external_nares_as_a_proportion_of_skull_length_excluding_sagittal_crests
 <0.30 0.30-0.5 0.5-0.6 >0.6 (3)_exclusive_of_sagittal_crests.;
 {5 Rostral_index_(antorbital_length_divided_by_maximal_skull_height_{excluding_cranial_crests}) 1.5_or_less
 1.5-3.0 >3.0;
 {6 Preorbital_rostrum <50%_skull_length 50-80%_skull_length >80%;
 {7 Dorsal_margin_of_nasal_+_antorbital_or_nasoantorbital_opening_bounded_by_slender_bar absent
 present_;
 {8 Premaxillary_crest absent low,_rounded,_confined_to_rostrum comb-
 like_free_margin_and_extends_from_above_anterior_end_of_nasoantorbital_fenestra_to_apex_of_skull
 _extends_from_tip_of_rostrum_to_apex_of_skull_and_confluent_with_fronto-parietal_crest
 tall,_narrow,_stands_on_anterior_half_of_premaxillae keel-
 like,_anterior_margin_extends_no_further_forward_than_midpoint_of_nasoantorbital_fenestra_;
 {9 Skull_broad_with_very_short_preorbital_region absent present_;
 {10 Ventral_margin_of_skull straight downcurved_caudally;
 {11 Posterior_extent_of_premaxillae terminates_level_with_frontals overlaps_frontals;
 {12 Nasal_process_of_maxilla vertical-subvertical inclined_backwards absent;
 {13 Maxilla-nasal_contact broad narrow absent;
 {14 Antorbital_fossa_on_the_ascending_process_of_the_maxilla present absent;
 {15 Nasal_opening terminal subterminal;
 {16 External_nasal_opening height_similar_to_or_greater_than_anteroposterior_length elongate;
 {17 Nares smaller_than_the_orbit_or_antorbital_opening form_the_largest_skull_opening;
 {18 Dorsal_border_of_the_antorbital_fenestra_lies_below_the_mid-height_of_the_naris absent present;
 {19 Antorbital_fenestra less_than_twice_as_long_as_it_is_deep at_least_as_twice_as_long_as_it_is_deep;
 {20 Naris_and_antorbital_opening separate confluent;
 {21 Nasoantorbital_fenestra <40%_skull_length_from_tip_of_rostrum_to_posterior_margin_of_orbit >40%;
 {22 Posterior_margin_of_antorbital_or_nasoantorbital_fenestra straight concave;
 {23 Lacrimal-jugal_bar inclined_anterodorsally vertical posterodorsally;
 {24 Orbit_shape subcircular tall,_oval;
 {25 Orbit larger_than_antorbital_opening similar_in_size,_or_smaller_than_antorbital_opening;
 {26 Dorsal_margin_of_orbit above_dorsal_margin_of_antorbital_or_nasoantorbital_opening
 level_with_dorsal_margin_of_nasoantorbital_opening or_below_it;
 {27 Frontal_extends_anterior_to_the_lacrimal-jugal_bar absent present_;
 {28 Fronto-parietal_crest absent flange-like,_short flange-like,_elongate rod-like,_short_rod-like,_elongate
 _sail-like;
 {29 Posterior_region_of_skull_rounded absent present;
 {30 Squamosal_position above,_or_level_with_the_orbit entirely_below_the_orbit;
 {31 Supratemporal_fenestra_largest_skull_opening_other_than_the_orbit absent present;
 {32 Separation_of_supratemporal_fenestrae
 wide,_formed_by_a_dorsally_facing_bridge_composed_of_the_parietals
 narrow,_parietals_form_sharp_sagittal_crest;
 {33 Occiput_faces_posteriorly posteroventrally ventrally;
 {34 Occipital_condyle on_the_posterior_face_of_the_occiput on_the_posteroventral_face_of_the_occiput;

- {35 Distal_ends_of_paroccipital_processes unexpanded rounded, tongue-like flange;
- {36 Basipterygoid_processes widely diverging (angle_between_processes_?35?) narrow (angle_<_35?);
- {37 Basipterygoid_processes separate_over_their_entire_length connected_by_a_bony_web, only_the_distal_articular_ends_separate;
- {38 Quadrate vertical inclined_backward subhorizontal;
- {39 Palatal_elements_reduced_to_thin_bars_of_bone absent present;
- {40 Position_of_the_jaw_joint posterior_to_the_orbit_or_under_the_posterior_third_of_the_orbit under_the_middle_third_of_the_orbit under_the_anterior_third_of_the_orbit;
- {41 Palatal_ridge absent present;
- {42 Dentary <50%_length_of_lower_jaw >50%;
- {43 Anterior_tip_of_the_mandible horizontal downturned;
- {44 Anterior_end_of_the_lower_jaw unexpanded_expanded_transversely;
- {45 Anterior_end_of_mandibular_symphysis laterally_compressed_or_as_wide_as_deep dorsoventrally_compressed;
- {46 Mandibular_symphysis unfused fused;
- {47 Length_of_symphysis less_than_30%_of_the_length_of_the_mandible more_than_30%_of_the_length_of_the_mandible;
- {48 Mandible_tips_fused_into_a_short_symphysis_bearing_a_forward_projecting_'tooth-like' prow_and_a_number_of_large, fang-like, procumbent_teeth_forming_a_fish_grab absent present;
- {49 Anterior_end_of_dentary level dorsally_expanded_forming_low_rounded_eminence high_rounded_eminence;
- {50 Mandibular_rami level_with_symphysis elevated_well_above_level_of_symphysis;
- {51 Dorsal_margin_of_the_dentary straight_or_slightly_concave markedly_concave convex sinuous;
- {52 Dentary_bony_sagittal_crest absent present;
- {53 Pre-dentary_region Pre-dentary_region_relatively_deep_with_convex_dorsal_profile, dentary_tapers_anteriorly pre-dentary_region_and_dentary_of_similar_depth_for_much_of_its_length;
- {54 Dimorphodontid_dentition absent present;
- {55 Teeth_small, peg-like_and_widely_spaced absent present;
- {56 Multicusped_teeth absent present;
- {57 Rostral_dentition more_than_11_pairs_of_teeth less_than_11_pairs;
- {58 Rostral_dentition more_than_nine_nine_or_less_relatively_straight_(or_slightly_recurved)_teeth;
- {59 Mandibular_dentition more_than_six_pairs_of_teeth six_or_less;
- {60 Heterodonty_in_the_mandibular_dentition present absent;
- {61 Anterior_dentary_teeth spacing_between_teeth_less_than_mesiodistal_diameter_of_the_teeth more_than_the_mesiodistal_diameter;
- {62 Posterior_dentary_teeth spacing_between_teeth_less_than_mesiodistal_diameter_of_the_teeth more_than_the_mesiodistal_diameter;
- {63 Dentition present absent;
- {64 Largest_teeth_in_caudal_half_of_dentition absent present;
- {65 First_three_pairs_of_teeth_large, 4th-6th_small, 7th-9th_large absent present;
- {66 Short, broad_teeth_in_at_least_part_of_the_dentition absent present;
- {67 Dentition_extends_to_jaw_tips jaw_tips_toothless, but_followed_by_tooth_row;
- {68 Teeth_relatively_elongate_with_a_long_cylindrical_crown_of_even_width_and_a_short_tapering_distal_tip absent present;
- {69 Total_of_more_than_192_long, fine_teeth absent present;
- {70 Laterally_compressed, triangular_teeth_in_at_least_part_of_the_dentition absent present;
- {71 Postexapophyses_on_cervical_vertebrae absent present;
- {72 Lateral_pneumatic_foramen_on_centrum_of_the_cervical absent present;
- {73 Mid-series_cervicals_length/_minnum_width ?_2.5 2.5-5 >5;
- {74 Cervical_ribs present highly_reduced_or_absent;
- {75 Neural_arch_of_cervicals high depressed_down_onto_or_even_confluent_with_the_centrum;
- {76 Neural_spines_of_mid-series_cervicals tall, blade-like tall, spike-like low_or_absent;
- {77 Notarium absent present;
- {78 Number_of_caudal_vertebrae more_than_15 15_or_fewer;

- {79 Combined_length_of_caudal_vertebrae longer_than_the_dorsal_series shorter;
- {80 Filiform_extensions_of_zygapophyses_and_hypapophyses absent present;
- {81 Sternum rectangular triangular semicircular square_with_posterolateral_projections;
- {82 Sternocoracoid_articulations,_position_with_respect_to_one_another lateral anterior_and_posterior;
- {83 Cristospine_of_sternum unconstricted constricted;
- {84 Cristopine,_shape shallow_and_elongated deep_and_short;
- {85 Coracoid less_than_two_thirds_length_of_scapula_
from_at_least_two_thirds_up_to_similar_length_to_scapula longer_than_scapula;
- {86 Coracoid_with_well-developed_brachial_flange absent present;
- {87 Coracoid,_shape semicircular broad_shaft narrow_shaft;
- {88 Coracoidal_contact_surface_with_sternum articulatory_surface flattened,_lacking_posterior_expansion
articulation_surface_oval,_with_posterior_expansion;
- {89 Shape_of_scapula elongate stout_with_constricted_shaft;
- {90 Scapula_posterior_end,_shape elongate_and_laterally_compressed suboval_and_expanded
slightly_bulbous;
- {91 Scapulocoracoid,_orientation_relative_to_vertebral_column subparallel rotated_laterally;
- {92 Scapula_articulates_with_vertebral_column absent present;
- {93 Appendicular_bones_with_thin_cortex_and_wide_lumen absent present;
- {94 Forelimb up_to_2.5_times_length_of_hind_limb_(f+t+mt) 2.5-3_times_length_of_hind_limb 3-
4_times_length_of_hind_limb at_least_4_times_length_hind_limb at_least_4_times_length_hind_limb;
- {95 Pneumatic_opening_in_palmar_surface_of_humerus absent present;
- {96 Pneumatic_opening_in_anconal_surface_of_humerus absent present;
- {97 Deltpectoral_crest_of_humerus small large_and_subtriangular_with_apex_directed_proximally proximo-
distally_elongate,_flange-shaped hatchet-shaped_tongue-shaped_with_necked_base antero-
posteriorly_elongate_with_rectangular_shape antero-
posteriorly_elongate,_main_axis_directed_anteromedially,_terminal_margin_rounded warped_
distally_expanded;
- {98 Distal_end_of_humerus D-shaped triangular;
- {99 Diameter_of_radius more_than_half_the_ulna less;
- {100 Ulna_shaft_anterior_surface:_shape flat longitudinal_ridge;
- {101 Ulna_considerably_shorter_than_dorsals+sacrals_similar_in_length_to_dorsals+sacrals;
- {102 Ulna_less_than_133%_humerus_133-150%_>150%;
- {103 Ulna/tibia_ratio 0.9-1.2 1.2-1.4_>1.4 <0.9;
- {104 Ornithocheiroid_carpus absent present;
- {105 Pteroid_less_than_30%_length_humerus 30-60% >60%;
- {106 Metacarpals_I-III disparate_lengths the_same_length;
- {107 Metacarpal_IV_proximal_cross-section,_shape anteroposteriorly_compressed subrectangular_;
- {108 Metacarpal_IV_shaft_cross-section,_shape subrectangular anteroposteriorly_compressed_;
- {109 Metacarpal_distal_end_between_condyles,_shape flat median_ridge;
- {110 Metacarpal_IV,_length/_max_dorso-ventral_height_of_proximal_articulation <3.5 3.5-4.5 >4.5;
- {111 Contact_between_distal_carpals_and_metacarpals_I-IV all_four_in_contact_
only_I_and_IV_contact_syncarpal only_IV_contacts_the_syncarpal;
- {112 Metacarpal_IV_?_humerus_ratio less_than_0.4 0.4-0.8 0.8-1.2 1.2-2.0 >2.0;
- {113 Unguals_of_manus_and_pes similar_in_size
manual_unguals_twice_the_size,_or_more,_of_pedal_unguals;
- {114 Manus_digit_iv_(wing-finger) 57.5%,_or_less,_of_total_forelimb_length >57.5% >65%_>65%;
- {115 Proceeding_distally,_phalanges_1-
4_of_digit_4_exhibit_a_rapid_decline_in_length,_contributing_40%,_30%,_20%_and_10%_to_the_wing-
finger_respectively absent present;
- {116 Manus_digit_iv_(wing-finger)_phalange_1_compared_to_length_of_tibiotarsus shorter
1_to_1.5_times_longer 1.5-2.0_times_longer more_than_twice_the_length;
- {117 Manual_digit_IV_phalanges_shaft_cross-sections,_shape round_to_subtriangular concave_posteriorly
oval ventral_ridge_;
- {118 Contribution_of_phalange_1_to_manus_digit_4 less_than_30% 30-40% more_than_40%;
- {119 Manus_digit_iv_phalanges_decline_in_length_distally phalanges_2_and/or_3_longer_than_phalange_1;
- {120 Preacetabular_process_of_iliac less_than_twice_

```

at_least_twice_the_length_of_the_postacetabular_process;
{121 Anterior_profile,_in_lateral_view,_of_pubis convex_or_straight slightly_concave deeply_concave;
{122 Pubis_and_ischium unfused
fused_to_form_a_plate_with_a_straight_ventral_margin_that_meets_the_posterodorsal_margin_at_an_acute_angle
ischium_with_convex_ventral_border_that_projects_below_level_of_the_pubis_and_obtuse_posterior_apex
narrow_ischium_with_steeply_oriented_posteroventral_margin dsungaripterid_ischiopubis
ischium_separated_from_pubis_by_deep_narrow_recess;
{123 Prepubis distal_expansion_longer_than_broad_or_similar_width_to_length transversely_expanded
cojoined_prepubes_forming_H_shape;
{124 Leg_length_(Femur+Tibia) less_than_1.5_x_length_of_dorsal+sacral_vertebral_series_
more_than_1.5_times;
{125 Femoral_neck,_shape indistinct constricted;
{126 Femur_caput directed_inward_at_about_135?_of_less
directed_steeply_almost_parallel_to_long_axis_of_femur_shaft_;
{127 Strongly_bowed_femur absent present;
{128 Prominent_anteriorly_directed_tubercle_on_dorsal_apex_of_external_trochanter_of_femur absent
present;
{129 Pneumatic_opening_in_posterior_face_of_collum_femoris absent present;
{130 Fibula subequal_in_length_to_the_tibia_less_than_80_percent_the_length_of_the_tibia_
reduced_to_a_small_splint_or_lost_altogether;
{131 Length_of_metatarsal_III_compared_to_tibia >30% <30%;
{132 Pes_digit_3 <75% >_75%_length_of_metatarsal_3;
{133 Length_of_metatarsal_4 similar_in_length_to_metatarsals_i-iii_ shorter_than_metatarsals_i-iii;
{134 Fifth_pedal_digit
_two_phalanges_or_more_and_combined_length_of_phalanges_>_66%_length_of_MTIII_
fifth_digit_strongly_reduced_(combined_lengths_of_phalanges_<_66%_length_of_MTIII)
one_very_short_phalange,_or_less;
{135 Phalange_two_of_pedal_digit straight_or_gently_curved arcuate_flexure_at_30-
40_%_length_of_phalange_subtends_angle_of_145-150?
angular_flexure_at_50%_length_of_phalange_subtends_angle_of_120?;
{136 Ascending_process_of_the_maxilla present absent;
;

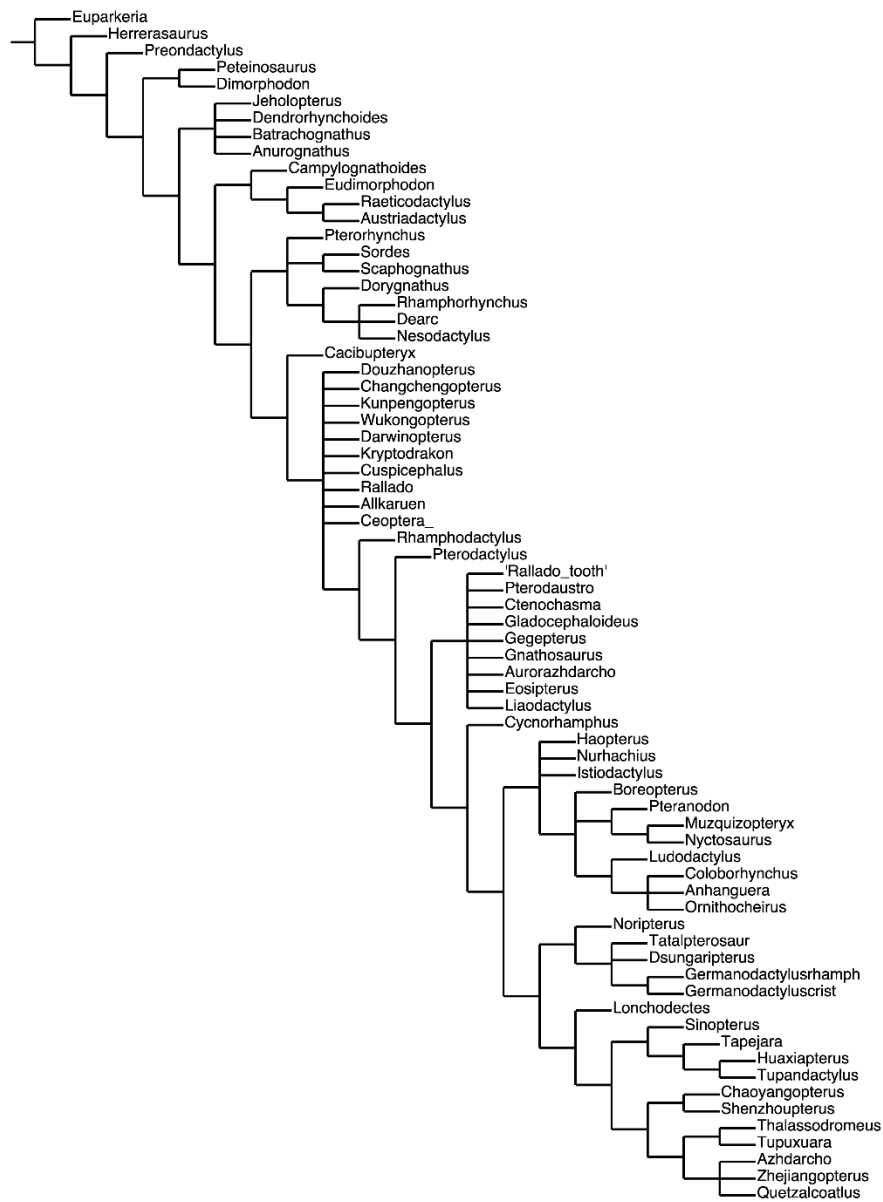
ccode + 4.6 23 26 38 40 73 85 94 102 105 111 112 114.118 130 134 *;

proc /;
comments 0
;

```

Martin-Silverstone et al., 2024 reduced consensus tree:

Strict consensus of 2500 trees (0 taxa excluded)



Appendix ii: Chapter 3. Supplementary Information: Phylogenetic Data Matrix

nstates cont;
mxram 300;
xread
275 181

&[continuous]

Euparkeria_capensis 3.65 8.50 1.044 0.0526 0.0563 0.679 0.2561 1.683 ? ? 1.018
0.1542 1.940 0.9572 0.5543 0.068 0.1084 6.87 1.62 ? 0.4076 1.670 0.95 1.461 2 0.942 3.471 .338 ? 3.71 ?
0.892 0.871 ? 0.243 0.2041 1.922 ? ? ? ? 0.767 0.183 1.476 0.857 1.000 0.4014 1.434 0.2291 0.6328 0.476

Ornithosuchus_longidens 2.67 11.50 0.913 0.0586 0.1885 ? 0.3331 1.633 ? ? 1.188 0.1205
? ? 0.5628 0.044 0.4762 3.92 3.49 ? ? 2.444 1.10 1.000 3 1.000 2.500 1.806 ? 5.70 ? 0.842 1.171 ? 0.132
0.2598 1.640 ? ? ? ? 0.704 0.262 1.526 0.839 1.000 0.4795 2.787 0.4288 0.6050 0.357

Herrerasaurus_ischigualastensis 3.10 ? 0.962 0.0302 0.0799 2.315 0.2333 1.892 ? ? 0.955 0.2038 ? 0.8308
0.6000 0.076 0.5000 8.60 5.68 ? 0.4229 1.947 ? 0.961 2 1.133 1.742 ? ? 4.61 ? 0.897 1.000 ? 0.189 0.1587
2.329 0.057 ? ? ? ? 0.613 0.453 1.971 0.913 1.005 0.5238 2.265 0.2226 0.7135 ?

Scleromochlus_taylori ? 13.18 1.052 0.1607 0.0835 ? 0.2124 2.535 ? ? 1.826 0.2348
1.813 0.6780 0.4472 0.062 0.0980 12.40 0.93 ? 0.4016 1.696 0.52 1.913 4 1.227 2.755 2.750 ? 8.86 ? 0.923
0.788 ? 0.128 0.1750 3.280 0.067 ? ? ? ? 0.323 1.007 1.641 1.078 1.000 0.4783 2.825 0.2718 0.4693 0.262

Preondactylus_buffarinii 3.41 29.86 0.875 0.1179 0.2812 5.235 0.2129 1.484 ? ? 1.094
? ? ? 0.6525 0.070 0.0750 17.69 2.13 ? 0.5691 1.377 1.57 1.554 4 7.188 5.459 ? ? 15.18 ?
1.358 0.766 0.1786 0.445 0.5117 2.371 1.103 1.143 1.159 0.779 4.559 ? 0.855 1.038 1.359
0.674 0.3690 4.696 0.4051 0.4467 ?

Austriadactylus_cristatus 3.88 13.75 0.808 0.1659 0.2122 3.042 0.1626 1.423 ? ? 1.105
0.0889 2.346 0.5657 0.5653 0.100 0.1242 13.27 2.27 ? 0.6170 1.241 1.63 ? ? 3.500 5.283 1.415 ? 9.38 ?
1.361 0.790 ? 0.436 ? ? 1.212 1.025 1.051 0.868 ? ? ? 0.777 1.272 ? 0.2230 ? ? ? ?

Peteinosaurus_zambellii ? ? ? ? ? ? ? ? ? ? ? ? ? ? 0.148 ? ? ? ? ? ? ? ? ? ? ? ? ? ? ? ? 2.252 ? 0.868 ?
0.815 ? ? 0.747 ? ? 0.890 0.3273 ? ? ? ?

Caviramus_schesaplanensis ? ? ? ? ? ? ? ? ? ? ? ? ? ? 0.068 0.1263 6.92 1.02 ? ? ? ? ? ? ? ?
? ?

Raeticodactylus_filisurenensis 3.06 13.57 0.884 0.2692 0.1474 3.111 0.2000 1.727 ? ? 1.106
0.1499 ? ? 0.5381 0.078 0.1976 8.84 1.22 ? 0.5594 1.429 2.86 2.181 ? ? ? ? ? 11.71 ? 1.293 ? 0.1971 ? ? ?
1.378 0.965 1.035 ? ? ? ? 0.683 1.482 0.522 0.3855 ? ? ? ?

Eudimorphodon_cromptonellus ? ? ? ? ? ? ? ? ? ? ? ? ? ? 0.048 ? ? ? ? ? ? ? ? ? ? 4.524
2.000 ? ? ? 1.107 0.851 ? 0.463 0.5000 2.088 0.992 1.139 1.139 ? ? ? ? 1.085 1.041
0.732 0.5537 ? ? ? ?

Eudimorphodon_rosenfeldi 2.49 15.01 0.792 0.2640 0.2248 5.710 0.1432 1.562 ? ? 1.833
0.1164 ? 0.3964 0.5525 0.066 0.2139 10.98 4.27 ? 0.7281 1.194 2.22 2.020 ? 6.073 9.731 1.243 ? 9.40 ?
1.339 0.726 0.2785 0.455 0.5049 2.053 1.466 0.937 0.991 0.864 ? ? 0.640 0.787 1.428 0.935 0.3875 5.184
0.2728 0.6995 0.632

Dolicorhamphus_depressirostris ? ? ? ? ? ? ? ? ? ? ? ? ? ? ? ? 0.020 ? ? 2.37 ? ? ? ? ? ? ? ? ? ? ?
 ?

Dolicorhamphus_bucklandi ? ? ? ? ? ? ? ? ? ? ? ? ? ? ? ? 0.028 0.3333 14.29 3.33 0.3302
 0.5867 ?

Fenghuangopterus_lii 2.57 14.53 0.996 ? ? ? 0.1612 ? ? ? ? ? 3.962 ? 0.7214 0.044 0.1334
 12.87 2.50 ? ? 1.375 2.09 1.951 3 2.669 2.339 0.800 ? 12.00 ? 1.349 1.000 0.1968 0.556 0.4877 2.027 1.984
 0.600 0.446 0.396 1.510 2.610 ? 0.905 1.754 0.435 0.2991 ? ? ? ?

Rhamphorhynchus_muensteri 3.64 17.37 0.763 0.3463 0.1375 4.276 0.0933 2.099 ? ? 1.311
 0.0935 1.310 0.2298 0.5790 0.036 0.4102 13.91 4.78 ? 0.6816 1.498 2.00 1.987 4 2.144 7.179 1.139 ? 7.28
 0.753 1.633 0.762 0.2033 0.560 0.6818 2.198 2.531 0.942 0.857 0.867 1.323 2.365 2.193 0.859 1.451 0.501
 0.4781 4.730 0.1875 0.5448 0.085

Nesodactylus_hesperius ? 1.287 2.19 2.143 4
 1.123 6.544 0.941 ? 7.75 0.717 1.720 0.653 ? 0.574 0.5247 2.604 2.946 ? ? ? 1.379 ? ? ? ? ? ? ? ? ? ?

Cacibuptyryx_caribensis 3.15 ? ? ? ? 2.833 ? 2.167 ? ? 0.867 ? 1.624 0.7241 ? 0.040
 ?

Qinglongopterus_guoi ? 9.96 1.002 0.3333 0.2376 ? 0.2376 ? ? ? ? ? ? ? 0.6455
 0.6400 0.028 0.3807 11.29 2.66 ? 0.6387 1.215 1.94 1.685 4 2.454 3.624 0.936 ? 7.09 ? 1.590 0.941 0.1413
 0.511 0.4152 2.328 1.781 1.009 0.937 0.584 1.798 ? ? 0.685 1.254 0.654 0.4641 4.570 0.3521 0.4000 0.240

Harpactognathus_gentryii 3.67 ? ? ? ? ? ? ? ? ? ? ? ? ? ? ? 0.028 ? ? ? ? ? ? ? ? ? ? ?
 ?

Angustinaripterus_longicephalus 4.02 ? 0.871 0.3114 0.2114 9.444 0.3159 2.646 ? ? 1.143 ? ? ? 0.5174
 0.036 0.1425 15.78 1.92 ?

Sericipterus_wucaiwanensis 4.08 14.27 ? 0.3010 ? ? ? ? ? ? ? ? 0.1279 ? ? ? 0.028 ? ? ?
 ? ? 1.866 2.37 2.019 ? ? ? 1.013 ? 6.81 ? ? 0.940 ? ? ? ? 1.271 0.922 ? 0.924 ? ? ? ? ? ? ? ? ?
 ? ?

Sordes_pilosus 3.51 19.20 0.736 0.2000 0.1931 2.753 0.2150 1.712 ? ? 1.176
 0.1601 1.360 0.6188 0.5034 0.026 0.2935 15.62 5.64 ? 0.4726 1.011 2.39 2.200 5 1.933 4.395 1.109 ? 11.66
 ? 1.639 0.867 0.1855 0.403 0.6333 2.338 1.068 1.081 1.038 0.755 3.320 1.559 2.589 0.790 1.411 0.390
 0.3293 1.574 0.2550 0.3269 0.359

Pterorhynchus_wellnhoferi 2.95 38.06 0.922 0.3215 ? ? ? ? 0.5318 5.471 1.204 ? ?
 0.3315 0.5125 0.038 0.1834 14.20 2.33 ? 0.4878 1.544 4.69 1.505 5 2.893 7.685 ? ? 16.77 ? 1.750 0.722
 0.2453 0.548 0.5507 ? 1.106 1.252 1.148 0.800 ? 2.206 2.384 0.808 1.167 0.347 ? ? ? ? ?

Kunpengopterus_sinensis 2.93 17.74 0.842 0.3789 ? ? ? ? 0.6632 4.025 1.100 ? ? ? ?
 ? 0.2444 11.69 3.79 ? ? 2.598 3.80 1.236 ? 1.792 4.502 1.210 ? 6.01 ? 1.635 0.823 0.4358
 0.635 0.4463 2.416 1.128 1.070 1.092 0.900 ? ? ? 1.110 1.356 0.355 0.3820 1.035 0.2718
 0.2393 0.220

Wukongopterus_lii 4.15 ? 0.860 0.2722 ? ? ? ? 0.5072 ? ? ? ? ? 0.4952 0.056
 0.1938 13.02 3.28 ? ? 2.039 ? ? 5 5.975 1.324 ? ? ? 1.602 ? 0.1176 0.591 ? 2.342 1.179
 1.243 1.287 1.127 ? ? 2.655 0.889 1.533 0.356 0.3367 1.790 0.4357 0.2307 0.199

Darwinopterus_zhengi ? 3.550 2.48 2.467 6

Elanodactylus_prolatus ? 3.638 6.39 1.370 ? ?
 ? 1.321 ? 12.31 ? 1.107 0.816 ? 0.848 0.5086 1.590 1.400 1.142 1.049 0.701 1.029 2.130 2.130 ? ? ? ? 1.132
 0.2248 0.2058 ?

Moganopterus_zhuiana 11.54 ? 0.913 0.8880 ? ? ? ? 0.2200 9.706 1.000 ? ? 0.0899 0.3067 0.064 0.3109
 34.25 14.35 ? 0.3796 7.250 ?

Feilongus_youngi 10.38 ? 0.893 0.5946 ? ? ? ? 0.2261 6.332 ? 0.0414 ? 0.0788 0.3009 0.076 0.4476 29.14
 15.31 ? 0.3536 6.364 ?
 ? ? ? ? ?

Ardeadactylus_longicollum 5.70 28.07 0.837 0.4952 ? ? ? ? 0.3096 3.404 1.318 0.0891
 6.789 ? 0.4803 0.058 0.4087 24.73 ? ? 0.4823 5.335 7.02 1.301 5 0.432 1.216 1.157 ? 11.50 ? 1.290 0.754
 0.6005 1.661 0.6815 1.500 2.055 0.776 0.466 0.393 1.198 2.117 2.307 1.143 1.505 0.226 0.2013 ? ? ? ?

Huanhepterus_quingyangensis 9.55 ? ? ? ? ? ? ? ? ? ? ? ? ? ? ? ? 0.100 ? ? 14.06 ? ? 8.258
 8.65 0.758 5 ? ? ? ? 7.54 ? 1.648 0.861 ? 0.875 0.5644 1.578 1.479 0.883 0.704 0.634 0.821 ? ? 0.931 2.040 ?
 0.2523 ? 0.2073 ? ?

Plataleorhynchus_streptophorodon ? ? ? ? ? ? ? ? ? ? ? ? ? ? ? ? 0.124 ? ? ? ? ? ? ? ? ? ? ? ? ?
 ?

Gnathosaurus_macrurus ? ? ? ? ? ? ? ? ? ? ? ? ? ? ? ? 0.120 0.3961 43.47 14.05 ? 0.5584 8.216 ? ? ? ? ? ? ? ? ?
 ?

Gnathosaurus_subulatus 12.44 ? ? 0.5019 ? ? ? ? 0.2927 5.179 1.461 0.0504 3.233 0.2884 0.5704
 0.140 ? ? 14.51 ?

Haopterus_gracilis 3.82 26.07 0.820 0.4240 ? ? ? ? 0.3555 7.616 ? ? ? ? 0.5405
 0.052 0.4719 13.09 7.96 ? 0.6728 1.395 3.00 1.017 ? ? ? 0.786 ? 11.78 ? 1.438 0.888 0.3736 1.180 ? ? 2.095
 0.799 0.649 0.331 ? ? ? ? ? ? ? ? 0.3160 0.1111 0.169

Ornithostoma_sedgwicki 5.43 ?
 ?

Volgadraco_bogolubovi ? 7.12 ? ? 2.400 4.76 0.801
 ?

Tethydraco_regalis ? 1.041
 ?

Pteranodon_sternbergi 6.14 43.18 0.914 0.7135 ? ? ? ? 0.1789 1.986 0.716 0.0325 ?
 0.0402 ? ? 0.6883 16.42 6.49 ? ? 2.150 4.09 0.937 ? 0.832 0.829 0.914 ? 13.55 ? 1.446 0.741 0.3726 2.367
 0.5438 1.542 2.684 0.798 0.582 0.324 1.283 2.075 2.169 1.003 1.397 0.315 0.2479 ? ? ? ?

Pteranodon_longiceps 4.78 ? 0.870 0.6939 ? ? ? ? 0.2257 2.086 0.761 0.0497 3.475
 0.0336 ? ? 0.6367 16.02 5.56 ? ? 2.070 ? ? 10 ? ? 0.903 ? ? ? 1.369 0.678 0.3003 2.154 0.4501 1.704 2.428
 0.814 0.593 0.297 1.132 2.423 2.040 0.982 1.408 0.316 0.3196 1.074 0.4130 0.0939 0.108

Alamodactylus_byrdi ? 0.975
 ?

Cretornis_hlavaci ?
 ? ? ? ? ? ? ? ? ? ? ? ? ? ? ? ? ?

1.124 0.5261 1.619 2.021 0.820 0.638 ? ? 1.889 ? 1.104 1.257 ? 0.1349 1.136 0.4430 ? ?

Liaoxipterus_brachyognathus ? ? ? ? ? ? ? ? ? ? ? ? ? ? ? ? 0.044 0.2863 22.39 5.34 ? 0.3418 ? ? ? ? ? ? ? ?
? ?

Istiodactylus_sinensis 5.21 38.25 0.902 0.2097 ? ? ? ? 0.6409 4.610 1.265 0.0576 ? ?
0.2331 0.060 0.1196 17.07 2.83 ? 0.2314 2.073 3.18 1.212 ? ? ? 0.896 ? 14.40 ? 1.751 0.483 ? 1.249 0.5819
1.716 2.046 0.892 0.715 ? ? ? ? 1.206 1.134 ? ? ? ? ? ?

Istiodactylus_latidens 6.29 38.02 0.755 0.1748 ? ? ? ? 0.4304 3.707 1.134 0.0509
3.833 ? 0.1539 0.052 0.1655 18.42 3.09 ? 0.2279 ? 3.60 1.105 ? ? ? 0.796 ? 10.75 ? 1.732
0.442 0.2520 ? 0.4913 ? ? ? ? ? ? ? 0.909 ? ? ? ? ? ? ?

"Pterodactylus"_polyodon 7.74 ?
? ?

Zhenyuanopterus_longirostris 8.17 32.30 0.908 0.5505 ? ? ? ? 0.2752 3.998 1.268
0.0397 ? ? 0.8073 0.172 0.5616 21.16 9.38 ? 0.8671 2.664 4.74 ? 6 0.593 1.012 1.333 ? 12.44 ? 1.248 0.526
0.4389 1.095 0.7071 1.317 1.714 0.764 0.583 0.528 ? ? ? 1.000 0.952 0.468 0.1100 ? ? ? ?

Boreopterus_giganticus 6.38 ? 0.876 0.5860 ? ? ? ? 0.2161 2.767 0.935 ? ? ? 0.6872
0.114 0.6353 15.09 13.21 ? 0.7897 ?

Boreopterus_cuiae 5.88 ? 0.851 0.5534 ? ? ? ? 0.2261 3.960 1.094 ? ? ? 0.6628
0.112 0.6500 20.13 11.91 ? 0.7771 2.198 ? ? ? ? 2.029 ? ? ? ? 1.392 ? 0.4091 1.190 ? 1.758
1.734 0.894 0.715 0.635 ? ? ? 1.038 1.000 ? 0.1585 ? ? ? ?

Hamipterus_tianshanensis 4.85 24.06 ? 0.5684 ? ? ? ? 0.2948 2.522 0.806 0.0695
1.431 0.1966 0.6652 0.068 0.4453 15.91 8.33 ? 0.5725 2.731 2.71 1.312 6 ? ? 0.905 ? 12.48 ? ? 0.500 0.4882
? ? 1.834 1.836 0.758 ? 0.219 ? 2.629 1.622 1.133 ? ? ? ? ? ? ?

Brasileodactylus_araripensis ? ? ? ? ? ? ? ? ? ? ? ? ? ? ? ? ? 5.54 ? ? ? ? ? ? ? ? ? ? ? ?
? ?

Barbosania_gracilirostris 3.25 29.25 0.844 0.5349 ? ? ? ? 0.2455 4.545 0.851 0.0598 ?
? 0.6733 0.044 0.5128 17.60 7.88 ? 0.7098 ? ? 0.927 ? 0.619 1.467 ? ? 11.86 ? 1.407 0.528 0.5785 0.981
0.8043 ? ? ? ? ? ? ? ? 0.801 ? ? ? ? ? ? ?

Cearadactylus_atrox 4.83 ? 0.846 0.4259 ? ? ? ? 0.3253 2.206 ? ? 3.238 ? 0.4171
0.062 0.2282 13.94 3.29 ? 0.4542 ?

Guidraco_venator 4.42 ? 0.868 0.5395 ? ? ? ? 0.2500 3.167 0.948 0.0423 ? ? 0.6342 0.088 0.5364
13.63 6.67 ? 0.7322 1.278 ?
? ? ? ? ?

Ludodactylus_colorhinus ?
? ?

Ludodactylus_sibbicki 4.52 ? 0.891 0.5049 ? ? ? ? 0.3055 2.668 0.983 0.0449 ? 0.1919 0.6882 0.080
0.3832 14.69 5.00 ? 0.6982 ?
? ? ? ? ? ?

Aetodactylus_halli ? ? ? ? ? ? ? ? ? ? ? ? ? ? 0.108 0.4078 29.60 10.49 ? 0.7540
? ?

Camposipterus_nasutus 4.97 ?

????????????????

Cimoliopterus_dunni 10.88 ?????????????????????????????????
????????????????????

Cimoliopterus_cuvieri 5.08 ?????????????????????????????????
????????????????????

Aerodracosedgwickii 5.62 ?????????????????????????????????
????????????????????

Liaoningopterus_gui 6.73 ?????????????????????0.068 0.3625 12.09 4.76 ??
2.207 ?????????????????????????????????

Anhanguera_robustus ?????????????????????0.071 0.4823 15.42 6.88 0.2728 0.5544 1.833 1.98 1.070
5 0.713 1.934 0.757 ? 11.59 ? 1.345 0.465 ? 0.983 ?????? 1.204 2.101 ? 0.955 ????? 0.921 ???

Anhanguera_piscator 5.43 27.52 0.845 0.4741 ????? 0.2921 2.823 1.828 0.0572 ?
0.3454 0.6452 0.089 0.4833 16.06 6.72 0.2796 0.6671 1.389 2.81 1.048 5 0.747 2.386 0.772 ? 11.08 ? 1.529
0.464 ? 1.004 0.6934 1.899 ?????? 2.754 ? 0.918 1.218 ? 0.2050 0.514 0.4879 ??

Anhanguera_bittersdorffi 6.00 ? 0.841 0.5019 ?????? 0.3022 3.326 0.989 0.0580 2.096 0.4173 0.6592 0.098
? 17.30 ? 0.2683 0.6732 ?????????????????????????????????
??????

Tropeognathus_mesembrinus 5.10 ? 0.850 0.4508 ?????? 0.3721 3.534 0.808 0.0433 1.879 0.4809
0.5589 0.048 0.2994 16.93 5.27 0.2491 0.6539 ?????????????????????????????????

Ornithocheirus_platystomus ?????????????????????????????????
????????????????

Ornithocheirus_simus ?????????????????????????????????
????????????????

Siroccopteryx_moroccensis ?????????????????????????????????
????????????

Coloborhynchus_capito ?????????????????????????????????
????????????

Coloborhynchus_wadleighi ?????????????????????????????????
????????????

Coloborhynchus_clavirostris ?????????????????????????????????
????????????

Eopteranodon_lui 4.03 24.34 0.949 0.3015 ?????? 0.4478 2.140 ?????? 0.6131
????? 2.555 5.08 1.259 ?????? 11.56 ? 1.495 0.898 0.5443 1.539 0.6076 1.692 2.025 0.773 0.522 0.347 ?
3.146 2.543 1.182 ??????

Huaxiapterus_jii 3.83 20.83 0.909 0.1096 ?????? 0.5257 2.201 ?????? 0.4752
14.72 3.32 0.6576 ? 3.399 4.43 1.171 ?????? 0.4123 10.60 ? 1.481 0.844 0.5128 1.671 0.6716 1.727 2.044
0.786 0.567 0.279 0.845 ? ? 1.266 1.410 0.355 0.2411 ??????

Sinopterus_dongi 3.45 30.94 0.721 0.1576 ?????? 0.6829 2.983 0.867 ??????
0.5184 13.13 5.40 0.5005 ? 2.448 4.00 1.140 5 ? ? 1.069 0.5071 11.11 ? 1.454 0.821 0.4896 1.577 0.7751

1.409 1.988 0.762 0.525 0.239 1.366 ? 2.535 1.226 1.415 0.208 0.2081 0.927 0.2607 0.2571 0.285

Sinopterus_benxiensis 3.36 ? 0.779 0.3346 ? ? ? ? 0.4705 3.003 ? 0.1009 ? ? ? ?
 0.5369 15.83 7.91 0.5468 ? 2.889 ? ? ? ? ? ? ? ? 1.919 0.857 0.5042 2.145 0.7692 1.267
 2.839 0.739 0.557 ? ? ? ? 1.806 1.375 ? 0.2273 ? ? ? ?

Sinopterus_corollatus 3.66 19.66 0.854 0.3073 ? ? ? ? 0.4417 2.321 ? ? ? ? ? ?
 0.5515 13.91 5.76 0.6613 ? 1.637 2.49 ? ? ? ? 1.175 0.5086 10.08 ? 1.479 0.806 0.5408 1.941 0.5944 1.655
 2.185 0.640 0.417 0.196 0.999 ? ? 1.319 1.513 0.285 0.1996 0.912 0.4092 0.1338 0.116

Bakonydraco_galaczi 5.68 ? ? ? ? ? ? ? ? ? ? ? ? ? ? 0.5000 20.17 12.63 0.4822
 ?

Keresdrakon_vilsoni 4.12 ? ? ? ? ? ? ? ? 1.482 ? ? ? ? ? ? ? ? 10.31 ? ? 2.519 1.80
 ? ? ? ? ? ? 5.79 ? 1.320 0.637 ? ? ? ? 2.156 ? ? ? ? 1.526 ? ? ? ? ? ? ? ? ? ?

Caiujara_dobruskii ? ? ? ? ? ? ? ? 1.542 0.807 ? ? 0.0338 ? ? 0.3677 9.78 2.23 0.3116 ? 1.712 ? 1.053
 6 0.497 0.776 ? 0.4396 12.19 ? 1.330 0.574 ? 1.673 ? 2.027 1.932
 0.907 0.955 0.291 1.489 ? ? 1.009 1.225 ? ? ? ? ? ?

Tupandactylus_navigans 3.04 ? ? 0.2531 ? ? ? ? 0.4747 2.071 0.766 0.1020 1.750 0.1104 ? ? ? ? ? ? ? ? ? ?
 ?

Tupandactylus_imperator 3.52 ? ? 0.1838 ? ? ? ? 0.6803 2.680 0.772 0.0257 ? ? ? ? 0.5100 12.86 2.92 0.5100
 ?

Vectidraco_daisymorrisae ? 1.750 5 ? ? ? ? ? ?
 ?

Europejara_olcadesorum ? ? ? ? ? ? ? ? ? ? ? ? ? ? ? ? 0.2505 11.59 1.96 0.2770 ? ?
 ?

Tapejara_wellnhoferi 2.46 14.96 0.770 0.2240 ? ? ? ? 0.4770 1.913 0.894 0.1300
 1.120 0.0415 ? ? 0.4387 7.04 1.18 0.3967 ? 2.722 2.48 0.928 ? 0.570 1.204 1.226 0.4700 5.93 ? 1.406 0.790
 0.4906 1.316 0.8068 1.365 1.966 0.835 0.646 0.435 ? 2.130 2.495 1.154 1.260 0.486 0.2908 ? ? ? ?

Microtuban_altivolans ? 1.282 0.3672 6.75 ? 1.363 0.700 ?
 1.807 0.8272 1.409 2.000 0.848 0.470 0.026 ? ? ? ? ? ? ? ? ? ? ? ? ? ?

Noriopterus_complicidens ? ? ? ? ? ? ? ? ? ? ? ? ? ? 0.028 ? ? ? ? ? 3.185 3.66 1.887 7 0.607 2.571 ? ? 9.59 ?
 1.368 0.902 ? 1.868 0.4174 1.771 2.289 0.713 ? ? 1.567 2.425 1.097
 1.145 1.839 0.220 0.2000 0.750 0.3808 0.3720 0.389

Noriopterus_parvus 3.66 ? 0.852 0.4682 ? ? ? ? 0.3394 2.002 1.089 0.0874 ?
 0.2628 0.4819 0.052 0.5363 18.84 10.33 ? 0.3000 1.481 2.10 1.630 ? ? ? ? ? 6.35 ? 1.412
 0.823 0.5456 1.917 0.6312 1.773 2.044 0.857 0.666 0.500 ? 1.666 ? 1.262 1.516 0.303 ? ? ? ? ?

Domeykodactylus_ceciliae ? ? ? ? ? ? ? ? ? ? ? ? ? ? ? ? 0.064 ? ? 8.38 ? ? ? ? ? ? ? ? ? ?
 ?

Dsungaripterus_weii 4.24 32.59 0.787 0.3941 ? ? ? ? 0.3218 2.072 1.180 0.0980
 1.312 0.3903 0.3685 0.044 0.4175 12.66 6.75 ? 0.6253 1.324 3.97 1.105 7 0.545 2.484 1.429 ? 8.97 ? 1.606
 0.814 ? 1.850 0.7534 1.777 2.398 0.770 0.798 0.582 ? 1.322 ? 1.440 1.571 ? 0.1600 ? ? ? ?

Tupuxuara_leonardii 6.25 43.73 0.722 0.2439 ? ? ? ? 0.4129 2.752 0.603 0.0316
 2.109 0.3496 ? ? 0.6211 18.49 14.03 ? ? 1.802 3.76 1.057 ? ? ? 1.187 ? 9.07 ? 1.258 0.694

0.5221 1.582 0.7732 1.678 2.185 0.611 0.410 ? ? ? ? 1.271 1.339 0.348 0.2232 ? 0.3765
0.1664 0.129

Tupuxuara_longicristatus 3.16 ?
? ?

Thalassodromeus_sethi 2.96 ? 0.927 0.4360 ? ? ? ? 0.6088 2.200 0.440 0.0480 ? ?
? ? 0.4776 12.12 6.50 ?

Lacusovagus_magnificens 8.51 ?
? ?

Xericeps_curvirostris ? ? ? ? ? ? ? ? ? ? ? ? ? ? ? ? 7.69 ? ? ? ? ? ? ? ? ? ? ? ?
? ?

Alanqa_saharica 10.42 ?
? ?

Argentinadraco_barrealensis ? ? ? ? ? ? ? ? ? ? ? ? ? ? ? ? 4.39 ? ? ? ? ? ? ? ? ? ?
? ?

Aerotitan_sudamericanus 7.70 ?
? ?

Eoazhdarcho_liaoxiensis ? ? ? ? ? ? ? ? ? ? ? ? ? ? 0.4444 27.81 ? ? ? 3.500 4.38
1.143 ? ? ? 1.136 0.5505 11.25 ? 1.356 0.364 0.4473 1.500 0.5333 1.641 1.978 0.781 0.522
0.281 ? ? ? 1.044 1.702 ? ? ? ? ? ?

Shenzhoupterus_chaoyangensis 2.64 ? 0.603 0.5000 ? ? ? ? 0.6027 2.109 0.429 ? ? ? ?
? 0.5000 12.97 5.79 ? ? 3.444 ? ? ? ? 1.000 ? ? ? 1.591 ? ? 2.121 ? 1.634 2.227 0.680 0.463 0.245 ? ? ? 1.545
1.363 ? 0.2806 ? ? ? ?

Jidapterus_edentus 3.12 24.39 0.895 0.5182 ? ? ? ? 0.4312 1.806 ? ? ? ? ? ?
0.5684 19.68 9.51 ? ? 2.605 4.03 1.216 ? 0.325 0.929 1.138 ? 8.85 ? 1.429 0.687 0.6166 1.910 0.5410 1.762
2.133 0.707 0.433 0.216 ? 2.380 ? 1.262 1.493 0.427 0.2416 0.961 0.3818 0.1647 0.141

Chaoyangopterus_zhangii 4.09 ? ? ? ? ? ? ? ? ? ? ? ? ? ? 0.4641 26.36 6.33 ? ? 3.733 5.64 1.099 ? ? ? 1.133
0.3052 10.89 ? 1.368 0.791 ? 1.965 0.5704 1.459 2.171 0.658
0.390 0.240 ? 1.695 1.385 1.440 1.559 0.399 0.2420 ? 0.2353 ? ?

Radiodactylus_langstoni ?
? ?

Montanazhdarcho_minor ? ? ? ? ? ? ? ? ? ? ? ? ? ? ? ? 5.33 ? ? 4.841 ? ? ? ? ? ?
0.5791 ? ? 1.652 0.719 ? 1.452 0.5816 2.375 ? ? ? ? ? ? ? ? ? ? ? ? ? ?

Azhdarcho_lanicollis 6.21 ? ? ? ? ? ? ? ? ? ? ? ? ? ? ? ? 6.83 ? ? 5.248 6.78 1.130
? ?

Albadraco_tharmisensis 5.68 ? ? ? ? ? ? ? ? ? ? ? ? ? ? ? ? 3.73 ? ? 4.828 ? ? ? ?
? ?

Mistralazhdarcho_maggii 11.43 ?
? 1.521 0.606 0.5536 ? 0.4334 1.238 ? ? ? ? ? ? ? ? ? ? ? ? ? ? ? ?

Leptostomia_begaensis 22.90 ? ? ? ? ? ? ? ? ? ? ? ? ? ? ? ? ? 28.64 ? ? ? ? ? ? ? ?

????????????????????

Apatorhamphus_gyrostega 4.67 ??????????????????????9.51 ??????????
????????????????????????????????

Aralazhdarcho_bostobensis ??????????????????????????????????????
????????????????????????????????

Phosphatodraco_mauritanicus ?????????????????????????????6.250 ???????
????????????????????????????????

Eurazhdarcho_langendorffensis ?????????????????????????????6.316 ???????
?????????????1.267 ?????????????????????

Zhejiangopterus_linhaiensis 5.40 ? 0.877 0.4440 ? ? ? 0.3814 2.686 0.993 0.0590 ? ?
? ? 0.5649 20.94 8.78 ? ? 9.124 11.62 1.407 7 ? 0.793 1.215 ? 12.02 ? 1.525 0.778 0.6255
2.074 0.9480 1.411 1.941 0.781 ? ? ? ? 1.434 1.582 0.156 0.2279 1.208 0.3341 0.1619 0.111

Cryodrakon_boreas ?????????????????????????????7.821 ??????????
? ? ? 2.480 ? 1.527 ? ? ? ? ? ? ? ? 0.2154 ? ? ? ?

Wellnhopterus_brevirostris 2.59 ?????????? 1.376 ?????????? 6.39 ? ? 8.457 ? ?
????????????????????????????????

Hatzegopteryx_thambema ?????????????????????????????18.05 ? ? 2.609 ? ? ? ?
????????????????????????????????

Arambourgiania_philadelphiae ?????????????????????????????8.781 ??????????
????????????????????????????????

Quetzalcoatlus_lawsoni 7.05 39.61 0.947 0.5914 ? ? ? ? 0.3123 3.319 1.015 ? 2.012
? ? ? 0.5846 30.31 19.28 ? ? 9.923 16.91 1.056 ? ? ? 1.112 0.5752 8.49 ? 1.521 0.635 0.5835 2.041 0.5397
1.736 2.474 0.519 0.303 0.067 1.339 2.184 2.441 1.619 1.460 0.222 0.1480 ? ? ? ?

Quetzalcoatlus_northropi ?????????????????????????????9.508 ??????????
? 1.362 0.812 ? ? 0.4995 3.596 ? ? ? ? ? ? ? ? ? ? ? ? ? ?

Dearc_sgiathanach ???
?????

Tacuadactylus_luciae ???
?????

Lusognathus_almadrava ???
?????

Brunn ???

&[num]

Euparkeria_capensis 00-100-000000010000000-000000000-----
00000000100--0000-00000-000000000000000000--000000100000-0000000000000-00100--
00100010000000001000110000000000-00-0---
00000??000—0000000000000010

Ornithosuchus_longidens 00-1?0-00000001?000000?2001001?0-----

00000000?0--1010-00000-0000000000??0??0??0?0?00100000-000000?????00100--
0010000000000000100011000?000000-000[01]00?000000000010100000000001000?00-?000?0??000--
0000000000001?0?

Herrerasaurus_ischigualastensis 00-1?0-00000010000100-000000000-----
00002000000--1000-00000-0000000000000000??0?0?00100000-00000000?????00200--
0010000000000000100011000000000000?000010000000?????????000010001040000-0----00110000000--
0000001000000030

Scleromochlus_taylori 10-?00-000010?1??01000?00?0?0100-----
010000000?0--1??0-0?20?-1?0??000?0000?????00?0?0?100000-00?00000?????00120--
0010??0000?????1??1??00?????100000?000000000000?????????0?01??01000?????--
--01?????000 00000001?00?004-

Preondactylus_buffarinii 10-1?0-00001??10101000-?0??0100-----
01001001000--?0?0??100-100000?????????????????0100000-0?000000?????00110--
?00101?0020100001011110000?????00?00??0??000?0?01?????????11?????01000?????00100100?0000
0000000001?00?0020

Austriadactylus_cristatus 10-1?0-?00010?101?1000-
00?0001?1010200001001001000--1000 00100-?000000?0??10?????0?????200000-
000?0000?????00120--
0001111002010000101111000?????000000000??000000?01?????001?????11?????01000?????01001??0?0
0????000?01???????

Peteinosaurus_zambellii ??????-
??
??00??000-0??0000?????0????-
?000101000201?0002022?000??
?????0010000000?00000?0?????????

Caviramus_schesaplanensis ??????-
??
?????010000111?110000?????00020--
000??100010?0?[01]1032??010??
??

Raeticodactylus_filisurenensis 10-1?0-10101??10101100-
00?010201020100001002000000--?000-00200-
1000000000??0?0??01??012000111?110100?????00021--
0011011000010001103211010?01000000??00?????????0?????????00?11????1010000?????0?100?0?0??
?????????1000?0??0

Eudimorphodon_cromptonellus ??????-?00??0?0??100?-
?????????????????010?200?00?????0?0??0-
??0??0?0?????????????????010000?000?00?????????0--
?00101000?01100[01]1042?10?????0??0??0??0??0?00?00?0101?0001?0?11?001010?????0??1?010??0?
?????????????10000?20

Eudimorphodon_rosenfeldi 10-1?0-00001??10101000-001110200-----
01003000000--1?00-00210-100000?00000100?????????0010000100?000001?????00110--
0001010002011001104211010?010000000?0??0000?00010101001?01100?101000000?00010010000
000?00?00?01??0?020

Eudimorphodon_ranzii 10-100-000010?10101000-001110200-----
01003000000--1000-00210-1000000000?????00--01??002000010000000010000-00110--

0001011002011001104211010??010??0000?00?1??0?00002010110100011000101000??0??1010010???
??00??000?01?0?00???

Parapsicephalus_purdoni 10-100-?01010000111000-203000210-----
01112000000--100??00100-1001000000001??00--
01000????????????????????????????????0?????0?1????[01]1??????0?????????????????
??

Dimorphodon_macronyx 10-1?0-00101??00111000-203000210-----
01111001000--110??00100-100100000??10?????01??0120000-0?0000000000-
2013200100124100211000011--
110000?011??0000?0010020?00012????00?00011100102000??0002010010000100132000010100000020

Dimorphodon_koi
????????????????????????[01]?????1????????????????????0--
??10????????????????001001????????????1?000-0?001000?00-
20?????1001????0201??00?????0?0?01110000????????????????????????????????
??

Dimorphodon_hanseni ???01?????01000-
?1????21??????0111100000102????10?????
10?10??00??????0??????0??0010000101010000-20242001001?4300201000011--
?10?0??
??????????????

Dimorphodon_jenkinsi
?????????1??????1??0??[02]??????????????0??????????????0????100?10010????00
10??0??2?100????0001????????????
??

Dimorphodon_weintraubi
????????????????????????[01]?????1????????????????????????????100?1????????????00
1000??0001110000
0?????????00?12????00?00?10?0102?00?00??2010010000?????????????????020

Herbstosaurus_pigmaeus
??
??
??10?0??130000??101100??

Campylognathoides_zitteli 10-1?0-000010?10111000-00??0210-----
02102000000--1000-00?00-0000100?????0?0??????01220000-0000001-000??10130--
100100000211100011--
10010??0?000000?0000020?00002?110001?01111??1010??001??2010010?011011310100101011?1021

Campylognathoides_liasicus 10-100-000010010111000-002110210-----
02102000000--1000-00200-00001000000010000--01??01220000-0000001-0000-10130--
100100000211100011--
100100?0100000000000000200000021110001001111??101000001?020100100011011310?00?010110102
1

Scaphognathus_crassirostris 10-1?0-000010210111100-002110210-----
01102000000--1000-00200-1100000000??10?????01?001120000-1000001-????00131--
102012010220100011--
10000000?00000000001002000000211??002000110??1030000100020110101002?11101[01]0000101101
122

Orientognathus_chaoyangensis 10-1?0-0000102??1?1100-?[02]????[12]?0-----
 011?2?????????????????0-11000?????????????????01120000-1000001-?????00131--
 ?02012010220100111--
 10010??010??0000?????010000002????00????01????0?0????0??5011?10??0201????110000101102121

Dorygnathus_banthenis 10-100-00001011111101-002110210-----
 00102000000--1000-00200-11000000000010000--01001112000101000001-0200-
 0013201102022010221100131--
 100100?0100000000000100200000021101003001111001030000100030110101002011[13]011001010110
 1122

Klobiodon_rochei
 ???
 ?????????????112000101000001-?????0112201102025010221?00131--
 ??010??
 ?????????????

Dolicorhamphus_depressirostris
 ???
 ?????????????10202010100000?????0-01??20??0202501022??02131--
 ??010??
 ?????????????

Dolicorhamphus_bucklandi
 ???
 ?????????????102000101000001-
 ??????01122011020????022????13?????010????????????????????????????????
 ???

Fenghuangopterus_lii 20-1?0-00001011??1100-?[02]?????0-----
 0?1?2?????????????????00200-11?000??0001?????0?011110000-1000001-?????0013?--
 102012010220?11111--
 100?0??010??0000?0?1?020000002?1010?200001???103000?????20110100?02011301???1?1?1101???

Rhamphorhynchus_muensteri 20-100-000010111110101-002110210-----
 00102000000--0000-00220-11000001-00010000--010011020000-1000001-0000-01131--
 102012210220110221--
 0001000011000000000010020000002110100[12]000111001060000100020110101012011[12]0110010101
 10112[12]

Nesodactylus_hesperius
 ??????????????????????????????????0????????????????????????????????????1?0????????????
 ??0?100000??
 ??????020?00?02?11000200?111??1060000100??011010?01??00?100010?1???????

Cacibupteryx_caribensis ???10???01010111110101-002000?10-----
 00102000000--0000-00100-?1000000000010000--
 0100?1?????????????????????????????020?????0?2????[01]2?????00?0????????????
 ??????????????????????????????????0????????????????????????????????????

Qinglongopterus_guoi 21?1?0-?0?0?01?1??1101-
 002?1?2?????????????0??20000?????????0?200-
 ??00?00????001?????0????112000??100?0?1-?????0?13?--102012?112201111?1--
 0001???010??0000?00?1?020000002????00????111??103000?00??3?1101?100?011101?????1?1101121

Harpactognathus_gentryii 11010101012101111?110?-
 ?????0?1001?001001?200?0?????????????-?????????????00--
 01???1?????????????????????????????020????1220???[01]2???00??0?????????????
 ???

Angustinarapterus_longicephalus 1111?10101010111111101-
 0021102?1001?00101102000000--1?0?00210-110000001?????????01???1120010-
 1001011-???0-00131--102025211120111121--
 000?0??
 ?????????????

Sericipterus_wucaiwanensis 1111?10101010111111101-
 ?????0?11001?001011?20000?0--???0-0?200-11?00??01?0??00?0--
 ???11?????1001001-0000-00?31?-102025211220111121--
 00??0?001000000????0?????00?02??????000111?010300100?????????02201????????????????

Sordes_pilosus 10-100-000010110111000-002110210 01102001000--
 1000-00210-11000101-00010000--01?001100000-1000001-0001010130--
 102033000220100011--
 100000?011000000000010020000002?110004001111??100000000?[45]011010100201110110000101101
 122

Pterorhynchus_wellnhoferi 10-100-00001011-11--100004110-?110110000----
 001000--?00-0022001100010?00010?????????1100000-1000001-?????10100--
 102033000220101011--
 100001?0?0?000????0100200?0?????????????110??100000????0011010??0201??01000101???????

Kunpengopterus_sinensis 10-1?0-000010?1-11--100004110-11101200?0----
 001000--1000-012100110001???1?????????????01100000-1?00001-?????10100--
 102033000220101031--
 200001???01001001000??020?00?02?110002?0??10??102000?????401?0??0?0?????????????11?1121

Wukongopterus_lii 10-1?0-00001011-1?--1?0?????0-?????????0----
 ??????????????2?01?????????????????01???1100000-1000001-?????10100--
 102033000220101031--
 20000??0?0100?00100010020000002????002??0110??109?????0??4?110100?????01?00001?11?1122

Darwinopterus_zhengi
 ???
 ??0?00?
 ?0???020000002????002?0?01???109000?????401101?0?????31?100001?11?2121

Darwinopterus_linglongtaensis 10-1?0-00001??1-11--100004110-1111220000----
 001000--1000-002100110011???10??0?????????01100000-1?00001-?????10100--
 102033000220101031--
 20000??01?100100??0011020?00?021110002?01111??109?000????40110100??20113?1000?01?1102122

Darwinopterus_robustodens 10-1?0-00001??1-11--100004110-1111220000----
 0010?0--1000-00210011001101-1???0?????????01100000-1?00001-?????10100--
 102033000220101031--
 200001?010100?001?001?020000002?11000200011???119000?1???4011010100201131?000001?1102122

Archaeoistiodactylus_linglongtaensis ???????00010?1-??--1?0?0?1?0-?????????0-?-
 ??????????????0?????????????????????0??0?110?0??10?00??1?00-
 ???????02033000?20101031--
 ???0??0?01?010?????????????????0??1?0??11??119000????04?11?????201??1100

0101?11?2?22

Darwinopterus_modularis 10-100-00001011-11--100004110-1111220000----
001000--1000-00210011001101-1??10?010001??1110000-1000001-????10100--
102033000220101031--
200001?0??100100?00?1?020000002?1??00200?110??19000??04?110?0?02011311000?01?1102122

Changchengopterus_pani
??
??01000001
?0??010?00?02??00?00?111??00000??401101??00201?01?0??1?11?2121

Dendrorhynchoides_curvidentatus 10-1-0-0001?020-0????0????1??0-----
0????????????????01????????001??10?10?100100-002000?0?00-1??0--
?0103300022?100011--
??00????100??1?0??100000002??004?001110?100000?0??501101?1?01????00?00??1??0?021

Luopterus_mutoudengensis 10-?-0-0001?02?-0--10000??1????????0-?-
??????1?????0??00????01??1?1?11?100-
?02000????????0?03300?20?00[01]11--
?00??0??0001????1?100000?02?????0??11?10000000?05?1101?1?3201??00100001?1?01020

Batrachognathus_volans 10-1-0-0001?020-0?--100000111-10-----0----0---?0--
1?00-000010?00110?????0?----10?10110010?-0020001-0000-1?220--
101033000220100011--
10000?????0001?00?????000020100004000110??100000?????110101?????1?0100?01?1??10??

Jeholopterus_ningchengensis 10-1-0-0001?020-0?--100000111-10-----0----0---?0--
1000-000010?001?0?????0?----10?1?1100100-?02000????00-
1?22????01033000220100011--
10000?????100??1100??010000002????00?001110?1040000??5011010100??11100100?01?11?1020

Anurognathus_ammoni 10?1-0-00011020-0?--1000001?1-10-----0----0---00--
1000-000010?00110?????00----10?101100100-0020001-0000-1?220--
101033000220100011--
100001?????0?1?0001010000002??????00111??104000?0??50110101??101??00100?0101101020

Kryptodrakon_progenitor
??
??
????0??????2?????00??1????0????000?11?000?00????????????????????

Painten_pterodactyloid 10-100-000010?1-01--100004110-10-----0----001000--
1100-00310011000001-1??0?????0??1100000-1000001-000??00100--
102033000220100211--
100000?000100001100010110000102????00?00111??10500000?0401110?0?03?113110110101101120

Cuspicephalus_scarfi 20-100-00001011-11--100004110-1110320000----
0?11?0--??0-20320011000101-11??0010--
0?0?01????????????????????020??0120??01??100?0????????????????
??

Germanodactylus_rhamphastinus 20-100-00001011-11--100004110-1110320000----
001100--1100-20320011000101-1??0?1??????1110000-?000001-0?0?-10130--
102033000120100011--
110000?0??100001??0?10??0000?20?00002?0?11?1??1??0?00?4??1?0010?301130?000?01011011??

Germanodactylus_cristatus 20-100-00001011-11--100004110-1110320000----
 001100--1100-20320011000101-1??0?1??????1110000-1000001-0?0?10130--
 102033000120100011--
 010100?0??0001100010??0000002??0020001110?1050??000??4??110010?301130100010101101133

Pterodactylus_antiquus 10-100-00001011-11--100004110-10-----0 001100--
 1100-11320011000101-2??0?10--0??1100000-1000001-0?00-00130--
 102033000120100011--
 100000?000100001100010100000002010100400011100105000000004011100100301130100110101101133
 3

Normannognathus_wellnhoferi 10-000-000?10?2?1????????????1122?000?-
 ?????????????????????????????????????10 ?????1?00200-
 100000??100?????????02012010110100?11--
 11000??
 ?????????????

Aurorazhdarcho_primordius
 ???
 ???
 ?0?1?10000002?110??200?111??1080000????201110?000?0113??????1??10?133

Cynorhamphus_suevicus 10-000-00021012-11--100002110-1[01]12220000----
 001100--1101111320011000101-211?0?10--010101000200-1001001-??0-0111110-012010110100011--
 1??000000000001?0??1??00000?02?110002000111??108000000??4?11100000301130100010101101133

Pterodactylus_micronyx 10-100-00000112-11--100004110-10-----0---001200--
 1100-11320011000101-21100?10--010001100000-1100001-0000-00020--
 102012000120101111--
 100000?00110010110001010000000211??002000111??105000000??4011100000201130110110101101133
 3

Liaodactylus_primus 10-1?0-00000112-11--110004110-?1103?0000?????0-
 -1??0-11320011000101-21100?1??01?001120000-1100001-??0-00020--
 101012011110101211--
 100000??
 ?????????????

Ctenochasma_elegans 10-100-00000112-11--100004110-1[01]103?0000----
 001200--1100-11320011000101-2??00?10--0?0??1100000-1100001-1000-00020--
 101012011110101211--
 10000?00?10010010001??00000002??00002000111??105000000??4??1100?0?3011301001?0101101133

Pterodaustro_guinazui 10-000-00000112-11--100004110-10-----0 001200--
 1100-11310?11000001-2??00?10--0??1100000-1100001-100??20020--
 101012010200201001--
 00000?000110010?10??110000000021100002000?110?1050??000004??1000003??13010011010111?133

Beipiaopterus_chenianus
 ???
 ??0??10010?1
 00?1?100?00022??00?00?11??1050??0??4??10000????????????1??133

Gegepterus_changi ??0????0000112-11--10000?110-11??300000----
 001200--1100-1?310011000001-2??0?10--0??10????11??001-??0??00020--

101012010?1?101201--
?0??00?001100100??????????22????002????????????????????[12]???0?003????0?
?????1???0????

Kepodactylus_inspertus
??
??
????????????????????????0101130101?
????????????????????001111?01050000?0?????100?0?????0?????1???????

Elanodactylus_prolatus
??
??
000?????000002?101001?01111?0105000000?040111000?0301130100110?011?1133

Moganopterus_zhuiana 10-100-00001??2-11--101004110-11101000?0----
001100--0?01311320??10?0?0??2?100?????????????120000-1?00001-?????00020--
102012010120111111--
10000?????23?1??
?????????????

Feilongus_youngi 10-100-000010?2-11--101?04110-1110100000----001000--
01010113?0011000101-2?100?10--0??01120000-1000001-?????00020--
102012010120111111--
10000?0?230101??
?????????????

Ardeadactylus_longicollum 10-101000001012-11--100004110-10-----0 001?00-
-1100-11320011000100121?00?10--010101100010-10?0001-1001010020--
102015010120101131--
100000000123010110001??00000002??0100110?0110?105000000?4?11100?0?3011301001101011011??

Huanhepterus_quingyangensis 10-
1?100000101????????????????1103?000????????????????????????????????????
????????1100010-100000?????????0--?02012010120101131--
10000?0?230?0110001?0?0?0?2?????1?0?1?1?1050?????????1?1????????130100
1?01?1??1???

Plataleorhynchus_streptophorodon 10-10100002?01??1?--1???????-??????????-
????????????????????????????1-??????10--
0?????1????????????????????????020????1120???13???10000????????????
??

Gnathosaurus_macrurus
??????10?0??1??
????????????100210-10??001-1000-
10?2????020????1120???23????00??001230101????????????????????
??

Gnathosaurus_subulatus 10-10110002101?-11--100004110-1110310000----
001000--1000-11320011000101-21100??0--0101?1100210-100?001-????1???0--
102012011120?01231--
100?0??
?????????????

Hapterus_gracilis 10-100-00001011-1?--1?000??10-?0-----0 010000--
?000-0?230?1?????01-?????0?0????????1120000-10010?1-?????10100--

?02033000220100011--
10000??0??0001?00?????1000020101??2000011??07000?????4?11?00100????????? ?????????14-

Ornithostoma_sedgwicki ??-10???0101002?????????????0-----
???00--
?????1?????????????????????????????????1-----
0???
?????????

Volgadraco_bogolubovi ??????-
???
?????1110000-1001????00?-??1--?1-----?--
??1001010101?11???
?1??????

Tethyraco_regalis
???
???
????????????????????????00110307110???

Pteranodon_sternbergi 20-0?0-10101002--0--110104110-10-----0---
0100?1200101200230111010101-1??00??????0?1110000-1001011-????00101?-?1-----
??0????0?0?????11??1?????20?10101?0?0?01?3?7????0?1?20??100??0?????????????1
??02???

Pteranodon_longiceps 20-000-10101002--0--110104110-10-----0---
010?01200101200240111010101-11100100--010111110000-1001011-0001100101--01-----
01100101010101111110111010200101011000001030711000011403110011010112011011011110214-

Alamodactylus_byrdi
???
???
????????????????????????1000010?306110?????????00?????????????????????????????????

Cretornis_hlavaci
???
???
????????????????????????1000010031?110?0??3?00?0?????????????????????????????????

Simurghia_robusta
???
???
????????????????????????00?????60?0???

Alcione_elainus
???
???
?????????110?02?01110?000000031601000??????100?10?????????????111102???

Muzquizopteryx_coahuilensis ?????????1?1??-?-110002110-10-----0---1--00-
-1101100220?11000101-1??0?????????1?????????????11-?????0103??11-----
01????02??01?111?10?11000?0?1?1?0?001??16010?????103?1?????????120?101??1?11?214?

Nyctosaurus_grandis
???
??11-

Boreopterus_cuiae 10-1?0-10101??1-10--110102110-10-----0----1----0--
 1110-002[12]0?11000101-1????????????1101000-1?01011-?????10120--
 100114?10220111211--
 10001??0??010101?????10????0?????????10?????????????????21????1?0?????????
 ???1?11?214-

Hamipterus_tianshanensis10-101000101002-10--100102110-1112330000----1----
 0--1110000220011001001-1110010100010011101010-1000001-1011000100--
 102124110120101131--
 100011?001010101?1??11??1110211?0??210100??207110?10?1402?100??101??1101101?1102???

Brasileodactylus_aripensis
 ?????0????0??
 ??????????1000010-1000001?101?????1--?02124??0121?01131--
 ?001??
 ????????????

Barbosania_gracilirostris 10-101000101001-1?--1?0?0?110-10-----0 0?11?0--
 1?10-0023?0?0?01?????001010?0????1000010-1?00001-1?1?00101--
 ?02124110121101131--
 10001?????????????1?1?10?1??02????10?0?00??207110????402?101??0211?0???
 ??1?1102???

Cearadactylus_atrox 10-101000101001-10--11010?110-?0-----0----
 01100?????????02300110101?1-?????010001111000010-1000001-1010-00101--
 102124?10121101131--
 10001??
 ????????????

Guidraco_venator 10-1?1000101??1-10--110102110-10-----0----
 ?????121111200230111010001-1??0????0?0?110??010-1?00001-?????10100--
 102124110121101131--
 10001??001??0101??
 ????????????

Ludodactylus_colorhinus 10-
 11100?01??
 100?????1?????????0?????????????????02?????00?1???13???1?0????????????
 ???

Ludodactylus_sibbicki 10-101000101??1-10--110102110-10-----0----
 01101111111200230111010001-11100?0100010?11000010-1?00001-100??10100--
 102124110021101131--
 10001??
 ????????????

Aetodactylus_halli ??-???000?2??0?????????????????0-----
 ??100????11000210-1120001-1000-1?100--
 10112?1?0120101131--
 ?001??
 ????????????

Camposipterus_nasutus 10-101000?211?2?????????????????0-----
 ??????????????????????????????????????100????1?????????0????????????
 ?02?????01?0???13???100?1??

101?????1????????????????????????????????02?2?001?????03???1?????????????????
 ???

Siroccopteryx_moroccensis 00-

101000?0?00????????????????????1004?01?????????????????????????????????????
 101?????1????????????????????????????????02?2?001???01131--
 2?0??
 ?????????????

Coloborhynchus_capito 00-

10120??0????????????????????1004?011?????????????????????????????????????
 ?????????1?????????0????????????????????0?2???01?1???131--
 2??
 ?????????????

Coloborhynchus_wadleighi 00-

11120??0100????????????????????1004?011?????????????????????????????????
 101?????1????????????????????????????????02?2???01?1???131--
 2?0??
 ?????????????

Coloborhynchus_clavirostris 00-

11120??0????????????????????1004?011?????????????????????????????????
 101?????1????????????????????????????????02?2???01?1???13???2?0?????????????
 ???

Eopteranodon_lii 20-2?0-11001000--?--100?????0-?110410110---

?????????????????001?011?1-1?????--???1?210001010??1?1-01?????1????11-----
 0?0?000101?????????????022????00?0?01???10801??1???4?????0?0201130111111?1111???

Huaxiapterus_jii 20-2?0-1?010?0--?--100??4110-?110410?10---

00?10?????????0?3?0?11?011?1-????????-0?????12100010100??1-0?????201220111-----
 0?0?0?0?01?0?0?1?????22??1000210?01???108011?????412110?110???13??????1?1111???

Sinopterus_dongi 20-2?0-110010?0--1--10002?1?0-1110410110---

0011011201?130?33?011?011?1-1???1?????????121000101001?11-?????201220111-----
 0?0?000101?0?0?110?1?0?22?11000210?01???108011111004131100110?0?13?111111?1?14-

Sinopterus_benxiensis 20-2?0-1?0010?0--?--100?????10-1112610110 0-

10?1120?013?0330011001101-1?????????????121000101001111-010??2012201?1-----
 0??001??0101?0?0????????????????????01????080?????0??3110?110?????????????
 ??????4-

Sinopterus_corollatus 20-2?0-110010?0--?--1?0?2???0-1112610110---

?????????0??10?????01?????????????1?????????121000101001?11-?????20?220111-----
 0??001??0101?0?0?????00?22??1000????01????0801?111??4?3110?110???13??11?111?1??14-

Bakonydraco_galaczi 20-200-

1?0310????????????????????11010011?????????????????????????????????????0--
 ???1121000111001111-01210001020111-----??--
 0??
 ????????

Keresdrakon_vilsoni 20-200-1?0310?0--?--1?0?????0-?110100110---

?????????????????0?????????????????00--?????121030[01]-100?01??002??10??201?1-----
 0?100100010?????????????00?121111001100011??108111?11?????????1?001??0111001111?1???

Caiuajara_dobruskii 20-210-11001000--?--100124110-?111011110----
 ?????112??13?0?[34]001?001101-1?101?00--0???0122000111001011-010??001021001-----
 0?10?100010??0?1?100100122?1?00?21?101??108011??1004??100?102??12??111?1111111???

Tupandactylus_navigans 20-210-110010?0--1--100124110-1111011100----
 00110??010?000230011001101-1??0??0??1????????????????????????????????1-----
 0??
 ????????

Tupandactylus_imperator 20-2?0-1?0010?0--?--1?0123110-1111011100----1----
 1120?01300230011001101-1??1?0??????1220001010????1-010??001?210?1-----
 0??
 ????????

Vectidraco_daisymorrisae
 ???
 ???
 ??10??3?1??011111???

Europejara_olcadesorum ??????-?0????????--1????411?-????????0----
 ???????1??002?001?0??0??????1??010?01210001110?1111-01???010210?1-----
 0??
 ????????

Tapejara_wellnhoferi 20-210-11001000--1--100124110-1111010110----
 001101120101300230011001101-11101110--01010121000111001111-01010001021001-----
 0?10010001010100??01001221110001101011001080111110040??100010301??00111?111111114-

Microtuban_altivolans
 ???
 ???
 1??????100?22??????000110??08011??1?4?3110??0????????????112?1???

Noripterus_complicidens ??????-
 ?????0??
 ???1??000-100?00??100110??1--?020510?0220??1?31--
 ???0?1101000101??1?11100??12??00?0010111010801111100?11100?0210113?11111001211?4-

Noripterus_parvus 210100-10001001-11--100012010-1111330101----1----
 1120001220220?11101101-11101?0100010?11110000-1001001-1001100101--
 102051000220101031--
 01010110010001010111????00?12????00?000011001080111110041?1100?02??1??????001211???

Domeykodactylus_ceciliae
 ?????????????????????????0?1?2??10??
 ?????????11?0??10??001-??10?0??1?-
 ?02051??0220??04????010??
 ???

Dsungaripterus_weii 210000-10001001-11--100012110-1112330101----1----
 1120001220220011101101-1110110100010111010000-1001001-1001000101--
 102051000220101041--
 0201011001000101011111001001121110001??0?0??10801111?0?1?1001123?1????111?001211???

Tupuxuara_leonardii 20-100-10001001--1--100124110-1100530120----1----

1100001220230011001101-111011111011111110000-1001011-1001000101--11-----
 011001000101??11?????001121?10001100??11?108011111004??100110?????????1112111??

Tupuxuara_longicristatus ???00-100010??-?-100?????0-11005?012?---
 ??????????????????0??0??1-?????11110????????????????????????????????1-----
 0?????????0?????????????????????0?????????????????????31?0??1?????????????
 ????????

Thalassodromeus_sethi 20-100-10101001--1--100124110-1100530120---
 010001100001220230011001101-1?1?110111011?111??000-100?011-1211000101--11-----
 0??
 ????????

Lacusovagus_magnificens 20-2?0-1100100?--?-1???????-?110100?10---
 ??????????????????1?????????????00--0????????????????????????????????1-----
 ?0??
 ????????

Xericeps_curvirostris
 ???
 ?????????????10??300-110101??1011?????0--?1?--
 0??
 ????????

Alaqa_saharica 20-100-
 10?011?1??111?
 ?????1??????10??01??1?1??????????1?-
 ?0??
 ????????

Argentinadraco_barrealensis
 ??????????????0??
 ???????????11??300-11?101??101100??200?1-----?--
 0??
 ????????

Aerotitan_sudamericanus 20-100-
 10?311?2??0--
 ?????0??????????????????????????????????????1?-
 ?1??
 ????????

Eoazhdarcho_liaoxiensis ??????-
 ??????0???--
 ??????110000-10?1001-00010??10?-?11-----
 ???000130?11?00?????000?22?????00?0?01?0?080?111?4?3110??10?????????????
 ??1?????

Shenzhoupterus_chaoyangensis 20-1?0-??010?2--1--10012?111-10-----0----1----
 1101?01301230?1100020??1??1?????????1110000-1?0??1-?????00121--?1-----
 0????0130?11?10?????00?22?????????01???1080?????0?31?0?1?0?????????????
 ?1??114-

Jidapterus_edentus 20-100-10001002--1--100?????1-?0-----0----
 ??????????????????0011?001?1-?1?????00--01?11110000-1001001-?????00121--11-----
 00?00013011101001000000?22111000100001???080?1?11004021100110301?????11111111211133


```
????????????????????????????????????????????????????????????????????????????????????
????????????????
```

```
;
```

```
nstates stand;
```

```
ccode + 52 55 65.66 81 85 87 99 103 111.112 120 124 140.141 160 162 169 176.177 179 182
```

```
185.187 197 210 217 246 254 269 271 273.274;
```

```
ccode - 53.54 56.64 67.80 82.84 86 88.98 100.102 104.110 113.119 121.123 125.139 142.159
```

```
161 163.168 170.175 178 180.181 183.184 188.196 198.209 211.216 218.245 247.253 255.268
```

```
270 272;
```

```
cnames
```

```
{0 Skull,_aspect_ratio,_length_to_maximum_height_preserved_exclusive_of_crests:_continuous;
```

```
{1 Skull,_length_to_squamosal_relative_to_dorsal_vertebra_length:_continuous;
```

```
{2 Mandible,_length_relative_to_skull_length_to_squamosal:_continuous;
```

```
{3
```

```
Rostrum,_length_to_narial/nasoantorbital_fenestra_relative_to_skull_length_to_squamosal:_continuous;
```

```
{4 External_naris,_length_relative_to_skull_length_to_squamosal:_continuous;
```

```
{5 External_naris,_length_relative_to_maximum_height_in_naris:_continuous;
```

```
{6 Antorbital_fenestra,_length_relative_to_skull_length_to_squamosal:_continuous;
```

```
{7 Antorbital_fenestra,_length_relative_to_maximum_height_in_fenestra:_continuous;
```

```
{8 Nasoantorbital_fenestra,_length_relative_to_skull_length_to_squamosal:_continuous;
```

```
{9
```

```
Nasoantorbital_fenestra,_aspect_ratio,_length_to_maximum_height_in_fenestra_preserved:_continuous;
```

```
{10 Orbit,_length_relative_to_height:_continuous;
```

```
{11 Supratemporal_fenestra,_length_relative_to_skull_length_to_squamosal:_continuous;
```

```
{12 Subtemporal_fenestra,_length_relative_to_width:_continuous;
```

```
{13 Basipterygoid_processes,_angle_divided_by_100:_continuous;
```

```
{14
```

```
Rostrum,_tooth_row,_length_to_posterior_margin_relative_to_skull_length_to_squamosal:_continuous;
```

```
{15 Teeth,_maximum_number_divided_by_1000:_continuous;
```

```
{16 Mandible,_symphysis,_length_relative_to_mandible_length:_continuous;
```

```
{17 Mandible,_length_relative_to_ramus_mid-depth:_continuous;
```

```
{18
```

```
Mandible,_symphysis,_aspect_ratio,_length_to_maximum_depth_preserved_exclusive_of_crests:_continuous;
```

```
{19 Mandible,_crest,_length_relative_to_mandible_length:_continuous;
```

```
{20 Mandible,_tooth_row,_length_relative_mandible_length:_continuous;
```

```
{21 Mid-cervical_vertebra,_maximum_length_relative_to_mid-width:_continuous;
```

```
{22 Mid-cervical_vertebra,_maximum_length_relative_to_dorsal_vertebra_length:_continuous;
```

```
{23 Dorsal_vertebra,_length_relative_to_maximum_diameter:_continuous;
```

```
{24 Synsacrum,_vertebra_number:_continuous;
```

```
{25 Caudal_vertebra,_length_relative_to_dorsal_vertebra_length:_continuous;
```

```
{26 Caudal_vertebra,_length_relative_to_diameter:_continuous;
```

```
{27 Scapula,_length_relative_to_coracoid_length:_continuous;
```

```
{28 Coracoid,_deep_flange,_length_relative_to_coracoid_length:_continuous;
```

```
{29 Humerus,_length_relative_to_dorsal_vertebra_length:_continuous;
```

```
{30
```

```
Humerus,_deltopectoral_crest,_proximodistal_constriction_width_relative_to_anterior_terminus_proximodistal_width:_continuous;
```

```
{31 Ulna_or_radius,_length_relative_to_humerus_length:_continuous;
```

```
{32 Radius,_mid-width_relative_to_ulna_mid-width:_continuous;
```

```
{33 Pteroid,_length_relative_to_ulna_or_radius_length:_continuous;
```

```
{34 Metacarpal_IV,_length_relative_to_humerus_length:_continuous;
```

```
{35 Metacarpal_IV,_midpoint_dorsoventral_width_relative_to_combined_ulna_and_radius_mid-width:_continuous;
```

{36
Metacarpal_IV,_proximal_end,_dorsoventral_width_relative_to_midpoint_dorsoventral_width:_continuous
;
{37 Manus,_digit_IV,_first_phalanx,_length_relative_to_humerus_length:_continuous;
{38 Manus,_digit_IV,_second_phalanx,_length_relative_to_first_phalanx_length:_continuous;
{39 Manus,_digit_IV,_third_wing_phalanx,_length_relative_to_first_phalanx_length:_continuous;
{40
Manus,_digit_IV,_fourth_wing_phalanx,_length_relative_to_first_phalanx_length:_continuous;
{41 Prepubis,_length_relative_to_maximum_width:_continuous;
{42 Pubis,_depth_relative_to_acetabulum_anteroposterior_length:_continuous;
{43
Ilium,_preacetabular_process,_length_relative_to_postacetabular_process_length:_continuous;
{44 Femur,_length_relative_to_humerus_length:_continuous;
{45 Tibiotarsus,_length_relative_to_femur_length:_continuous;
{46 Fibula,_free_length_relative_to_tibiotarsus_length:_continuous;
{47 Metatarsal_III,_length_relative_to_tibiotarsus_length:_continuous;
{48 Pes,_digit_III,_second_phalanx,_length_relative_to_mid-width:_continuous;
{49 Pes,_digit_IV,_first_phalanx,_length_relative_to_metatarsal_III_length:_continuous;
{50
Pes,_digit_IV,_second_phalanx,_length_relative_to_pedal_digit_IV_first_phalanx_length:_continuous;
{51
Pes,_digit_IV,_third_phalanx,_length_relative_to_pedal_digit_IV_first_phalanx_length:_continuous;
{52 Rostrum,_anterior_tip,_shape:_ordered flat rounded pointed;
{53 Rostrum,_rostral_process: absent present;
{54 Rostrum,_rostral_process,_cross-section: triangular elliptical;
{55 Rostrum,_anterior_end,_orientation:_ordered upturned straight downturned;
{56 Palate,_anterior_end,_fossa: absent present;
{57 Rostrum,_anterior_end,_lateral_expansion: absent present;
{58 Jaws,_anterior_end,_lateral_expansion,_horizontal_outline: elliptical triangular quadrangular;
{59 Rostrum,_anterior_portion,_occlusal_margins,_shape: rounded ridged;
{60 Rostrum,_middle_portion,_expansion: absent present;
{61 Rostrum,_posterior_portion,_occlusal_margins,_shape: rounded ridged;
{62 Rostrum,_shape: laterally_compressed anteroposteriorly_truncated dorsoventrally_depressed
laterally_flattened;
{63 Rostrum,_taper_in_sagittal_plane: subparallel attenuated;
{64 Rostrum,_taper_in_horizontal_plane: attenuated subparallel;
{65 Skull,_lateral_margins,_curvature_in_horizontal_plane:_ordered concave
straight convex;
{66 Skull,_dorsal_margin,_curvature_in_sagittal_plane_exclusive_of_cranial_crests:_ordered convex
straight concave;
{67 External_naris,_dorsal_and_ventral_edges,_orientation: acute_angle subparallel;
{68 Nasal/nasoantorbital_fenestra,_anterior_end,_position_relative_to_premaxillary_toothrow: dorsal
posterior;
{69 Jugal,_lateral_surface,_antorbital/nasoantorbital_fossa: present absent;
{70 Antorbital_fenestra,_dorsal_and_ventral_edges,_orientation: subparallel angle;
{71 Antorbital_fenestra,_ventral_edge,_position_relative_to_external_naris_ventral_edge: level ventral;
{72 External_naris_and_antorbital_fenestra,_configuration: separate confluent_(nasoantorbital_fenestra);
{73 Antorbital/nasoantorbital_fenestra,_posterior_edge,_shape: subangular beveled;
{74 Nasoantorbital_fenestra,_dorsal_and_ventral_edges,_orientation: acute_angle
subparallel;
{75 Orbit_outline: subcircular inverted_piriform_to_ovate inverted_triangle;
{76 Orbit,_dorsal_position_in_skull:
middle_of_the_skull_with_the_ventral_margin_of_the_orbit_below_the_middle_of_the_antorbital_(or_nasoantorbital)_fenestra_and_the_dorsal_margin_of_the_orbit_above_the_dorsal_margin_of_the_antorbital_(or_nasoantorbital)_fenestra
high_in_the_skull_with_the_ventral_margin_of_the_orbit_the_same_level_or_above_the_middle_of_the_

antorbital_(or_nasoantorbital)_fenestra
 low_in_the_skull_with_the_entire_orbit_lower_than_the_dorsal_margin_of_the_antorbital_(or_nasoantorbital)_fenestra;
 {77 Infratemporal_fenestra,_outline: trapezoidal inverted_triangle upright_triangle oval elliptical;
 {78 Infratemporal_fenestra,_position_relative_to_orbit: posterior_to_orbit reaches_under_orbit;
 {79 Infratemporal_fenestra,_orientation: subvertical inclined;
 {80 Premaxilla,_premaxillary_bar,_width: wide narrow;
 {81 Premaxilla,_maxillary_process,_posterior_end,_position: _ordered contacts_nasal posterior_half_of_external_naris anterior_half_of_external_naris;
 {82 Premaxilla,_premaxillary_bar,_posterior_end,_position: between_nasals between_frontals;
 {83 Premaxilla,_crest: absent present;
 {84 Premaxilla,_crest,_anterior_end,_position_relative_to_skull_anterior_end: level posterior;
 {85 Premaxilla,_crest,_anterior_margin,_orientation: _ordered inclined_posteriorly subvertical curving_anterodorsally;
 {86 Premaxilla,_crest,_shape: tall_triangle_decreasing_in_height_posteriorly low_blade low_with_anterior_hump comb-like_with_straight_dorsal_margin semicircular tall_triangle_increasing_in_height_posteriorly rectangular;
 {87 Premaxilla,_crest,_posterior_end,_position: _ordered anterior_to_naris/nasoantorbital_fenestra_anterior_end between_naris/nasoantorbital_fenestra_anterior_end_and_orbit above_orbit above_occiput;
 {88 Premaxilla,_crest,_dorsal_spine: absent present;
 {89 Premaxilla,_crest,_thickness: thin,_single_plate thick,_two_plates_separated_by_trabeculae;
 {90 Premaxilla,_crest,_texture: striated smooth branching_grooves;
 {91 Maxilla,_posterior_end,_shape: narrow ventral_expansion;
 {92 Maxilla,_nasal_process,_shape: broad tapered parallel_sided;
 {93 Maxilla,_lateral_surface,_antorbital_fossa: present absent;
 {94 Maxilla,_nasal_contact,_position: main_body_of_nasal descending_process_of_nasal;
 {95 Maxilla,_premaxillary_process_and_posterior_ramus,_configuration: posterior_ramus_wider both_narrow premaxillary_process_wider both_wide;
 {96 Nasal,_descending_process: present absent;
 {97 Nasal,_descending_process,_position: lateral medial;
 {98 Nasal,_descending_process,_length: short elongate;
 {99 Nasal,_descending_process,_orientation: _ordered inclined_anteriorly ventral inclined_posteriorly;
 {100 Nasal,_descending_process,_lateral_pneumatic_foramen: absent present;
 {101 Frontal,_crest: absent present;
 {102 Frontal,_crest,_shape: blunt elongate expanded;
 {103 Frontal,_crest,_anterior_end,_position: _ordered anterior_to_orbit above_orbit posterior_to_orbit;
 {104 Frontal,_anterior_end,_position_relative_to_preorbital_bar_anterior_margin: anterior posterior;
 {105 Lacrimal,_foramen: absent present;
 {106 Lacrimal,_posterior_margin,_orbital_process: absent present;
 {107 Parietal,_crest: absent present;
 {108 Parietal,_crest,_shape: low expanded_into_rounded_margin tapered_into_triangular_process elongate_process;
 {109 Squamosal,_shape: unexpanded rounded expanded;
 {110 Squamosal,_position_relative_to_base_of_lacrimal_process_of_jugal: above below;
 {111 Quadrangle,_inclination_relative_to_ventral_margin_of_skull: _ordered acute Perpendicular ~120° ~150°;
 {112 Quadrangle,_mandible_articulation,_position_relative_to_orbit: _ordered posterior_to_orbit posterior_to_center_below_orbit below_orbit_center anterior_to_center_below_orbit anterior_to_orbit;
 {113 Quadrangle,_ascending_process,_shape: wide thin;
 {114 Jugal,_anterior_end,_position_relative_to_nasoantorbital_fenestra_anterior_end: posterior level;

{115 Jugal,_maxillary_ramus: absent present;
 {116 Jugal,_ventral_margin,_curvature_in_parasagittal_plane: straight concave;
 {117 Jugal,_postorbital_process_and_lacrimal_configuration: do_not_contact
 contact_to_form_lower_orbital_bar;
 {118 Jugal,_ascending_and_postorbital_processes_configuration: separated_by_distinct_angle
 infilled_by_concave_flange;
 {119 Jugal,_ascending_process_base_width: broad narrow;
 {120 Jugal,_ascending_process_inclination: _ordered anterodorsal subvertical posterodorsal;
 {121 Jugal,_postorbital_process_anterior_margin_orbital_process: absent present;
 {122 Jugal,_posterior_process: present absent;
 {123 Jugal,_posterior_process_orientation: posterior ventral;
 {124 Occiput,_orientation: _ordered posterior posteroventral ventral;
 {125 Basioccipital,_length_relative_to_width: shorter_than_wide longer_than_wide;
 {126 Basisphenoid,_main_body_length: shorter_than_wide longer_than_wide;
 {127 Basisphenoid,_elongate_basipterygoid_processes: absent present;
 {128 Supraoccipital,_crest: absent present;
 {129 Supraoccipital,_pneumatic_foramina: absent present;
 {130 Palate,_posterior_end_shape: concave convex;
 {131 Palate,_median_ridge: absent present;
 {132 Palate,_median_ridge_position: tapering_anteriorly confined_posteriorly;
 {133 Palate,_median_ridge_shape: narrow_strip wide_keel;
 {134 Palatine_shape: broad_plate thin_bars;
 {135 Choanae_and_maxilla_configuration: contact do_not_contact;
 {136 Pterygoid,_ventral_margin_position_relative_to_jaw_occlusal_margin: dorsal
 ventral;
 {137 Interpterygoid_vacuity_length_relative_to_subtemporal_fenestra_length:
 longer_than_subtemporal_fenestra shorter_than_subtemporal_fenestra;
 {138 Mandible,_articulation_helical_shape: absent present;
 {139 Jaws,_lateral_surface_row_of_foramina_parallel_to_occlusal_margin: present absent;
 {140 Mandible,_anterior_end_orientation: _ordered upturned straight downturned;
 {141 Mandible,_anterior_tip_shape: _ordered blunt pointed prow;
 {142 Mandible,_odontoid_process: absent present;
 {143 Mandible,_symphysis_shape:
 laterally_compressed anteroposteriorly_shortened dorsoventrally_depressed laterally_flattened;
 {144 Mandible,_anterior_end_lateral_expansion: absent present;
 {145 Mandible,_symphysis_dorsal_eminence: absent present;
 {146 Mandible,_symphysis_dorsal_eminence_height: low high;
 {147 Mandible,_symphysis_fusion: absent present;
 {148 Mandible,_symphysis_taper_in_horizontal_plane: attenuated subparallel;
 {149 Mandible,_anterior_end_lateral_surfaces_texture: flat cup-shaped_structures pitted;
 {150 Mandible,_anterior_portion_occlusal_margins_shape: rounded ridged;
 {151 Mandible,_middle_portion_expansion: absent present;
 {152 Mandible,_posterior_portion_occlusal_margins_shape: rounded ridged;
 {153 Mandible,_ramus_dorsal_eminence: present absent;
 {154 Mandible,_ramus_dorsal_eminence_shape: rounded pointed;
 {155 Mandible,_symphysis_occlusal_surface_median_sulcus: absent present;
 {156 Mandible,_symphysis_occlusal_surface_anterior_end_shape: flat fossa keel;
 {157 Mandible,_symphysis_occlusal_surface_shape: flat parasagittal_ridges median_ridge;
 {158 Mandible,_symphyseal_cavity: absent present;
 {159
 Mandible,_symphyseal_cavity_dorsal_shelf_posterior_end_position_relative_to_ventral_symphysis_post
 erior_end:
 dorsal_shelf_extends_posterior_to_ventral_symphysis
 ventral_symphysis_extends_posterior_to_dorsal_shelf;
 {160 Mandible,_ramus_dorsal_margin_curvature_along_length: _ordered convex
 straight concave;

{161 Mandible,_ramus,_orientation: straight_to_upturned downcurved;
 {162 Mandible,_retroarticular_process,_orientation_relative_to_ramus:_ordered posteroventral subparallel posterodorsal;
 {163 Mandible,_retroarticular_process,_outline_in_parasagittal_plane: triangular subcircular elongate blunt rectangular;
 {164 Mandible,_symphysis,_ventral_margin,_shape: flat keel crest;
 {165 Mandible,_crest,_shape: blade-like_and_low massive_and_deep;
 {166 Mandible,_crest,_anterior_end,_position_relative_to_mandible_anterior_end: posterior level;
 {167 Dentary,_position_relative_to_angular_and_surangular: does_not_separate separates;
 {168 Dentition: present absent;
 {169 Dentition,_spacing_along_jaws:_ordered mesial_teeth_spaced_wider_apart even_along_the_jaws distal_teeth_spaced_wider_apart;
 {170 Dentition,_tooth_shape,_variation: isodont heterodont;
 {171 Dentition,_mesial_teeth,_shape: recurved_triangle slender_needle recurved_spike curved_cone labiolingually_compressed_triangle bulbous_triangle;
 {172 Dentition,_cheek_teeth,_shape: recurved_triangle bulbous_triangle slender_needle curved_cone labiolingually_compressed_triangle recurved_spike;
 {173 Dentition,_texture: smooth striated mesial_and_distal_keels median_carina veined;
 {174 Dentition,_maximum_crown_height_relative_to_mesiodistal_base_width: less_than_four_times_width more_than_four_times_width;
 {175 Dentition,_lateral_orientation: vertical lateral;
 {176 Dentition,_mesial_teeth,_spacing_between_successive_teeth:_ordered nearly_touching at_most_diameter_of_teeth more_than_diameter_of_teeth;
 {177 Dentition,_cheek_teeth,_spacing_between_successive_teeth:_ordered nearly_touching at_most_diameter_of_teeth more_than_diameter_of_teeth;
 {178 Dentition,_size_variation: even_transition_along_tooth_row distinct_disparity_in_size_between_mesial_and_distal_teeth;
 {179 Dentition,_upper_teeth,_size_relative_to_lower_teeth:_ordered upper_teeth_significantly_larger subequal_lower_teeth_significantly_larger;
 {180 Dentition,_maximum_curvature_relative_to_mesiodistal_base_width: displacement_of_curvature_less_than_width displacement_of_curvature_more_than_width;
 {181 Dentition,_curvature_orientation: posterior lingual anterior;
 {182 Dentition,_inclination:_ordered upright mesial_teeth_procumbent procumbent;
 {183 Dentition,_cheek_alveoli,_shape: set_in_grooves low undulating_occlusal_margins raised_rims pedestals;
 {184 Dentition,_cheek_teeth,_denticles: present absent;
 {185 Dentition,_cheek_teeth,_largest_denticles,_shape:_ordered serrations cuspules crenulations low_cusps tall_cusps;
 {186 Dentition,_cheek_teeth,_maximum_denticle_number:_ordered more_than_50 between_six_and_49 five;
 {187 Dentition,_upper_tooth_row,_anterior_end,_position:_ordered posterior_to_rostrum_tip rostrum_tip rostrum_anterior_surface;
 {188 Dentition,_maxillary_teeth,_position_of_largest_teeth: mesial middle distal;
 {189 Dentition,_fifth_and_sixth_teeth,_subequal_in_size_and_distinctly_smaller_than_fourth_and_seventh: absent present;
 {190 Dentition,_lower_tooth_row,_anterior_end,_position: mandible_tip posterior_to_mandible_tip;
 {191 Jaws,_occlusal_margin,_curvature_in_sagittal_plane: straight dorsally_reflected;
 {192 Cervical_vertebrae,_atlantoaxis,_fusion: unfused fused;
 {193 Cervical_vertebrae,_lateral_to_neural_canal,_pneumatic_foramina: absent present;
 {194 Cervical_vertebrae,_middle-series,_midsection,_cross-section: pentagonal dorsoventrally_depressed wide_suboval laterally_compressed;
 {195 Cervical_vertebrae,_middle-series,_neural_arch,_lateral_surface,_pneumatic_foramen: absent present;

{196 Cervical_vertebrae,_middle-series,_centrum,_lateral_surface,_pneumatic_foramen: absent present;
 {197 Cervical_vertebrae,_IV–VI,_neural_spines,_height:_ordered tall low extremely_reduced;
 {198 Cervical_vertebrae,_IV–VI,_neural_spine,_shape: rectangular subtriangular fan
 ridge;
 {199 Cervical_vertebrae,_middle-series,_transverse_crest_or_ridge,_dorsal_reflection: absent present;
 {200 Cervical_vertebrae,_middle-series,_postexapophyses: absent present;
 {201 Cervical_vertebrae,_middle-series,_neural_arch_and_centrum,_configuration:
 distinct confluent;
 {202 Cervical_vertebrae,_middle-series,_ribs,_shape: elongate reduced;
 {203 Cervical_vertebrae,_VIII,_neural_spine,_height: tall low;
 {204 Cervical_vertebrae,_IX,_shape: similar_to_dorsal_vertebrae similar_to_cervicals;
 {205 Dorsal_vertebrae,_notarium: absent present;
 {206 Dorsal_vertebrae,_anterior_series,_supraneural_plate: absent present;
 {207 Synsacrum,_sacral_ribs,_configuration: contact_at_iliac contact_medial_to_iliac;
 {208 Synsacrum,_supraneural_plate: absent present;
 {209 Caudal_vertebrae,_number: more_than_15 at_most_15;
 {210 Caudal_vertebrae,_zygapophyses,_length:_ordered short elongate extremely_elongate;
 {211 Caudal_vertebrae,_centrum,_shape: single duplex;
 {212 Scapulocoracoid,_orientation_relative_to_vertebral_column: subparallel
 rotated_laterally;
 {213 Scapula_proximal_end,_shape: elongate_and_compressed suboval_and_expanded;
 {214 Scapula,_shape: elongate_process stout_with_constricted_shaft;
 {215 Scapula,_articulation_with_vertebral_column: absent present;
 {216 Coracoid,_ventral_margin,_shape: flat broad_tubercle crest;
 {217 Coracoid,_shape:_ordered semicircular broad_shaft narrow_shaft;
 {218 Sternum,_sternocoracoid_articulations,_configuration: lateral_to_one_another
 anterior_and_posterior_to_one_another;
 {219 Sternum,_posterior_to_sternocoracoid_articulations,_constriction: present absent;
 {220 Sternum,_cristospine,_shape: shallow deep;
 {221 Sternum,_cristospine,_length: stout elongate;
 {222 Sternocoracoid_articulations,_shape: flattened oval;
 {223 Sternocoracoid_articulations,_posterior_expansion: absent present;
 {224 Sternum,_plate,_shape: narrow quadrangular semicircular triangular laterally_expanded;
 {225 Humerus,_proximal_end,_ventral_surface,_pneumatic_foramen: absent present;
 {226 Humerus,_proximal_end,_articulation_surface,_outline: crescent horseshoe;
 {227 Humerus,_proximal_end,_dorsal_surface,_pneumatic_foramen: absent present
 {228 Humerus,_shaft,_curvature: straight bowed;
 {229 Humerus,_mid-shaft,_shape: constricted subcylindrical;
 {230
 Humerus,_entepicondyle,_dorsoventral_width_relative_to_ectepicondyle_dorsoventral_width:
 entepicondyle_wider_than_ectepicondyle ectepicondyle_wider_than_entepicondyle;
 {231 Humerus,_distal_end,_anterior_surface,_between_distal_condyles,_pneumatic_foramen: absent
 present;
 {232 Humerus,_distal_aspect,_pneumatic_foramen: absent present;
 {233 Humerus,_distal_aspect,_outline: hourglass crescentic_or_D-shape triangular
 trapezoidal;
 {234 Humerus,_deltopectoral_crest,_position: proximal more_distal_on_shaft;
 {235 Humerus,_deltopectoral_crest,_shape: subtriangular_with_proximal_apex
 proximodistally_long_and_proximally_leaning_trapezoid proximally_curving_hook
 oblong_process_with_constricted_neck anteroposteriorly_short_and_rectangular
 proximodistally_long_and_proximally_expanded hatchet-shape
 distally_leaning_trapezoid anteroposteriorly_tall_and_rectangular_process
 anteroposteriorly_tall_and_proximally_leaning_trapezoid;
 {236 Humerus,_deltopectoral_crest,_curvature: perpendicular_to_shaft warped_distally;
 {237 Humerus,_ulnar_crest,_size: reduced developed;
 {238 Humerus,_ulnar_crest,_orientation: posterior ventral;

```

{239 Ulna,_shaft,_proximal_end,_anterior_surface,_longitudinal_ridge: absent present;
{240 Ulna,_distal_tuberculum,_position: middle_of_the_distal_end ventral_part_of_the_distal_end;
{241 Radius,_distal_end,_cross-section: suboval subtriangular_with_large_anterior_process;
{242
Distal_syncarpal_ventral_articular_facet_for_wing_metacarpal,_size_relative_to_dorsal_facet:
ventral_facet_larger subequal_in_size;
{243 Distal_syncarpal,_cross-section: rectangular triangular;
{244 Pteroid,_shape: angled_at_midsection stout_hook
straight_and_tapered_with_expanded_proximal_end straight_with_expanded_ends
proximally_curved_slender_rod curved_and_subparallel_sided;
{245 Medial_carpal,_shape: longer_than_wide wider_than_long;
{246 Metacarpals,_number_articulating_with_carpus:_ordered five four two one;
{247 Metacarpals_I-III,_distal_ends,_relative_positions: disparate approximate;
{248 Metacarpal_IV,_proximal_end,_cross-section: anteroposteriorly_compressed
broad;
{249 Metacarpal_IV,_shaft,_cross-section: cylindrical anteroposteriorly_compressed_oval;
{250 Metacarpal_IV,_distal_end,_intercondylar_sulcus,_median_ridge: absent present;
{251 Manus,_unguals,_size_relative_to_pedal_unguals: less_than_twice_size_of_pedal_unguals
more_than_twice_size_of_pedal_unguals;
{252 Manus,_digit_IV,_first_phalanx,_proximal_end,_ventral_surface,_pneumatic_foramen: absent
present;
{253 Manus,_digit_IV,_second_or_third_phalanges,_shaft,_cross-section: subtriangular
concave_posteriorly oval ventral_keel;
{254 Pubis,_anterior_margin,_curvature_in_sagittal_plane:_ordered convex
straight_slightly_concave deeply_concave;
{255 Pubis_and_ischium,_ventral_contact,_configuration: confluent oval_opening;
{256 Ischium,_ventral_margin,_curvature_in_parasagittal_plane: straight convex;
{257 Prepubis,_shaft,_constriction: absent present;
{258 Prepubis,_shape:
elongate_paddle medially_curved_with_short_lateral_process triradiate expanded_fan;
{259 Ilium,_preacetabular_process,_anterior_margin,_shape: rounded triangular sharp_rod;
{260 Ilium,_preacetabular_process,_orientation: straight dorsiflected;
{261 Ilium,_postacetabular_process,_orientation: subhorizontal posterodorsal;
{262 Ilium,_postacetabular_process,_shaft,_constriction: absent present;
{263 Ilium,_postacetabular_process,_terminus,_expansion: absent present;
{264 Acetabulum,_outline: oval subcircular;
{265 Ilium,_postacetabular_process,_dorsal_margin,_shape: flat convex;
{266 Femur,_curvature: strongly_bowed straight_to_slightly_curved;
{267 Femur,_proximal_end,_pneumatic_foramen: absent present;
{268 Femur,_neck,_shape: indistinct constricted;
{269 Femur,_greater_trochanter,_shape:_ordered reduced distinct_process hooked_process;
{270 Femur,_distal_end,_epicondyles,_size: reduced_and_confluent_with_distal_condyles
expanded_into_distinct_distal_flanges;
{271 Femur,_neck,_angle_relative_to_shaft:_ordered perpendicular less_than_145° more_than_145°;
{272 Metatarsal_IV,_length_relative_to_metatarsals_I-III: subequal significantly_shorter;
{273 Pes,_digit_V,_number_of_phalanges:_ordered four three two one zero;
{274 Pedal_digit_V_ultimate_phalanx,_shape:_ordered straight curved bent_at_midsection nubbin;

nstates stand; hold 130000;
rseed 0; rseed []; collapse auto;
mult= replic 2000 keepall ratchet; best;
procedure/;

```


Dolicorhamphus_bucklandi ? ? ? ? ? ? ? ? ? ? ? ? ? ? ? ? 0.028 0.3333 14.29 3.33 0.3302 0.5867 ? ? ? ? ?
? ?

Fenghuangopterus_lii 2.57 14.53 0.996 ? ? ? 0.1612 ? ? ? ? ? 3.962 ? 0.7214 0.044
0.1334 12.87 2.50 ? ? 1.375 2.09 1.951 3.000 2.669 2.339 0.800 ? 12.00 ? 1.349 1.000 0.1968 0.556 0.4877
2.027 1.984 0.600 0.446 0.396 1.510 2.610 ? 0.905 1.754 0.435 0.2991 ? ? ? ?

Rhamphorhynchus_muensteri 3.64 17.37 0.763 0.3463 0.1375 4.276 0.0933 2.099 ? ? 1.311 0.0935
1.310 0.2298 0.5790 0.036 0.4102 13.91 4.78 ? 0.6816 1.498 2.00 1.987 4.000 2.144 7.179 1.139 ? 7.28
0.753 1.633 0.762 0.2033 0.560 0.6818 2.198 2.531 0.942 0.857 0.867 1.323 2.365 2.193 0.859 1.451 0.501
0.4781 4.730 0.1875 0.5448 0.085

Nesodactylus_hesperius ? 1.287 2.19 2.143
4.000 1.123 6.544 0.941 ? 7.75 0.717 1.720 0.653 ? 0.574 0.5247 2.604 2.946 ? ? ? 1.379 ? ? ? ? ? ? ? ? ? ?

Cacibupteryx_caribensis 3.15 ? ? ? ? 2.833 ? 2.167 ? ? 0.867 ? 1.624 0.7241 ? 0.040
? ?

Qinglongopterus_guoi ? 9.96 1.002 0.3333 0.2376 ? 0.2376 ? ? ? ? ? ? 0.6455 0.6400 0.028 0.3807 11.29
2.66 ? 0.6387 1.215 1.94 1.685 4.000 2.454 3.624 0.936 ? 7.09 ? 1.590 0.941 0.1413 0.511 0.4152 2.328
1.781 1.009 0.937 0.584 1.798 ? ? 0.685 1.254 0.654 0.4641 4.570 0.3521 0.4000 0.240

Harpactognathus_gentryii 3.67 ? ? ? ? ? ? ? ? ? ? ? ? ? ? ? ? 0.028 ? ? ? ? ? ? ? ? ? ? ? ? ? ?
? ?

Angustinarapterus_longicephalus 4.02 ? 0.871 0.3114 0.2114 9.444 0.3159 2.646 ? ? 1.143 ? ? ? 0.5174
0.036 0.1425 15.78 1.92 ?

Sericipterus_wucaiwanensis 4.08 14.27 ? 0.3010 ? ? ? ? ? ? ? 0.1279 ? ? ? 0.028 ? ? ?
? ? 1.866 2.37 2.019 ? ? ? 1.013 ? 6.81 ? ? 0.940 ? ? ? ? 1.271 0.922 ? 0.924 ? ? ? ? ? ? ? ? ? ? ?
? ?

Sordes_pilosus 3.51 19.20 0.736 0.2000 0.1931 2.753 0.2150 1.712 ? ? 1.176
0.1601 1.360 0.6188 0.5034 0.026 0.2935 15.62 5.64 ? 0.4726 1.011 2.39 2.200 5.000 1.933 4.395 1.109 ?
11.66 ? 1.639 0.867 0.1855 0.403 0.6333 2.338 1.068 1.081 1.038 0.755 3.320 1.559 2.589 0.790 1.411 0.390
0.3293 1.574 0.2550 0.3269 0.359

Pterorhynchus_wellnhoferi 2.95 38.06 0.922 0.3215 ? ? ? ? 0.5318 5.471 1.204 ? ?
0.3315 0.5125 0.038 0.1834 14.20 2.33 ? 0.4878 1.544 4.69 1.505 5.000 2.893 7.685 ? ? 16.77 ? 1.750 0.722
0.2453 0.548 0.5507 ? 1.106 1.252 1.148 0.800 ? 2.206 2.384 0.808 1.167 0.347 ? ? ? ? ?

Kunpengopterus_sinensis 2.93 17.74 0.842 0.3789 ? ? ? ? 0.6632 4.025 1.100 ? ? ? ?
? 0.2444 11.69 3.79 ? ? 2.598 3.80 1.236 ? 1.792 4.502 1.210 ? 6.01 ? 1.635 0.823 0.4358
0.635 0.4463 2.416 1.128 1.070 1.092 0.900 ? ? ? 1.110 1.356 0.355 0.3820 1.035 0.2718
0.2393 0.220

Wukongopterus_lii 4.15 ? 0.860 0.2722 ? ? ? ? 0.5072 ? ? ? ? ? 0.4952 0.056
0.1938 13.02 3.28 ? ? 2.039 ? ? 5.000 ? 5.975 1.324 ? ? ? 1.602 ? 0.1176 0.591 ? 2.342 1.179 1.243 1.287
1.127 ? ? 2.655 0.889 1.533 0.356 0.3367 1.790 0.4357 0.2307 0.199

Darwinopterus_zhengi ? 3.550 2.48 2.467 6.00
1.495 6.467 1.439 ? 9.34 ? 1.227 0.830 0.5161 0.656 ? ? 1.098 1.054 0.999 0.848 ? ? 3.236
0.830 1.744 0.448 0.3185 1.905 ? ? ?

Darwinopterus_linglongtaensis 3.78 22.88 0.842 0.4130 ? ? ? ? 0.3275 2.927 0.976 ? ? ? 0.4833 ? 0.2197

20.72 3.18 ? ? 1.610 3.82 1.810 5.000 1.921 4.224 1.215 ? 7.71 ? 1.484 0.834 0.4849 0.574 0.5771 2.027
1.497 1.135 1.180 1.184 0.769 2.963 2.846 0.990 1.250 0.460 0.3220 1.345 0.3493 0.2304 0.368

Darwinopterus_robustodens 5.00 31.38 0.863 0.3486 ? ? ? ? 0.4343 3.800 0.841
0.0662 ? ? 0.3441 0.040 0.2661 23.18 4.00 ? 0.3960 2.839 2.87 1.546 ? 2.514 3.732 1.129 ? 8.97 ? 1.600
0.571 0.4375 0.600 0.3571 2.167 1.300 1.154 1.154 1.031 1.070 0.947 2.873
0.860 1.395 ? 0.3500 1.000 0.3333 0.1429 0.143

Archaeoistiodactylus_linglongtaensis 4.20 ? ? ? ? ? ? ? ? 3.577 ? ? ? ? ? ? ? ? ? ? 2.493 ? ? ? ? ? ? ? ? 1.489
1.000 0.5100 0.596 0.5000 ? ? ? ? ? ? 2.597 2.636 0.936 1.409 0.251 0.3335 ? ? ? ?

Darwinopterus_modularis 4.65 29.58 0.834 0.3455 ? ? ? ? 0.4432 4.284 1.169 0.0852
? ? 0.4846 0.054 0.2167 24.88 5.59 ? 0.5475 2.020 2.49 1.639 5.000 3.747 7.527 1.038 ? 9.84 ? 1.465 0.918
0.4063 0.601 0.5940 2.627 1.181 1.146 1.229 1.104 1.118 2.364 2.462 0.909 1.350 ? 0.3520 1.841 0.3360
0.2808 1.217

Changchengopterus_pani ? 1.167 1.17 1.333
3.000 1.133 3.007 1.222 ? 6.48 ? 1.421 1.000 0.4620 0.602 0.3509 ? 1.158 1.067 1.000 ? ? ? ? 0.811 1.190
0.471 0.4091 ? ? ? ?

Dendrorhynchoides_curvidentatus ? 10.21 1.083 0.1068 ? ? ? ? ? ? ? ? 2.466 ? ? ? 0.0517
18.21 1.02 ? ? ? ? 1.516 ? 0.935 0.852 1.182 ? 14.76 ? 1.298 0.908 0.1114 0.308 0.4349 2.614 1.623 0.822
0.628 ? ? ? ? 0.723 1.344 0.518 0.4523 1.211 0.2417 0.4524 0.300

Luopterus_mutoudengensis ? ? 0.801 0.1272 ? ? ? ? 0.1917 1.460 2.136 0.1127 3.218
? ? ? 0.0989 12.87 ? ? ? 1.181 ? ? 5.000 ? 2.000 1.889 ? ? ? 1.556 1.000 0.1215 0.323 0.4695 2.404 1.852
0.820 0.500 0.100 ? 1.871 2.528 0.778 1.286 0.556 0.4444 1.506 0.1667 0.7500 0.500

Batrachognathus_volans ? 12.29 0.977 0.0208 ? ? ? ? 0.1816 0.859 1.398 0.1406
2.923 ? 0.6351 0.048 0.0644 11.53 1.11 ? ? 1.170 1.76 1.737 ? ? ? 1.033 ? 13.13 ? 1.609 0.823 ? 0.326 ?
2.594 ? ? ? ? ? ? ? 0.628 1.616 0.292 0.3833 1.545 0.1477 0.5742 0.620

Jeholopterus_ningchengensis 2.76 7.52 1.065 0.0877 ? ? ? ? 0.2596 0.920 1.095 ?
2.399 ? 0.6883 0.028 0.0926 13.01 1.23 ? 0.6377 1.126 1.75 1.507 5.000 0.403 0.868 1.532 ? 13.13 ? 1.275
0.819 0.1529 0.326 0.3821 2.562 1.480 0.891 0.633 0.178 1.416 ? 3.055 0.702 1.149 0.457 0.4517 1.494
0.1590 0.6528 0.494

Anurognathus_ammoni 1.66 14.15 0.891 0.0419 ? ? ? ? 0.1830 1.175 1.211 0.1655
2.546 ? 0.4894 0.030 0.1651 12.88 1.33 ? 0.3678 1.384 3.12 1.321 5.000 0.556 0.894 1.220 ? 13.85 ? 1.433
0.839 0.1389 0.285 0.5540 2.279 1.686 0.798 0.462 ? ? 1.622 3.139 0.796 1.463 0.475 0.4649 2.469 0.1857
0.5240 0.487

Kryptodrakon_progenitor ?
? ? 1.027 ? 2.547 ?

Painten_pterodactyloid 3.83 25.87 0.797 0.4424 ? ? ? ? 0.3042 2.241 1.065 0.0767 ?
? 0.5215 0.042 0.4741 19.96 9.52 ? 0.5753 1.375 3.05 1.275 5.000 0.579 2.229 1.515 ? 9.50 ? 1.359 0.638
0.3412 0.630 0.4827 ? 1.140 1.095 1.107 0.864 1.540 2.825 2.408 0.953 1.174 0.483 0.3190 0.698 0.3412
0.2057 0.173

Cuspicephalus_scarfi 5.93 ? ? 0.3659 ? ? ? ? 0.4755 5.167 0.906 0.0450 ? ? 0.6204
0.116 ?

Germanodactylus_rhamphastinus 4.54 34.81 0.862 0.3118 ? ? ? ? 0.4105 3.043 1.065
0.0446 ? ? 0.5242 0.058 0.4718 17.43 10.50 ? 0.5016 2.693 5.01 1.074 5.000 ? ? 1.253 ? 11.64 ? 1.448 0.875
? 1.068 0.7015 1.317 1.427 0.824 0.772 0.705 1.169 2.064 3.640 1.032 1.471 0.469 0.3179 ? ? ? ?

Germanodactylus_cristatus 4.33 26.29 0.752 0.3921 ? ? ? ? 0.3552 2.404 1.149 0.0680
 ? ? 0.5213 0.052 0.4112 16.90 6.63 ? 0.6260 3.312 3.43 1.194 5.000 0.499 1.424 1.266 ? 13.40 ? 1.274 0.812
 0.5467 1.093 0.7204 1.783 1.381 0.943 0.825 0.718 1.528 1.966 3.408 0.958 1.434 0.383 0.3340 1.091
 0.3395 0.1957 0.092

Pterodactylus_antiquus 6.16 27.95 0.802 0.4560 ? ? ? ? 0.2467 3.194 1.474 0.0766 ?
 ? 0.4625 0.079 0.3878 23.05 9.75 ? 0.5105 5.090 6.79 1.313 5.000 0.489 1.168 1.359 ? 10.53 ? 1.339 0.855
 0.5036 0.991 0.7031 1.556 1.306 0.945 0.840 0.641 1.154 2.127 3.154 0.994 1.388 0.373 0.3668 0.969
 0.3336 0.1637 0.177

Normannognathus_wellnhoferi 4.90 ?
 ?

Aurorazhdarcho_primordius ? 1.165 ? 0.480
 1.333 1.250 ? 10.89 ? 1.329 0.933 0.6538 1.511 ? ? 1.915 0.592 0.423 0.422 1.094 3.235 ?
 1.226 1.510 0.346 0.1823 0.963 0.3278 0.1555 0.161

Cynorhamphus_suevicus 4.42 20.62 0.827 0.4032 ? ? ? ? 0.3364 3.569 1.427
 0.1623 6.016 ? 0.0514 0.012 0.3065 15.23 3.99 ? 0.0928 2.224 3.84 1.286 5.000 0.432 1.535 1.057 ? 9.30 ?
 1.305 0.810 0.7317 1.630 0.6160 1.788 2.123 0.818 0.595 0.499 1.190 1.666 2.645 1.152 1.482 0.339 0.2280
 ? ? ? ?

Pterodactylus_micronyx 5.32 30.83 0.777 0.5025 ? ? ? ? 0.1885 3.262 2.138 0.0620
 3.253 0.6449 0.2631 0.072 0.3878 25.00 8.72 ? 0.3248 3.038 5.44 1.192 5.000 0.624 1.587
 1.099 ? 13.12 ? 1.102 0.764 0.5169 1.328 0.5138 1.874 1.646 0.778 0.594 0.518 1.303 2.443 2.731 1.039
 1.379 0.301 0.2585 0.997 0.3410 0.1976 0.213

Liaodactylus_primus 6.69 ? 0.880 0.5000 ? ? ? ? 0.3113 3.322 1.087 0.0685 2.327 0.3762 0.5515 0.152
 0.3050 33.94 10.23 ? 0.5888 ?
 ? ? ? ? ? ? ? ?

Ctenochasma_elegans 8.11 28.39 0.806 0.6119 ? ? ? ? 0.1265 3.214 1.719 0.0878
 3.561 0.1758 0.6095 0.406 0.5873 24.33 22.42 ? 0.7242 4.210 4.66 ? 5.000 0.479 1.110 1.236 ? 11.96 ?
 1.235 0.765 0.5138 1.047 0.9256 1.366 1.400 0.919 0.718 0.667 1.255 2.452 3.389 0.857 1.442 0.327 0.3730
 1.054 0.3146 0.2332 0.152

Pterodaustro_guinazui 10.77 38.38 0.961 0.6873 ? ? ? ? 0.1419 3.790 1.262 0.0377
 ? ? 0.7238 1.000 0.5955 26.11 15.67 ? 0.8843 4.294 5.21 1.228 7.00 0.822 2.854 1.039 ? 11.61 ? 1.435 0.757
 ? 1.052 ? 1.865 1.604 0.975 0.753 0.602 1.273 2.940 ? 0.855 1.556 0.530 0.5125 1.690 0.3537 0.2212 0.168

Beipiaopterus_chenianus ? 3.984 8.81 0.966
 5.000 0.404 1.066 1.123 0.4221 18.43 ? 1.349 0.819 0.2735 1.035 0.6092 1.687 0.927 1.575 1.317 1.102 ? ?
 ? 0.706 1.993 0.380 0.3428 0.927 0.3146 0.1107 0.119

Gegepterus_changi 9.94 39.19 0.861 0.6700 ? ? ? ? 0.1879 4.429 1.212 0.0667 ?
 ? 0.4224 0.151 ? 30.98 19.08 ? 0.4718 3.672 5.06 0.987 ? ? ? ? 0.3852 ? ? ? ? ? ? ? ? 1.015 ? ? ? 2.171 ? ? ?
 ? ? ? ? ? ?

Kepodactylus_inspersatus ? 2.712 ? ? ? ? ? ? ? ?
 ? ? ? ? ? ? 1.250 ? ? ? ? ? ? ? ? 0.858 ? ? ? ? ? ? ? ?

Elanodactylus_prolatus ? 3.638 6.39 1.370 ? ?
 ? 1.321 ? 12.31 ? 1.107 0.816 ? 0.848 0.5086 1.590 1.400 1.142 1.049 0.701 1.029 2.130 2.130 ? ? ? ? 1.132
 0.2248 0.2058 ?

0.695 1.274 0.715 ? 1.504 0.5248 ? ? ? ? ? ? ? ? 1.003 ? ? ? ? ? ?

Muzquizopteryx_coahuilensis 4.08 ? ? ? ? ? ? ? ? 2.688 1.714 ? ? ? ? ? ? ? ? ? ? ?
8.00 ? ? ? ? ? 0.702 1.391 0.773 0.6011 ? ? ? ? ? ? ? 0.957 2.425 ? 0.969 1.397 ? 0.2018 ? ? ? ?

Nyctosaurus_grandis ? ? ? ? ? ? ? ? ? ? ? ? ? ? ? ? 2.345 ? ? ? ? ? ? ? ?
0.716 1.300 0.678 ? 0.910 0.8025 1.898 ? ? ? ? ? ? ? 0.878 ? ? ? ? ? ? ?

Nyctosaurus_lamegoi ?
0.740 ?

Nyctosaurus_nanus ? 0.995 ? ? ? ? ?
6.75 0.596 ?

Nyctosaurus_gracilis 5.83 31.98 0.885 0.6637 ? ? ? ? 0.2690 2.759 1.109 0.0788
1.935 0.5217 ? ? 0.5612 21.58 12.11 ? ? 2.173 3.60 1.088 9.00 0.462 0.828 0.898 ? 8.88 0.626 1.837 0.697
0.7837 2.996 0.5522 1.576 3.523 0.796 0.453 0.377 0.902 3.719 2.138 0.913 1.352 0.292 0.2755 ? ? ? ?

Serradraco_sagittirostris ?
? ?

Aussiedraco_molnari ? ? ? ? ? ? ? ? ? ? ? ? ? ? ? ? ? 4.88 ? ? ? ? ? ? ? ? ? ? ?
? ?

Hongshanopterus_lacustris ? ? ? 0.4895 ? ? ? ? 0.2795 ? ? 0.0770 2.996 0.4516 0.5000 0.072 ? ? ? ? ?
1.325 ?

Targaryendraco_wiedenrothi ? ? ? ? ? ? ? ? ? ? ? ? ? ? ? ? ? 3.38 ? ? ? ? ? ? ? ? ? ? ?
? ? 0.672 ?

Lonchodectes_compressirostris 6.90 ? ? ? ? ? ? ? ? ? ? ? ? ? ? ? ? ? 3.29 ? ? ? ? ? ? ? ?
? ?

Ikandraco_avatar 7.07 ? 0.907 0.5002 ? ? ? ? 0.3366 3.782 1.500 0.0579 4.070
0.1988 0.6059 0.080 0.5136 20.24 9.38 0.4588 0.5815 2.648 ? ? ? ? ? ? ? ? 1.644 0.524
0.7117 1.264 0.8331 1.460 2.060 0.954 ? ? ? ? ? ? ? ? ? ? ? ? ?

Ikandraco_machaerorhynchus ? ? ? ? ? ? ? ? ? ? ? ? ? ? ? ? ? 3.10 ? ? ? ? ? ? ? ? ? ? ?
? ?

Lonchodraco_giganteus 3.26 ? ? ? ? ? ? ? ? ? ? ? ? ? ? ? ? ? 4.92 ? ? ? ? ? ? ? ? ? ? ?
? ? ? 0.683 ?

Lonchodraco_microdon 9.46 ?
? ?

Lonchodraco_denticulatus 1.66 ?
? ?

Nurhachius_ignaciobritoi 5.16 27.86 0.881 0.3779 ? ? ? ? 0.5968 6.399 1.402 0.0648
5.966 ? 0.3506 0.047 0.3207 21.68 7.04 ? 0.3750 2.311 3.25 1.407 ? ? ? 0.810 ? 10.15 ? 1.709 0.454 0.3798
1.124 0.5261 1.619 2.021 0.820 0.638 ? ? 1.889 ? 1.104 1.257 ? 0.1349 1.136 0.4430 ? ?

Liaoxipterus_brachyognathus ? ? ? ? ? ? ? ? ? ? ? ? ? ? 0.044 0.2863 22.39 5.34 ? 0.3418 ? ? ? ? ? ? ? ?
? ?

Istiodactylus_sinensis 5.21 38.25 0.902 0.2097 ? ? ? ? 0.6409 4.610 1.265 0.0576 ? ?
 0.2331 0.060 0.1196 17.07 2.83 ? 0.2314 2.073 3.18 1.212 ? ? ? 0.896 ? 14.40 ? 1.751 0.483 ? 1.249 0.5819
 1.716 2.046 0.892 0.715 ? ? ? ? 1.206 1.134 ? ? ? ? ?

Istiodactylus_latidens 6.29 38.02 0.755 0.1748 ? ? ? ? 0.4304 3.707 1.134 0.0509
 3.833 ? 0.1539 0.052 0.1655 18.42 3.09 ? 0.2279 ? 3.60 1.105 ? ? ? 0.796 ? 10.75 ? 1.732
 0.442 0.2520 ? 0.4913 ? ? ? ? ? ? 0.909 ? ? ? ? ? ?

Pterodactylus_polyodon 7.74 ?
 ?

Zhenyuanopterus_longirostris 8.17 32.30 0.908 0.5505 ? ? ? ? 0.2752 3.998 1.268
 0.0397 ? ? 0.8073 0.172 0.5616 21.16 9.38 ? 0.8671 2.664 4.74 ? 6.00 0.593 1.012 1.333 ?
 12.44 ? 1.248 0.526 0.4389 1.095 0.7071 1.317 1.714 0.764 0.583 0.528 ? ? ? 1.000 0.952
 0.468 0.1100 ? ? ? ?

Boreopterus_giganticus 6.38 ? 0.876 0.5860 ? ? ? ? 0.2161 2.767 0.935 ? ? ? 0.6872
 0.114 0.6353 15.09 13.21 ? 0.7897 ?

Boreopterus_cuiae 5.88 ? 0.851 0.5534 ? ? ? ? 0.2261 3.960 1.094 ? ? ? 0.6628
 0.112 0.6500 20.13 11.91 ? 0.7771 2.198 ? ? ? ? 2.029 ? ? ? ? 1.392 ? 0.4091 1.190 ? 1.758
 1.734 0.894 0.715 0.635 ? ? ? 1.038 1.000 ? 0.1585 ? ? ? ?

Hamipterus_tianshanensis 4.85 24.06 ? 0.5684 ? ? ? ? 0.2948 2.522 0.806 0.0695
 1.431 0.1966 0.6652 0.068 0.4453 15.91 8.33 ? 0.5725 2.731 2.71 1.312 6.00 ? ? 0.905 ? 12.48 ? ? 0.500
 0.4882 ? ? 1.834 1.836 0.758 ? 0.219 ? 2.629 1.622 1.133 ? ? ? ? ? ? ?

Brasileodactylus_araripensis ? ? ? ? ? ? ? ? ? ? ? ? ? ? ? ? 5.54 ? ? ? ? ? ? ? ? ? ? ?
 ?

Barbosania_gracilirostris 3.25 29.25 0.844 0.5349 ? ? ? ? 0.2455 4.545 0.851 0.0598 ?
 ? 0.6733 0.044 0.5128 17.60 7.88 ? 0.7098 ? ? 0.927 ? 0.619 1.467 ? ? 11.86 ? 1.407 0.528 0.5785 0.981
 0.8043 ? ? ? ? ? ? ? ? 0.801 ? ? ? ? ? ? ?

Cearadactylus_atrox 4.83 ? 0.846 0.4259 ? ? ? ? 0.3253 2.206 ? ? 3.238 ? 0.4171
 0.062 0.2282 13.94 3.29 ? 0.4542 ?

Guidraco_venator 4.42 ? 0.868 0.5395 ? ? ? ? 0.2500 3.167 0.948 0.0423 ? ? 0.6342 0.088 0.5364
 13.63 6.67 ? 0.7322 1.278 ?
 ? ? ? ? ?

Ludodactylus_colorhinus ?
 ?

Ludodactylus_sibbicki 4.52 ? 0.891 0.5049 ? ? ? ? 0.3055 2.668 0.983 0.0449 ? 0.1919 0.6882 0.080
 0.3832 14.69 5.00 ? 0.6982 ?
 ? ? ? ? ? ?

Aetodactylus_halli ? ? ? ? ? ? ? ? ? ? ? ? ? ? 0.108 0.4078 29.60 10.49 ? 0.7540
 ?

Camposipterus_nasutus 4.97 ?
 ?

Cimoliopterus_dunni 10.88 ?
 ?

Sinopterus_benxiensis 3.36 ? 0.779 0.3346 ? ? ? ? 0.4705 3.003 ? 0.1009 ? ? ? ?
0.5369 15.83 7.91 0.5468 ? 2.889 ? ? ? ? ? ? ? ? 1.919 0.857 0.5042 2.145 0.7692 1.267
2.839 0.739 0.557 ? ? ? ? 1.806 1.375 ? 0.2273 ? ? ? ?

Sinopterus_corollatus 3.66 19.66 0.854 0.3073 ? ? ? ? 0.4417 2.321 ? ? ? ? ? ?
0.5515 13.91 5.76 0.6613 ? 1.637 2.49 ? ? ? ? 1.175 0.5086 10.08 ? 1.479 0.806 0.5408 1.941 0.5944 1.655
2.185 0.640 0.417 0.196 0.999 ? ? 1.319 1.513 0.285 0.1996 0.912 0.4092 0.1338 0.116

Bakonydraco_galaczi 5.68 ? ? ? ? ? ? ? ? ? ? ? ? 0.5000 20.17 12.63 0.4822
? ?

Keresdrakon_vilsoni 4.12 ? ? ? ? ? ? ? ? 1.482 ? ? ? ? ? ? ? ? 10.31 ? ? 2.519 1.80
? ? ? ? ? ? 5.79 ? 1.320 0.637 ? ? ? ? 2.156 ? ? ? ? 1.526 ? ? ? ? ? ? ? ?

Caiuajara_dobruskii ? ? ? ? ? ? ? ? 1.542 0.807 ? ? 0.0338 ? ? 0.3677 9.78 2.23 0.3116 ? 1.712 ? 1.053
6.00 0.497 0.776 ? 0.4396 12.19 ? 1.330 0.574 ? 1.673 ? 2.027 1.932
0.907 0.955 0.291 1.489 ? ? 1.009 1.225 ? ? ? ? ? ?

Tupandactylus_navigans 3.04 ? ? 0.2531 ? ? ? ? 0.4747 2.071 0.766 0.1020 1.750 0.1104 ? ? ? ? ? ? ? ? ? ?
? ?

Tupandactylus_imperator 3.52 ? ? 0.1838 ? ? ? ? 0.6803 2.680 0.772 0.0257 ? ? ? ? 0.5100 12.86 2.92 0.5100
? ?

Vectidraco_daisymorrisae ? 1.750 5.000 ? ?
? ?

Europejara_olcadesorum ? ? ? ? ? ? ? ? ? ? ? ? ? ? ? ? 0.2505 11.59 1.96 0.2770 ? ?
? ?

Tapejara_wellnhoferi 2.46 14.96 0.770 0.2240 ? ? ? ? 0.4770 1.913 0.894 0.1300
1.120 0.0415 ? ? 0.4387 7.04 1.18 0.3967 ? 2.722 2.48 0.928 ? 0.570 1.204 1.226 0.4700 5.93 ? 1.406 0.790
0.4906 1.316 0.8068 1.365 1.966 0.835 0.646 0.435 ? 2.130 2.495 1.154 1.260 0.486 0.2908 ? ? ? ?

Microtuban_altivolans ? 1.282
0.3672 6.75 ? 1.363 0.700 ? 1.807 0.8272 1.409 2.000 0.848 0.470 0.026 ? ? ? ? ? ? ? ? ? ? ? ?

Noriopterus_complicidens ? ? ? ? ? ? ? ? ? ? ? ? ? ? ? ? 0.028 ? ? ? ? ? ? 3.185 3.66 1.887
7.00 0.607 2.571 ? ? 9.59 ? 1.368 0.902 ? 1.868 0.4174 1.771 2.289 0.713 ? ? 1.567 2.425
1.097 1.145 1.839 0.220 0.2000 0.750 0.3808 0.3720 0.389

Noriopterus_parvus 3.66 ? 0.852 0.4682 ? ? ? ? 0.3394 2.002 1.089 0.0874 ?
0.2628 0.4819 0.052 0.5363 18.84 10.33 ? 0.3000 1.481 2.10 1.630 ? ? ? ? ? 6.35 ? 1.412
0.823 0.5456 1.917 0.6312 1.773 2.044 0.857 0.666 0.500 ? 1.666 ? 1.262 1.516 0.303 ? ? ? ? ?

Domeykodactylus_ceciliae ? ? ? ? ? ? ? ? ? ? ? ? ? ? ? ? 0.064 ? ? 8.38 ? ? ? ? ? ? ? ? ? ?
? ?

Dsungaripterus_weii 4.24 32.59 0.787 0.3941 ? ? ? ? 0.3218 2.072 1.180 0.0980
1.312 0.3903 0.3685 0.044 0.4175 12.66 6.75 ? 0.6253 1.324 3.97 1.105 7.00 0.545 2.484
1.429 ? 8.97 ? 1.606 0.814 ? 1.850 0.7534 1.777 2.398 0.770 0.798 0.582 ? 1.322 ? 1.440
1.571 ? 0.1600 ? ? ? ?

Tupuxuara_leonardii 6.25 43.73 0.722 0.2439 ? ? ? ? 0.4129 2.752 0.603 0.0316
2.109 0.3496 ? ? 0.6211 18.49 14.03 ? ? 1.802 3.76 1.057 ? ? ? 1.187 ? 9.07 ? 1.258 0.694
0.5221 1.582 0.7732 1.678 2.185 0.611 0.410 ? ? ? ? 1.271 1.339 0.348 0.2232 ? 0.3765

?????000010001040000-0---00110000000 0000001000000030

Scleromochlus_taylori 10-?00-000010?1??01000?00?0?0100--
 ----010000000?0--1??0-0?20?-1?0??000?0000?????00??0
 ?100000-00?00000?????00120--0010??0000?????1??1???
 00????100000?0000000000000?????0?01??1000?????
 ----01?????00000000001?00?004-

Preondactylus_buffarinii 10-1?0-00001??10101000-?0??0100---
 ----01001001000--??0????100-100000?????????????
 100000-0?000000?????00110?00101?002010000101111000
 0?????00?00??0??000?0?01?????????11????01000?????
 ?00100100?00000000000001?00?0020

Austriadactylus_cristatus 10-1?0-?00010?101?1000-00?0001?101
 0200001001001000--1000-00100-?000000?0??10?????0???
 ??200000-000?0000?????001200001111002010000101111000????0000
 00000??000000?01????001????11????01000?????01001????000??00
 0?01?????????

Peteinosaurus_zambellii ??????-?????????????????????
 ??
 ?00????000-0??00000?????0????-?000101000201?0002022
 ??000???
 ??????????0010000000?000000?0?????????

Caviramus_schesaplanensis ??????-?????????????????????
 ??
 ??????010000111?110000?????00020000??100010?0? [01] 1
 032??010?????????????????????????????????????
 ??

Raeticodactylus_filisurenensis 10-1?0-10101??10101100-00?0102010
 20100001002000000--?000-00200-1000000000?????01?
 ??012000111?110100?????00021--001101100001000110321
 1010??01000000????00?????????0?????????00?11????101000
 0?????0?100??0?0?????????????1000?0???

Eudimorphodon_cromptonellus ??????-?00????0?0??100?-?????????
 ??????????010?200?00?????0?0??0-??0??0?????????
 ??????010000?000?00?????????????0--?00101000?01100 [01] 1
 042?10??????0??0?????0??00?00?0101?0001?0?11?0010
 10????0?????1?010?0?????????????100000?20

Eudimorphodon_rosenfeldi 10-1?0-00001??10101000-001110200-
 -01003000000--1?00-00210-100000?00000100?????????
 010000100?000001?????0011000010100020110011042110
 10??0100000000?0??0000?00010101001??01100?10100000
 0?00010010000000?00?00?01??0?020

Eudimorphodon_ranzii 10-100-000010?10101000-001110200--
 ----01003000000--1000-00210-1000000000????0?00 01??002000010000
 000010000-00110--0001011002011001104211010??010??0000?00?1???
 0?00002010110100011000101000?0??1010010?????00??000?01?0?00
 ???

Parapsicephalus_purdoni 10100-?01010000111000-203000210-
 -----01112000000--100??00100-1001000000001??0001000
 ???[01]1?????
 ??0??
 ???

Dimorphodon_macronyx 10-1?0-00101??00111000-203000210-
 -----01111001000--110??00100-100100000???10??????01??
 ?0120000-0?0000000000-2013200100124100211000011110000?011??00
 00?0010020?00012????00?00011100102000??
 0002010010000100132000010100000020

Dimorphodon_koi ???[01]?????1?
 ??????????????????????0--????10????????????????????001001?????
 ??????1??000-0?001000?00-20?????1001?????0201????00??
 ??0?0?0?01110000??
 ???

Dimorphodon_hanseni ?????????01????????01000-?1????21?
 ?????????0111100000102????10?????-10?10?00??????0?????
 ?????0??0010000101010000-20242001001?4300201000011--?10?0?????
 ???
 ???

Dimorphodon_jenkinsi ??????????1?????????1??0??[02]?????
 ?????????0????????????????????0?????100?10010????0010?????
 ??2?100????0001?
 ???
 ???

Dimorphodon_weintraubi ?????????????????????????????????????[01]?????1
 ??????????????????????????????????100?1????????????????001000?????
 ???
 ?????????00011100000????????????00?12????00?00??10?0102
 200?00??2010010000????????????????????????????????020

Herbstosaurus_pigmaeus ?????????????????????????????????????
 ???
 ???
 ??????????????????????????????????10?0????????????????????????
 ??????????????????????????????130000?????101100???

Campylognathoides_zitteli 10-1?0-000010?10111000-00????0210--
 -----02102000000--1000-00?00-0000100?????????0?????????
 1220000-0000001-000??10130--100100000211100011--1001
 0??0?000000?0000020?00002?110001?01111??1010??001
 ??2010010?011011310100101011?1021

Campylognathoides_liasicus 10-100-000010010111000-002110210-02102000
 000--1000-00200-00001000000010000--01??
 01220000-0000001-0000-10130--1001000002111000111001
 00?0100000000000000200000021110001001111??101000001?02010010
 001011310?00?0101101021

Scaphognathus_crassirostris 10-1?0-000010210111100-002110210-
 -----01102000000--100000200-1100000000???10??????01?00

1120000-1000001-?????00131--102012010220100011 1000
0000??00000000001002000000211?002000110??103000010002011010
1002?11101 [01]0000101101122

Orientognathus_chaoyangensis 10-1?0-0000102??1?1100-? [02]????
[12]?0011?2????????????????0-11000????????????????01120000-10
00001-?????00131?02012010220100111--10010??010??0000??????0100
00002????00??01????0?0????0?5011?10??0201???11000010110212
1

Dorygnathus_banthenis 10-100-00001011111101-002110210-
-----0010200000--1000-00200-1100000000001000001001
112000101000001-0200-0013201102022010221100131--100100?010000
0000000100200000021101003001111001030000100030110101002011
[13]0110010101101122

Klobiodon_rochei??
??112000101000001-?????01122011
02025010221?00131--?010????????????????????????????????????
??

Dolicorhamphus_depressirostris ??????????????????????????????
??
??????10202010100000?????0-01??20??0202501022??02131
--?010??
??

Dolicorhamphus_bucklandi ??????????????????????????????
??
??????102000101000001-?????01122011020????022????13?
????010??
??

Fenghuangopterus_lii 20-1?0-00001011??11100-? [02]?????0--0?1?2??????
?????00200-11?000??0001?????0??011110000-1000001-?????0013?
--102012010220?11111 100?0??010??0000?0?1?020000002?1010?2000
01??103000?????20110100?02011301???1?1?1101???

Rhamphorhynchus_muensteri 20-100-000010111110101-002110210-----0010
2000000--0000-00220-11000001-00010000010011020000-1000001-0000
-01131--10201221022011022100010000110000000000100200000021101
00 [12]000111001060000100020110101012011 [12]011001010110112 [12]

Nesodactylus_hesperius ??????????????????????????????
????????????????????????????????1?0????????????????????
??
?????????0?100000?????020?00?02?11000200?111??1060
000100??011010?01????00?100010??1??????

Cacibupteryx_caribensis ???10??01010111110101-002000?10-
-----0010200000--0000-00100-?1000000000010000--0100?1????????
????????????????????020?????0?2???? [01]2????0
0?0??
?0??

Qinglongopterus_guoi 21?1?0-?0?0?01?1??1101-002?1?2???

??????0??20000??????0?200-??00?00??001??????0?
 ???112000??100?0?1-?????0?13?--102012?112201111?10
 001??010??0000?00?1?020000002????00????111??103000
 ?00??3?1101?100?011101?????1?1101121

Harpactognathus_gentryii 11010101012101111?110?-?????0??1
 001?001001?200?0????????????-????????????0001
 ???1????????????????????020????1220???[01]2??
 ?00??0????????????????????????????????????
 ?????????????????????????????????????

Angustinaripterus_longicephalus 1111?10101010111111101-0021102?1001?00101
 102000000--1?0??00210-110000001????????01???1120010-1001011-
 ???0-00131--102025211120111121--000?0????????????????
 ?????????????????
 ?????????????????????

Sericopterus_wucaiwanensis 1111?10101010111111101-?????0?11
 001?001011?20000?0--??0-0?200-11?00??01?0?00?0--??
 ??11??????1001001-0000-00?31?-102025211220111121--0
 0??0?001000000????0?????00?02?????000111?0103001
 0?????????02201????????????????

Sordes_pilosus 10-100-000010110111000-002110210----
 ---01102001000--1000-00210-11000101-00010000--01?001100000-1000
 001-0001010130--102033000220100011--100000?01100000000010020
 000002?110004001111??1000000000?[45]01101010020111011000010110
 1122

Pterorhynchus_wellnhoferi 10-100-00001011-11--100004110-?110
 10000001000--?00-0022001100010??00010????????
 1100000-1000001-?????10100--102033000220101011 1000
 01?0?0?000????0100200?0?????????110??100000??
 ??0011010??0201??01000101????0??2?

Kunpengopterus_sinensis 10-1?0-000010?1-11100004110-111
 01200?0----001000 1000-012100110001????1????????
 01100000-1?00001-?????10100--102033000220101031200
 001????01001001000??020?00?02?110002?0??10??102000??
 ???401?0??0?0????????????1?11?1121

Wukongopterus_lii 10-1?0-00001011-1?--1?0?????0-????????0????????
 ???????2?01????????????????01???1100000-1000001-?????10100--
 102033000220101031 20000?0?0100?00100010020000002????002??0
 110??109?????0??4?110100????????01?00001?11?1122

Darwinopterus_zhengi ?????????????????????????????
 ???
 ???
 ?????????????0?00?0?0?020000002????002?0?01???10900
 0?????401101?0?????31?100001?11?2121

Darwinopterus_linglongtaensis 10-1?0-00001??1-11100004110-111
 1220000----001000 1000-002100110011???10?0????????
 01100000-1?00001-?????10100--102033000220101031200
 00?01?100100??0011020?00?021110002?01111??109?000?

????40110100??20113?1000?01?1102122

Darwinopterus_robustodens 10-1?0-00001??1-11100004110-111
1220000----0010?0--1000-00210011001101-1???0?????????
01100000-1?00001-?????10100--102033000220101031--200
001?010100?001?001?020000002?11000200011????119000?1???4011010
100201131?000001?1102122

Archaeoistiodactylus_linglongtaensis ???????00010?1-??--1?0?0?1?0-?????????0-?
--???
??0?110?0??10?00??1?00-?????????02033000?20101031--?
??0??0?01?010?????????????????????0??1?0??11??119000
?????04?11??????201??11000101?11?2?22

Darwinopterus_modularis 10-100-00001011-11--100004110-1111
20000001000--1000-00210011001101-1??10?010001???1110000-100000
1-?????10100--102033000220101031200001?0??100100?00?1?0200000
02?1??00200?110??19000?????04?110??0?02011311000?01?1102122

Changchengopterus_pani ??
???
??01000001?0??010?00?02????00?00
?111???00000????401101??00201??01?0??1?11?2121

Dendrorhynchoides_curvidentatus 10-1-0-0001?020-0?????0?????1?0-----0????
?????????????????01?????????????001??10?10?100100-002000?0?00-1??
?0--?0103300022?100011--??00?????100??1??0??100000002?????004
?001110?100000?0??501101?1?01?????00?00??1??0?021

Luoopterus_mutoudengensis 10-?-0-0001?02?-0?--10000???1?????????0-?--
?????????1? ??????0????00?????01??1??1?11??100-?02000?????????
?????0?03300??20?00 [01] 11--??00?????0????0001?????1?100000?02?????
??0??11??10000000?05?1101?1?3201??00100001?1?01020

Batrachognathus_volans 10-1-0-0001?020-0?--100000111-10-----0----0---?0--
1?00-000010????00110?????0? 10?10110010?-0020001-0000-1?220-
-101033000220100011--10000?????????0001????0000020100004000
110??1000000??????110101??????1?0100?01?1??10??

Jeholopterus_ningchengensis 10-1-0-0001?020-0?100000111-10-----0----0---
?0--1000-000010????001?0?????0?10?1?1100100-?02000?????00-1?22???
?01033000220100011--10000?????100??1100??0100000002?????00?00
1110?10400000??5011010100??11100100?01?11?1020

Anurognathus_ammoni 10?1-0-00011020-0?--1000001?1-10--
-----0----0---00--1000-000010????00110????????0010?10110
0100-0020001-0000-1?220--101033000220100011--100001??????0??1?
00010100000002?????????00111??104000?0??50110101??101??00100?
0101101020

Kryptodrakon_progenitor ??
???
???
?????????????????????????????????0?????????2?????????00??1????0??
?????000?11?000?00????????????????????????????????

Painten_pterodactyloid 10-100-000010?1-01--100004110-10----
 ---0001000--1100-00310011000001-1????0??????0??110
 0000-1000001-000??00100--102033000220100211--100000?
 000100001100010110000102????00??00111??10500000??04
 01110?0?03?1131110110101101120

Cuspicephalus_scarfi 20-100-00001011-11100004110-1110320000----0?11?0
 --??0-20320011000101-11??0010--0?0?01?????????????????????
 ??020??0120??01??100?0?????????????????????????????????
 ???

Germanodactylus_rhampastinus 20-100-00001011-11100004110-1
 110320000----001100--1100-20320011000101-1????0?1?????
 ???1110000-?000001-0?0?-10130--10203300012010001111
 0000?0??100001??0?10??0000?20?00002?0?111??1?????
 ?00?4??1?0010?301130?000?01011011??

Germanodactylus_cristatus 20-100-00001011-11100004110-1110320000----0
 01100--1100-20320011000101-1????0?1????????1110000-1000001-0?0??
 10130--102033000120100011010100?0????0001100010??0000002????0
 020001110?1050??000??4??110010?301130100010101101133

Pterodactylus_antiquus 10-100-00001011-11--100004110-10---
 ----0----001100--1100-11320011000101-2????0?100????110
 0000-1000001-0?00-00130--102033000120100011100000?0
 001000011000101000000020101004000111001050000000040111001003
 01130100110101101133

Normannognathus_wellnhoferi 10-000-000?10?2?1????????????????1122?000?-?
 ???10--?
 ?????1?00200-100000??100????????????02012010110100?11--11000?????
 ??
 ??

Aurorazhdarcho_primordius ?????????????????????????????????
 ??
 ??
 ?????????????????????0?1?100000002?110??200?111??108
 0000????201110?000?0113?????????1??10?133

Cycnorhamphus_suevicus 10-000-00021012-11--100002110-1
 [01]12220000----001100--1101111320011000101-211?0?10--0101010002
 00-1001001-????0-01111--10-012010110100011--1??0000000000001?0??
 1??00000?02?110002000111??108000000??4?1110000030113010001010
 1101133

Pterodactylus_micronyx 10-100-00000112-11--100004110-10----
 ---0001200--1100-11320011000101-21100?10--010001100000-1100001-
 0000-00020--102012000120101111100000?001100101100010100000002
 11??002000111??105000000??40
 11100000201130110110101101133

Liaodactylus_primus 10-1?0-00000112-11110004110-?1103?0000----????0
 --1??011320011000101-21100?1????01?001120000-1100001-??0-00020
 --101012011110101211100000?????????????????????????????????
 ???

Ctenochasma_elegans 10-100-00000112-11100004110-1[01]103?0000----0012
 00--1100-11320011000101-2??00?10--0?0??1100000-1100001-1000-000
 20--10101201111010121110000?000?10010010001??00000002??000020
 00111??105000000??4??1100?0?3011301001?0101101133

Pterodaustro_guinazui 10-000-00000112-11--100004110-10----
 ---0----001200--1100-11310?11000001-2??00?10 0????100
 0000-1100001-100??20020--10101201020020100100000?0
 00110010?10??110000000021100002000?110?1050??000004??1000003
 ??13010011010111?133

Beipiaopterus_chenianus ?????????????????????????????????
 ???
 ???
 ??????????0?10010?100?1?100?00022??00?00?11??1050
 ???0??4??10000????????????1????133

Gegepterus_changi ???0????0000112-11--10000?110-11??00000----00120
 0--1100-1?310011000001-2????0?100????10?????11??001-??0??00020-
 -101012010?1?101201?0?00?001100100????????????22????002?????
 ?????????????????[12]??0?003????0?????1??0?????

Kepodactylus_insperatus ?????????????????????????????????
 ???
 ???
 ??????????0101130101?????????????????????001111?01050
 00??0??????100?0?????0?????1?????????

Elanodactylus_prolatus ?????????????????????????????????
 ???
 ???
 ??????????0??2301011000?????000002?101001?01111?010500
 0000?040111000?0301130100110?011?1133

Moganopterus_zhuiana 10-100-00001??2-11--101004110-1110
 1000?0001100--0?01311320??10?0?0??2?100????????????120000-1?000
 01-?????00020--10201201012011111100
 00?????23?1??
 ???

Feilongus_youngi 10-100-000010?2-11101?04110-1110100000----001000--010
 10113?0011000101-2?100?100??01120000-1000001-?????00020--1020
 12010120111111 10000?0??230101????????????????????????
 ???

Ardeadactylus_longicollum 10-101000001012-11--100004110-10--
 -----0----001?00--1100-11320011000100121?00?100101011
 00010-10?0001-1001010020--102015010120101131100000
 000123010110001??00000002??0100110?0110?105000000??11100?0?3
 011301001101011011??

Huanhepterus_quingyangensis 10-1?100000101????????????????1103?000??
 ???
 ??????1100010-100000?????????0?02012010120101131-
 -10000?0??230?0110001??0??0?2?????1?0?1?1??1050

?????????1?1?????????1301001?01?1??1???

Plataleorhynchus_streptophorodon 10-10100002?01??1?--1??????-?
?????????-????????????????????????????????1-?????100?????1?????????
?????????????????????020?????1120?????13???10000?????????????????
??

Gnathosaurus_macrurus ??????10?0????1?????????????????????????????????
??100210-10??001-1000-10?
2????020?????1120?????23?????00????001230101?????????????????????
??

Gnathosaurus_subulatus 10-10110002101?-11100004110-1110310000----00100
0--1000-11320011000101-21100??0--0101?1100210-100?001-?????1???
0--102012011120?01231--100?0?????????????????????????????????
??

Haopterus_gracilis 10-100-00001011-1?--1?000??10-?0-----0----010000
--?000-0?230?1?????01-?????0?0?????????1120000-10010?1-?????10100
--?02033000220100011 10000??0?????0001?00??????1000020101??2000
011???07000?????4?11?00100?????????????????????????14-

Ornithostoma_sedgwicki ??-10???0101002?????????????????0--?????????????????
????????????????????????????????????00--?????1?????? ??????????????????10
???
????????????????????????

Volgadraco_bogolubovi ??????-???
??1110000-1001?????00?-???
?1--?1-----?--??1001010101?11?????????????????????????????
??1???????

Tethydraco_regalis ??
???
???
00110307110???

Pteranodon_sternbergi 20-0?0-10101002--0--110104110-10-----0----0100?1
200101200230111010101-1??00?????????0??1110000-1001011-?????0010
1?-?1 ???0?????0?0?????11??1?????20?10101?0?0?01?3?7?????0?1?20??
100?0?????????????????1??02???

Pteranodon_longiceps 20-000-10101002--0--110104110-10----
---0----010?01200101200240111010101-1110010001011111
0000-1001011-0001100101--010110010101010111111011101020010101
1000001030711000011403110011010112011011011110214-

Alamodactylus_byrdi ??
???
???
0010?306110????????????00????????????????????????????????

Cretornis_hlavaci ??
???
???
031?110?0?????3??00?0????????????????????????????????

Zhenyuanopterus_longirostris 10-1?0-00101??1-10110104110-111
 2310??0---0110?0 1111000220011000101-1??0??????0?
 ?11??000-1?00011-?????10100--100114?10220111231 10001??0?10
 10101?1111?10?111102?????2?0?001??207110?????4??110?1??????0
 ??????1?11?214-

Boreopterus_giganticus 10-1?0-10101??1-10--110102110-10---
 ---0---1---0--111000220011000101-11??0??????0?1110
 1000-1?01011-?????10120--?00114110220111211--100011?
 ??
 ??

Boreopterus_cuiaie 10-1?0-10101??1-10--110102110-10-----0----1----0--
 1110-002[12]0?11000101-1????????????????1101000-1?01011-?????10120
 --100114?10220111211--10001??0??010101??????10?????0??????????1
 0?????????????????21??1?0?????????????1?11?214-

Hamipterus_tianshanensis10-101000101002-10100102110-1112330000----1----0
 1110000220011001001-1110010100010011101010-1000001-10110
 00100--102124110120101131100011?001010101?1??11??11110211?0?
 ?210100???207110?10?1402?100???101??11101101?1102???

Brasileodactylus_araripensis ??????0?????0????????????????????????????
 ???1000010-1000001?101
 ??????1--?02124?0121?01131--?001????????????????????????????
 ???

Barbosania_gracilirostris 10-101000101001-1?--1?0?0?110-10---
 ---0 0?11?0--1?10-0023?0??0?01??0??001010?0?????10
 00010-1?00001-1?1??00101--?02124110121101131--10001?
 ??????????????1?1?10?1??02?????10?0?00???207110?????
 402?101?0211??0??????1?1102???

Cearadactylus_atrox 10-101000101001-10--11010?110-?0-----0----01100?
 ??????????02300110101?1-?????0100011111000010-1000001-1010-0010
 1--102124?10121101131--10001????????????????????????????
 ???

Guidraco_venator 10-1?1000101??1-10--110102110-10-----0----?????1
 211111200230111010001-1??0?????0?0?110??010-1?00001-?????1010
 0--102124110121101131--10001??001??0101????????????????????
 ???

Ludodactylus_colorhinus 10-11100??01????????????????????????????
 ???100?????1????????????
 ??????02?????00?1????13??1?0????????????????????????????
 ???

Ludodactylus_sibbicki 10-101000101??1-10--110102110-10-----0 011011
 111111200230111010001-11100?0100010?11000010-1?00001-100??101
 00--102124110021101131--10001????????????????????????????
 ???

Aetodactylus_halli ??-???000?2??0????????????????????0----????????
 ?????????????????????????????????100?????11000210-1120001-1000-1?100-
 -10112?1?0120101131--?001????????????????????????????????

????02??2??001????03??1??
??

Siroccopteryx_moroccensis 00-101000?0?00????????????????????1004?01????
??101?????1????????????????
????????????02??2??001??01131--2?0????????????????????????????????
??

Coloborhynchus_capito 00-10120??0????????????????????1004?011????????
??1?????????0????????????
?????0??2??01?1??131--2????????????????????????????????????
??

Coloborhynchus_wadleighi 00-11120??0100????????????????1004?011???
??101?????1????????????
????????????02??2??01?1??1131--2?0????????????????????????????
??

Coloborhynchus_clavirostris 00-11120??0????????????????1004?011???
??101?????1????????????
????????????02??2??01?1??13??2?0????????????????????????????
??

Eopteranodon_lii 20-2?0-11001000--?--100?????0-?110410110????????
?????001??011?1-1??????-? ?????1?210001010?1?1-01?????1????110??
0??000101????????????0?22????00?0?01???10801??1???4?????0?020
11301111111?1111???

Huaxiapterus_jii 20-2?0-1??010?0--?--100??4110-?110410?10----00?10????
??0??3?0?11?011?1-??????00????12100010100??1-0????2012201110
??0????0?1??0??1??????22??1000210?01???108011?????412110?110
??13?????????1?1111???

Sinopterus_dongi 20-2?0-110010?0--110002?1?0-1110410110----0011011201?
130?33?011?011?1-1??1??????????121000101001?11-?????201220111
0??0??000101?0??110?1?0?22?11000210?011??1080111110041311001
10?0?13?1111111??1?14-

Sinopterus_benxiensis 20-2?0-1?0010?0--?--100????10-11126
101100-10?1120?013?0330011001101-1????????????
121000101001111-010??2012201?10??001??0101??0????????????
?????01????080?????0??3110?110????????????1?????4-

Sinopterus_corollatus 20-2?0-110010?0--?1?0?2????0-1112610110 ??????
??0??10?????01????????????1????????????121000101001?11-?????20?22
01110??001??0101?0????????00?2??1000????01????0801?111??4?311
0?110??13????1?111?1??14-

Bakonydraco_galaczi 20 200-1?0310????????????????11010011?????
??0--????1121000111001111-01210
001020111-----?? 0????????????????????????????
??

Keresdrakon_vilsoni 20-200-1?0310?0--?--1?0?????0-?110100110----?????
?????????????0????????????????00--?????121030[01]-100?01??002??10?
?201?1 0?100100010????????????00?121111001100011??108111?11

?????????1?001???0111001111?1???

Caiuajara_dobruskii 20-210-11001000--?100124110-?111011110----?????1
12??13?0?[34]001?001101-1?101?00--0????0122000111001011-010?00
1021001 0?10?100010??0?1?100100122?1?00?21?101??108011??1
004???100?102??12??111?1111111???

Tupandactylus_navigans 20-210-110010?0--1100124110-1111011100 00110?
??010?000230011001101-1??0??0?????1?????????????????????
???1 0???
?????????????????????????????????????

Tupandactylus_imperator 20-2?0-1?0010?0--? 1?0123110-1111011100----111
20?01300230011001101-1???1?0?????????1220001010?????1-010??001?2
10?10???
?????????????????????????????????

Vectidraco_daisymorrisae ???
??
??
??
??3?1??011111???????????

Europejara_olcadesorum ??????-??0?????????--1????411?-?????????0 ??????
???1??002?001?0??0?????????1??010?01210001110?1111-01????010
210?10???
?????????????????????????????????

Tapejara_wellnhoferi 20-210-11001000--1100124110-1111010110----001101
120101300230011001101-1110111001010121000111001111-0101000102
10010?10010001010100??01001221110001101011001080111110040?
?100010301??00111?111111114-

Microtuban_altivolans ???
??
??
110??08011??1??4?3110??0????????????????????112?1???

Noripterus_complicidens ??????-?????0????????????????????????????
??1??000-100?00??100110??
?1--?020510?0220??1?31--????0?1101000101??1?11100?????12????00?
0010111010801111100??11100?0210113?111111001211?4-

Noripterus_parvus 210100-10001001-11 00012010-1111330101----1----11
20001220220?11101101-11101?0100010?11110000-1001001-100110010
1--102051000220101031010110010001010111?????00?12????00?00
0011001080111110041?1100?02??1?????????001211???

Domeykodactylus_ceciliae ?????????????????????????????????????0??1?2????10?????????
??11??0??10??001-???10?0?
?1?-?02051??0220??04?????010?????????????????????????????????
??

Dsungaripterus_wei 210000-10001001-11100012110-1112330101----11120
001220220011101101-1110110100010111010000-1001001-1001000101-
-10205100022010104102010110010001010111111001001121110001???
0?0??108011111?0?11?1001123?1?????1111?001211???

Tupuxuara_leonardii 20-100-10001001--1100124110-1100530120----111000
01220230011001101-11101111101111110000-1001011-1001000101--
11011001000101??11?????001121?10001100??11?108011111004???10
0110?????????????1112111??

Tupuxuara_longicristatus ???00-100010??--?100?????0-11005?012?????????
?????????0??0??1-?????11110?????????????????????????????1
0?????????0?????????????????0?????????????????????31?0??1?
?????????????????

Thalassodromeus_sethi 20-100-10101001--1--100124110-11005301200100011
00001220230011001101-1?1?110111011?111??000-100?011-121100010
1--110???
?????????????????????

Lacusovagus_magnificens 20-2?0-1100100?--?--1????????-?110100?10----?????
?????????????1?????????????????0--0?????????????????????????
???1?0???
?????????????????????

Xericeps_curvirostris ??
??10??300-110101??1011?????
?0--?1-----?--0???
???

Alaqa_saharica 20-100-10?011?1?????????????????????????????????????
????????????????????????????111?????1?????????10??01??1?1?????????????
1?-?0???
?????????????????????????????????

Argentinadraco_barrealensis ??????????????0?????????????????????????????
??11??300-11?101??101
100??200?1-----?0???
???

Aerotitan_sudamericanus 20-100-10?311?2?????????????????????????????????
?????????????????????????????????????0--?????0?????????????????????????
?????1?-?1???
?????????????????????????????????

Eoazhdarcho_liaoxiensis ??????-?????0?????????????????????????????????
?????????????????0????????????????????????????--?????110000-10?1001-00010??1
0?-?11????000130?11?00?????000?22?????00?0?01?0?080??111??4?3
110??10?????????????????1??1?????

Shenzhoupterus_chaoyangensis 20-1?0-???010?2--1 10012?111-10-----0----
11101?01301230?1100020??1??1?????????????1110000-1?0??1-?????00
121--?1 0????0130?11?10?????????00?22?????????01??1080?????
0??31?0?1?0?????????????1?1??114-

Jidapterus_edentus 20-100-10001002--1--100?????1-?0-----0?????????????
?????????0011?001?1-?1?????0--01??11110000-1001001-?????00121--11
00?000130111010010000000?22111000100001?????080?1?11004021100
110301?????11111111211133


```

{2 Mandible,_length_relative_to_skull_length_to_squamosal:_continuous;
{3
Rostrum,_length_to_narial/nasoantorbital_fenestra_relative_to_skull_length_to_squamosal:_continuous;
{4 External_naris,_length_relative_to_skull_length_to_squamosal:_continuous;
{5 External_naris,_length_relative_to_maximum_height_in_naris:_continuous;
{6 Antorbital_fenestra,_length_relative_to_skull_length_to_squamosal:_continuous;
{7 Antorbital_fenestra,_length_relative_to_maximum_height_in_fenestra:_continuous;
{8 Nasoantorbital_fenestra,_length_relative_to_skull_length_to_squamosal:_continuous;
{9
Nasoantorbital_fenestra,_aspect_ratio,_length_to_maximum_height_in_fenestra_preserved:_continuous;
{10 Orbit,_length_relative_to_height:_continuous;
{11 Supratemporal_fenestra,_length_relative_to_skull_length_to_squamosal:_continuous;
{12 Subtemporal_fenestra,_length_relative_to_width:_continuous;
{13 Basipterygoid_processes,_angle_divided_by_100:_continuous;
{14
Rostrum,_tooth_row,_length_to_posterior_margin_relative_to_skull_length_to_squamosal:_continuous;
{15 Teeth,_maximum_number_divided_by_1000:_continuous;
{16 Mandible,_symphysis,_length_relative_to_mandible_length:_continuous;
{17 Mandible,_length_relative_to_ramus_mid-depth:_continuous;
{18
Mandible,_symphysis,_aspect_ratio,_length_to_maximum_depth_preserved_exclusive_of_crest
s:_continuous;
{19 Mandible,_crest,_length_relative_to_mandible_length:_continuous;
{20 Mandible,_tooth_row,_length_relative_mandible_length:_continuous;
{21 Mid-cervical vertebra,_maximum_length_relative_to_mid-width:_continuous;
{22 Mid-cervical vertebra,_maximum_length_relative_to_dorsal vertebra_length:_continuous;
{23 Dorsal vertebra,_length_relative_to_maximum_diameter:_continuous;
{24 Synsacrum,_vertebra_number:_continuous;
{25 Caudal vertebra,_length_relative_to_dorsal vertebra_length:_continuous;
{26 Caudal vertebra,_length_relative_to_diameter:_continuous;
{27 Scapula,_length_relative_to_coracoid_length:_continuous;
{28 Coracoid,_deep_flange,_length_relative_to_coracoid_length:_continuous;
{29 Humerus,_length_relative_to_dorsal vertebra_length:_continuous;
{30
Humerus,_deltopectoral_crest,_proximodistal_constriction_width_relative_to_anterior_terminus_proximo
distal_width:_continuous;
{31 Ulna_or_radius,_length_relative_to_humerus_length:_continuous;
{32 Radius,_mid-width_relative_to_ulna_mid-width:_continuous;
{33 Pteroid,_length_relative_to_ulna_or_radius_length:_continuous;
{34 Metacarpal_IV,_length_relative_to_humerus_length:_continuous;
{35 Metacarpal_IV,_midpoint,_dorsoventral_width_relative_to_combined_ulna_and_radius_mid-
width:_continuous;
{36
Metacarpal_IV,_proximal_end,_dorsoventral_width_relative_to_midpoint_dorsoventral_width:_continuous
;
{37 Manus,_digit_IV,_first_phalanx,_length_relative_to_humerus_length:_continuous;
{38 Manus,_digit_IV,_second_phalanx,_length_relative_to_first_phalanx_length:_continuous;
{39 Manus,_digit_IV,_third_wing_phalanx,_length_relative_to_first_phalanx_length:_continuous;
{40
Manus,_digit_IV,_fourth_wing_phalanx,_length_relative_to_first_phalanx_length:_continuous;
{41 Prepubis,_length_relative_to_maximum_width:_continuous;
{42 Pubis,_depth_relative_to_acetabulum_anteroposterior_length:_continuous;
{43
Ilium,_preacetabular_process,_length_relative_to_postacetabular_process_length:_continuous;
{44 Femur,_length_relative_to_humerus_length:_continuous;
{45 Tibiotarsus,_length_relative_to_femur_length:_continuous;

```

{46 Fibula, _free_length_relative_to_tibiotarsus_length: continuous;
 {47 Metatarsal_III, _length_relative_to_tibiotarsus_length: continuous;
 {48 Pes, _digit_III, _second_phalanx, _length_relative_to_mid-width: continuous;
 {49 Pes, _digit_IV, _first_phalanx, _length_relative_to_metatarsal_III_length: continuous;
 {50
 Pes, _digit_IV, _second_phalanx, _length_relative_to_pedal_digit_IV_first_phalanx_length: continuous;
 {51
 Pes, _digit_IV, _third_phalanx, _length_relative_to_pedal_digit_IV_first_phalanx_length: continuous;
 {52 Rostrum, _anterior_tip, _shape: ordered flat rounded pointed;
 {53 Rostrum, _rostral_process: absent present;
 {54 Rostrum, _rostral_process, _cross-section: triangular elliptical;
 {55 Rostrum, _anterior_end, _orientation: ordered upturned straight downturned;
 {56 Palate, _anterior_end, _fossa: absent present;
 {57 Rostrum, _anterior_end, _lateral_expansion: absent present;
 {58 Jaws, _anterior_end, _lateral_expansion, _horizontal_outline: elliptical triangular quadrangular;
 {59 Rostrum, _anterior_portion, _occlusal_margins, _shape: rounded ridged;
 {60 Rostrum, _middle_portion, _expansion: absent present;
 {61 Rostrum, _posterior_portion, _occlusal_margins, _shape: rounded ridged;
 {62 Rostrum, _shape: laterally_compressed anteroposteriorly_truncated dorsoventrally_depressed
 laterally_flattened;
 {63 Rostrum, _taper_in_sagittal_plane: subparallel attenuated;
 {64 Rostrum, _taper_in_horizontal_plane: attenuated subparallel;
 {65 Skull, _lateral_margins, _curvature_in_horizontal_plane: ordered concave
 straight convex;
 {66 Skull, _dorsal_margin, _curvature_in_sagittal_plane_exclusive_of_cranial_crests: ordered convex
 straight concave;
 {67 External_naris, _dorsal_and_ventral_edges, _orientation: acute_angle subparallel;
 {68 Narial/nasoantorbital_fenestra, _anterior_end, _position_relative_to_premaxillary_toothrow: dorsal
 posterior;
 {69 Jugal, _lateral_surface, _antorbital/nasoantorbital_fossa: present absent;
 {70 Antorbital_fenestra, _dorsal_and_ventral_edges, _orientation: subparallel angle;
 {71 Antorbital_fenestra, _ventral_edge, _position_relative_to_external_naris_ventral_edge: level ventral;
 {72 External_naris_and_antorbital_fenestra, _configuration: separate confluent_(nasoantorbital_fenestra);
 {73 Antorbital/nasoantorbital_fenestra, _posterior_edge, _shape: subangular beveled;
 {74 Nasoantorbital_fenestra, _dorsal_and_ventral_edges, _orientation: acute_angle
 subparallel;
 {75 Orbit_outline: subcircular inverted_piriform_to_ovate inverted_triangle;
 {76 Orbit, _dorsal_position_in_skull:
 middle_of_the_skull_with_the_ventral_margin_of_the_orbit_below_the_middle_of_the_antorbital_(or_nasoantorbital)_fenestra_and_the_dorsal_margin_of_the_orbit_above_the_dorsal_margin_of_the_antorbital_(or_nasoantorbital)_fenestra
 high_in_the_skull_with_the_ventral_margin_of_the_orbit_the_same_level_or_above_the_middle_of_the_antorbital_(or_nasoantorbital)_fenestra
 low_in_the_skull_with_the_entire_orbit_lower_than_the_dorsal_margin_of_the_antorbital_(or_nasoantorbital)_fenestra;
 {77 Infratemporal_fenestra, _outline: trapezoidal inverted_triangle upright_triangle oval
 elliptical;
 {78 Infratemporal_fenestra, _position_relative_to_orbit: posterior_to_orbit_reaches_under_orbit;
 {79 Infratemporal_fenestra, _orientation: subvertical inclined;
 {80 Premaxilla, _premaxillary_bar, _width: wide narrow;
 {81 Premaxilla, _maxillary_process, _posterior_end, _position: ordered contacts_nasal
 posterior_half_of_external_naris anterior_half_of_external_naris;
 {82 Premaxilla, _premaxillary_bar, _posterior_end, _position: between_nasals
 between_frontals;
 {83 Premaxilla, _crest: absent present;
 {84 Premaxilla, _crest, _anterior_end, _position_relative_to_skull_anterior_end: level

posterior;

{85 Premaxilla, _crest, _anterior_margin, _orientation: _ordered inclined_posteriorly subvertical curving anterodorsally;

{86 Premaxilla, _crest, _shape: tall_triangle_decreasing_in_height_posteriorly low_blade low_with_anterior_hump comb-like_with_straight_dorsal_margin semicircular tall_triangle_increasing_in_height_posteriorly rectangular;

{87 Premaxilla, _crest, _posterior_end, _position: _ordered anterior_to_naris/nasoantorbital_fenestra_anterior_end between_naris/nasoantorbital_fenestra_anterior_end_and_orbit above_orbit above_occiput;

{88 Premaxilla, _crest, _dorsal_spine: absent present;

{89 Premaxilla, _crest, _thickness: thin, _single_plate thick, _two_plates_separated_by_trabeculae;

{90 Premaxilla, _crest, _texture: striated smooth branching_grooves;

{91 Maxilla, _posterior_end, _shape: narrow ventral_expansion;

{92 Maxilla, _nasal_process, _shape: broad tapered parallel_sided;

{93 Maxilla, _lateral_surface, _antorbital_fossa: present absent;

{94 Maxilla, _nasal_contact, _position: main_body_of_nasal descending_process_of_nasal;

{95 Maxilla, _premaxillary_process_and_posterior_ramus, _configuration: posterior_ramus_wider both_narrow premaxillary_process_wider both_wide;

{96 Nasal, _descending_process: present absent;

{97 Nasal, _descending_process, _position: lateral medial;

{98 Nasal, _descending_process, _length: short elongate;

{99 Nasal, _descending_process, _orientation: _ordered inclined_anteriorly ventral inclined_posteriorly;

{100 Nasal, _descending_process, _lateral_pneumatic_foramen: absent present;

{101 Frontal, _crest: absent present;

{102 Frontal, _crest, _shape: blunt elongate expanded;

{103 Frontal, _crest, _anterior_end, _position: _ordered anterior_to_orbit above_orbit posterior_to_orbit;

{104 Frontal, _anterior_end, _position_relative_to_preorbital_bar_anterior_margin: anterior posterior;

{105 Lacrimal, _foramen: absent present;

{106 Lacrimal, _posterior_margin, _orbital_process: absent present;

{107 Parietal, _crest: absent present;

{108 Parietal, _crest, _shape: low expanded_into_rounded_margin tapered_into_triangular_process elongate_process;

{109 Squamosal, _shape: unexpanded rounded expanded;

{110 Squamosal, _position_relative_to_base_of_lacrimal_process_of_jugal: above below;

{111 Quadrate, _inclination_relative_to_ventral_margin_of_skull: _ordered acute Perpendicular $\sim 120^\circ \sim 150^\circ$;

{112 Quadrate, _mandible_articulation, _position_relative_to_orbit: _ordered posterior_to_orbit posterior_to_center_below_orbit below_orbit_center anterior_to_center_below_orbit anterior_to_orbit;

{113 Quadrate, _ascending_process, _shape: wide thin;

{114 Jugal, _anterior_end, _position_relative_to_nasoantorbital_fenestra_anterior_end: posterior level;

{115 Jugal, _maxillary_ramus: absent present;

{116 Jugal, _ventral_margin, _curvature_in_parasagittal_plane: straight concave;

{117 Jugal, _postorbital_process_and_lacrimal, _configuration: do_not_contact contact_to_form_lower_orbital_bar;

{118 Jugal, _ascending_and_postorbital_processes, _configuration: separated_by_distinct_angle infilled_by_concave_flange;

{119 Jugal, _ascending_process, _base, _width: broad narrow;

{120 Jugal, _ascending_process, _inclination: _ordered anterodorsal subvertical posterodorsal;

{121 Jugal, _postorbital_process, _anterior_margin, _orbital_process: absent present;

{122 Jugal, _posterior_process: present absent;

{123 Jugal, _posterior_process, _orientation: posterior ventral;

{124 Occiput, _orientation: _ordered posterior posteroventral ventral;

{125 Basioccipital, _length_relative_to_width: shorter_than_wide longer_than_wide;

{126 Basisphenoid, _main_body, _length: shorter_than_wide longer_than_wide;

{127 Basisphenoid,_elongate_basipterygoid_processes: absent present;
 {128 Supraoccipital,_crest: absent present;
 {129 Supraoccipital,_pneumatic_foramina: absent present;
 {130 Palate,_posterior_end,_shape: concave convex;
 {131 Palate,_median_ridge: absent present;
 {132 Palate,_median_ridge,_position: tapering_anteriorly confined_posteriorly;
 {133 Palate,_median_ridge,_shape: narrow_strip wide_keel;
 {134 Palatine,_shape: broad_plate thin_bars;
 {135 Choanae_and_maxilla,_configuration: contact do_not_contact;
 {136 Pterygoid,_ventral_margin,_position_relative_to_jaw_occlusal_margin: dorsal ventral;
 {137 Interpterygoid_vacuity,_length_relative_to_subtemporal_fenestra_length: longer_than_subtemporal_fenestra shorter_than_subtemporal_fenestra;
 {138 Mandible,_articulation,_helical_shape: absent present;
 {139 Jaws,_lateral_surface,_row_of_foramina_parallel_to_occlusal_margin: present absent;
 {140 Mandible,_anterior_end,_orientation: ordered_upturned straight downturned;
 {141 Mandible,_anterior_tip,_shape: ordered_blunt pointed prow;
 {142 Mandible,_odontoid_process: absent present;
 {143 Mandible,_symphysis,_shape: laterally_compressed anteroposteriorly_shortened dorsoventrally_depressed laterally_flattened;
 {144 Mandible,_anterior_end,_lateral_expansion: absent present;
 {145 Mandible,_symphysis,_dorsal_eminence: absent present;
 {146 Mandible,_symphysis,_dorsal_eminence,_height: low high;
 {147 Mandible,_symphysis,_fusion: absent present;
 {148 Mandible,_symphysis,_taper_in_horizontal_plane: attenuated subparallel;
 {149 Mandible,_anterior_end,_lateral_surfaces,_texture: flat_cup-shaped_structures pitted;
 {150 Mandible,_anterior_portion,_occlusal_margins,_shape: rounded ridged;
 {151 Mandible,_middle_portion,_expansion: absent present;
 {152 Mandible,_posterior_portion,_occlusal_margins,_shape: rounded ridged;
 {153 Mandible,_ramus,_dorsal_eminence: present absent;
 {154 Mandible,_ramus,_dorsal_eminence,_shape: rounded pointed;
 {155 Mandible,_symphysis,_occlusal_surface,_median_sulcus: absent present;
 {156 Mandible,_symphysis,_occlusal_surface,_anterior_end,_shape: flat fossa keel;
 {157 Mandible,_symphysis,_occlusal_surface,_shape: flat parasagittal_ridges median_ridge;
 {158 Mandible,_symphyseal_cavity: absent present;
 {159 Mandible,_symphyseal_cavity,_dorsal_shelf,_posterior_end,_position_relative_to_ventral_symphysis_posterior_end: dorsal_shelf_extends_posterior_to_ventral_symphysis ventral_symphysis_extends_posterior_to_dorsal_shelf;
 {160 Mandible,_ramus,_dorsal_margin,_curvature_along_length: ordered_convex straight concave;
 {161 Mandible,_ramus,_orientation: straight_to_upturned downcurved;
 {162 Mandible,_retroarticular_process,_orientation_relative_to_ramus: ordered_posteroventral subparallel posterodorsal;
 {163 Mandible,_retroarticular_process,_outline_in_parasagittal_plane: triangular subcircular elongate blunt rectangular;
 {164 Mandible,_symphysis,_ventral_margin,_shape: flat keel crest;
 {165 Mandible,_crest,_shape: blade-like_and_low massive_and_deep;
 {166 Mandible,_crest,_anterior_end,_position_relative_to_mandible_anterior_end: posterior level;
 {167 Dentary,_position_relative_to_angular_and_surangular: does_not_separate separates;
 {168 Dentition: present absent;
 {169 Dentition,_spacing_along_jaws: ordered_mesial_teeth_spaced_wider_apart even_along_the_jaws distal_teeth_spaced_wider_apart;
 {170 Dentition,_tooth_shape,_variation: isodont heterodont;
 {171 Dentition,_mesial_teeth,_shape: recurved_triangle slender_needle recurved_spike

curved_cone labiolingually_compressed_triangle bulbous_triangle;
 {172 Dentition,_cheek_teeth,_shape: recurved_triangle bulbous_triangle slender_needle
 curved_cone labiolingually_compressed_triangle recurved_spike;
 {173 Dentition,_texture: smooth striated mesial_and_distal_keels median_carina;
 {174 Dentition,_maximum_crown_height_relative_to_mesiodistal_base_width:
 less_than_four_times_width more_than_four_times_width;
 {175 Dentition,_lateral_orientation: vertical lateral;
 {176 Dentition,_mesial_teeth,_spacing_between_successive_teeth:_ordered nearly_touching
 at_most_diameter_of_teeth more_than_diameter_of_teeth;
 {177 Dentition,_cheek_teeth,_spacing_between_successive_teeth:_ordered nearly_touching
 at_most_diameter_of_teeth more_than_diameter_of_teeth;
 {178 Dentition,_size_variation: even_transition_along_tooth_row
 distinct_disparity_in_size_between_mesial_and_distal_teeth;
 {179 Dentition,_upper_teeth,_size_relative_to_lower_teeth:_ordered upper_teeth_significantly_larger
 subequal_lower_teeth_significantly_larger;
 {180 Dentition,_maximum_curvature_relative_to_mesiodistal_base_width:
 displacement_of_curvature_less_than_width displacement_of_curvature_more_than_width;
 {181 Dentition,_curvature_orientation: posterior lingual anterior;
 {182 Dentition,_inclination:_ordered upright mesial_teeth_procumbent procumbent;
 {183 Dentition,_cheek_alveoli,_shape: set_in_grooves low undulating_occlusal_margins raised_rims
 pedestals;
 {184 Dentition,_cheek_teeth,_denticles: present absent;
 {185 Dentition,_cheek_teeth,_largest_denticles,_shape:_ordered serrations cuspules crenulations
 low_cusps tall_cusps;
 {186 Dentition,_cheek_teeth,_maximum_denticle_number:_ordered more_than_50
 between_six_and_49 five;
 {187 Dentition,_upper_tooth_row,_anterior_end,_position:_ordered posterior_to_rostrum_tip
 rostrum_tip rostrum_anterior_surface;
 {188 Dentition,_maxillary_teeth,_position_of_largest_teeth: mesial middle distal;
 {189
 Dentition,_fifth_and_sixth_teeth,_subequal_in_size_and_distinctly_smaller_than_fourth_and_seventh:
 absent present;
 {190 Dentition,_lower_tooth_row,_anterior_end,_position: mandible_tip posterior_to_mandible_tip;
 {191 Jaws,_occlusal_margin,_curvature_in_sagittal_plane: straight dorsally_reflected;
 {192 Cervical_vertebrae,_atlantoaxis,_fusion: unfused fused;
 {193 Cervical_vertebrae,_lateral_to_neural_canal,_pneumatic_foramina: absent
 present;
 {194 Cervical_vertebrae,_middle-series,_midsection,_cross-section: pentagonal
 dorsoventrally_depressed wide_suboval laterally_compressed;
 {195 Cervical_vertebrae,_middle-series,_neural_arch,_lateral_surface,_pneumatic_foramen: absent
 present;
 {196 Cervical_vertebrae,_middle-series,_centrum,_lateral_surface,_pneumatic_foramen: absent present;
 {197 Cervical_vertebrae,_IV-VI,_neural_spines,_height:_ordered tall low extremely_reduced;
 {198 Cervical_vertebrae,_IV-VI,_neural_spine,_shape: rectangular subtriangular fan
 ridge;
 {199 Cervical_vertebrae,_middle-series,_transverse_crest_or_ridge,_dorsal_reflection: absent present;
 {200 Cervical_vertebrae,_middle-series,_postexapophyses: absent present;
 {201 Cervical_vertebrae,_middle-series,_neural_arch_and_centrum,_configuration:
 distinct confluent;
 {202 Cervical_vertebrae,_middle-series,_ribs,_shape: elongate reduced;
 {203 Cervical_vertebrae,_VIII,_neural_spine,_height: tall low;
 {204 Cervical_vertebrae,_IX,_shape: similar_to_dorsal_vertebrae similar_to_cervicals;
 {205 Dorsal_vertebrae,_notarium: absent present;
 {206 Dorsal_vertebrae,_anterior_series,_supraneural_plate: absent present;
 {207 Symsacrum,_sacral_ribs,_configuration: contact_at_iliac contact_medial_to_iliac;
 {208 Symsacrum,_supraneural_plate: absent present;

{209 Caudal_vertebrae,_number: more_than_15 at_most_15;
 {210 Caudal_vertebrae,_zygapophyses,_length: _ordered short elongate extremely_elongate;
 {211 Caudal_vertebrae,_centrum,_shape: single duplex;
 {212 Scapulocoracoid,_orientation_relative_to_vertebral_column: subparallel
 rotated_laterally;
 {213 Scapula_proximal_end,_shape: elongate_and_compressed suboval_and_expanded;
 {214 Scapula,_shape: elongate_process stout_with_constricted_shaft;
 {215 Scapula,_articulation_with_vertebral_column: absent present;
 {216 Coracoid,_ventral_margin,_shape: flat broad_tubercle crest;
 {217 Coracoid,_shape: _ordered semicircular broad_shaft narrow_shaft;
 {218 Sternum,_sternocoracoid_articulations,_configuration: lateral_to_one_another
 anterior_and_posterior_to_one_another;
 {219 Sternum,_posterior_to_sternocoracoid_articulations,_constriction: present absent;
 {220 Sternum,_cristospine,_shape: shallow deep;
 {221 Sternum,_cristospine,_length: stout elongate;
 {222 Sternocoracoid_articulations,_shape: flattened oval;
 {223 Sternocoracoid_articulations,_posterior_expansion: absent present;
 {224 Sternum,_plate,_shape: narrow quadrangular semicircular triangular laterally_expanded;
 {225 Humerus,_proximal_end,_ventral_surface,_pneumatic_foramen: absent present;
 {226 Humerus,_proximal_end,_articulation_surface,_outline: crescent horseshoe;
 {227 Humerus,_proximal_end,_dorsal_surface,_pneumatic_foramen: absent present
 {228 Humerus,_shaft,_curvature: straight bowed;
 {229 Humerus,_mid-shaft,_shape: constricted subcylindrical;
 {230
 Humerus,_entepicondyle,_dorsoventral_width_relative_to_ectepicondyle_dorsoventral_width:
 entepicondyle_wider_than_ectepicondyle ectepicondyle_wider_than_entepicondyle;
 {231 Humerus,_distal_end,_anterior_surface,_between_distal_condyles,_pneumatic_foramen: absent
 present;
 {232 Humerus,_distal_aspect,_pneumatic_foramen: absent present;
 {233 Humerus,_distal_aspect,_outline: hourglass crescentic_or_D-shape triangular
 trapezoidal;
 {234 Humerus,_deltopectoral_crest,_position: proximal more_distal_on_shaft;
 {235 Humerus,_deltopectoral_crest,_shape: subtriangular_with_proximal_apex
 proximodistally_long_and_proximally_leaning_trapezoid proximally_curving_hook
 oblong_process_with_constricted_neck anteroposteriorly_short_and_rectangular
 proximodistally_long_and_proximally_expanded hatchet-shape
 distally_leaning_trapezoid anteroposteriorly_tall_and_rectangular_process
 anteroposteriorly_tall_and_proximally_leaning_trapezoid;
 {236 Humerus,_deltopectoral_crest,_curvature: perpendicular_to_shaft warped_distally;
 {237 Humerus,_ulnar_crest,_size: reduced developed;
 {238 Humerus,_ulnar_crest,_orientation: posterior ventral;
 {239 Ulna,_shaft,_proximal_end,_anterior_surface,_longitudinal_ridge: absent present;
 {240 Ulna,_distal_tuberculum,_position: middle_of_the_distal_end ventral_part_of_the_distal_end;
 {241 Radius,_distal_end,_cross-section: suboval subtriangular_with_large_anterior_process;
 {242
 Distal_syncarpal_ventral_articular_facet_for_wing_metacarpal,_size_relative_to_dorsal_facet:
 ventral_facet_larger subequal_in_size;
 {243 Distal_syncarpal,_cross-section: rectangular triangular;
 {244 Pteroid,_shape: angled_at_midsection stout_hook
 straight_and_tapered_with_expanded_proximal_end straight_with_expanded_ends
 proximally_curved_slender_rod curved_and_subparallel_sided;
 {245 Medial_carpal,_shape: longer_than_wide wider_than_long;
 {246 Metacarpals,_number_articulating_with_carpus: _ordered five four two one;
 {247 Metacarpals_I-III,_distal_ends,_relative_positions: disparate approximate;
 {248 Metacarpal_IV,_proximal_end,_cross-section: anteroposteriorly_compressed
 broad;

{249 Metacarpal_IV,_shaft,_cross-section: cylindrical anteroposteriorly_compressed_oval;
 {250 Metacarpal_IV,_distal_end,_intercondylar_sulcus,_median_ridge: absent present;
 {251 Manus,_unguals,_size_relative_to_pedal_unguals: less_than_twice_size_of_pedal_unguals
 more_than_twice_size_of_pedal_unguals;
 {252 Manus,_digit_IV,_first_phalanx,_proximal_end,_ventral_surface,_pneumatic_foramen: absent
 present;
 {253 Manus,_digit_IV,_second_or_third_phalanges,_shaft,_cross-section: subtriangular
 concave_posteriorly oval ventral_keel;
 {254 Pubis,_anterior_margin,_curvature_in_sagittal_plane: _ordered convex
 straight slightly_concave deeply_concave;
 {255 Pubis_and_ischium,_ventral_contact,_configuration: confluent oval_opening;
 {256 Ischium,_ventral_margin,_curvature_in_parasagittal_plane: straight convex;
 {257 Prepubis,_shaft,_constriction: absent present;
 {258 Prepubis,_shape:
 elongate_paddle medially_curved_with_short_lateral_process triradiate expanded_fan;
 {259 Ilium,_preacetabular_process,_anterior_margin,_shape: rounded triangular sharp_rod;
 {260 Ilium,_preacetabular_process,_orientation: straight dorsiflected;
 {261 Ilium,_postacetabular_process,_orientation: subhorizontal posterodorsal;
 {262 Ilium,_postacetabular_process,_shaft,_constriction: absent present;
 {263 Ilium,_postacetabular_process,_terminus,_expansion: absent present;
 {264 Acetabulum,_outline: oval subcircular;
 {265 Ilium,_postacetabular_process,_dorsal_margin,_shape: flat convex;
 {266 Femur,_curvature: strongly_bowed straight_to_slightly_curved;
 {267 Femur,_proximal_end,_pneumatic_foramen: absent present;
 {268 Femur,_neck,_shape: indistinct constricted;
 {269 Femur,_greater_trochanter,_shape: _ordered reduced distinct_process hooked_process;
 {270 Femur,_distal_end,_epicondyles,_size: reduced_and_confluent_with_distal_condyles
 expanded_into_distinct_distal_flanges;
 {271 Femur,_neck,_angle_relative_to_shaft:_ordered perpendicular less_than_145° more_than_145°;
 {272 Metatarsal_IV,_length_relative_to_metatarsals_I-III: subequal significantly_shorter;
 {273 Pes,_digit_V,_number_of_phalanges:_ordered four three two one zero;
 {274 Pedal_digit_V_ultimate_phalanx,_shape:_ordered straight curved bent_at_midsection nubbin;

nstates stand; hold 130000;
 rseed 0; rseed []; collapse auto;
 mult= replic 2000 keepall ratchet; best;
 procedure/;